A one dimensional analysis of singularities of the d-dimensional stochastic Burgers equation.

Neate, Andrew

A one dimensional analysis of singularities of the d-dimensional stochastic Burgers equation

Andrew Neate

Submitted to the University of Wales in fulfilment of the requirements for the Degree of Doctor of Philosophy

Swansea University

2005

Declaration

This work has not previously been accepted in substance for any degree and is not being concurrently submitted in candidature for any degree.

Signed .... (candidate)

Date ....

Statement 1

This thesis is the result of my own investigations, except where otherwise stated. Other sources are acknowledged by explicit references. A bibliography is appended.

Signed .... (candidate)

Date ....

Statement 2

I hereby give consent for my thesis, if accepted, to be available for photocopying and inter-library loan, and for the title and summary to be made available to outside organisations.

Signed .... (candidate)

Date ....

Contents

Abstract

This thesis presents a one dimensional analysis of the singularities of the d-dimensional stochastic Burgers equation using the 'reduced action function'. In particular, we investigate the geometry of the caustic, the Maxwell set and the Hamilton-Jacobi level surfaces, and describe some turbulent phenomena.

Chapter 1 begins by introducing the stochastic Burgers equation and its related Stratonovich heat equation. Some earlier geometric results of Davies, Truman and Zhao are presented together with the derivation of the reduced action function.

In Chapter 2 we present a complete analysis of the caustic in terms of the derivatives of the reduced action function, which leads to a new method for identifying the singular (cool) parts of the caustic.

Chapter 3 investigates the spontaneous formation of swallowtails on the caustic and Hamilton-Jacobi level surfaces. Using a circle of ideas due to Arnol'd, Cayley and Klein, we find necessary conditions for these swallowtail perestroikas and relate these conditions to the reduced action function.

In Chapter 4 we find an explicit formula for the Maxwell set by considering the double points of the level surfaces in the two dimensional polynomial case. We extend this to higher dimensions using a double discriminant of the reduced action function and then consider the geometric properties of the Maxwell set in terms of the pre-Maxwell set.

We conclude in Chapter 5 by using our earlier work to model turbulence in the Burgers fluid. We show that the number of cusps on the level surfaces can change infinitely rapidly causing 'real turbulence' and also that the number of swallowtails on the caustic can change infinitely rapidly causing 'complex turbulence'. These processes are both inherently stochastic in nature. We determine their intermittence in terms of the recurrent behaviour of two processes derived from the reduced action.

Acknowledgements

Firstly, I would like to thank my supervisor, Professor Aubrey Truman, and my co-supervisor, Dr Ian Davies, for their encouragement, help and guidance over the past three years. Thanks should also go to everyone within the Mathematics Department for making it such a pleasant and rewarding place to complete seven years of study. A special mention should go to Elinor Park, Alexander Potrykus and all my other fellow Ph.D. students for their friendship and support.

I would also like to thank the Engineering and Physical Sciences Research Council (EPSRC) for providing the financial support for my postgraduate studies.

Finally, I wish to thank my parents, especially as they proof read this thesis, and also my sister, Lindsay, who provided encouragement from exotic locations as she travelled around the world.

Chapter 1

Introduction

Summary

We begin with a summary of results on the inviscid limit of the minimal entropy solution to the stochastic Burgers equation. This includes a brief outline of the relationships between the Burgers equation, the heat equation and the Hamilton-Jacobi equation, and the introduction of the classical mechanical flow map derived from the Euler-Lagrange equation. We consider how discontinuities develop in the inviscid limit of the Burgers fluid velocity field and define the caustic, Maxwell set and Hamilton-Jacobi level surface. The main geometrical results of Davies, Truman and Zhao (DTZ) are then outlined and examples given. We show how the method of stationary phase can be used to reduce this d-dimensional problem into a simpler one dimensional problem. The chapter concludes with some results on polynomials which are needed in later sections.

1.1 The inviscid limit of Burgers equation

Burgers equations have been used both in studying turbulence and modelling the large scale structure of the universe [5, 16, 37]. They have also played a part in Arnol'd's pioneering work on caustics and Maslov's seminal works in semiclassical quantum mechanics which inspired much of the early work in this subject [2, 3, 29, 30].

We will consider the stochastic, viscous Burgers equation for the velocity field $v^\mu(x,t) \in \mathbb{R}^d$, where $x \in \mathbb{R}^d$ and $t > 0$,

$$\frac{\partial v^\mu}{\partial t} + (v^\mu \cdot \nabla)\, v^\mu = \frac{\mu^2}{2}\Delta v^\mu - \nabla V(x) - \epsilon \nabla k_t(x) \dot{W}_t, \tag{1.1}$$

with initial condition,

$$v^\mu(x,0) = \nabla S_0(x) + \mathrm{O}(\mu^2).$$

Here $V(x)$ and $k_t(x)$ are two potentials, $\dot{W}_t$ denotes white noise and μ^2 is the coefficient of viscosity which we assume to be small.

We are interested in the advent of discontinuities in the inviscid limit of the velocity field,

$$v^0(x,t) = \lim_{\mu \searrow 0} v^\mu(x,t).$$

Using the Hopf-Cole transformation,

$$v^\mu(x,t) = -\mu^2 \nabla \ln u^\mu(x,t),$$

the stochastic Burgers equation (1.1) is transformed into the Stratonovich heat equation for the scalar temperature $u^\mu(x,t) \in \mathbb{R}$,

$$\frac{\partial u^\mu}{\partial t} = \frac{\mu^2}{2} \Delta u^\mu + \mu^{-2} V(x) u^\mu + \epsilon \mu^{-2} k_t(x) u^\mu \circ \dot{W}_t, \tag{1.2}$$

with initial condition,

$$u^\mu(x,0) = \exp\left(-\frac{S_0(x)}{\mu^2}\right) T_0(x).$$

The convergence factor T_0 is related to the initial Burgers fluid density. Note that the Hopf-Cole transformation has changed the Itô integral in equation (1.1) into a Stratonovich integral in equation (1.2).

Now let,

$$A[X] := \frac{1}{2} \int_0^t \dot{X}^2(s)\,\mathrm{d}s - \int_0^t V(X(s))\,\mathrm{d}s - \epsilon \int_0^t k_s(X(s))\,\mathrm{d}W_s,$$

and select a path X which minimises $A[X]$. This requires,

$$\mathrm{d}\dot{X}(s) + \nabla V(X(s))\,\mathrm{d}s + \epsilon \nabla k_s(X(s))\,\mathrm{d}W_s = 0. \tag{1.3}$$

We then define the stochastic action as,

$$A(X(0),x,t) := \inf_{\substack{X(\cdot) \\ X(t)=x}} A[X].$$

Setting,

$$\mathcal{A}(X(0),x,t) := S_0(X(0)) + A(X(0),x,t),$$

and then minimising $\mathcal{A}(X(0), x, t)$ over $X(0)$ gives,

$$\dot{X}(0) = \nabla S_0(X(0)).$$

Moreover, it follows that,

$$\mathcal{S}_t(x) := \inf_{X(0)} [\mathcal{A}(X(0), x, t)],$$

is the minimal solution of the Hamilton-Jacobi equation,

$$\mathrm{d}\mathcal{S}_t + \left(\frac{1}{2}|\nabla \mathcal{S}_t|^2 + V(x)\right) \mathrm{d}t + \epsilon k_t(x)\, \mathrm{d}W_t = 0, \tag{1.4}$$

where,

$$\mathcal{S}_{t=0}(x) = S_0(x).$$

Following the work of Freidlin et al [20], as $\mu \to 0$,

$$-\mu^2 \ln u^\mu(x,t) \to \inf_{X(0)} [\mathcal{A}(X(0), x, t)] = \mathcal{S}_t(x).$$

This gives the minimal entropy solution of the Burgers equation as $v^0(x,t) = \nabla \mathcal{S}_t(x)$ [11]. We now consider the behaviour of $v^0(x,t)$.

Definition 1.1. *The stochastic wavefront $\mathcal{W}_t$ at time t is given by the level surface,*

$$\mathcal{W}_t = \{x : \quad \mathcal{S}_t(x) = 0\}.$$

For small μ and fixed t, the solution of the Stratonovich heat equation $u^\mu(x,t)$ switches continuously from being exponentially large to exponentially small as x crosses the wavefront $\mathcal{W}_t$. However, when $\mu \to 0$, $u^\mu(x,t)$ and $v^\mu(x,t)$ can also switch discontinuously.

Define the classical mechanical flow map $\Phi_s : \mathbb{R}^d \to \mathbb{R}^d$ by,

$$\mathrm{d}\dot{\Phi}_s + \nabla V(\Phi_s)\, \mathrm{d}s + \epsilon \nabla k_s(\Phi_s)\, \mathrm{d}W_s = 0, \tag{1.5}$$

where,

$$\Phi_0 = \mathrm{id}, \qquad \dot{\Phi}_0 = \nabla S_0.$$

Since $X(t) = x$, it follows that,

$$X(s) = \Phi_s\left(\Phi_t^{-1}(x)\right),$$

where we accept that the inverse image $x_0(x,t) = \Phi_t^{-1}(x)$ is not necessarily unique. Given some regularity and boundedness, the global inverse function theorem gives a caustic time $T(\omega) > 0$ such that for $0 < t < T(\omega)$, Φ_t is a random diffeomorphism [41]. This means that the pre-image $\Phi_t^{-1}(x)$ is unique before the caustic time $T(\omega)$. Moreover, almost surely,

$$v^0(x,t) = \dot{\Phi}_t\left(\Phi_t^{-1}(x)\right),$$

is a classical solution of the stochastic Burgers equation.

The method of characteristics suggests that discontinuities in $v^0(x,t)$ are associated with the non-uniqueness of the real pre-image $x_0(x,t)$. When this occurs, the classical mechanical flow map Φ_t focuses an infinitesimal volume of points $\mathrm{d}x_0$ into a zero volume $\mathrm{d}X(t)$.

Definition 1.2. *The caustic C_t at time t is defined to be the set,*

$$C_t = \left\{x: \quad \det\left(\frac{\partial X(t)}{\partial x_0}\right) = 0\right\}.$$

Before the caustic time (when the pre-image $x_0(x,t)$ is unique) Truman and Zhao [41] demonstrated that the solution to the heat equation can be expressed as,

$$u^\mu(x,t) \sim \theta \exp\left\{-\frac{S_0(x,t)}{\mu^2}\right\}, \tag{1.6}$$

where,

$$S_0(x,t) := \mathcal{A}\left(x_0(x,t),x,t\right) = S_0\left(x_0(x,t)\right) + A\left(x_0(x,t),x,t\right),$$

and θ is an asymptotic series in μ^2 such that for any integer m,

$$\theta = \sum_{j=0}^{m} \mu^{2j} f_j(x,t), \tag{1.7}$$

where each f_j can be found explicitly. Moreover, if y_s^μ is chosen to be the Nelson diffusion process given by,

$$\mathrm{d}y_s^\mu = \mu\,\mathrm{d}B_s - \nabla\sum_{j=0}^{m}\mu^{2j}S_j(y_s^\mu, t-s)\,\mathrm{d}s, \qquad y_0^\mu = x, \qquad y_t^\mu = x_0(x,t),$$

then Hamilton-Jacobi theory gives for each integer m,

$$\begin{aligned} v^\mu(x,t) \quad &= \quad \sum_{j=0}^{m}\mu^{2j}v_j(x,t) - \mu^2\nabla\ln\mathbb{E}\Bigg\{\exp\left(\frac{-\mu^{2m}}{2}\int_0^t \nabla\cdot v_m(y_s^\mu, t-s)\,\mathrm{d}s\right. \\ &\left.\left. +\frac{1}{2}\sum_{j=m+1}^{2m}\mu^{2(j-1)}\sum_{\substack{0\le i_1\le i_2\le m\\ i_1+i_2=j}}\int_0^t v_{i_1}\cdot v_{i_2}(y_s^\mu, t-s)\,\mathrm{d}s\right)\right\}, \end{aligned} \tag{1.8}$$

where $v_j(x,t) = \nabla S_j(x,t)$ and S_j satisfies the Hamilton-Jacobi continuity equations,

$$\frac{\partial S_j}{\partial t} + \frac{1}{2} \sum_{\substack{i_1,i_2\geq 0 \\ i_1+i_2=j}} \nabla S_{i_1} \cdot \nabla S_{i_2} = \frac{1}{2}\Delta S_{j-1},$$

for $j = 0, 1, 2, \ldots$, with the convention $\frac{1}{2}\Delta S_{-1} = -V - \epsilon k_t \dot{W}_t$. As $\mu \sim 0$,

$$v^\mu(x,t) \sim \nabla S_0(x,t) + \mathrm{O}(\mu^2),$$

$S_0(x,t)$ being Hamilton's principal function $\mathcal{S}_t(x)$ as expected.

Now assume that at time t the point x has n real pre-images. That is, let,

$$\Phi_t^{-1}\{x\} = \{x_0(1)(x,t), x_0(2)(x,t), \ldots, x_0(n)(x,t)\},$$

where each $x_0(i)(x,t) \in \mathbb{R}^d$. Assuming none of these pre-images are repeated, the Feynman-Kac formula and Laplace's method in infinite dimensions may be used to show that the solution of the heat equation can again be expressed as an asymptotic series in μ^2 [41]. Thus, in a similar manner to equation (1.6),

$$u^\mu(x,t) \sim \sum_{i=1}^{n} \theta_i \exp\left(-\frac{S_0^i(x,t)}{\mu^2}\right), \tag{1.9}$$

where,

$$S_0^i(x,t) := \mathcal{A}\left(x_0(i)(x,t), x, t\right) = S_0\left(x_0(i)(x,t)\right) + A\left(x_0(i)(x,t), x, t\right),$$

each θ_i being an asymptotic series in μ^2, as in equation (1.7). There is also a series for v^μ in this case; however, unlike equation (1.8), there is no simple form for the remainder term. It is important to note that,

$$\mathcal{S}_t(x) = \min_{i=1,2,\ldots,n} S_0^i(x,t).$$

This leads naturally to the concept of the Hamilton-Jacobi level surfaces.

Definition 1.3. *The Hamilton-Jacobi level surface H_t^c corresponding to the level c, is defined to be the set,*

$$H_t^c = \left\{x : \quad S_0^i(x,t) = c \text{ for some } i\right\}.$$

The zero level surface H_t^0 includes the stochastic wavefront $\mathcal{W}_t$.

As $\mu \to 0$, the dominant term in the asymptotic series for $v^\mu(x,t)$ comes from the minimising $x_0(i)(x,t)$ which we denote $\tilde{x}_0(x,t)$. Assuming $\tilde{x}_0(x,t)$ is unique, we obtain the corresponding inviscid limit of the Burgers fluid velocity as,

$$v^0(x,t) = \dot{\Phi}_t(\tilde{x}_0(x,t)).$$

If the minimiser $\tilde{x}_0(x,t)$ suddenly jumps between two pre-images $x_0(i)(x,t)$ and $x_0(j)(x,t)$, a jump discontinuity will also occur in the inviscid limit of the Burgers velocity field.

There are two ways in which the minimiser $\tilde{x}_0(x,t)$ can change. Firstly, two pre-images can coalesce to form a repeated root which then disappears (becomes complex). As we will show later, this occurs as x crosses the caustic. If one of these pre-images is the minimising $x_0(i)(x,t)$, then $\tilde{x}_0(x,t)$ will jump and the caustic will be described as cool. Alternatively, two pre-images can return the same value of the action. When these pre-images both minimise the action, $\tilde{x}_0(x,t)$ will jump between them. This leads to the following definition.

Definition 1.4. *The Maxwell set M_t is the set,*

$$\begin{aligned} M_t &= \{x : \exists\, x_0, \check{x}_0 \in \mathbb{R}^d \ s.t. \\ &\qquad x = \Phi_t(x_0) = \Phi_t(\check{x}_0),\ x_0 \neq \check{x}_0 \ \text{and}\ \mathcal{A}(x_0,x,t) = \mathcal{A}(\check{x}_0,x,t)\}. \end{aligned}$$

If x is on the Maxwell set, then it has at least two pre-images returning the same value of the action. If these pre-images are also the global minimisers of the action, then v^0 will have a jump discontinuity and the Maxwell set is said to be cool.

We conclude this section with a simple example illustrating a caustic, zero level surface, wavefront and Maxwell set. This also indicates how the number of pre-images for a point x changes by a multiple of two as it crosses the caustic.

Example 1.5 (The generic Cusp). Let $V = 0$, $k_t = 0$ and

$$S_0(x_0,y_0) = x_0^2 y_0/2.$$

This initial condition leads to the generic Cusp, a semicubical parabolic caustic shown in Figure 1.1. The caustic C_t (long dash) is given by,

$$x_t(x_0) = t^2 x_0^3, \qquad y_t(x_0) = \frac{3}{2} t x_0^2 - \frac{1}{t}.$$

The zero level surface H_t^0 (solid line) is,

$$\begin{aligned} x_{(t,0)}(x_0) &= \frac{x_0}{2}\left(1 \pm \sqrt{1 - t^2 x_0^2}\right), \\ y_{(t,0)}(x_0) &= \frac{1}{2t}\left(t^2 x_0^2 - 1 \pm \sqrt{1 - t^2 x_0^2}\right). \end{aligned}$$

Finally, the Maxwell set is,

$$x = 0 \quad \text{for} \quad y > -\frac{1}{t}.$$

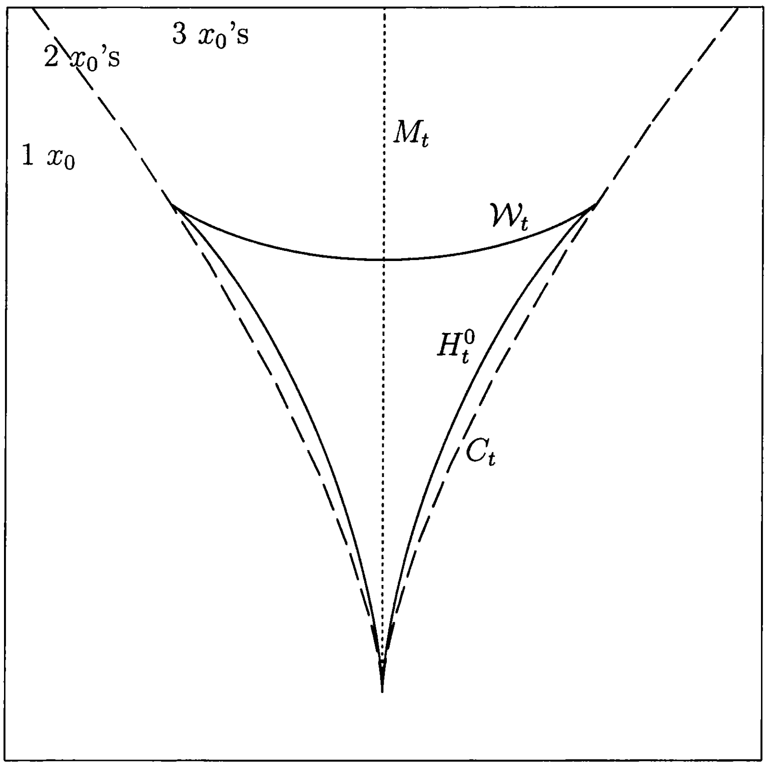

Figure 1.1: The cusp caustic (long dash), tricorn zero level surface (solid) and Maxwell set (dotted) for the generic Cusp.

1.2 Notation

Throughout this thesis $x, x_0, x_t, x_{(t,c)}$ etc will denote vectors for which normally $x = \Phi_t(x_0)$. Cartesian coordinates of these vectors will be indicated using a sub/superscript where relevant; thus $x = (x_1, x_2, \ldots, x_d)$, $x_0 = (x_0^1, x_0^2, \ldots, x_0^d)$ etc. The only exception will be in the discussion of explicit examples in two and three dimensions when we will use (x, y) and (x_0, y_0) etc to denote the vectors.

1.3 Geometrical results

We now summarise the geometrical relationships between the Hamilton-Jacobi level surfaces and the caustic as established by DTZ [12].

Consider the deterministic case where $\epsilon = 0$, $t > 0$ and $x, x_0 \in \mathbb{R}^d$ are given by $x_0 = (x_0^1, x_0^2, \ldots, x_0^d)$ and $x = (x_1, x_2, \ldots, x_d)$. Then,

$$\mathcal{A}(x_0, x, t) = S_0(x_0) + A(x_0, x, t),$$

where

$$A(x_0, x, t) = \inf_{\substack{X(0)=x_0 \\ X(t)=x}} \left[\int_0^t \left\{ \frac{1}{2}\dot{X}(s)^2 \text{-} V(X(s)) \right\} \mathrm{d}s \right].$$

The corresponding Euler-Lagrange equation (1.3) is,

$$\ddot{X}(s) = -\nabla V(X(s)) \quad \text{for } s \in [0, t],$$

where,

$$X(t) = x, \qquad X(0) = x_0.$$

This is greatly simplified by considering the free case ($V = 0$) so that,

$$\mathcal{A}(x_0, x, t) = \frac{(x - x_0)^2}{2t} + S_0(x_0). \tag{1.10}$$

Assuming that $\mathcal{A}(x_0, x, t)$ is C^4 in space variables for times $t > 0$, this gives,

$$\frac{\partial \mathcal{A}}{\partial x_0^\alpha} = 0, \quad \alpha = 1, 2, \ldots, d \qquad \Leftrightarrow \qquad x = \Phi_t(x_0) = x_0 + t\nabla S_0(x_0). \tag{1.11}$$

We will see that equation (1.11) is true in enormous generality.

The Hamilton-Jacobi level surface H_t^c is obtained by eliminating x_0 between,

$$\mathcal{A}(x_0, x, t) = c \qquad \text{and} \qquad \frac{\partial \mathcal{A}}{\partial x_0^\alpha}(x_0, x, t) = 0, \tag{1.12}$$

for $\alpha = 1, 2, \ldots, d$. Alternatively, eliminating x gives the pre-level surface $\Phi_t^{-1} H_t^c$. Similarly, the caustic C_t (and pre-caustic $\Phi_t^{-1} C_t$) are obtained by eliminating x_0 (or x) between,

$$\det \left(\frac{\partial^2 \mathcal{A}}{\partial x_0^\alpha \partial x_0^\beta}(x_0, x, t) \right)_{\alpha,\beta=1,2,\ldots,d} = 0 \qquad \text{and} \qquad \frac{\partial \mathcal{A}}{\partial x_0^\alpha}(x_0, x, t) = 0, \tag{1.13}$$

for $\alpha = 1, 2, \ldots, d$. These pre-surfaces are the algebraic inverses of C_t and H_t^c which are not necessarily the same as their topological inverses. This distinction is of fundamental importance.

In the free case, the equation for the zero pre-level surface is the eikonal equation,

$$\frac{t}{2}\left|\nabla S_0(x_0)\right|^2 + S_0(x_0) = 0,$$

and the derivative map $D\Phi_t(x_0)$ is given by the Hessian,

$$D\Phi_t(x_0) = I + t\nabla^2 S_0(x_0). \tag{1.14}$$

These, together with the key identity,

$$\nabla_{x_0}\left\{\frac{t}{2}\left|\nabla S_0(x_0)\right|^2 + S_0(x_0)\right\} = \left(1 + t\nabla^2 S_0(x_0)\right)\nabla S_0(x_0), \tag{1.15}$$

give the following results in two dimensions.

Definition 1.6. *A curve $x = x(\gamma)$, $\gamma \in N(\gamma_0, \delta)$, is said to have a generalised cusp at $\gamma = \gamma_0$, γ being an intrinsic variable such as arc length, if*

$$\left.\frac{\mathrm{d}x}{\mathrm{d}\gamma}\right|_{\gamma=\gamma_0} = 0.$$

Lemma 1.7 (2-dim free case). *Assume the pre-level surface meets the pre-caustic at x_0 where,*

$$\left|\left(I + t\nabla^2 S_0(x_0)\right)\nabla S_0(x_0)\right| \neq 0 \text{ and } \dim\left(\ker\left(I + t\nabla^2 S_0(x_0)\right)\right) = 1.$$

Then T_{x_0}, the tangent plane to the pre-level surface, is spanned by,

$$\ker\left(I + t\nabla^2 S_0(x_0)\right).$$

Proposition 1.8 (2-dim free case). *Assume that,*

$$\left|\left(I + t\nabla^2 S_0(x_0)\right)\nabla S_0(x_0)\right| \neq 0,$$

so that x_0 is not a singular point of $\Phi_t^{-1}H_t^c$, then $\Phi_t(x_0)$ can only be a generalised cusp if $\Phi_t(x_0) \in C_t$, the caustic. Moreover, if

$$x = \Phi_t(x_0) \in \Phi_t\left(\Phi_t^{-1}C_t \cap \Phi_t^{-1}H_t^c\right),$$

x will indeed be a generalised cusp of the level surface.

These results are best understood by considering Example 1.5 (the generic Cusp) in more detail. Figure 1.2 shows that a point lying inside the semicubical parabolic caustic is on three different level surfaces and has three distinct real pre-images each lying on a separate pre-level surface. A cusp only occurs on a

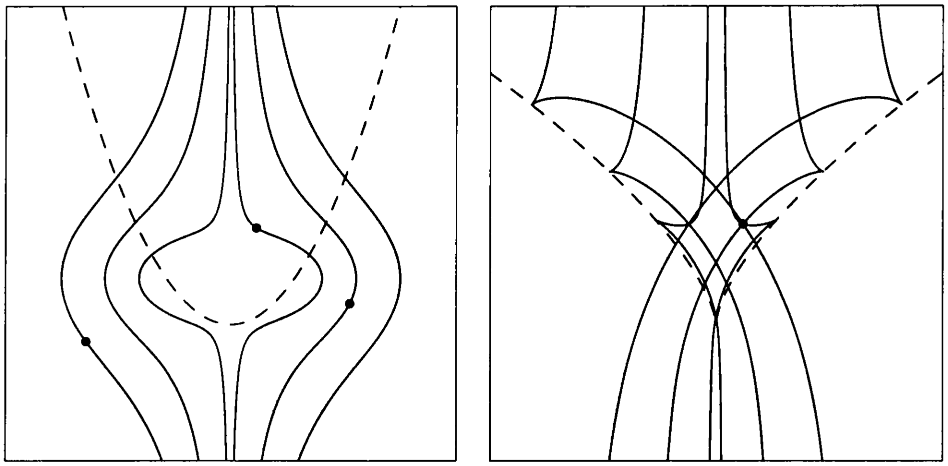

Figure 1.2: The caustic (dashed) and level surfaces ($c > 0$) (solid) and their pre-images for the generic Cusp.

level surface when its corresponding pre-level surface intersects the pre-caustic. Thus, if the normal to the pre-level surface is well defined and non zero, a level surface can only have a cusp on the caustic. However, a level surface does not have to be cusped at every point of intersection it has with the caustic.

These results can be generalised to d-dimensions and also to systems with deterministic and noisy potentials. Let the stochastic action be defined by,

$$A(x_0, p_0, t) := \frac{1}{2}\int_0^t \dot{X}(s)^2 \, \mathrm{d}s - \int_0^t \Big[V(X(s)) \, \mathrm{d}s + \epsilon k_s(X(s)) \, \mathrm{d}W_s \Big], \quad (1.16)$$

where $X(s) = X(s, x_0, p_0) \in \mathbb{R}^d$. The Euler-Lagrange equation (1.3) again holds so that,

$$\mathrm{d}\dot{X}(s) = -\nabla V(X(s)) \, \mathrm{d}s - \epsilon \nabla k_s(X(s)) \, \mathrm{d}W_s, \qquad s \in [0, t],$$

with $X(0) = x_0$, $\dot{X}(0) = p_0$ and $x_0, p_0 \in \mathbb{R}^d$. We assume that X_s is $\mathcal{F}_s$ measurable and unique. If $\mathrm{d}u_s \, \mathrm{d}\dot{X}(s) = 0$ then,

$$\int_0^t u(s) \, \mathrm{d}\dot{X}(s) = u(t)\dot{X}(t) - u(0)\dot{X}(0) - \int_0^t \dot{u}(s)\dot{X}(s) \, \mathrm{d}s.$$

In particular, this holds when $u_s = \frac{\partial X_s}{\partial x_0^\alpha}$ where $\alpha = 1, 2 \ldots, d$. Using Kunita [28], mild regularity gives,

$$\frac{\mathrm{d}}{\mathrm{d}s}\left(\frac{\partial X_s}{\partial x_0^\alpha}\right) = \frac{\partial \dot{X}_s}{\partial x_0^\alpha} \qquad \alpha = 1, 2, \ldots, d,$$

almost surely.

Lemma 1.9 (*d* **dims**). *Assume $S_0, V \in C^2$ and $k_t \in C^{2,0}$, $\nabla V, \nabla k_t$ Lipschitz with Hessians $\nabla^2 V, \nabla^2 k_t$ and all second derivatives with respect to space variables of V and k_t bounded. Then for p_0, possibly x_0 dependent,*

$$\frac{\partial A}{\partial x_0^\alpha}(x_0, p_0, t) = \dot{X}(t) \cdot \frac{\partial X(t)}{\partial x_0^\alpha} - \dot{X}_\alpha(0), \qquad \alpha = 1, 2, \ldots, d.$$

This lemma is used to establish the stochastic mechanical flow map. Let

$$A(x_0, x, t) = A(x_0, p_0, t)|_{p_0 = p_0(x_0, x, t)}$$

where $p_0(x_0, x, t)$ is the random minimiser (assumed unique) of $A(x_0, p_0, t)$ when $X(t, x_0, p_0) = x$. For the existence of $p_0(x_0, x, t)$, we require the map $p_0 \mapsto X(t, x_0, p_0)$ where $X(t, x_0, p_0) \in \mathbb{R}^d$ to be onto for all x_0. This is guaranteed for small values of t by methods of Kolokoltsov et al [26].

Theorem 1.10 (*d* **dims**). *Let the stochastic flow map be denoted by Φ_t. Then $\Phi_t(x_0) = x$ is equivalent to,*

$$\frac{\partial}{\partial x_0^\alpha}\left[S_0(x_0) + A(x_0, x, t)\right] = 0, \qquad \alpha = 1, 2, \ldots, d.$$

We now define the stochastic action corresponding to the initial momentum $\nabla S_0(x_0)$ by,

$$\mathcal{A}(x_0, x, t) := A(x_0, x, t) + S_0(x_0).$$

Assume that $\mathcal{A}(x_0, x, t)$ is C^4 in space variables with $\det\left(\frac{\partial^2 \mathcal{A}}{\partial x_0^\alpha \partial x^\beta}\right) \neq 0$.

Proposition 1.11 (*d* **dims**). *Almost surely, the random classical flow map has Frechet derivative,*

$$\left(D\Phi_t\right)(x_0) = \left(-\frac{\partial^2 \mathcal{A}}{\partial x \partial x_0}\right)^{-1} \left(\frac{\partial^2 \mathcal{A}}{(\partial x_0)^2}(x_0, x, t)\right),$$

and the normal to the pre-level surface is,

$$n(x_0) = -\left(\frac{\partial^2 \mathcal{A}}{(\partial x_0)^2}\right)\left(\frac{\partial^2 \mathcal{A}}{\partial x_0 \partial x}\right)^{-1} \dot{X}\left(t, x_0, \nabla S_0(x_0)\right).$$

This proposition provides direct generalisations of equations (1.14) and (1.15) from the free case.

Corollary 1.12 (2 dims). *Let the pre-level surface meet the pre-caustic at a point x_0, where $n(x_0) \neq 0$ and*

$$\ker\left(\frac{\partial^2 \mathcal{A}}{(\partial x_0)^2}(x_0, \Phi_t(x_0), t)\right) = \langle e_0 \rangle,$$

e_0 being the zero eigenvector. Then T_{x_0}, the tangent plane to the pre-level surface at x_0, is spanned by e_0.

Proposition 1.13 (2 dims). *Assume that at $x_0 \in \Phi_t^{-1} H_t^c$ the above normal is non zero so that the pre-level surface does not have a generalised cusp at x_0. Then the level surface can only have a generalised cusp at $\Phi_t(x_0)$ if $\Phi_t(x_0) \in C_t$, the caustic surface. Moreover, if*

$$x = \Phi_t(x_0) \in \Phi_t \left\{\Phi_t^{-1} C_t \cap \Phi_t^{-1} H_t^c\right\},$$

the level surface will have a generalised cusp at x.

Finally, we quote the following result for the three dimensional case to illustrate how these ideas can be extended to higher dimensions.

Theorem 1.14 (3 dims). *Let,*

$$x \in Cusp\,(H_t^c) = \left\{x \in \Phi_t\left(\Phi_t^{-1} C_t \cap \Phi_t^{-1} H_t^c\right), \quad x = \Phi_t(x_0), \quad n(x_0) \neq 0\right\}.$$

Then, in 3 dimensions in the stochastic case with probability one, T_x, the tangent space to the level surface at x, is at most one dimensional.

1.4 The method of stationary phase

In this section we consider the asymptotic behaviour of the integral,

$$I(\mu) = \int_\Omega T_0(x_0) \exp\left\{-\frac{\mathrm{i}}{\mu^2} F(x_0)\right\} \mathrm{d}x_0, \tag{1.17}$$

as $\mu \to 0$, where $\Omega \subset \mathbb{R}$ is some bounded set with $T_0 \in C_0^\infty(\Omega)$ and $F \in C^\infty(\Omega)$. Such integrals play an important role in establishing the one dimensional analysis that we use in this thesis. All the results in this section are stated without proofs; these may be found in any standard text on the subject [17, 29].

Begin by considering the one dimensional case where $F(x_0)$ has no critical points in the interval $\Omega = [a, b]$. Then,

$$I(\mu) \;=\; \int_a^b T_0(x_0) \exp\left\{-\frac{\mathrm{i}}{\mu^2} F(x_0)\right\} \mathrm{d}x_0$$

$$= -\int_a^b \frac{\mathrm{i}}{\mu^2} F'(x_0) \frac{T_0(x_0)}{-\frac{\mathrm{i}}{\mu^2} F'(x_0)} \exp\left\{-\frac{\mathrm{i}}{\mu^2} F(x_0)\right\} \mathrm{d}x_0$$

$$= -\int_a^b \frac{\mathrm{d}}{\mathrm{d}x_0} \left(\frac{T_0(x_0)}{-\frac{\mathrm{i}}{\mu^2} F'(x_0)}\right) \exp\left\{-\frac{\mathrm{i}}{\mu^2} F(x_0)\right\} \mathrm{d}x_0.$$

If we define,

$$S(x_0) = \frac{\mathrm{d}}{\mathrm{d}x_0} \left(\frac{T_0(x_0)}{-\mathrm{i}F'(x_0)}\right),$$

then,

$$I(\mu) = -\mu^2 \int_a^b S(x_0) \exp\left\{-\frac{\mathrm{i}}{\mu^2} F(x_0)\right\} \mathrm{d}x_0.$$

This process can be repeated and after N repetitions $I(\mu) \sim \mathrm{O}(\mu^{2N})$. Therefore,

$$I(\mu) \sim \mathrm{O}(\mu^{\infty}) \quad \text{as} \quad \mu \to 0.$$

Thus, the main contribution to $I(\mu)$ as $\mu \to 0$ must come from the critical points of F. Intuitively, the exponential term in the integrand is oscillating rapidly whilst T_0 is oscillating slowly and cancelling out the integrand. It is only when the oscillation of the exponential slows at a critical point of F that there is a contribution to the value of the integral.

Assuming the critical points are isolated, it is sufficient to determine the behaviour of the integral given the existence of a single critical point.

Theorem 1.15. *Let $T_0 \in C_0^{\infty}[a,b]$ and $F \in C^{\infty}[a,b]$ where F is real valued. Furthermore, let F have a unique critical point in $[a,b]$ at $\tilde{x}_0$ and let that critical point be non-degenerate. That is, there exists $\tilde{x}_0 \in [a,b]$ such that $F'(\tilde{x}_0) = 0$, $F''(\tilde{x}_0) \neq 0$ and $F'(x_0) \neq 0$ for all $x_0 \neq \tilde{x}_0$ with $x_0 \in [a,b]$. Then,*

$$I(\mu) = \exp\left\{-\frac{\mathrm{i}}{\mu^2} F(\tilde{x}_0)\right\} \sum_{j=0}^{k-1} a_j(T_0, F)\mu^{2j+1} + R_k(\mu),$$

where,

$$a_j(T_0,F) = \frac{\Gamma(j+\frac{1}{2})}{(2j)!} \exp\left\{-\frac{\mathrm{i}\pi\sigma}{4}(2j+1)\right\} \left(\frac{\mathrm{d}}{\mathrm{d}x_0}\right)^{2j} \left[h(x_0)^{-\frac{2j+1}{2}} T_0(x_0)\right]_{x_0=\tilde{x}_0}$$

and

$$h(x_0) = 2\sqrt{\sigma(F(x_0) - F(\tilde{x}_0))}(x_0 - \tilde{x}_0)^{-1}, \qquad \sigma = \operatorname{sgn} F''(\tilde{x}_0).$$

Moreover, for $\mu^2 < 1$ there exists a constant $c_k \in \mathbb{R}$ such that,

$$R_k(\mu) \leq c_k \mu^{2k} ||T_0||_{C^{k+1}[a,b]}.$$

By considering the first term in this series, we obtain the following corollary.

Corollary 1.16. *Under the conditions of Theorem 1.15, as* $\mu \to 0$,

$$I(\mu) \sim \left(\frac{2\pi\mu^2}{|F''(\tilde{x}_0)|}\right)^{\frac{1}{2}} T_0(\tilde{x}_0) \exp\left\{-\frac{\mathrm{i}}{\mu^2}F(\tilde{x}_0) - \frac{\mathrm{i}\pi\sigma}{4}\right\},$$

to first order in μ.

The n-dimensional case may be broken down using the Morse lemma. This allows F to be broken into a sum of squares in some neighbourhood of its critical point. We can then apply the one dimensional formula from Corollary 1.16 successively to each variable in turn. This leads to the following theorem taken from [17].

Theorem 1.17. *Let* $\Omega \subset \mathbb{R}^n$ *be a bounded domain,* $T_0 \in C_0^\infty(\Omega)$ *and* $F \in C^\infty(\Omega)$ *where* F *is real valued. Furthermore, let* F *have a unique critical point in* Ω *at* $\tilde{x}_0$ *and let that critical point be non-degenerate. That is, there exists* $\tilde{x}_0 \in \Omega$ *such that* $\nabla F(\tilde{x}_0) = 0$, $\det(F''(\tilde{x}_0)) \neq 0$ *and* $\nabla F(x_0) \neq 0$ *for all* $x_0 \neq \tilde{x}_0$ *with* $x_0 \in \Omega$. *Then,*

$$I(\mu) \sim (2\pi\mu^2)^{\frac{n}{2}} \left|\det(F''(\tilde{x}_0))\right|^{-\frac{1}{2}} T_0(\tilde{x}_0) \exp\left\{-\frac{\mathrm{i}}{\mu^2}F(\tilde{x}_0) - \frac{\mathrm{i}\pi\Sigma}{4}\right\},$$

where F'' *is the Hessian of* F *and* Σ *is the signature of the quadratic form with the matrix* F.

1.5 The reduced action function

We now outline a one dimensional analysis first investigated by Reynolds, Truman and Williams (RTW) [35] which allows us to simplify the analysis of the stochastic Burgers equation. Using these ideas, we can consider the degeneracy that occurs from the non-uniqueness of x_0 by only considering one component of the vector x_0.

Definition 1.18. *The* d*-dimensional classical flow map* Φ_t *is globally reducible if, for any* $x = (x_1, x_2, \ldots, x_d)$ *and* $x_0 = (x_0^1, x_0^2, \ldots, x_0^d)$ *where* $x = \Phi_t(x_0)$, *it is possible to write each coordinate* x_0^α *as a function of the lower coordinates. That is,*

$$x = \Phi_t(x_0) \qquad \Rightarrow \qquad x_0^\alpha = x_0^\alpha(x, x_0^1, x_0^2, \ldots x_0^{\alpha-1}, t), \tag{1.18}$$

for $\alpha = d, d-1, \ldots, 2$.

Therefore, using Theorem 1.10, the flow map is globally reducible if we can find a chain of C^2 functions $x_0^d, x_0^{d-1}, \ldots, x_0^2$ such that,

$$\begin{aligned}
x_0^d = x_0^d(x, x_0^1, x_0^2, \ldots x_0^{d-1}, t) &\Leftrightarrow \frac{\partial \mathcal{A}}{\partial x_0^d}(x_0, x, t) = 0,\\
x_0^{d-1} = x_0^{d-1}(x, x_0^1, x_0^2, \ldots x_0^{d-2}, t) &\Leftrightarrow \frac{\partial \mathcal{A}}{\partial x_0^{d-1}}(x_0^1, x_0^2, \ldots, x_0^d(\ldots), x, t) = 0,\\
&\vdots\\
x_0^2 = x_0^2(x, x_0^1, t) &\Leftrightarrow\\
&\frac{\partial \mathcal{A}}{\partial x_0^2}(x_0^1, x_0^2, x_0^3(x, x_0^1, x_0^2, t), \ldots, x_0^d(\ldots), x, t) = 0,
\end{aligned}$$

where $x_0^d(\ldots)$ is the expression gained by substituting each of the appropriate functions $x_0^{d-1}, x_0^{d-2}, \ldots,$ repeatedly into $x_0^d(x, x_0^1, x_0^2, \ldots, x_0^{d-1}, t)$. This requires that no roots are repeated to ensure that none of the second derivatives of $\mathcal{A}$ vanish. We assume also that there is a favoured ordering of coordinates and a corresponding decomposition of Φ_t which allows the non-uniqueness to be reduced to the level of the x_0^1 coordinate.

This assumption appears to be quite restrictive. However, for some local reducibility at x, we only require there to be at most one integer α with $1 \leq \alpha \leq d$ such that,

$$\frac{\partial \mathcal{A}}{\partial x_0^\alpha} = \frac{\partial^2 \mathcal{A}}{(\partial x_0^\alpha)^2} = 0 \qquad \text{when} \qquad \nabla_{x_0} \mathcal{A} = 0.$$

This allows us to apply the ideas of reducibility to a large class of problems.

Definition 1.19. *Assume Φ_t is globally reducible. Then the reduced action function is the univariate function gained from evaluating the action with the equations (1.18). That is,*

$$f_{(x,t)}(x_0^1) := f(x_0^1, x, t) = \mathcal{A}(x_0^1, x_0^2(x, x_0^1, t), x_0^3(\ldots), \ldots, x, t).$$

Before we introduce the main properties of the reduced action we need the following lemma of RTW.

Lemma 1.20. *If Φ_t is globally reducible, modulo the above assumptions,*

$$\begin{aligned}
&\left| \det\left(\frac{\partial^2 \mathcal{A}}{(\partial x_0)^2}(x_0, x, t) \right)\Big|_{x_0 = (x_0^1, x_0^2(x, x_0^1, t), \ldots, x_0^d(\ldots))} \right|\\
&= \prod_{\alpha=1}^{d} \left| \left[\left(\frac{\partial}{\partial x_0^\alpha} \right)^2 \mathcal{A}(x_0^1, \ldots, x_0^\alpha, x_0^{\alpha+1}(\ldots), \ldots, x_0^d(\ldots), x, t) \right]_{\substack{x_0^2 = x_0^2(x, x_0^1, t)\\ \vdots \\ x_0^\alpha = x_0^\alpha(\ldots)}} \right|
\end{aligned}$$

where the first term is $f''_{(x,t)}(x_0^1)$ and the last $d-1$ terms are non zero.

Proof. We consider the asymptotic behaviour of the integral,

$$I(\mu) = \int_{\mathbb{R}^d} T_0(x_0) \exp\left(-\frac{\mathrm{i}}{\mu^2}\mathcal{A}(x_0, x, t)\right) \mathrm{d}x_0.$$

Firstly, we apply the principle of stationary phase to the integral,

$$\begin{aligned} I(\mu) \sim\ & \left(2\pi\mu^2\right)^{\frac{1}{2}} \exp\left\{-\frac{\mathrm{i}\pi\sigma_d}{4}\right\} \int \mathrm{d}x_0^1 \ldots \int \mathrm{d}x_0^{d-1} \\ & \left[T_0(x_0) \left(\frac{\partial^2 \mathcal{A}}{\left(\partial x_0^d\right)^2}\right)^{-\frac{1}{2}} \exp\left\{-\frac{\mathrm{i}}{\mu^2}\mathcal{A}(x_0, x, t)\right\}\right]_{x_0^d = x_0^d\left(x, x_0^1, \ldots x_0^{d-1}, t\right)}. \end{aligned}$$

Repeating this $(d-1)$ times gives,

$$\begin{aligned} I(\mu) \sim\ & \left(2\pi\mu^2\right)^{\frac{d-1}{2}} \exp\left\{-\sum_{k=2}^{d} \frac{\mathrm{i}\pi\sigma_k}{4}\right\} \int \mathrm{d}x_0^1 \\ & \left[T_0(x_0) \left(\prod_{k=2}^{d} \frac{\partial^2 \mathcal{A}}{\left(\partial x_0^k\right)^2}\right)^{-\frac{1}{2}} \exp\left\{-\frac{\mathrm{i}}{\mu^2} f_{(x,t)}(x_0^1)\right\}\right]_{\substack{x_0^d = x_0^d\left(x, x_0^1, \ldots x_0^{d-1}, t\right) \\ \vdots \\ x_0^2 = x_0^2\left(x, x_0^1, t\right)}} \end{aligned}$$

where,

$$\sigma_k = \operatorname{sgn}\left[\frac{\partial^2 \mathcal{A}}{\left(\partial x_0^k\right)^2}\right]_{\substack{x_0^d = x_0^d\left(x, x_0^1, \ldots x_0^{d-1}, t\right) \\ \vdots \\ x_0^k = x_0^k\left(x, x_0^1, \ldots x_0^{k-1}, t\right)}}.$$

Alternatively, we can expand the integrand using Taylor's theorem and diagonalise the leading term in the exponential giving a product of Gaussian integrals. Thus we gain an alternative expansion of $I(\mu)$. The result follows by comparing the leading terms in these asymptotic expansions. □

We can also express this factorisation using the initial momentum of the system.

Lemma 1.21. *Assuming that the conditions of Lemma 1.10 are satisfied,*

$$\frac{\partial \mathcal{A}}{\partial x_0^\alpha} = -p_0^\alpha(x_0, x, t) + \frac{\partial S_0}{\partial x_0^\alpha}(x_0),$$

where p_0^α denotes the α coordinate of the initial momentum.

Proof. If we fix $X(t) = x$, then the result follows from Lemma 1.9 where,

$$\dot{X}_\alpha(0) = p_0^\alpha(x_0, x, t).$$

□

The factorisation in Lemma 1.20 can then be written in terms of the reduced initial momenta,

$$\left|\det\left(\frac{\partial^2 \mathcal{A}}{(\partial x_0)^2}(x_0, x, t)\right)\Big|_{x_0=(x_0^1, x_0^2(x, x_0^1, t), \ldots, x_0^d(\ldots))}\right|$$

$$= \prod_{\alpha=1}^{d}\left|\frac{\partial}{\partial x_0^\alpha}\left(\left[p_0^\alpha(x_0, x, t) + \frac{\partial S_0}{\partial x_0^\alpha}(x_0)\right]_{\substack{x_0^{\alpha+1}=x_0^{\alpha+1}(\ldots)\\ \vdots \\ x_0^d = x_0^d(\ldots)}}\right)_{\substack{x_0^2=x_0^2(x,x_0^1,t)\\ \vdots \\ x_0^\alpha=x_0^\alpha(\ldots)}}\right|.$$

Lemma 1.20 also leads to the following important theorem.

Theorem 1.22. *Let the classical mechanical flow map Φ_t be globally reducible. Then:*

1. $\frac{\partial f_{(x,t)}}{\partial x_0^1}(x_0^1) = 0$ *and the equations (1.18)* $\Leftrightarrow x = \Phi_t x_0$,
2. $\frac{\partial f_{(x,t)}}{\partial x_0^1}(x_0^1) = \frac{\partial^2 f_{(x,t)}}{(\partial x_0^1)^2}(x_0^1) = 0$ *and the equations (1.18)* $\Leftrightarrow x = \Phi_t x_0$ *is such that the number of real solutions x_0 of this equation changes.*

If $x_0(i)(x,t)$ denotes the real pre-images of x as in Section 1.1, then

$$\begin{aligned} x_0(i)(x,t) : &= \left(x_0^1(i)(x,t), x_0^2(i)(x,t), \ldots, x_0^d(i)(x,t)\right) \\ &= \left(x_0^1(i)(x,t), x_0^2(x, x_0^1(i)(x,t), t), \ldots, x_0^d(x, x_0^1(i)(x,t), \ldots, t)\right), \end{aligned}$$

where $x_0^1(i)(x,t)$ is then an enumeration of the real roots x_0^1 of $f'_{(x,t)}(x_0^1) = 0$.

The reduced action function allows us to perform a one dimensional analysis on many aspects of the stochastic Burgers equation. For instance, the caustic surface can be found by eliminating the x_0^1 variable between,

$$f'_{(x,t)}(x_0^1) = 0 \qquad \text{and} \qquad f''_{(x,t)}(x_0^1) = 0. \tag{1.19}$$

This allows us to view the caustic as the bifurcation set of the univariate function f [21]. The level surfaces can be found by eliminating x_0^1 between,

$$f_{(x,t)}(x_0^1) = c \qquad \text{and} \qquad f'_{(x,t)}(x_0^1) = 0. \tag{1.20}$$

For polynomial f, these eliminations can be made by taking resultants with respect to x_0^1, as will be outlined in Section 1.6.

1.6 Some results on polynomials

We now outline a selection of results on the roots of polynomials which will be needed later in this thesis. We begin with the concept of resultants which allows us to analyse when a pair of polynomials have a common root. This leads to the definition of the discriminant of a polynomial which provides a condition for a polynomial to have a repeated root. We conclude with a collection of results on the exact number of real roots of a polynomial. All of the results can be found in Burnside and Panton [6], although we also give other specific references.

We begin by considering two arbitrary real polynomials $f(x)$ and $g(x)$. Let,

$$f(x) = a_0 \prod_{i=1}^{m} (x - \alpha_i) \quad \text{and} \quad g(x) = b_0 \prod_{i=1}^{n} (x - \beta_i),$$

so that $f(x)$ is a polynomial of degree m with leading coefficient a_0 and roots α_i and $g(x)$ is a polynomial of degree n with leading coefficient b_0 and roots β_i. These polynomials have a common root if and only if one of $g(\alpha_1), g(\alpha_2), \ldots, g(\alpha_m)$ is zero. Clearly, if this holds then,

$$\prod_{i=1}^{m} g(\alpha_i) = b_0^m \prod_{i=1}^{m} \prod_{j=1}^{n} (\alpha_i - \beta_j) = 0.$$

Similarly, there will be a common root if and only if,

$$\prod_{i=1}^{n} f(\beta_i) = a_0^n \prod_{i=1}^{n} \prod_{j=1}^{m} (\beta_i - \alpha_j) = 0.$$

This leads naturally to the following definition.

Definition 1.23. *Let $f(x)$ be a polynomial of degree m with roots $\alpha_1, \alpha_2, \ldots,$ α_m and leading coefficient a_0 and $g(x)$ be a polynomial of degree n with roots $\beta_1, \beta_2, \ldots, \beta_n$ and leading coefficient b_0. Then the resultant of $f(x)$ and $g(x)$ with respect to x is,*

$$R_x(f(x), g(x)) := a_0^n b_0^m \prod_{i=1}^{n} \prod_{j=1}^{m} (\beta_i - \alpha_j).$$

Lemma 1.24. *Let $f(x)$ be a polynomial of degree m with roots $\alpha_1, \alpha_2, \ldots,$ α_m and leading coefficient a_0 and $g(x)$ be a polynomial of degree n with roots $\beta_1, \beta_2, \ldots, \beta_n$ and leading coefficient b_0. Then,*

$$R_x(f(x), g(x)) = (-1)^{mn} b_0^m \prod_{i=1}^{n} f(\beta_i) = a_0^n \prod_{j=1}^{m} g(\alpha_j).$$

Lemma 1.25. *Let $f(x)$ and $g(x)$ be two polynomials with leading coefficients a_0 and b_0 respectively. Assuming that $a_0 \neq 0$ and $b_0 \neq 0$, then $f(x)$ and $g(x)$ have a common root if and only if $R_x(f(x), g(x)) = 0$.*

Lemma 1.24 provides an interesting symmetry property for resultants. However, calculating a resultant using either Definition 1.23 or Lemma 1.24 is impractical as this involves finding all of the roots of at least one of the polynomials. Instead, we use the following method of elimination due to Euler and Sylvester.

Lemma 1.26. *Let,*

$$f(x) = a_0x^m + a_1x^{m-1} + \ldots + a_{m-1}x + a_m$$

and

$$g(x) = b_0x^n + b_1x^{n-1} + \ldots + b_{n-1}x + b_n,$$

be real polynomials. Then the resultant of $f(x)$ and $g(x)$ is the determinant of the $(n+m) \times (n+m)$ Sylvester matrix,

$$R_x(f(x), g(x)) = \begin{vmatrix} a_0 & a_1 & a_2 & \ldots & a_m & 0 & 0 & \ldots & 0 \\ 0 & a_0 & a_1 & \ldots & a_{m-1} & a_m & 0 & \ldots & 0 \\ 0 & 0 & \ddots & \ddots & \ddots & \ddots & \ddots & \ddots & 0 \\ 0 & 0 & \ldots & \ldots & \ldots & \ldots & \ldots & \ldots & a_m \\ b_0 & b_1 & b_2 & \ldots & b_n & 0 & 0 & \ldots & 0 \\ 0 & b_0 & b_1 & \ldots & b_{n-1} & b_n & 0 & \ldots & 0 \\ 0 & 0 & \ddots & \ddots & \ddots & \ddots & \ddots & \ddots & 0 \\ 0 & 0 & \ldots & \ldots & \ldots & \ldots & \ldots & \ldots & b_n \end{vmatrix}.$$

Alternatively, the resultant can be calculated using an algorithm derived by Pohst and Zassenhaus [32].

If the polynomial $f(x)$ has a repeated root α_i then,

$$f(\alpha_i) = f'(\alpha_i) = 0.$$

This leads to the definition of the discriminant of the polynomial $f(x)$ in terms of the resultant of $f(x)$ and its derivative $f'(x)$.

Definition 1.27. *The discriminant of a polynomial $f(x)$ with leading coefficient a_0 is the resultant,*

$$D_x(f(x)) := \frac{1}{a_0} R_x(f(x), f'(x)).$$

Lemma 1.28. *Let $f(x)$ be a polynomial of degree m with roots $\alpha_1, \alpha_2, \ldots, \alpha_m$ and leading coefficient a_0. Then the discriminant of f is,*

$$D_x(f(x)) = a_0^{2m-2} \prod_{i<k} (\alpha_i - \alpha_k)^2.$$

Lemma 1.29. *Let $f(x)$ be a polynomial with leading coefficient a_0. Assuming that $a_0 \neq 0$, then $f(x)$ has a repeated root if and only if,*

$$D_x(f(x)) = 0.$$

A concise account of the complete relationships between resultants and discriminants and their inherent symmetry properties can be found in Van Der Waerden [42].

There are well known explicit forms for the discriminant for the cubic and quartic cases. Moreover, in these cases the discriminant reveals the exact number of real roots. The following two results are taken from Ferrar [18].

Theorem 1.30 (Cubics). *Let $f(x) = \alpha x^3 + 3\beta x^2 + 3\gamma x + \delta$ be a real cubic polynomial in x. Then the polynomial can be reduced by the substitution $z = \alpha x + \beta$ to,*

$$f_0(z) = z^3 + Hz + G,$$

and the discriminant of the cubic is then given by,

$$D_x(f(x)) = -\frac{27G^2 + 4H^3}{\alpha^2}.$$

Moreover, if the discriminant of a cubic is positive, the cubic has three distinct real roots; if it is zero, it has three real roots two of which are repeated; and if it is negative, it has one real root and two complex roots.

Theorem 1.31 (Quartics). *Let $f(x) = \alpha x^4 + 4\beta x^3 + 6\gamma x^2 + 4\delta x + \epsilon$ be a real quartic polynomial in x and define,*

$$\begin{aligned} G_f &= \alpha^2\delta - 3\alpha\beta\gamma + 2\beta^3, \\ H_f &= \alpha\gamma - \beta^2, \\ I_f &= \alpha\epsilon - 4\beta\delta + 3\gamma^2, \\ J_f &= \alpha\gamma\epsilon + 2\beta\gamma\delta - \alpha\delta^2 - \epsilon\beta^2 - \gamma^3. \end{aligned}$$

Then the polynomial can be reduced by the transformation $z = \alpha x + \beta$ to,

$$f_0(z) = z^4 + 6H_f z^2 + 4G_f z + \alpha^2 I_f - 3H_f^2,$$

and the discriminant $D_x(p)$ is given by,

$$D_x(f(x)) = I_f^3 - 27J_f^2.$$

We now consider how many real roots there are for a given polynomial using a collection of results taken from Burnside and Panton [6].

Theorem 1.32 (Fourier and Budan's Theorem). *Let $a, b \in \mathbb{R}$ with $a < b$ and let $f(x)$ be some real polynomial in x of degree $n \in \mathbb{N}$. Then the difference between the number of sign changes in the sequence,*

$$f(a), f'(a), f''(a), \ldots, f^{(n)}(a),$$

and the number of sign changes in the sequence,

$$f(b), f'(b), f''(b), \ldots, f^{(n)}(b),$$

is an upper bound to the number of real roots of $f(x)$ which lie in the interval (a, b). Moreover, when the number of real roots is m less than this upper bound, m will be an even number.

Corollary 1.33 (Descartes' Rule of Sign). *Let $f(x)$ be a real polynomial of degree $n \in \mathbb{N}$ and write $f(x)$ in descending order of powers of x. Working from the highest power down, count the changes of sign of the coefficients. This is an upper bound to the number of real positive roots of $f(x)$. Similarly an upper bound to the number of negative real roots of $f(x)$ is found by counting the changes of sign in $f(-x)$.*

Next we outline Sturm's theorem which establishes the exact number of real roots of a real polynomial in any given interval. Let $f(x)$ be a polynomial in x and define,

$$f_0(x) := f(x), \qquad f_1(x) := f'(x).$$

Now let $Q_2(x)$ be the polynomial quotient and $R_2(x)$ be the polynomial remainder of $f_0(x)$ divided by $f_1(x)$. That is Q_2 and R_2 are the unique real polynomials such that,

$$f_0(x) = Q_2(x) f_1(x) + R_2(x),$$

with the degree of $R_2(x)$ less than the degree of $f_1(x)$. Define,

$$f_2(x) := -R_2(x).$$

Let $R_m(x)$ denote the polynomial remainder of $f_{m-1}(x)$ and $f_{m-2}(x)$. Then we define,

$$f_m(x) := -R_m(x) \qquad \text{for } m \geq 3.$$

This sequence of functions is continued until we encounter $f_M(x)$ which is a constant.

Definition 1.34. *The sequence of functions,*

$$f_0(x), f_1(x), f_2(x), \ldots, f_M(x),$$

is known as the Sturm chain and the functions are called Sturm functions.

Theorem 1.35 (Sturm's Theorem). *Let any two real quantities a and b be substituted for x in the Sturm chain of M polynomials. Then the difference between the number of changes of sign in the series when a is substituted for x and the number of changes of sign when b is substituted for x, is exactly the number of roots of $f(x) = 0$ in the interval (a, b), where each multiple root is counted once only.*

Chapter 2

A one dimensional analysis of the caustic

Summary

In this chapter we demonstrate how the reduced action function can be used to analyse the caustic. We begin by defining the subcaustic as the region of the caustic where the tangent plane drops a dimension. We show how the subcaustic and other geometrical features can be identified in terms of critical points of the reduced action function. Using a formula of Kac, we derive an equation for the cusp density on both the caustic and the Hamilton-Jacobi level surfaces. We conclude with a new method for analysing the hot and cool parts of the caustic producing an exact analytic solution for the three dimensional polynomial swallowtail and a numerical solution for the non-generic swallowtail.

2.1 Parameterising the caustic

It is useful to express the caustic as a parameterised curve as in Example 1.5. Let $x = \Phi_t(x_0)$, where Φ_t is the d-dimensional classical mechanical flow map which is assumed to be globally reducible, $x = (x_1, x_2, \ldots, x_d)$ and $x_0 = (x_0^1, x_0^2, \ldots, x_0^d)$. As explained in Section 1.5, local reducibility is sufficient for the following analysis, but we assume global reducibility to ensure the results are simple and clear. Recall from Definition 1.2 that the caustic is given by,

$$0 = \det\left(\frac{\partial X(t)}{\partial x_0}\right) = \det\left(\frac{\partial \Phi_t(x_0)}{\partial x_0^\alpha}\right)_{\alpha=1,2,\ldots,d.} \tag{2.1}$$

This is an equation involving only x_0 and t, and is therefore the equation of the pre-caustic. Assuming a favoured ordering of the coordinates, we may solve (2.1) locally to give a parameterisation of the pre-caustic in terms of $\lambda_1, \lambda_2, \ldots, \lambda_{d-1} \in \mathbb{R}$ as,

$$x_0^1 = \lambda_1, \quad x_0^2 = \lambda_2, \ldots, \quad x_0^{d-1} = \lambda_{d-1}, \quad x_0^d = x_{0,\mathrm{C}}^d\left(\lambda_1, \lambda_2, \ldots, \lambda_{d-1}\right),$$

where the additional subscript C is to denote the caustic. The parameters have been restricted to be real so that only real pre-images are considered.

Definition 2.1. *For a parameter $\lambda = (\lambda_1, \lambda_2, \ldots, \lambda_{d-1}) \in \mathbb{R}^{d-1}$ the pre-parameterisation of the caustic is given by,*

$$\begin{aligned} x_t(\lambda) &:= \Phi_t\left(\lambda, x_{0,\mathrm{C}}^d(\lambda)\right) \\ &= \Phi_t\left(\lambda_1, \lambda_2, \ldots, \lambda_{d-1}, x_{0,\mathrm{C}}^d(\lambda_1, \lambda_2, \ldots, \lambda_{d-1})\right). \end{aligned}$$

This style of pre-parameterisation will occur repeatedly in our work not only for the caustic but also for the level surfaces and Maxwell set.

Corollary 2.2. *Let $x_t(\lambda)$ denote the pre-parameterisation of the caustic where $\lambda = (\lambda_1, \lambda_2, \ldots, \lambda_{d-1}) \in \mathbb{R}^{d-1}$. Then,*

$$f'_{(x_t(\lambda),t)}(\lambda_1) = f''_{(x_t(\lambda),t)}(\lambda_1) = 0.$$

Proof. From Theorem 1.22,

$$f'_{(x_t(\lambda),t)}(\lambda_1) = 0,$$

since $x_t(\lambda) = \Phi_t(\lambda, x_{0,\mathrm{C}}^d(\lambda))$. Moreover, as $x_t(\lambda) \in C_t$, it follows from Lemma 1.20 that,

$$f''_{(x_t(\lambda),t)}(\lambda_1) = 0. \qquad \square$$

Thus, there is a critical point of inflexion on the reduced action function $f_{(x,t)}(x_0^1)$ at $x_0^1 = \lambda_1$ when x is replaced by the pre-parameterisation of the caustic $x_t(\lambda)$. This enables us to visualise the crossing of the caustic in terms of the critical points of $f_{(x,t)}(x_0^1)$. Consider an example where for x on one side of the caustic there are four real critical points on $f_{(x,t)}(x_0^1)$. Let these be enumerated $x_0^1(i)(x,t)$ for $i = 1$ to 4, and denote the minimising critical point by $\tilde{x}_0^1(x,t)$.

Figure 2.1 illustrates how the minimiser jumps from (a) to (b) as x crosses the caustic if the point of inflexion is the global minimiser of the reduced action function $f_{(x,t)}(x_0^1)$. If this occurs, x is said to be on the cool part of the caustic and, as was explained in the Introduction, $v^0(x,t)$ will have a jump discontinuity. We will return to this topic in Section 2.6.

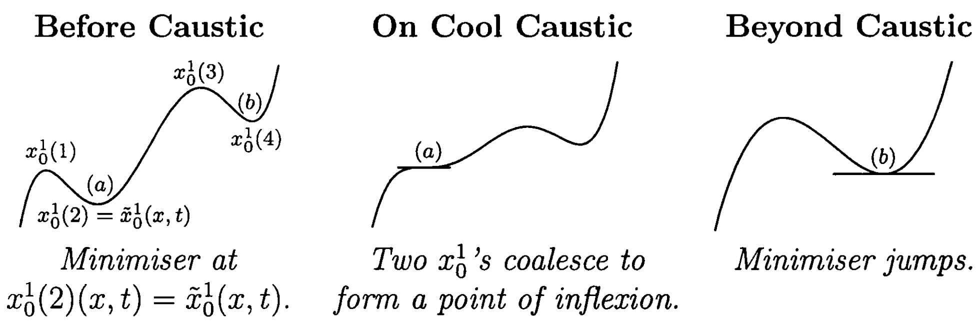

Figure 2.1: The graph of $f_{(x,t)}(x_0^1)$ as x crosses the caustic.

The geometric results of Section 1.3 required that the parameterisation used was intrinsic. Lemma 2.3 is necessary to ensure that this holds for the pre-parameterisation.

Lemma 2.3. *Let Φ_t denote the classical mechanical flow map and let $x_t(\lambda)$ denote the pre-parameterisation of a two dimensional curve where,*

$$x_t(\lambda) = \Phi_t(\lambda, x_0^2(\lambda)),$$

for $\lambda \in \mathbb{R}$ and $x_0^2 \in C^1(\mathbb{R})$. Then λ is an intrinsic parameter of the curve $x_t(\lambda)$ if $\ker(D\Phi_t)$ is at most one dimensional.

Proof. Let s denote the arc length of the curve $x_t(\lambda)$ so that,

$$\begin{aligned}\left(\frac{\mathrm{d}s}{\mathrm{d}\lambda}(\lambda)\right)^2 = \frac{\mathrm{d}x_t}{\mathrm{d}\lambda}(\lambda)\cdot\frac{\mathrm{d}x_t}{\mathrm{d}\lambda}(\lambda) &= \left(\frac{\mathrm{d}x_0}{\mathrm{d}\lambda}\right)^T (D\Phi_t)^T(D\Phi_t)\frac{\mathrm{d}x_0}{\mathrm{d}\lambda} \\ &= (\nu_1^2+\nu_2^2)\left(1+\left(\frac{\mathrm{d}x_0^2}{\mathrm{d}\lambda}\right)^2\right),\end{aligned}$$

where $x_0(\lambda) = (\lambda, x_0^2(\lambda))$ and ν_i are the eigenvalues of $D\Phi_t$. Therefore, if $\ker(D\Phi_t)$ is at most one dimensional,

$$\frac{\mathrm{d}\lambda}{\mathrm{d}s} < \infty,$$

and so,

$$\frac{\mathrm{d}x_t}{\mathrm{d}\lambda} = 0 \quad \Rightarrow \quad \frac{\mathrm{d}x_t}{\mathrm{d}s} = \frac{\mathrm{d}x_t}{\mathrm{d}\lambda}\frac{\mathrm{d}\lambda}{\mathrm{d}s} = 0.$$ □

2.2 Caustic geometry and the subcaustic

We begin our investigation of the geometry of the caustic by considering the behaviour of its tangent plane.

Lemma 2.4. *Let $x_t(\lambda)$ denote the pre-parameterisation of the caustic where $\lambda = (\lambda_1, \lambda_2, \ldots, \lambda_{d-1}) \in \mathbb{R}^{d-1}$. Then, there exist scalars ξ_α, not all zero, where $\alpha = 1, 2, \ldots, d$, such that,*

$$\sum_{\alpha=1}^{d-1} \xi_\alpha \frac{\partial x_t}{\partial \lambda_\alpha}(\lambda) + \xi_d \left.\frac{\partial \Phi_t(x_0)}{\partial x_0^d}\right|_{x_0=(\lambda, x^d_{0,\mathrm{C}}(\lambda))} = 0.$$

Proof. Let $x_0 = (\lambda, x^d_{0,\mathrm{C}}(\lambda))$ then, from equation (2.1), there exist scalars ξ_α (not all zero) such that,

$$\sum_{\alpha=1}^{d} \xi_\alpha \frac{\partial \Phi_t(x_0)}{\partial x_0^\alpha} = 0. \tag{2.2}$$

However,

$$\frac{\partial x_t}{\partial \lambda_\alpha} = \left[\frac{\partial \Phi_t(x_0)}{\partial x_0^\alpha} + \frac{\partial \Phi_t(x_0)}{\partial x_0^d}\frac{\partial x_0^d}{\partial \lambda_\alpha}\right]_{x_0=(\lambda, x^d_{0,\mathrm{C}}(\lambda))},$$

for $\alpha = 1, \ldots, d-1$. Substituting into equation (2.2) gives the result. □

When $\xi_d = 0$, the derivatives of the caustic become linearly dependent and the tangent space to the caustic reduces to a $(d-2)$-dimensional space. This will have a profound effect on the geometry of the caustic which we now investigate in both the two and three dimensional cases.

Definition 2.5. *The subcaustic of a d-dimensional caustic is defined to be that part of the caustic where the tangent space is at most $(d-2)$-dimensional.*

In two dimensions, the pre-caustic is given by $x_0^1 = \lambda$ and $x_0^2 = x^2_{0,\mathrm{C}}(\lambda)$ (we have dropped the subscript from λ since $\lambda = \lambda_1$). The caustic is then given by $x_t(\lambda) = \Phi_t(\lambda, x^2_{0,\mathrm{C}}(\lambda))$ and there exist scalars ξ_1 and ξ_2 not both zero such that,

$$\xi_1 \frac{\partial x_t}{\partial \lambda}(\lambda) + \xi_2 \frac{\partial \Phi_t}{\partial x_0^2}(\lambda, x^2_{0,\mathrm{C}}(\lambda)) = 0.$$

If we set $\xi_2 = 0$, this forces,

$$\frac{\partial x_t}{\partial \lambda} = 0, \tag{2.3}$$

so that the caustic has a generalised cusp. Hence, in two dimensions, the subcaustic corresponds to cusped points of the caustic.

In three dimensions, the pre-caustic is given by $x_0^1 = \lambda_1$, $x_0^2 = \lambda_2$ and $x_0^3 = x^3_{0,\mathrm{C}}(\lambda_1, \lambda_2)$. The pre-parameterisation of the caustic is then $x_t(\lambda_1, \lambda_2) = \Phi_t(\lambda_1, \lambda_2, x^3_{0,\mathrm{C}}(\lambda_1, \lambda_2))$ and so there exist scalars ξ_1, ξ_2 and ξ_3 such that,

$$\xi_1 \frac{\partial x_t}{\partial \lambda_1} + \xi_2 \frac{\partial x_t}{\partial \lambda_2} + \xi_3 \frac{\partial \Phi_t}{\partial x_0^3}(\lambda_1, \lambda_2, x^3_{0,\mathrm{C}}(\lambda_1, \lambda_2)) = 0.$$

The subcaustic then corresponds to forcing $\xi_3 = 0$ which requires,

$$\sqrt{\left|\frac{\partial x_t}{\partial \lambda_1}\right|^2 \left|\frac{\partial x_t}{\partial \lambda_2}\right|^2 - \left(\frac{\partial x_t}{\partial \lambda_1} \cdot \frac{\partial x_t}{\partial \lambda_2}\right)^2} = 0, \tag{2.4}$$

or equivalently,

$$\begin{vmatrix} \frac{\partial x_t}{\partial \lambda_1} \cdot \frac{\partial x_t}{\partial \lambda_1} & \frac{\partial x_t}{\partial \lambda_1} \cdot \frac{\partial x_t}{\partial \lambda_2} \\ \frac{\partial x_t}{\partial \lambda_2} \cdot \frac{\partial x_t}{\partial \lambda_1} & \frac{\partial x_t}{\partial \lambda_2} \cdot \frac{\partial x_t}{\partial \lambda_2} \end{vmatrix} = \left| \begin{pmatrix} \frac{\partial x_t}{\partial \lambda_1} \\ \frac{\partial x_t}{\partial \lambda_2} \end{pmatrix} \begin{pmatrix} \frac{\partial x_t}{\partial \lambda_1}^T & \frac{\partial x_t}{\partial \lambda_2}^T \end{pmatrix} \right| = 0. \tag{2.5}$$

Assuming a favoured ordering of coordinates, equation (2.5) can be solved locally to give $\lambda_2 = \lambda_2(\lambda_1)$. The pre-parameterisation of the subcaustic is then,

$$x_t^{\mathrm{SC}}(\lambda_1) = (\Phi_t(\lambda_1, \lambda_2(\lambda_1)), x_{0,\mathrm{C}}^3(\lambda_1, \lambda_2(\lambda_1))).$$

The subcaustic contains all points of the caustic where the tangent space is at most one dimensional and therefore corresponds to creases in the caustic.

This analysis can be extended to the general d-dimensional case.

Lemma 2.6. *There exist $\xi_\alpha \in \mathbb{R}$ such that,*

$$\sum_{\alpha=1}^{p} \xi_\alpha \frac{\partial x_t}{\partial \lambda_\alpha} = 0,$$

where $d - 1 \geq p \geq 1$ if and only if,

$$\det_{\alpha,\beta=1,\ldots,p} \left(\frac{\partial x_t}{\partial \lambda_\alpha} \cdot \frac{\partial x_t}{\partial \lambda_\beta}\right) = 0. \tag{2.6}$$

Proof. Let,

$$v = \sum_{\alpha=1}^{p} \xi_\alpha \frac{\partial x_t}{\partial \lambda_\alpha}$$

and

$$\mathcal{V} = \mathrm{Span}\left\{\frac{\partial x_t}{\partial \lambda_\alpha} \quad \text{for } \alpha = 1, \ldots, p\right\}.$$

Since $v \in \mathcal{V}$, it follows that $v = 0$ if and only if $v \in \mathcal{V}^\perp$. Therefore,

$$\frac{\partial x_t}{\partial \lambda_\beta} \cdot v = \sum_{\alpha=1}^{p} \xi_\alpha \frac{\partial x_t}{\partial \lambda_\alpha} \cdot \frac{\partial x_t}{\partial \lambda_\beta} = 0,$$

which will only have a non-trivial solution if equation (2.6) holds. □

Proposition 2.7. *The pre-parameterisation of the subcaustic is given by,*

$$x_t^{\mathrm{sc}}(\lambda_1, \lambda_2, \ldots, \lambda_{d-2}) = \Phi_t\left(\lambda, x_{0,\mathrm{C}}^d(\lambda)\right)\big|_{\lambda_{d-1}=\lambda_{d-1}(\lambda_1,\ldots,\lambda_{d-2})},$$

where $\lambda_{d-1}(\ldots)$ *is determined by,*

$$\det_{\alpha,\beta=1,\ldots,d-1}\left(\frac{\partial x_t}{\partial \lambda_\alpha}\cdot\frac{\partial x_t}{\partial \lambda_\beta}\right) = 0. \tag{2.7}$$

Proof. This follows from Lemmas 2.4 and 2.6 where we assume that equation (2.7) can be solved locally for λ_{d-1}. □

We now give some three dimensional examples to show how the shape of the caustic is related to its subcaustic.

Example 2.8 (The butterfly). Let $V = 0$, $k_t = 0$ and

$$S_0(x_0, y_0, z_0) = x_0^3 y_0 + x_0^2 z_0.$$

The butterfly initial condition is the three dimensional equivalent of the generic cusp from Example 1.5. The determinant equation (2.7) for the subcaustic is,

$$9\left(\lambda_2 - 2\lambda_1 t - 9\lambda_1^3 t\right)^2\left(1 + 4\lambda_1^2 t^2 + 9\lambda_1^4 t^2\right) = 0,$$

which gives,

$$\lambda_2(\lambda_1) = 2\lambda_1 t + 9\lambda_1^3 t.$$

The subcaustic is then,

$$\begin{aligned}
x_t^{\mathrm{sc}}(\lambda_1) &= -2\lambda_1^3 t^2\left(1 + 9\lambda_1^2\right),\\
y_t^{\mathrm{sc}}(\lambda_1) &= 2\lambda_1 t\left(1 + 5\lambda_1^2\right),\\
z_t^{\mathrm{sc}}(\lambda_1) &= -\frac{1}{2t}\left(1 + 6\lambda_1^2 t^2 + 45\lambda_1^4 t^2\right).
\end{aligned}$$

This is shown in Figure 2.2 where the subcaustic is drawn in black.

Example 2.9 (The 3D polynomial swallowtail). Let $V = 0$, $k_t = 0$ and

$$S_0(x_0, y_0, z_0) = x_0^7 + x_0^3 y_0 + x_0^2 z_0.$$

This initial condition is the simplest polynomial to produce a three dimensional swallowtail caustic [34]. The determinant equation (2.7) for the subcaustic is,

$$9\left(35\lambda_1^4 + \lambda_2 - 2\lambda_1 t - 9\lambda_1^3 t\right)^2\left(1 + 4\lambda_1^2 t^2 + 9\lambda_1^4 t^2\right) = 0,$$

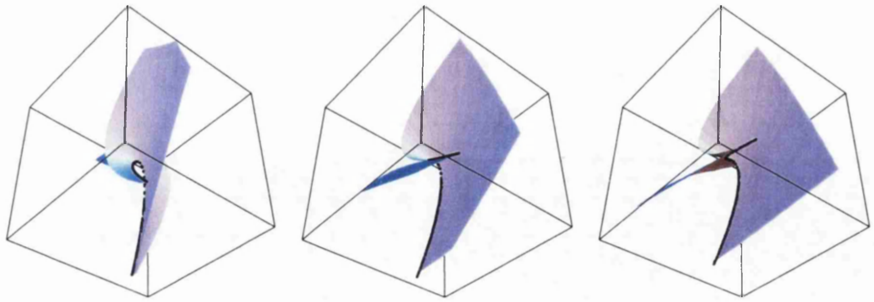

Figure 2.2: The butterfly caustic plotted with subcaustic for times $t = 1, 2, 3$.

so that,

$$\lambda_2(\lambda_1) = -35\lambda_1^4 + 2\lambda_1 t + 9\lambda_1^3 t.$$

The subcaustic is,

$$\begin{aligned} x_t^{sc}(\lambda_1) &= 2\lambda_1^3 t\left(35\lambda_1^3 - t - 9\lambda_1^2 t\right), \\ y_t^{sc}(\lambda_1) &= -\lambda_1\left(35\lambda_1^3 - 2t - 10\lambda_1^2 t\right), \\ z_t^{sc}(\lambda_1) &= \frac{1}{2t}\left(-1 + 168\lambda_1^5 t - 6\lambda_1^2 t^2 - 45\lambda_1^4 t^2\right). \end{aligned}$$

Moreover, the subcaustic is itself cusped when $70\lambda_1^3 - 15\lambda_1^2 t - t = 0$, which always has exactly one real solution by Descarte's rule of sign (Corollary 1.33). The subcaustic is shown in Figure 2.3 where it is clearly cusped.

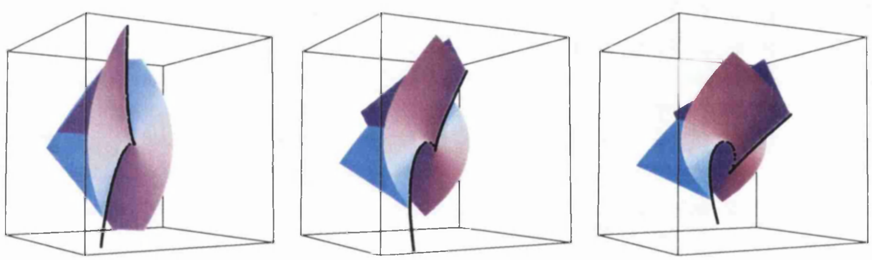

Figure 2.3: The 3D polynomial swallowtail caustic plotted with subcaustic.

2.3 Caustic geometry and the reduced action function

In two dimensions there is a well known classification of the double points of an algebraic curve as acnodes (isolated points), crunodes (points of self-intersection) and cusps (Figure 2.4) [10, 22]. We consider the relationships between these features and the critical points of the reduced action function.

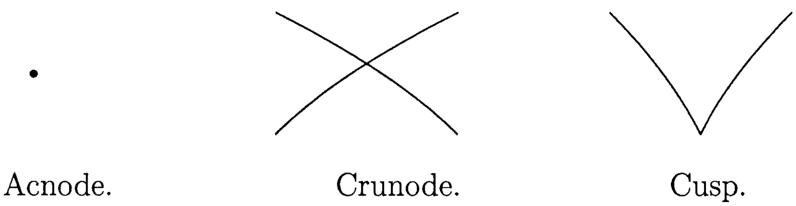

Figure 2.4: The classification of double points.

Theorem 2.10. *Let $x_t(\lambda)$ be the pre-parameterisation of the caustic where $\lambda \in \mathbb{R}$. If $x_t(\tilde{\lambda})$ is a generalised cusp on the caustic, then,*

$$f'_{(x_t(\tilde{\lambda}),t)}(\tilde{\lambda}) = f''_{(x_t(\tilde{\lambda}),t)}(\tilde{\lambda}) = f'''_{(x_t(\tilde{\lambda}),t)}(\tilde{\lambda}) = 0.$$

Proof. From Corollary 2.2,

$$f'_{(x_t(\lambda),t)}(\lambda) = f''_{(x_t(\lambda),t)}(\lambda) = 0, \tag{2.8}$$

for all $\lambda \in \mathbb{R}$. Differentiating the second part of equation (2.8) with respect to λ gives,

$$0 = \frac{\mathrm{d}x_t}{\mathrm{d}\lambda}(\lambda) \cdot \nabla_x f''_{(x_t(\lambda),t)}(\lambda) + f'''_{(x_t(\lambda),t)}(\lambda).$$

Setting $\lambda = \tilde{\lambda}$ forces,

$$f'''_{(x_t(\tilde{\lambda}),t)}(\tilde{\lambda}) = 0.$$ □

Theorem 2.11. *Let $x_t(\lambda)$ be the pre-parameterisation of the caustic where $\lambda \in \mathbb{R}$. If*

$$f'_{(x_t(\tilde{\lambda}),t)}(\tilde{\lambda}) = f''_{(x_t(\tilde{\lambda}),t)}(\tilde{\lambda}) = f'''_{(x_t(\tilde{\lambda}),t)}(\tilde{\lambda}) = 0,$$

and the vectors,

$$\nabla_x f'_{(x_t(\tilde{\lambda}),t)}(\tilde{\lambda}), \qquad \nabla_x f''_{(x_t(\tilde{\lambda}),t)}(\tilde{\lambda}),$$

are linearly independent, then there is a generalised cusp on the caustic at $x_t(\tilde{\lambda})$.

Proof. Differentiating the two equations (2.8) with respect to λ yields,

$$\frac{\mathrm{d}x_t}{\mathrm{d}\lambda}(\lambda) \cdot \nabla_x f'_{(x_t(\lambda),t)}(\lambda) = 0, \qquad \frac{\mathrm{d}x_t}{\mathrm{d}\lambda}(\lambda) \cdot \nabla_x f''_{(x_t(\lambda),t)}(\lambda) + f'''_{(x_t(\lambda),t)}(\lambda) = 0.$$

Setting $\lambda = \tilde{\lambda}$ forces,

$$\frac{\mathrm{d}x_t}{\mathrm{d}\lambda}(\tilde{\lambda}) \cdot \nabla_x f'_{(x_t(\tilde{\lambda}),t)}(\tilde{\lambda}) = 0, \qquad \frac{\mathrm{d}x_t}{\mathrm{d}\lambda}(\tilde{\lambda}) \cdot \nabla_x f''_{(x_t(\tilde{\lambda}),t)}(\tilde{\lambda}) = 0.$$

Therefore, since $\nabla_x f'_{(x_t(\tilde{\lambda}),t)}(\tilde{\lambda})$ and $\nabla_x f''_{(x_t(\tilde{\lambda}),t)}(\tilde{\lambda})$ are linearly independent,

$$\frac{\mathrm{d}x_t}{\mathrm{d}\lambda}(\tilde{\lambda}) = 0. \qquad \square$$

Lemma 2.12. *Let $x_t(\lambda)$ denote the pre-parameterisation of the caustic where $\lambda \in \mathbb{R}$. There is a point of self-intersection (a crunode) at $x_t(\lambda)$ if and only if there exists a solution,*

$$f'_{(x_t(\lambda),t)}(x_0^1) = f''_{(x_t(\lambda),t)}(x_0^1) = 0, \tag{2.9}$$

with $x_0^1 \neq \lambda$.

Proof. If a point on the caustic is a point of self-intersection, it must have two distinct pre-images on the pre-caustic to give two distinct tangent directions on the caustic. Therefore, there must be two values for x_0^1 such that equation (2.9) holds. $\square$

These results can be extended to d-dimensions if we assume that the derivatives,

$$\left\{ \frac{\partial \Phi_t(x_0)}{\partial x_0^2}, \frac{\partial \Phi_t(x_0)}{\partial x_0^3}, \ldots, \frac{\partial \Phi_t(x_0)}{\partial x_0^d} \right\},$$

are linearly independent.

Theorem 2.13. *Let $x_t(\lambda)$ denote the pre-parameterisation of the caustic where $\lambda = (\lambda_1, \lambda_2, \ldots, \lambda_{d-1}) \in \mathbb{R}^{d-1}$. If $x_t(\tilde{\lambda})$ is on the subcaustic, then,*

$$f'_{(x_t(\tilde{\lambda}),t)}(\tilde{\lambda}_1) = f''_{(x_t(\tilde{\lambda}),t)}(\tilde{\lambda}_1) = f'''_{(x_t(\tilde{\lambda}),t)}(\tilde{\lambda}_1) = 0. \tag{2.10}$$

Proof. The first two parts of equation (2.10) follow directly from Corollary 2.2. Differentiating the equation,

$$f''_{(x_t(\lambda),t)}(\lambda_1) = 0,$$

with respect to each λ_α gives,

$$0 = \frac{\partial x_t}{\partial \lambda_1}(\lambda) \cdot \nabla_x f''_{(x_t(\lambda),t)}(\lambda_1) + f'''_{(x_t(\lambda),t)}(\lambda_1), \tag{2.11}$$

$$0 = \frac{\partial x_t}{\partial \lambda_\alpha}(\lambda) \cdot \nabla_x f''_{(x_t(\lambda),t)}(\lambda_1), \tag{2.12}$$

where $\alpha = 2, \ldots, d-1$. If $x_t(\tilde{\lambda})$ is on the subcaustic, then there exist scalars ξ_α with $\xi_1 \neq 0$ such that,

$$\sum_{\alpha=1}^{d-1} \xi_\alpha \frac{\partial x_t}{\partial \lambda_\alpha}(\tilde{\lambda}) = 0. \tag{2.13}$$

Taking the dot product of (2.13) with $\nabla_x f''_{(x_t(\tilde{\lambda}),t)}(\tilde{\lambda}_1)$ and then substituting in equations (2.12) gives,

$$\xi_1 \frac{\partial x_t}{\partial \lambda_1}(\tilde{\lambda}) \cdot \nabla_x f''_{(x_t(\tilde{\lambda}),t)}(\tilde{\lambda}_1) = 0,$$

where $\xi_1 \neq 0$. Therefore, it follows from equation (2.11) that,

$$f'''_{(x_t(\tilde{\lambda}),t)}(\tilde{\lambda}_1) = 0. \qquad \square$$

Theorem 2.14. *Let $x_t(\lambda)$ denote the pre-parameterisation of the caustic where $\lambda = (\lambda_1, \lambda_2, \dots, \lambda_{d-1}) \in \mathbb{R}^{d-1}$. If*

$$f'_{(x_t(\tilde{\lambda}),t)}(\tilde{\lambda}_1) = f''_{(x_t(\tilde{\lambda}),t)}(\tilde{\lambda}_1) = f'''_{(x_t(\tilde{\lambda}),t)}(\tilde{\lambda}_1) = 0,$$

and the vectors,

$$\nabla_x f'_{(x_t(\tilde{\lambda}),t)}(\tilde{\lambda}_1), \qquad \nabla_x f''_{(x_t(\tilde{\lambda}),t)}(\tilde{\lambda}_1),$$

are linearly independent, then $x_t(\tilde{\lambda}_1)$ is on the subcaustic.

Proof. Differentiating the equation,

$$f'_{(x_t(\lambda),t)}(\lambda_1) = 0,$$

with respect to each λ_α and then setting $\lambda = \tilde{\lambda}$ gives,

$$\frac{\mathrm{d}x_t}{\mathrm{d}\lambda_\alpha}(\tilde{\lambda}) \cdot \nabla_x f'_{(x_t(\tilde{\lambda}))}(\tilde{\lambda}_1) = 0,$$

for $\alpha = 1, \dots, d-1$. Moreover, when $\lambda = \tilde{\lambda}$ equations (2.11) and (2.12) reduce to give,

$$\frac{\mathrm{d}x_t}{\mathrm{d}\lambda_\alpha}(\tilde{\lambda}) \cdot \nabla_x f''_{(x_t(\tilde{\lambda}))}(\tilde{\lambda}_1) = 0.$$

Since $\nabla_x f'_{(x_t(\tilde{\lambda}))}(\tilde{\lambda}_1)$ and $\nabla_x f''_{(x_t(\tilde{\lambda}))}(\tilde{\lambda}_1)$ are linearly independent, they span a plane in $\mathbb{R}^d$ leaving $(d-2)$ directions orthogonal to both vectors. Therefore, the vectors $\frac{\mathrm{d}x_t}{\mathrm{d}\lambda_\alpha}(\lambda)$ for $\alpha = 1, \dots, d-1$, must form a linearly dependent set. $\square$

We can extend Theorem 2.13 to describe the dimension of the tangent plane in all generality.

Proposition 2.15. *Let $x_t(\lambda)$ denote the pre-parameterisation of the caustic where $\lambda = (\lambda_1, \lambda_2, \dots, \lambda_{d-1}) \in \mathbb{R}^{d-1}$. If we assume $f_{(x_t(\lambda),t)}(x_0^1) \in C^{p+1}$ then, in d-dimensions, if the tangent to the caustic is at most $(d-p+1)$-dimensional at $x_t(\tilde{\lambda})$,*

$$f'_{(x_t(\tilde{\lambda}),t)}(\tilde{\lambda}_1) = f''_{(x_t(\tilde{\lambda}),t)}(\tilde{\lambda}_1) = \dots = f^{(p)}_{(x_t(\tilde{\lambda}),t)}(\tilde{\lambda}_1) = 0.$$

Proof. On the subcaustic, where $\lambda_{d-1} = \lambda_{d-1}(\lambda_1, \ldots, \lambda_{d-2})$ as determined in equation (2.7), the tangent plane is at most $(d-2)$-dimensional and from Theorem 2.13,

$$f'''_{(x_t(\lambda_1,\ldots,\lambda_{d-1}(\ldots)),t)}(\lambda_1) = 0.$$

Differentiating this gives,

$$\begin{aligned} 0 &= \nabla_x f'''_{(x_t(\lambda_1,\ldots,\lambda_{d-1}(\ldots)),t)}(\lambda_1) \cdot \left(\frac{\mathrm{d}x_t}{\mathrm{d}\lambda_1} + \frac{\mathrm{d}x_t}{\mathrm{d}\lambda_{d-1}} \frac{\mathrm{d}\lambda_{d-1}}{\mathrm{d}\lambda_1} \right) \\ &\quad + f^{(4)}_{(x_t(\lambda_1,\ldots,\lambda_{d-1}(\ldots)),t)}(\lambda_1), \\ 0 &= \nabla_x f'''_{(x_t(\lambda_1,\ldots,\lambda_{d-1}(\ldots)),t)}(\lambda_1) \cdot \left(\frac{\mathrm{d}x_t}{\mathrm{d}\lambda_\alpha} + \frac{\mathrm{d}x_t}{\mathrm{d}\lambda_{d-1}} \frac{\mathrm{d}\lambda_{d-1}}{\mathrm{d}\lambda_\alpha} \right), \end{aligned}$$

where $\alpha = 1, \ldots, d-2$, and $\frac{\mathrm{d}x_t}{\mathrm{d}\lambda_{d-1}}$ can be expressed as a linear combination of the derivatives $\frac{\mathrm{d}x_t}{\mathrm{d}\lambda_1}$ through $\frac{\mathrm{d}x_t}{\mathrm{d}\lambda_{d-2}}$.

However, if the tangent plane is at most $(d-3)$-dimensional so that $x_t(\ldots)$ is on the sub^{2}caustic (the subsubcaustic) then,

$$f^{(4)}_{(x_t(\lambda),t)}(\lambda_1) = 0.$$

Moreover, assuming a favoured ordering of coordinates, we can solve locally an equivalent equation to (2.7) to give $\lambda_{d-2} = \lambda_{d-2}(\lambda_1, \ldots, \lambda_{d-3})$.

Repeating this process we conclude that,

$$f^{(p)}_{(x_t(\lambda),t)}(\lambda_1) = 0,$$

on the sub^{p}caustic where the tangent plane is at most $(d-p+1)$-dimensional. □

Finally, Lemma 2.12 extends to d-dimensions without any need for further proof.

Lemma 2.16. *Let $x_t(\lambda)$ denote the pre-parameterisation of the caustic where $\lambda = (\lambda_1, \lambda_2, \ldots, \lambda_{d-1}) \in \mathbb{R}^{d-1}$. The caustic surface intersects itself at $x_t(\lambda)$ if and only if there exists a solution,*

$$f'_{(x_t(\lambda),t)}(x_0^1) = f''_{(x_t(\lambda),t)}(x_0^1) = 0,$$

with $x_0^1 \neq \lambda_1$.

The acnodes of the caustic will be considered in Chapter 3.

2.4 The cusp density

We can combine the two dimensional results of Section 2.3 with a lemma of Kac to derive explicit formulae for the density of cusps on both the caustic and the Hamilton-Jacobi level surfaces.

Lemma 2.17 (Kac's Lemma). *If $f(x)$ is continuous for $a \leq x \leq b$ and continuously differentiable for $a < x < b$ then, assuming $f(x)$ has a finite number of turning points, the number of zeros of $f(x)$ in (a, b) is given by,*

$$n(a, b; f) = \lim_{R\to\infty} (2\pi)^{-1} \int_{-R}^{R} \int_{a}^{b} \cos\left(\xi f(x)\right) |f'(x)| \, \mathrm{d}x \, \mathrm{d}\xi,$$

where multiple zeros are counted once and if either a or b is a zero it is counted as $\frac{1}{2}$.

Proof. See Kac [24]. □

Theorem 2.18. *Let $x_t(\lambda)$ denote the pre-parameterisation of the caustic where $\lambda \in \mathbb{R}$. The number of generalised cusps on the caustic C_t is given by,*

$$\lim_{R\to\infty} (2\pi)^{-1} \int_{-R}^{R} \int_{a}^{b} \cos\left(\xi \left\{ f'''_{(x_t(\lambda),t)}(\lambda) \right\}\right) \times \left| \frac{\mathrm{d}x_t}{\mathrm{d}\lambda}(\lambda) \cdot \nabla_x f'''_{(x_t(\lambda),t)}(\lambda) + f^{(4)}_{(x_t(\lambda),t)}(\lambda) \right| \mathrm{d}\lambda \, \mathrm{d}\xi,$$

if the vectors

$$\nabla_x f'_{(x_t(\lambda),t)}(\lambda), \qquad \nabla_x f''_{(x_t(\lambda),t)}(\lambda),$$

are linearly independent for all $\lambda \in \mathbb{R}$ with $f'''_{(x_t(\lambda),t)}(\lambda) = 0$.

Proof. From Theorem 2.11, assuming that the above vectors are linearly independent, the caustic has a generalised cusp at $x_t(\lambda)$ if,

$$f'''_{(x_t(\lambda),t)}(\lambda) = 0.$$

Therefore, the number of cusps on the caustic is given by the number of real solutions λ for this equation and the result follows from Kac's Lemma. □

Formally, this result is a consequence of the fact that if at time t there are n_t cusps on the caustic at $\lambda^1(t)$, $\lambda^2(t)$,...,$\lambda^{n_t}(t)$, then,

$$\sum_{i=1}^{n_t} \delta\left\{\lambda - \lambda^i(t)\right\} \mathrm{d}\lambda = \delta\left\{ f'''_{(x_t(\lambda),t)}(\lambda) \right\} \left| \frac{\mathrm{d}}{\mathrm{d}\lambda} \left(f'''_{(x_t(\lambda),t)}(\lambda) \right) \right| \mathrm{d}\lambda,$$

and

$$\delta\left\{f'''_{(x_t(\lambda),t)}(\lambda)\right\} = (2\pi)^{-1}\int_{-\infty}^{\infty} \mathrm{d}\xi \exp\left\{\mathrm{i}\xi f'''_{(x_t(\lambda),t)}(\lambda)\right\}.$$

Theorem 2.19. *Let $x_t(\lambda)$ denote the pre-parameterisation of the caustic where $\lambda \in \mathbb{R}$. The number of generalised cusps on a level surface H_t^c is given by,*

$$\lim_{R\to\infty}(2\pi)^{-1}\int_{-R}^{R}\int_{a}^{b}\cos\left(\xi\left\{f_{(x_t(\lambda),t)}(\lambda)-c\right\}\right)\left|\frac{\mathrm{d}x_t}{\mathrm{d}\lambda}(\lambda)\cdot\nabla_x f_{(x_t(\lambda),t)}(\lambda)\right| \mathrm{d}\lambda\,\mathrm{d}\xi.$$

Proof. The key geometric result of DTZ, Theorem 1.14, shows that the cusps of the level surface correspond to points where the pre-level surface intersects the pre-caustic. Therefore, the cusps of the level surface will be given by the roots of,

$$f_{(x_t(\lambda),t)}(\lambda) - c = 0.$$

The result then follows from Kac's Lemma. □

2.5 Hot and cool parts of the caustic

In Section 1.1 we introduced the division of the caustic into two distinct regions. Across one region the inviscid limit of the Burgers fluid velocity is continuous (the hot part) whilst across the other region the fluid velocity is discontinuous (the cool part).

Definition 2.20. *Let x be a point on the caustic and let, $x_0(i)(x,t)$ for $i = 1, 2, \ldots, n$ denote an enumeration of the real roots of,*

$$\nabla_{x_0}\mathcal{A}(x_0, x, t) = 0,$$

so that for some i, $x_0(i)(x,t) \in \Phi_t^{-1}C_t$. The point x is defined to be cool if

$$\mathcal{A}(x_0(i)(x,t), x, t) \leq \mathcal{A}(x_0(j)(x,t), x, t),$$

for all $j = 1, 2, \ldots, n$. If the caustic is not cool it is defined to be hot.

The label 'cool' arises from the following lemma.

Lemma 2.21. *In two dimensions, a point $\tilde{x}$ is on the cool part of the caustic if and only if for x on one side of the caustic $v^0(x,t) \to 0$ as $x \to \tilde{x}$.*

Proof. See Reynolds [34]. □

Lemma 2.22. *The inviscid limit of the Burgers velocity field $v^0(x,t)$ will be discontinuous as x crosses a cool part of the caustic, but continuous as x crosses a hot part of the caustic.*

Proof. See Reynolds [34] □

Previous techniques developed by Reynolds [34] and RTW [35] found the cool parts of the caustic either by examining how the multiplicity of pre-images of a point x changes as it crosses the caustic, or by identifying those critical points which minimise the action. Instead we use the reduced action function to develop a new technique based on the identification of the boundaries between the hot and cool parts.

Lemma 2.23. *Let $x_t(\lambda)$ denote the pre-parameterisation of the caustic where $\lambda = (\lambda_1, \lambda_2, \ldots, \lambda_{d-1}) \in \mathbb{R}^{d-1}$. Then, $x_t(\lambda)$ is on the cool part of the caustic if and only if,*

$$f_{(x_t(\lambda),t)}(\lambda_1) \leq f_{(x_t(\lambda),t)}(x_0^1(i)(x_t(\lambda),t)),$$

for all $i = 1, 2, \ldots, n$, where $x_0^1(i)(x,t)$ denotes an enumeration of the real roots for x_0^1 to,

$$f'_{(x,t)}(x_0^1) = 0.$$

Proof. This follows from Definition 2.20 and Theorem 1.22. □

Definition 2.24. *The pre-normalised reduced action function evaluated on the caustic is defined by,*

$$\mathcal{F}_\lambda(x_0^1) := f_{(x_t(\lambda),t)}(x_0^1) - f_{(x_t(\lambda),t)}(\lambda_1).$$

Lemma 2.25. *If $\mathcal{F}_\lambda$ denotes the pre-normalised reduced action function evaluated on the caustic, then,*

$$\mathcal{F}_\lambda(\lambda_1) = \mathcal{F}'_\lambda(\lambda_1) = \mathcal{F}''_\lambda(\lambda_1) = 0.$$

Proof. This follows from Corollary 2.2. □

From Lemma 2.25, $\mathcal{F}_\lambda(x_0^1)$ has a critical point of inflexion at $x_0^1 = \lambda_1$. As λ varies, the curve $\mathcal{F}_\lambda(x_0^1)$ will deform; however, there will always be an inflexion at $x_0^1 = \lambda_1$ at which $\mathcal{F}_\lambda(\lambda_1) = 0$. When this inflexion is the minimising critical point of $\mathcal{F}_\lambda$, the caustic at $x_t(\lambda)$ will be cool, and when it is not the minimising critical point, the caustic at $x_t(\lambda)$ will be hot.

Corollary 2.26. *If $\mathcal{F}_\lambda(x_0^1)$ is a real analytic function of x_0^1 in a neighbourhood of $\lambda_1 \in \mathbb{R}$, then,*

$$\mathcal{F}_\lambda(x_0^1) = (x_0^1 - \lambda_1)^3 \tilde{F}(x_0^1), \tag{2.14}$$

where $\tilde{F}$ is real analytic.

Proof. This follows from Lemma 2.25. □

Proposition 2.27. *If $\mathcal{F}_\lambda(x_0^1)$ is a real analytic function of x_0^1, then a necessary condition for $x_t(\lambda) \in C_t$ to be a possible hot/cool boundary is that either:*

1. $\tilde{F}(x_0^1)$*; or,*
2. $\tilde{G}(x_0^1) = 3\tilde{F}(x_0^1) + (x_0^1 - \lambda_1)\tilde{F}'(x_0^1)$*,*

has a repeated root at $x_0^1 = r$ where normally $r \neq \lambda_1$.

Proof. There are two ways in which the inflexion at $x_0^1 = \lambda_1$ can switch between being and not being the minimising critical point of $\mathcal{F}_\lambda(x_0^1)$, assuming that the curve deforms continuously with λ.

Firstly, λ could be such that there is a repeated root of $\mathcal{F}_\lambda(x_0^1) = 0$ at some value $x_0^1 = r_{\tilde{F}} \neq \lambda_1$; $r_{\tilde{F}}$ would be a repeated root of $\tilde{F}(x_0^1) = 0$. Therefore, there would be a critical point at $x_0^1 = r_{\tilde{F}}$ where $\mathcal{F}_\lambda(r_{\tilde{F}}) = 0$ (see Figure 2.5 column 1). If we let $\lambda \mapsto \lambda \pm \delta\lambda$, then this critical point will either sink below the zero level making the caustic hot or rise above the zero level making the caustic cool (we assume that there are no other critical points $x_0^1 = x_0^c$ where $\mathcal{F}_\lambda(x_0^c) < 0$).

Secondly, λ could be such that there is an inflexion of $\mathcal{F}_\lambda(x_0^1)$ at $x_0^1 = r_{\tilde{G}} \neq \lambda_1$ where $\mathcal{F}_\lambda(r_{\tilde{G}}) < 0$; $r_{\tilde{G}}$ would be a repeated root of $\tilde{G}(x_0^1) = 0$ (see Figure 2.5 column 2). The point $x_t(\lambda)$ would then correspond to a self-intersection on the caustic. If the inflexion at $x_0^1 = r_{\tilde{G}}$ disappeared (became complex) as $\lambda \mapsto \lambda \pm \delta\lambda$, the caustic would become cool, whereas if it split into a maximum and a mimimum the caustic would become hot (again provided that there were no other critical points $x_0^1 = x_0^c$ where $\mathcal{F}_\lambda(x_0^c) < 0$). □

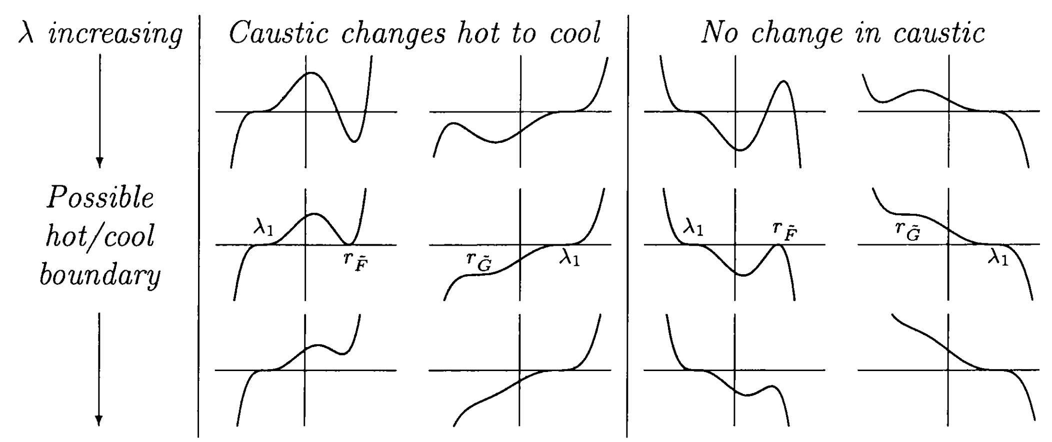

Figure 2.5: Graphs of $\mathcal{F}_\lambda(x_0^1)$ plotted as a function of x_0^1.

Corollary 2.28. *If $\mathcal{F}_\lambda(x_0^1)$ is a polynomial in x_0^1 then a necessary condition for $x_t(\lambda)$ to be a possible hot/cool boundary is that either:*

1. $D_{x_0^1}\left(\tilde{F}(x_0^1)\right) = 0$; *or,*

2. $D_{x_0^1}\left(\tilde{G}(x_0^1)\right) = 0$,

where D_x denotes the discriminant taken with respect to x.

Proof. This follows from Proposition 2.27 and Lemma 1.29. □

The conditions in Proposition 2.27 and Corollary 2.28 are not sufficient because they include cases where the repeated roots $r_{\tilde{F}}$ and $r_{\tilde{G}}$ are complex, where there are other critical points $x_0^1 = x_0^c$ with $\mathcal{F}_\lambda(x_0^c) < 0$, and where $\mathcal{F}_\lambda(r_{\tilde{G}}) > 0$ (see Figure 2.5 columns 3 and 4). Consequently, we can divide the points $x_t(\lambda)$, where λ are the results of Proposition 2.27 or Corollary 2.28 (the 'possible hot/cool boundaries') into two distinct categories; 'genuine hot/cool boundaries' where the caustic will change from hot to cool and 'false positive boundaries' where the caustic will not change.

In two dimensions, the possible hot/cool boundaries are single points and the false positive boundaries can be eliminated by testing each individually.

Proposition 2.29. *Let $\mathcal{F}_\lambda(x_0^1)$ be the pre-normalised reduced action function and let $\tilde{F}$ and $\tilde{G}$ be defined as in Proposition 2.27.*

1. *If $x_0^1 = r_{\tilde{F}}$ is a repeated root of $\tilde{F}(x_0^1) = 0$ and $\tilde{F}''(r_{\tilde{F}})\,(r_{\tilde{F}} - \lambda_1) < 0$, then $x_t(\lambda)$ is a false positive boundary point.*

2. *If $x_0^1 = r_{\tilde{G}}$ is a repeated root of $\tilde{G}(x_0^1) = 0$ and $\mathcal{F}_\lambda(r_{\tilde{G}}) > 0$, then $x_t(\lambda)$ is a false positive boundary point.*

Proof. If $x_0^1 = r_{\tilde{F}}$ is a repeated root of $\tilde{F}(x_0^1) = 0$ then,

$$\mathcal{F}_\lambda''(r_{\tilde{F}}) = (r_{\tilde{F}} - \lambda_1)^3 \tilde{F}''(r_{\tilde{F}}).$$

Therefore, $r_{\tilde{F}}$ is a local maximum of $\mathcal{F}_\lambda$ if $\tilde{F}''(r_{\tilde{F}})\,(r_{\tilde{F}} - \lambda_1) < 0$ and so $x_t(\lambda)$ is a false positive boundary.

If $x_0^1 = r_{\tilde{G}}$ is a repeated root of $\tilde{G}(x_0^1) = 0$ and $\mathcal{F}_\lambda(r_{\tilde{G}}) > 0$, then this second inflexion will occur at a higher level than the inflexion at λ_1 which is fixed at the zero level. Therefore, the inflexion at $r_{\tilde{G}}$ will not affect the hot/cool nature of the caustic. □

We conclude with an example to show the simplicity of our method.

Example 2.30 (The polynomial swallowtail). Let $V = 0$, $k_t = 0$ and

$$S_0(x_0, y_0) = x_0^5 + x_0^2 y_0.$$

This initial condition was first investigated by Reynolds [34] and is the simplest polynomial initial condition to produce a two dimensional swallowtail caustic. A simple calculation gives,

$$\tilde{F}(x_0) = 12\lambda^2 - 3\lambda t + 6\lambda x_0 - t x_0 + 2x_0^2,$$

$$\tilde{G}(x_0) = 15\lambda^2 - 4\lambda t + 10\lambda x_0 - 2t x_0 + 5x_0^2,$$

which have discriminants,

$$D_{x_0}(\tilde{F}(x_0)) = 60\lambda^2 - 12\lambda t - t^2, \qquad D_{x_0}(\tilde{G}(x_0)) = 50\lambda^2 - 10\lambda t - t^2.$$

Thus, from Corollary 2.28, the possible hot/cool boundaries are the points $x_t(\lambda)$ where,

$$\lambda = \frac{t}{30}\left(3 \pm 2\sqrt{6}\right), \qquad \lambda = \frac{t}{10}\left(1 \pm \sqrt{3}\right).$$

If $\lambda = \frac{t}{30}\left(3 \pm 2\sqrt{6}\right)$, the corresponding repeated root of $\tilde{F}(x_0)$ is given by,

$$r_{\tilde{F}} = -\frac{t}{10}\left(-1 \pm \sqrt{6}\right).$$

Therefore,

$$\tilde{F}''(r_{\tilde{F}})\left(r_{\tilde{F}} - \lambda_1\right) = \mp\frac{2}{3}t\sqrt{6},$$

and so by part 1 of Proposition 2.29, $x_t\left(\frac{t}{30}\left(3 - 2\sqrt{6}\right)\right)$ is a false positive boundary.

If $\lambda = \frac{t}{10}\left(1 \pm \sqrt{3}\right)$, the corresponding repeated root of $\tilde{G}(x_0)$ is given by,

$$r_{\tilde{G}} = \frac{t}{10}\left(1 \mp \sqrt{3}\right).$$

Thus,

$$\mathcal{F}_\lambda(r_{\tilde{G}}) = \mp\frac{t^3\sqrt{3}}{250}$$

and so by part 2 of Proposition 2.29, $x_t\left(\frac{t}{10}\left(1 - \sqrt{3}\right)\right)$ is a false positive boundary.

Thus, there are at most two genuine hot/cool boundary points which divide the caustic into three sections where:

$$\begin{array}{rcccl} -\infty & < & \lambda & < & \frac{t}{30}(3 - 2\sqrt{6}), \\ \frac{t}{30}(3 - 2\sqrt{6}) & \le & \lambda & \le & \frac{t}{10}(1 + \sqrt{3}), \\ \frac{t}{10}(1 + \sqrt{3}) & < & \lambda & < & \infty. \end{array}$$

If we determine whether the caustic at $x_t(\lambda)$ is hot or cool for a fixed λ value in one interval, we will establish if the caustic is hot or cool for λ throughout that interval. Thus, we consider the configuration of the critical points of $\mathcal{F}_\lambda(x_0)$ at our fixed λ. Other than the known inflexion at $x_0 = \lambda$, the critical points will be the roots,

$$\tilde{G}(x_0) = 0.$$

Firstly choose $\lambda = -t$. Then $\tilde{G}(x_0) = 19t^2 - 12tx_0 + 5x_0^2$ which has no real roots for x_0 and so the only critical point of $\mathcal{F}_\lambda(x_0)$ is the inflexion at $x_0 = \lambda$, making the caustic cool.

Next choose $\lambda = 0$. Then $\tilde{G}(x_0) = x_0\,(5x_0 - 2t)$ and the inflexion at $x_0 = \lambda = 0$ is actually a maximum. There is one other critical point $x_0 = 2t/5$ which must occur at a lower level, making the caustic hot.

Finally choose $\lambda = t$. Then $\tilde{G}(x_0) = 11t^2 + 8tx_0 + 5x_0^2$, which again has no real roots. As in the first case, the caustic is cool.

In conclusion, the caustic $x_t(\lambda)$ is hot when $\lambda \in \left(\frac{t}{30}(3 - 2\sqrt{6}), \frac{t}{10}(1 + \sqrt{3})\right)$ and cool for all other $\lambda \in \mathbb{R}$. This gives boundary points on the caustic,

$$\begin{aligned}
\kappa &= \left(-\frac{t^5}{500}, -\frac{1}{2t} + \frac{t^3}{50}\right), \\
\psi &= \left(-\frac{t^5(3 + 8\sqrt{6})}{18000}, -\frac{1}{2t} + \frac{t^3(9 - \sqrt{6})}{450}\right),
\end{aligned}$$

which are shown in Figure 2.6.

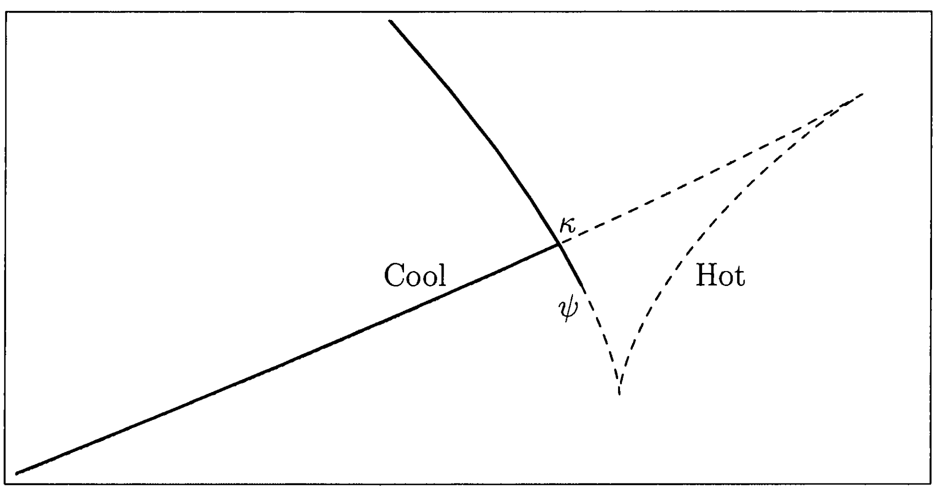

Figure 2.6: Hot and cool parts of the polynomial swallowtail caustic when $t = 1$.

2.6 The three dimensional polynomial swallowtail

We now find an explicit analytic expression for the boundary between the hot and cool parts of the three dimensional polynomial swallowtail. Previously, it has only been possible to find the hot and cool parts of this caustic numerically [34].

Let $V = 0$, $k_t = 0$ and

$$S_0(x_0, y_0, z_0) = x_0^7 + x_0^3 y_0 + x_0^2 z_0.$$

This gives,

$$\begin{aligned}\mathcal{F}_{(\lambda_1,\lambda_2)}(x_0) &= \frac{1}{2}(\lambda_1 - x_0)^3(-30\lambda_1^4 - 2\lambda_2 + 3\lambda_1 t + 8\lambda_1^3 t - 20\lambda_1^3 x_0 + tx_0 \\ &\qquad +6\lambda_1^2 t x_0 - 12\lambda_1^2 x_0^2 + 3\lambda_1 t x_0^2 - 6\lambda_1 x_0^3 + tx_0^3 - 2x_0^4),\end{aligned}$$

so that,

$$\begin{aligned}\tilde{F}(x_0) &= -30\lambda_1^4 - 2\lambda_2 + 3\lambda_1 t + 8\lambda_1^3 t - 20\lambda_1^3 x_0 + tx_0 + 6\lambda_1^2 t x_0 - 12\lambda_1^2 x_0^2 \\ &\quad +3\lambda_1 t x_0^2 - 6\lambda_1 x_0^3 + tx_0^3 - 2x_0^4, \\ \tilde{G}(x_0) &= -35\lambda_1^4 - 3\lambda_2 + 4\lambda_1 t + 9\lambda_1^3 t - 28\lambda_1^3 x_0 + 2tx_0 + 9\lambda_1^2 t x_0 - 21\lambda_1^2 x_0^2 \\ &\quad +6\lambda_1 t x_0^2 - 14\lambda_1 x_0^3 + 3tx_0^3 - 7x_0^4.\end{aligned}$$

2.6.1 Repeated roots of $\tilde{F}$

Following Corollary 2.28, we use the discriminant to find the values of $\lambda = (\lambda_1, \lambda_2)$ for which $\tilde{F}(x_0)$ has a repeated root. As $\tilde{F}(x_0)$ is a quartic in x_0, we use Theorem 1.31 to define,

$$\begin{aligned}G_{\tilde{F}} &= \frac{1}{32}(-280\lambda_1^3 + 32t + 60\lambda_1^2 t + 6\lambda_1 t^2 + t^3), \\ H_{\tilde{F}} &= \frac{1}{16}(28\lambda_1^2 - 4\lambda_1 t - t^2), \\ I_{\tilde{F}} &= \frac{1}{4}(168\lambda_1^4 + 16\lambda_2 - 18\lambda_1 t - 32\lambda_1^3 t - t^2 - 3\lambda_1^2 t^2), \\ J_{\tilde{F}} &= \frac{1}{8}(-196\lambda_1^6 - 28\lambda_1^2\lambda_2 + 14\lambda_1^3 t + 56\lambda_1^5 t + 4\lambda_1\lambda_2 t + t^2 + \lambda_1^2 t^2 + 7\lambda_1^4 t^2 \\ &\quad +\lambda_2 t^2 - \lambda_1 t^3 - 2\lambda_1^3 t^3).\end{aligned}$$

Thus,

$$D_{x_0}(\tilde{F}(x_0))$$

$$\begin{aligned}
= \quad & 4096\lambda_2^3 + 3\lambda_2^2(35952\,\lambda_1^4 - 4608\lambda_1 t - 6176\lambda_1^3 t - 256t^2 - 408\lambda_1^2 t^2 \\
& -72\lambda_1 t^3 - 9t^4) + 6\lambda_2(176400\lambda_1^8 - 44856\lambda_1^5 t - 64848\lambda_1^7 t + 2844\lambda_1^2 t^2 \\
& +6276\lambda_1^4 t^2 + 1640\lambda_1^6 t^2 + 252\lambda_1 t^3 + 962\lambda_1^3 t^3 + 276\lambda_1^5 t^3 - t^4 + 75\lambda_1^2 t^4 \\
& +81\lambda_1^4 t^4 + 9\lambda_1 t^5 + 18\lambda_1^3 t^5) + 3704400\lambda_1^{12} - 1375920\lambda_1^9 t - 2116800\lambda_1^{11} t \\
& +168588\lambda_1^6 t^2 + 464184\lambda_1^8 t^2 + 251496\lambda_1^{10} t^2 - 6588\lambda_1^3 t^3 - 16740\lambda_1^5 t^3 \\
& +12492\lambda_1^7 t^3 + 21664\lambda_1^9 t^3 - 27t^4 - 1026\lambda_1^2 t^4 - 5517\lambda_1^4 t^4 - 6258\lambda_1^6 t^4 \\
& +45\lambda_1^8 t^4 - 258\lambda_1^3 t^5 - 576\lambda_1^5 t^5 - 108\lambda_1^7 t^5 - t^6 - 36\lambda_1^2 t^6 - 135\lambda_1^4 t^6 \\
& -135\lambda_1^6 t^6.
\end{aligned}$$

This is a cubic in λ_2 and so we find its real roots $\lambda_2 = \lambda_2(\lambda_1)$.

Lemma 2.31. *Let $t > 0$ and*

$$\begin{aligned}
f_0(\lambda_1) \quad = \quad & 1568\lambda_1^6 - 672t\lambda_1^5 - 12t^2\lambda_1^4 + 4t(3t^2 - 70)\lambda_1^3 + 3t^2(t^2 + 20)\lambda_1^2 \\
& +6t^3\lambda_1 + t^4 + 16t^2,
\end{aligned}$$

then $f_0(\lambda_1) = 0$ has no real solutions for λ_1.

Proof. This follows by applying Sturm's Theorem (Theorem 1.35) to $f_0(\lambda_1)$. □

Lemma 2.32. *The equation $D_{x_0}(\tilde{F}(x_0)) = 0$ has exactly one real solution for λ_2 if $G_{\tilde{F}} \neq 0$.*

Proof. From Lemma 2.32, $f_0(\lambda)$ has no real zeros and so is always positive. Therefore, assuming $G_{\tilde{F}} \neq 0$,

$$D_{\lambda_2}(D_{x_0}(\tilde{F}(x_0))) = 2916 \times G_{\tilde{F}}^2 \times f_0(\lambda_1)^3 > 0.$$

Hence, by Theorem 1.29, the cubic $D_{x_0}(\tilde{F}(x_0)) = 0$ will have exactly one real solution. □

Proposition 2.33. *Assume that $G_{\tilde{F}} \neq 0$, then $\tilde{F}(x_0)$ can only be a real polynomial with a real repeated root if,*

$$\begin{aligned}
& \lambda_2 = \lambda_2^{\tilde{F}}(\lambda_1) \\
:= \quad & \frac{1}{4096}\Big(-35952\lambda_1^4 + 4608\lambda_1 t + 6176\lambda_1^3 t + 256t^2 + 408\lambda_1^2 t^2 + 72\lambda_1 t^3 \\
& +9t^4 + \{P_{\tilde{F}}(\lambda_1) - Q_{\tilde{F}}(\lambda_1)\}^{\frac{1}{3}} + \{P_{\tilde{F}}(\lambda_1) + Q_{\tilde{F}}(\lambda_1)\}^{\frac{1}{3}}\Big), \qquad (2.15)
\end{aligned}$$

where,

$$\begin{aligned}
P_{\tilde{F}}(\lambda_1) &= 27\left(14269853696\lambda_1^{12} - 14611251200\lambda_1^{9}t - 12231303168\lambda_1^{11}t\right. \\
&+3403939840\lambda_1^{6}t^2 + 9392947200\lambda_1^{8}t^2 + 4441479168\lambda_1^{10}t^2 \\
&-293601280\lambda_1^{3}t^3 - 14588313260\lambda_1^{5}t^3 - 1458831360\lambda_1^{7}t^3 \\
&-1629788160\lambda_1^{9}t^3 + 8388608t^4 + 62914560\lambda_1^{2}t^4 + 32440320\lambda_1^{4}t^4 \\
&+182190080\lambda_1^{6}t^4 + 437556480\lambda_1^{8}t^4 + 6291456\lambda_1 t^5 - 4587520\lambda_1^{3}t^5 \\
&-81838080\lambda_1^{5}t^5 + 1631232\lambda_1^{7}t^5 + 1048576t^6 + 6930432\lambda_1^{2}t^6 \\
&-3072000\lambda_1^{4}t^6 - 8522496\lambda_1^{6}t^6 + 835584\lambda_1 t^7 + 1081344\lambda_1^{3}t^7 \\
&-2375424\lambda_1^{5}t^7 + 69632t^8 + 417792\lambda_1^{2}t^8 + 45648\lambda_1^{4}t^8 + 41472\lambda_1 t^9 \\
&\left.+54432\lambda_1^{3}t^9 + 2304t^{10} + 8856\lambda_1^{2}t^{10} + 648\lambda_1 t^{11} + 27t^{12}\right), \\
Q_{\tilde{F}}(\lambda_1) &= 110592\left|280\lambda_1^3 - 32t - 60\lambda_1^2 t - 6\lambda_1 t^2 - t^3\right| \\
&\times\left(1568\lambda_1^6 - 280\lambda_1^3 t - 672\lambda_1^5 t + 16t^2 + 60\lambda_1^2 t^2 - 12\lambda_1^4 t^2 + 6\lambda_1 t^3\right. \\
&\qquad\left.+12\lambda_1^3 t^3 + t^4 + 3\lambda_1^2 t^4\right)^{\frac{3}{2}}.
\end{aligned}$$

Proof. This is the real solution of a cubic given that it has exactly one real root [31]. □

We now consider the case $G_{\tilde{F}} = 0$ by returning to the original quartic $\tilde{F}(x_0)$.

Lemma 2.34. *If $G_{\tilde{F}} = 0$ then $\tilde{F}(x_0)$ has a repeated real root if and only if,*

$$4I_{\tilde{F}} - 3H_{\tilde{F}}^2 = 0.$$

Proof. If $G_{\tilde{F}} = 0$, then by Theorem 1.31 we can transform $\tilde{F}$ into a quadratic in z^2,

$$z^4 + 6H_p z^2 + \alpha^2 I_p - 3H_p^2 = 0,$$

which will have a repeated root if either $4I_{\tilde{F}} - 12H_{\tilde{F}}^2 = 0$ or $4I_{\tilde{F}} - 3H_{\tilde{F}}^2 = 0$.

If $4I_{\tilde{F}} - 3H_{\tilde{F}}^2 = 0$, the quartic equation is $z^4 + 6H_{\tilde{F}}z^2 = 0$, which has a real repeated root $z = 0$.

If $4I_{\tilde{F}} - 12H_{\tilde{F}}^2 = 0$, the equation becomes $(z^2 + 3H_{\tilde{F}})^2 = 0$, which has two repeated roots $z = \pm\sqrt{-3H_{\tilde{F}}}$. However, if $G_{\tilde{F}} = 0$ then $H_{\tilde{F}} \geq 0$ and these are two distinct complex repeated roots. □

Theorem 2.35. *The polynomial $\tilde{F}(x_0)$ can only be a real polynomial with a real repeated root if*

$$\lambda_2 = \lambda_2^{\tilde{F}}(\lambda_1),$$

where $\lambda_2^{\tilde{F}}(\lambda_1)$ is defined in equation (2.15).

Proof. When $G_{\tilde{F}} \neq 0$, this reiterates Proposition 2.33. It remains to show that Lemma 2.34 is equivalent to the above.

Assuming λ_1 is such that $G_{\tilde{F}} = 0$, we can solve $4I_{\tilde{F}} - 3H_{\tilde{F}}^2 = 0$ for λ_2 to give,

$$\lambda_2(\lambda_1) = \frac{1}{4096}(-40656\lambda_1^4 + 4608\lambda_1 t + 7520\lambda_1^3 t + 256t^2 + 648\lambda_1^2 t^2 + 24\lambda_1 t^3 + 3t^4).$$

However, $Q_{\tilde{F}}(\lambda_1) = 0$ so,

$$\begin{aligned}\lambda_2^{\tilde{F}}(\lambda_1) &= \frac{1}{4096}\Big(-35952\lambda_1^4 + 4608\lambda_1 t + 6176\lambda_1^3 t + 256t^2 + 408\lambda_1^2 t^2 \\ &\quad +72\lambda_1 t^3 + 9t^4 + 2\left\{P_{\tilde{F}}(\lambda_1)\right\}^{\frac{1}{3}}\Big).\end{aligned}$$

Moreover,

$$\lambda_2^{\tilde{F}}(\lambda_1) - \lambda_2(\lambda_1) = \frac{1}{2048}\left(3(28\lambda_1^2 - 4\lambda_1 t - t^2)^2 + P_{\tilde{F}}(\lambda_1)^{\frac{1}{3}}\right) = 0. \qquad \square$$

Although $Q_{\tilde{F}}(\lambda_1)$ is cusped when λ_1 satisfies $G_{\tilde{F}} = 0$, it is clear that $\lambda_2^{\tilde{F}}(\lambda_1)$ is not. This follows by considering the Taylor expansion in a neighbourhood of λ_1 where $|P_{\tilde{F}}(\lambda_1)| < |Q_{\tilde{F}}(\lambda_1)|$. Then,

$$\begin{aligned}&(P_{\tilde{F}}(\lambda_1) + Q_{\tilde{F}}(\lambda_1))^{\frac{1}{3}} + (P_{\tilde{F}}(\lambda_1) - Q_{\tilde{F}}(\lambda_1))^{\frac{1}{3}} \\ &= P_{\tilde{F}}(\lambda_1)^{\frac{1}{3}}\left\{\left(1 + \frac{Q_{\tilde{F}}(\lambda_1)}{P_{\tilde{F}}(\lambda_1)}\right)^{\frac{1}{3}} + \left(1 - \frac{Q_{\tilde{F}}(\lambda_1)}{P_{\tilde{F}}(\lambda_1)}\right)^{\frac{1}{3}}\right\} \\ &= P_{\tilde{F}}(\lambda_1)^{\frac{1}{3}}\left\{2 + \frac{2Q_{\tilde{F}}(\lambda_1)^2}{-9P_{\tilde{F}}(\lambda_1)^2} + \frac{20Q_{\tilde{F}}(\lambda_1)^4}{-243P_{\tilde{F}}(\lambda_1)^4} + \dots\right\},\end{aligned}$$

which only involves even powers of $Q_{\tilde{F}}$ and so is not cusped.

2.6.2 Repeated roots of $\tilde{G}$

We apply the analysis of Section 2.6.1 to $\tilde{G}$. The discriminant of $\tilde{G}$ is given by,

$$\begin{aligned}&D_{x_0}(\tilde{G}(x_0)) \\ &= \frac{27}{256}\big(47059600\lambda_1^{12} - 18823840\lambda_1^9 t - 24202080\lambda_1^{11} t + 2458624\lambda_1^6 t^2 \\ &\quad +5416656\lambda_1^8 t^2 + 2103276\lambda_1^{10} t^2 - 98784\lambda_1^3 t^3 - 131712\lambda_1^5 t^3 + 411600\lambda_1^7 t^3 \\ &\quad +310072\lambda_1^9 t^3 - 784t^4 - 21168\lambda_1^2 t^4 - 94668\lambda_1^4 t^4 - 81340\lambda_1^6 t^4 + 7791\lambda_1^8 t^4\end{aligned}$$

$$
\begin{aligned}
&-4312\lambda_1^3t^5 - 5796\lambda_1^5t^5 + 3654\lambda_1^7t^5 - 32t^6 - 816\lambda_1^2t^6 - 2664\lambda_1^4t^6 \\
&-2349\lambda_1^6t^6) + \frac{81\lambda_2}{128}\left(2689120\lambda_1^8 - 729904\lambda_1^5t - 883568\lambda_1^7t + 49392\lambda_1^2t^2\right. \\
&+79576\lambda_1^4t^2 + 4802\lambda_1^6t^2 + 5488\lambda_1t^3 + 17444\lambda_1^3t^3 + 1862\lambda_1^5t^3 - 28t^4 \\
&\left.+1414\lambda_1^2t^4 + 903\lambda_1^4t^4 + 216\lambda_1t^5 + 387\lambda_1^3t^5\right) + \frac{81\lambda_2^2}{256}(653072\lambda_1^4 \\
&-87808\lambda_1t - 98784\lambda_1^3t - 6272t^2 - 7448\lambda_1^2t^2 - 1512\lambda_1t^3 - 243t^4) \\
&+9261\lambda_2^3.
\end{aligned}
$$

Working exactly as in items 2.31 to 2.35, we reach the following conclusion.

Theorem 2.36. *The polynomial $\tilde{G}(x_0)$ can only be a real polynomial with a real repeated root if*

$$
\begin{aligned}
\lambda_2 &= \lambda_2^{\tilde{G}}(\lambda_1) \\
&:= \frac{1}{87808}\left(-653072\lambda_1^4 + 87808\lambda_1t + 98784\lambda_1^3t + 6272t^2 + 7448\lambda_1^2t^2\right. \\
&\qquad +1512\lambda_1t^3 + 243t^4 \\
&\qquad \left.+\{P_{\tilde{G}}(\lambda_1) - Q_{\tilde{G}}(\lambda_1)\}^{\frac{1}{3}} + \{P_{\tilde{G}}(\lambda_1) + Q_{\tilde{G}}(\lambda_1)\}^{\frac{1}{3}}\right), \qquad (2.16)
\end{aligned}
$$

where,

$$
\begin{aligned}
&P_{\tilde{G}}(\lambda_1) = \\
&\quad 2664613881638912\lambda_1^{12} - (2850893879443456\lambda_1^9 + 2283954755690496\lambda_1^{11})t \\
&\quad +(796028810493952\lambda_1^6 + 1832717493927936\lambda_1^8 + 845202101839872\lambda_1^{10})t^2 \\
&\quad -(84627647627264\lambda_1^3 + 341155204497408\lambda_1^5 + 295535613198336\lambda_1^7 \\
&\quad +321899108894720\lambda_1^9)t^3 + (3022415986688 + 18134495920128\lambda_1^2 \\
&\quad +7083787468800\lambda_1^4 + 54450713010176\lambda_1^6 + 82238345145600\lambda_1^8)t^4 \\
&\quad +(1942981705728\lambda_1 - 3373232128000\lambda_1^3 - 20229273071616\lambda_1^5 \\
&\quad +2502094930944\lambda_1^7)t^5 + (416353222656 + 2016710922240\lambda_1^2 \\
&\quad -1337968429056\lambda_1^4 - 1204816114432\lambda_1^6)t^6 + (284384120832\lambda_1 \\
&\quad +139868660736\lambda_1^3 - 675993136896\lambda_1^5)t^7 + (30469727232 \\
&\quad +128152088064\lambda_1^2 - 18343447920\lambda_1^4)t^8 + (15554923776\lambda_1 \\
&\quad +12602368800\lambda_1^3)t^9 + (1111065984 + 2985989832\lambda_1^2)t^{10} \\
&\quad +267846264\lambda_1t^{11} + 14348907t^{12}, \\
&Q_{\tilde{G}}(\lambda_1) = \\
&\quad 175616\left|5488\lambda_1^3 - 784t - 1176\lambda_1^2t - 126\lambda_1t^2 - 27t^3\right| \\
&\quad \times\Big(48020\lambda_1^6 - 10976\lambda_1^3t - 20580\lambda_1^5t + 784t^2 + 2352\lambda_1^2t^2 - 735\lambda_1^4t^2
\end{aligned}
$$

$$+252\lambda_1 t^3 + 350\lambda_1^3 t^3 + 54t^4 + 135\lambda_1^2 t^4\Big)^{\frac{3}{2}}.$$

Proof. This follows exactly as Theorem 2.35. □

2.6.3 Eliminating the false positive boundaries

We have identified two curves of values for $\lambda = (\lambda_1, \lambda_2)$ on which $x_t(\lambda)$ is a possible hot/cool boundary, namely $\lambda_2 = \lambda_2^{\tilde{F}}(\lambda_1)$ and $\lambda_2 = \lambda_2^{\tilde{G}}(\lambda_1)$. We now need to establish those parts of the curves $x_t(\lambda_1, \lambda_2^{\tilde{F}}(\lambda_1))$ and $x_t(\lambda_1, \lambda_2^{\tilde{G}}(\lambda_1))$ that are genuine hot/cool boundaries; however, as they are curves we cannot test each point individually. Instead we find the points on these curves that separate the genuine hot/cool boundaries from the false positive boundaries. Hence, we find values of λ_1 at which this separation occurs.

Lemma 2.37. *The pre-normalised reduced action function $\mathcal{F}_\lambda(x_0)$ has at most two real critical points other than the inflexion at $x_0 = \lambda_1$, counting repetitions.*

Proof. The number of real critical points is given by the number of real zeros of,

$$\tilde{G}'(x_0) = -28\lambda_1^3 + 2t + 9\lambda_1^2 t - 42\lambda_1^2 x_0 + 12\lambda_1 t x_0 - 42\lambda_1 x_0^2 + 9t x_0^2 - 28x_0^3,$$

which has discriminant,

$$\begin{aligned} D_{x_0}(\tilde{G}'(x_0)) &= 48020\lambda_1^6 - 10976\lambda_1^3 t - 20580\lambda_1^5 t + 784t^2 + 2352\lambda_1^2 t^2 \\ &\quad -735\lambda_1^4 t^2 + 252\lambda_1 t^3 + 350\lambda_1^3 t^3 + 54t^4 + 135\lambda_1^2 t^4. \end{aligned}$$

Sturm's Theorem (Theorem 1.35) shows that this discriminant has no real roots and hence, must always be positive. Therefore, by Theorem 1.30, $\tilde{G}(x_0)$ has exactly one critical point and so has at most two real zeros. □

Lemma 2.38. *There is only one value of λ_1 at which the curves $x_t(\lambda_1, \lambda_2^{\tilde{F}}(\lambda_1))$ and $x_t(\lambda_1, \lambda_2^{\tilde{G}}(\lambda_1))$ may change from a genuine hot/cool boundary to a false positive boundary, namely when,*

$$\lambda_1 = \tilde{\lambda}_1(t) :=$$
$$\frac{1}{14}\left(t + \left\{\frac{5t^5}{98 + 5t^2 + 14\sqrt{49 + 5t^2}}\right\}^{\frac{1}{3}} + \left\{\frac{98t + 5t^3 + 14t\sqrt{49 + 5t^2}}{5}\right\}^{\frac{1}{3}}\right).$$

Proof. Lemma 2.37 restricts the possible combinations of critical points on the pre-normalised reduced action function evaluated on the curves $\lambda_2 = \lambda_2^{\tilde{F}}(\lambda_1)$

and $\lambda_2 = \lambda_2^{\tilde{G}}(\lambda_1)$ to those shown as possible hot/cool boundaries in Figure 2.5 (row 2). Therefore, the curve $x_t(\lambda_1, \lambda_2^{\tilde{F}}(\lambda_1))$ can only change from a genuine hot/cool boundary to a false positive boundary if the repeated root $r_{\tilde{F}}$ coalesces with the inflexion at $x_0^1 = \lambda_1$, and the curve $x_t(\lambda_1, \lambda_2^{\tilde{G}}(\lambda_1))$ can only change if the two inflexions on $\mathcal{F}_{(\lambda_1, \lambda_2^{\tilde{G}}(\lambda_1))}$ coalesce.

If either of these occur then,

$$\mathcal{F}_\lambda(x_0) = \mathcal{F}'_\lambda(x_0) = \mathcal{F}''_\lambda(x_0) = \mathcal{F}'''_\lambda(x_0) = \mathcal{F}^{(4)}_\lambda(x_0) = 0,$$

and so from Proposition 2.15, $x_t(\lambda)$ is a cusp on the subcaustic. There is only one such point on the three dimensional polynomial swallowtail (see Example 2.9) which is where λ_1 is the only real root of,

$$70\lambda_1^3 - 15\lambda_1^2 t - t = 0. \qquad \square$$

From the construction of $x_t(\lambda_1, \lambda_2^{\tilde{F}}(\lambda_1))$ and $x_t(\lambda_1, \lambda_2^{\tilde{G}}(\lambda_1))$, it is apparent that both curves will pass through the cusp on the subcaustic as both $\tilde{F}$ and $\tilde{G}$ will have a repeated root at this point.

Proposition 2.39. *For $\lambda_1 > \tilde{\lambda}_1(t)$ the curve $x_t(\lambda_1, \lambda_2^{\tilde{F}}(\lambda_1))$ is a false positive boundary.*

Proof. If $\lambda_2 = \lambda_2^{\tilde{F}}(\lambda_1)$ then $\tilde{F}(x_0)$ will have a repeated root $r_{\tilde{F}}$. Since $\mathcal{F}_\lambda(x_0) \to \pm\infty$ as $x_0 \to \pm\infty$, it follows from Lemma 2.37 that $x_t(\lambda_1, \lambda_2^{\tilde{F}}(\lambda_1))$ is a false positive boundary if $r_{\tilde{F}} < \lambda_1$.

We test one point on the curve, where $\lambda_1 = t + 1 > \tilde{\lambda}_1(t)$, to find whether the curve is a false positive boundary for all $\lambda_1 > \tilde{\lambda}_1(t)$.

When $\lambda_1 = t + 1$, the repeated root is $r_{\tilde{F}} = a(t)/b(t)$ where,

$$\begin{aligned} a(t) &= 5880 + 37184t + 102940t^2 + 160393t^3 + 150855t^4 + 84988t^5 \\ &\quad +26317t^6 + 3428t^7 + \lambda_2^{\tilde{F}}(t+1)\left(392 + 1044t + 1030t^2 + 311t^3\right), \\ b(t) &= 8\lambda_2^{\tilde{F}}(t+1)\left(28 + 52t + 23t^2\right) \\ &\quad +t\left(392 + 1488t + 2438t^2 + 2086t^3 + 950t^5 + 181t^6\right) \end{aligned}$$

and

$$\begin{aligned} \lambda_2^{\tilde{F}}(t+1) &= \frac{1}{4096}\Big(- 35952 - 133024t - 191912t^2 - 124392t^3 - 29287t^4 \\ &\quad +(P_{\tilde{F}}(t+1) - Q_{\tilde{F}}(t+1))^{\frac{1}{3}} + (P_{\tilde{F}}(t+1) + Q_{\tilde{F}}(t+1))^{\frac{1}{3}}\Big). \end{aligned}$$

Since $P_{\tilde{F}}(t+1) \pm Q_{\tilde{F}}(t+1) > 0$, it follows that,

$$a(t) - (t+1)b(t) > 0. \qquad (2.17)$$

Moreover,

$$\begin{aligned} P_{\tilde{F}}(1+t) - Q_{\tilde{F}}(t+1) &< P_{\tilde{F}}(1+t) \\ &< \left(1742t^4 + 7855t^3 + 11675t^2 + 8179t + 2426\right)^3, \end{aligned}$$

and

$$\begin{aligned} &P_{\tilde{F}}(1+t) + Q_{\tilde{F}}(t+1) \\ &\quad < P_{\tilde{F}}(1+t) \\ &\qquad\quad +4096\left(280 + 748t + 714t^2 + 213t^3\right)\left(30t^3 + 101t^2 + 106t + 42\right)^3 \\ &\quad < \left(6676t^4 + 29315t^3 + 47663t^2 + 33773t + 9558\right)^3. \end{aligned}$$

Therefore,

$$b(t) < -3t^2\left(8 + 11470t^2 + 6534t^3 + 29t^4\right) < 0,$$

and it follows from inequality (2.17) that $r_{\tilde{F}} < t + 1$. $\square$

Proposition 2.40. *For $\lambda_1 < \tilde{\lambda}_1$, the curve $x_t(\lambda_1, \lambda_2^{\tilde{G}}(\lambda_1))$ is a false positive boundary.*

Proof. If $\lambda_2 = \lambda_2^{\tilde{G}}(\lambda_1)$ then $\tilde{G}(x_0)$ will have a repeated root $r_{\tilde{G}}$. Since $\mathcal{F}_\lambda(x_0) \to \pm\infty$ as $x_0 \to \pm\infty$, it follows from Lemma 2.37 that $x_t(\lambda_1, \lambda_2^{\tilde{G}}(\lambda_1))$ will be a false positive boundary if $r_{\tilde{G}} > \lambda_1$.

Again we test a single point of the curve, $\lambda_1 = 0 < \tilde{\lambda}_1(t)$, to show that the curve is a false positive boundary for all $\lambda_1 < \tilde{\lambda}_1(t)$. When $\lambda_1 = 0$, the repeated root is given by,

$$r_{\tilde{G}} = \frac{1568\lambda_2^{\tilde{G}}(0) - 28t^2 + 81\lambda_2^{\tilde{G}}(0)t^2}{4t(196 + 63\lambda_2^{\tilde{G}}(0) + 9t^2)},$$

where,

$$\lambda_2^{\tilde{G}}(0) = \frac{1}{87808}\left(6272t^2 + 243t^4 + (P_{\tilde{G}}(0) - Q_{\tilde{G}}(0))^{\frac{1}{3}} + (P_{\tilde{G}}(0) + Q_{\tilde{G}}(0))^{\frac{1}{3}}\right).$$

Since $P_{\tilde{G}}(0) \pm Q_{\tilde{G}}(0) > 0$, it follows that,

$$\lambda_2^{\tilde{G}}(0) > \frac{6272t^2 + 243t^4}{87808} > \frac{28t^2}{1568 + 81t^2},$$

and so $r_{\tilde{G}} > 0 = \lambda_1$.

$\square$

We can combine Propositions 2.39 and 2.40 to conclude that:

Theorem 2.41. *The only curve which could be a genuine hot/cool boundary on the polynomial swallowtail is given by* $x_t(\lambda_1, \lambda_2(\lambda_1))$ *where,*

$$\lambda_2(\lambda_1) := \begin{cases} \lambda_2^{\tilde{F}}(\lambda_1) & \text{if} \quad \lambda_1 < \tilde{\lambda}_1, \\ \lambda_2^{\tilde{G}}(\lambda_1) & \text{if} \quad \lambda_1 > \tilde{\lambda}_1. \end{cases} \tag{2.18}$$

This is a continuous function of λ_1.

2.6.4 Identifying the hot and cool parts

The curve $\lambda_2 = \lambda_2(\lambda_1)$ in Theorem 2.41 divides the (λ_1, λ_2) plane into two parts. We identify a point on each side of the curve and analyse whether $x_t(\lambda_1, \lambda_2)$ is hot or cool.

Theorem 2.42. *A point on the caustic* $x_t(\lambda_1, \lambda_2)$ *will be:*

1. HOT *if* $\lambda_2 < \lambda_2(\lambda_1)$*; or,*
2. COOL *if* $\lambda_2 \geq \lambda_2(\lambda_1)$*,*

where $\lambda_2(\lambda_1)$ *is given in equation (2.18).*

Proof. Consider the point $x_t(\lambda)$ where $\lambda = (0, 0)$. This lies on the subcaustic and therefore, at this point the function $\mathcal{F}_\lambda(x_0)$ has a quadruple repeated root $x_0 = 0$,

$$\mathcal{F}_{(0,0)}(x_0) = \frac{1}{2} x_0^4 \left(2x_0^3 - t x_0^2 - t\right),$$

and

$$\mathcal{F}_{(0,0)}^{(4)}(0) = -12t < 0.$$

Therefore, there is a maximum at $x_0 = 0$ and by Lemma 2.37 there is only one other critical point (which must then be a minimum). Thus, at $x_t(0, 0)$, the caustic will be hot. Moreover, since $\lambda_2 = 0 < \lambda_2(0)$, we conclude that a point $x_t(\lambda_1, \lambda_2)$ is on a hot part of the caustic if $\lambda_2 < \lambda_2(\lambda_1)$.

Now let $\lambda = (0, \lambda_2^{\tilde{G}}(0))$. Then from the proof of Proposition 2.40, it follows that the caustic is cool. Moreover,

$$\frac{\mathrm{d}}{\mathrm{d}t}\left(\lambda_2^{\tilde{G}}(0) - \lambda_2(0)\right) = \frac{t}{351232}\left(6272 + 801t^2\right) > 0,$$

so that $\lambda_2^{\tilde{G}}(0) - \lambda_2(0)$ is an increasing function of t. When $t = 0$, $\lambda_2^{\tilde{G}}(0) - \lambda_2(0) = 0$ and so $\lambda_2^{\tilde{G}}(0) > \lambda_2(0)$ for all $t \geq 0$. Thus, we conclude that the caustic is cool if $\lambda_2 > \lambda_2(\lambda_1)$. □

The hot and cool parts of the caustic are shown in Figures 2.7 and 2.8. The cool parts are indicated by a mesh drawn onto the surface.

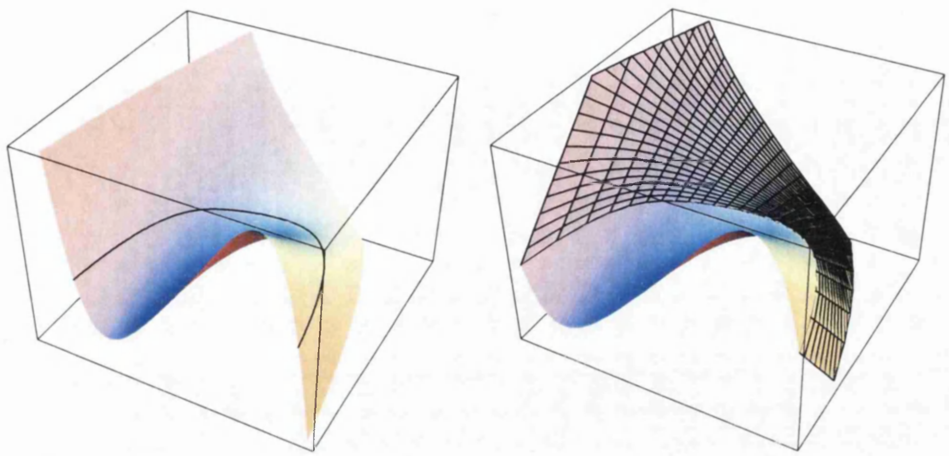

Boundary on the pre-caustic. *Hot and cool parts.*

Figure 2.7: Hot and cool parts of the 3D polynomial swallowtail pre-caustic when $t = 1$.

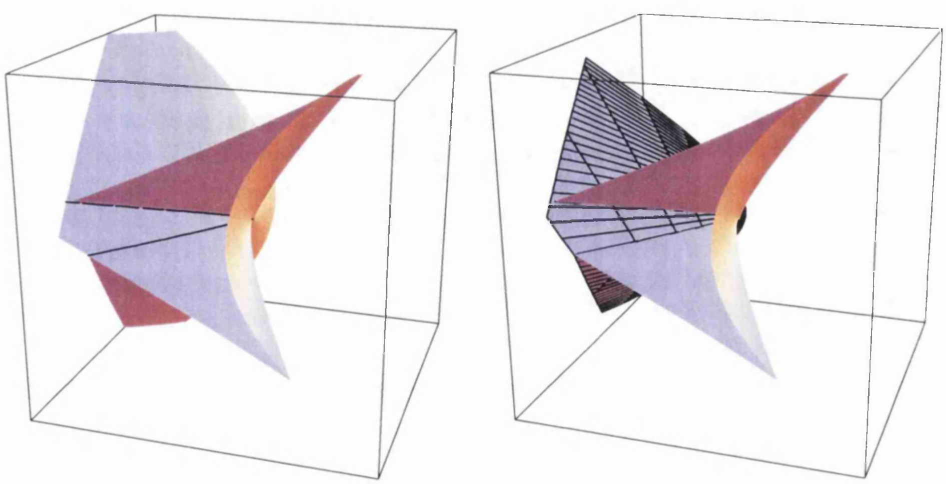

Boundary on the caustic. *Hot and cool parts.*

Figure 2.8: Hot and cool parts of the 3D polynomial swallowtail caustic when $t = 1$.

2.7 The non-generic swallowtail

Our final example is a two dimensional caustic which mutates with time. Let $V = 0$, $k_t = 0$ and

$$S_0(x_0, y_0) = x_0^5 + |x_0|^{\frac{3}{2}} y_0.$$

This caustic was first investigated by DTZ [12]. It begins with a single swallowtail, but develops a second when $t = t_c = 1.05327\ldots$ and the two swallowtails then move together to form a five pointed star which finally becomes an arrowhead within a swallowtail. This development is shown in Figure 2.9 where the caustic $x_t(\lambda)$ has been separated into two parts corresponding to $\lambda > 0$ (solid line) and $\lambda < 0$ (dashed line). This separation has been highlighted because the initial condition gives two separate and distinct parameterisations for the two cases. The development of the second swallowtail will be discussed in Chapter 3.

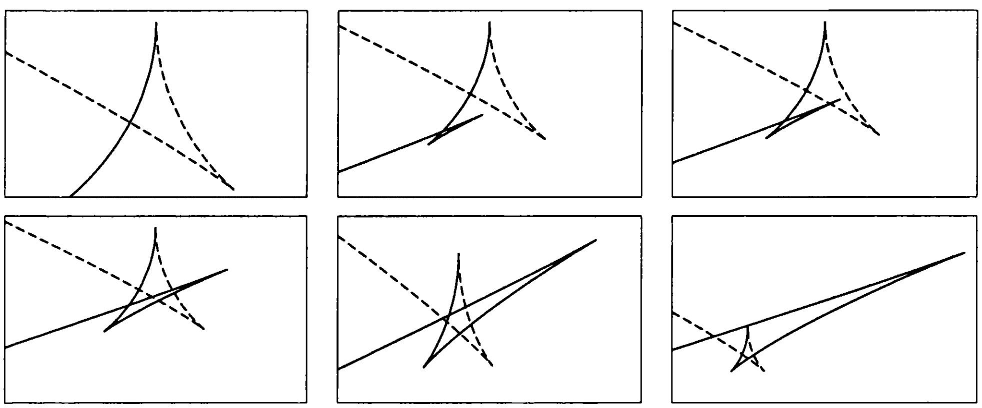

Figure 2.9: The non-generic swallowtail caustic when $t = 1$, 1.2, 1.23, 1.3, 1.4 and 1.6

Due to the complexity of the equations, we solve this example numerically making use of the geometry whenever possible to reduce the workload. The pre-normalised reduced action function evaluated on the caustic is given by,

$$\mathcal{F}_\lambda(x_0) = \begin{cases} \mathcal{F}_\lambda^1(x_0) & \text{if } \lambda > 0, \\ \mathcal{F}_\lambda^2(x_0) & \text{if } \lambda < 0, \end{cases}$$

where,

$$\mathcal{F}^1_\lambda(x_0) = \begin{cases} -\frac{1}{6t}\left(\lambda^{\frac{1}{2}} - x_0{}^{\frac{1}{2}}\right)^3 \tilde{F}_{1a}(x_0) & \text{if } x_0 > 0, \\ -\frac{1}{6t}\tilde{F}_{1b}(x_0) & \text{if } x_0 < 0, \end{cases}$$

$$\mathcal{F}^2_\lambda(x_0) = \begin{cases} \frac{1}{6t}\tilde{F}_{2a}(x_0) & \text{if } x_0 > 0, \\ -\frac{1}{6t}\left(|\lambda|^{\frac{1}{2}} - |x_0|^{\frac{1}{2}}\right)^3 \tilde{F}_{2b}(x_0) & \text{if } x_0 < 0. \end{cases}$$

The functions $\tilde{F}$ are given by,

$$\begin{aligned}
\tilde{F}_{1a} &= 56\lambda^{\frac{7}{2}}t - 6\lambda^{\frac{3}{2}}t^2 + (3 + 168\lambda^3 t - 18\lambda t^2)x_0^{\frac{1}{2}} + (126\lambda^{\frac{5}{2}}t - 9\lambda^{\frac{1}{2}}t^2)x_0 \\
&\quad +(90\lambda^2 t - 3t^2)x_0^{\frac{3}{2}} + 60\lambda^{\frac{3}{2}}tx_0^2 + 36\lambda t x_0^{\frac{5}{2}} + 18\lambda^{\frac{1}{2}}tx_0^3 + 6tx_0^{\frac{7}{2}} + \lambda^{\frac{1}{2}}, \\
\tilde{F}_{1b} &= \lambda^2 + 56\lambda^5 t - 6\lambda^3 t^2 + (8\lambda^{\frac{1}{2}} + 160\lambda^{\frac{7}{2}}t - 24\lambda^{\frac{3}{2}}t^2)(-x_0)^{\frac{3}{2}} \\
&\quad -(6\lambda + 210\lambda^4 t - 27\lambda^2 t^2)x_0 - 3x_0^2 - 3t^2x_0^3 - 6tx_0^5, \\
\tilde{F}_{2a} &= -\lambda^2 - 56\lambda^5 t - 6\lambda^3 t^2 - (8(-\lambda)^{\frac{1}{2}} + 160(-\lambda)^{\frac{7}{2}}t + 24(-\lambda)^{\frac{3}{2}}t^2)x_0^{\frac{3}{2}} \\
&\quad +(6\lambda + 210\lambda^4 t + 27\lambda^2 t^2)x_0 + 3x_0^2 - 3t^2x_0^3 + 6tx_0^5, \\
\tilde{F}_{2b} &= -(-\lambda)^{\frac{1}{2}} - 56(-\lambda)^{\frac{7}{2}}t - 6(-\lambda)^{\frac{3}{2}}t^2 - (3 + 168\lambda^3 t + 18\lambda t^2)(-x_0)^{\frac{1}{2}} \\
&\quad -(126(-\lambda)^{\frac{5}{2}}t + 9(-\lambda)^{\frac{1}{2}}t^2)x_0 + (90\lambda^2 t + 3t^2)(-x_0)^{\frac{3}{2}} \\
&\quad -60(-\lambda)^{\frac{3}{2}}tx_0^2 - 36\lambda t(-x_0)^{\frac{5}{2}} - 18(-\lambda)^{\frac{1}{2}}tx_0^3 + 6t(-x_0)^{\frac{7}{2}},
\end{aligned}$$

and therefore,

$$\begin{aligned}
\tilde{G}_{1a} &= 2 + 70\lambda^3 t - 9\lambda t^2 + (60\lambda^{\frac{5}{2}}t - 6\lambda^{\frac{1}{2}}t^2)x_0^{\frac{1}{2}} + (50\lambda^2 t - 3t^2)x_0 \\
&\quad +40\lambda^{\frac{3}{2}}tx_0^{\frac{3}{2}} + 30\lambda t x_0^2 + 20\lambda^{\frac{1}{2}}tx_0^{\frac{5}{2}} + 10tx_0^3, \\
\tilde{G}_{1b} &= 2\lambda + 70\lambda^4 t - 9\lambda^2 t^2 + (4\lambda^{\frac{1}{2}} + 80\lambda^{\frac{7}{2}}t - 12\lambda^{\frac{3}{2}}t^2)(-x_0)^{\frac{1}{2}} + 2x_0 + 3t^2x_0^2 \\
&\quad +10tx_0^4, \\
\tilde{G}_{2a} &= 2\lambda + 70\lambda^4 t + 9\lambda^2 t^2 - (4(-\lambda)^{\frac{1}{2}} + 80(-\lambda)^{\frac{7}{2}}t + 12(-\lambda)^{\frac{3}{2}}t^2)x_0^{\frac{1}{2}} + 2x_0 \\
&\quad -3t^2x_0^2 + 10tx_0^4, \\
\tilde{G}_{2b} &= -70\lambda^3 t - 9\lambda t^2 + (60(-\lambda)^{\frac{5}{2}}t + 6(-\lambda)^{\frac{1}{2}}t^2)(-x_0)^{\frac{1}{2}} - (50\lambda^2 t + 3t^2)x_0 \\
&\quad -40(-\lambda)^{\frac{3}{2}}t(-x_0)^{\frac{3}{2}} - 30\lambda t x_0^2 + 20(-\lambda)^{\frac{1}{2}}t(-x_0)^{\frac{5}{2}} - 10tx_0^3 - 2.
\end{aligned}$$

In this example, the factor is $\left(\sqrt{\pm\lambda} - \sqrt{\pm x_0}\right)^3$ since the initial condition is non-polynomial; moreover, there is no factorisation when λ and x_0 have opposite signs.

We now substitute $x_0 = \pm X_0^2$ into all of these functions, where $X_0 > 0$ and the sign is chosen to be appropriate for the domain of x_0. Thus, all of the

$\tilde{F}$ and $\tilde{G}$ are polynomials in X_0. If D_x denotes the discriminant taken with respect to x, then the repeated roots are given by the zeros of:

$$\begin{aligned}
D_{X_0}\left(\tilde{G}_{1a}\right) &= K_1(t)\left(-1-20\lambda^3 t+3\lambda t^2\right)P_1(\lambda,t),\\
D_{X_0}\left(\tilde{G}_{1b}\right) &= \lambda K_2(t)Q_1(\lambda,t),\\
D_{X_0}\left(\tilde{G}_{2a}\right) &= \lambda K_3(t)Q_2(\lambda,t),\\
D_{X_0}\left(\tilde{G}_{2b}\right) &= K_4(t)\left(1+20\lambda^3 t+3\lambda t^2\right)P_2(\lambda,t),\\
D_{X_0}\left(\tilde{F}_{1a}\right) &= K_5(t)\left(-1-20\lambda^3 t+3\lambda t^2\right)^2\left(-1-56\lambda^3 t+6\lambda t^2\right)R_1(\lambda,t),\\
D_{X_0}\left(\tilde{F}_{1b}\right) &= K_6(t)\lambda^6\left(-1-56\lambda^3 t+6\lambda t^2\right)S_1(\lambda,t),\\
D_{X_0}\left(\tilde{F}_{2a}\right) &= K_7(t)\lambda^6\left(1+56\lambda^3 t+6\lambda t^2\right)S_2(\lambda,t),\\
D_{X_0}\left(\tilde{F}_{1b}\right) &= K_8(t)\left(1+56\lambda^3 t+6\lambda t^2\right)\left(1+20\lambda^3 t+3\lambda t^2\right)^2 R_2(\lambda,t).
\end{aligned}$$

The $K_i(t)$ are functions of t only with $K_i(t) \neq 0$ for all $t > 0$. However, the P_i are polynomials of degree 10 in λ and t, the Q_i are polynomials of degree 25 in λ and t, the R_i are polynomials of degree 12 in λ and t, and the S_i are polynomials of degree 30 in λ and t. They are all too complicated to include here but can be found in Appendix A.

Using Sturm's Theorem (Theorem 1.35), it can be shown that the only roots in which we are interested are those arising from P_i, Q_i, R_i and S_i. The other solutions lead to the conclusion that either $X_0 = 0$ or $X_0 < 0$ and so can be discarded. We can also show that the polynomials P_2 and R_2 have no solutions for $\lambda < 0$ and so may also be discarded. Geometrically, roots of P_2 would correspond to points where the negative part of the caustic intersects itself which clearly does not occur (see Figure 2.9).

Moreover, R_1 only has roots in the interval $(t_c, 1.95111\ldots)$ in which the upper bound is the only real root of,

$$-145557134975 + 1512891415t^5 - 19064571344t^{10} + 678785292t^{15} = 0.$$

Roots of P_1 correspond to points where the positive part of the caustic intersects itself. This does not happen before time t_c after which a point of self-intersection moves along the curve until it reaches the join at $(0,0)$ when,

$$(x_t(\lambda), y_t(\lambda)) = \left(\frac{1}{2}\lambda\left(-2-70\lambda^3 t+9\lambda t^2\right), \frac{4}{3t}\sqrt{\lambda}\left(3\lambda t^2-20\lambda^3 t-1\right)\right) = 0,$$

which occurs at,

$$t^5 - 10 = 0 \quad \Rightarrow \quad t = \sqrt[5]{10}.$$

There is no longer a point of self-intersection on the positive part of the caustic after this time; therefore, we only need to find roots of P_1 for $t \in (t_c, \sqrt[5]{10})$.

Finally, there are self-intersections where the positive and negative parts meet, given by roots of Q_1 and Q_2. It is only necessary to solve one of these equations as they will both yield the same points of self-intersection.

Thus, the work has been reduced to finding solutions of,

$$P_1 = 0 \quad \text{for } t \in (t_c, \sqrt[5]{10}), \qquad R_1 = 0 \quad \text{for } t \in (t_c, 1.95111\ldots),$$

and,

$$Q_1 = 0, \qquad S_1 = 0, \qquad S_2 = 0.$$

We now proceed to solve these equations numerically. For a fixed time t we:

1. solve one of these equations for λ and select those values which are real and have the appropriate sign,
2. identify those values λ which give real positive repeated roots for X_0,
3. plot the function $F(x_0)$ at these values for λ and identify those which are genuine hot/cool boundary points.

The genuine boundaries are listed in the following table and illustrated in Figure 2.10 where the cool parts are drawn with a thick solid line and hot parts with a dashed line.

t	Cool	Hot
1.0	$-\infty< \lambda <-0.1778$ $0.01860< \lambda <\infty$	$-0.1778< \lambda <0.01860$
1.2	$-\infty< \lambda <-0.1373$ $0.01387< \lambda <0.04787$ $0.2807< \lambda <\infty$	$-0.1373< \lambda <0.01387$ $0.04787< \lambda <0.2807$
1.23	$-\infty< \lambda <-0.1321$ $0.01329< \lambda <0.04031$ $0.2935< \lambda <\infty$	$-0.1321< \lambda <0.01329$ $0.04031< \lambda <0.2935$
1.3	$-\infty< \lambda <-0.1210$ $0.01206< \lambda <0.02662$ $0.3196< \lambda <\infty$	$-0.1210< \lambda <0.01206$ $0.02662< \lambda <0.3196$
1.4	$-\infty< \lambda <-0.1114$ $0.01054< \lambda <0.01348$ $0.3525< \lambda <\infty$	$-0.1114< \lambda <0.01054$ $0.01348< \lambda <0.3525$
1.6	$-\infty< \lambda <-0.1018$ $0.4083< \lambda <\infty$	$-0.1018< \lambda <0.4083$

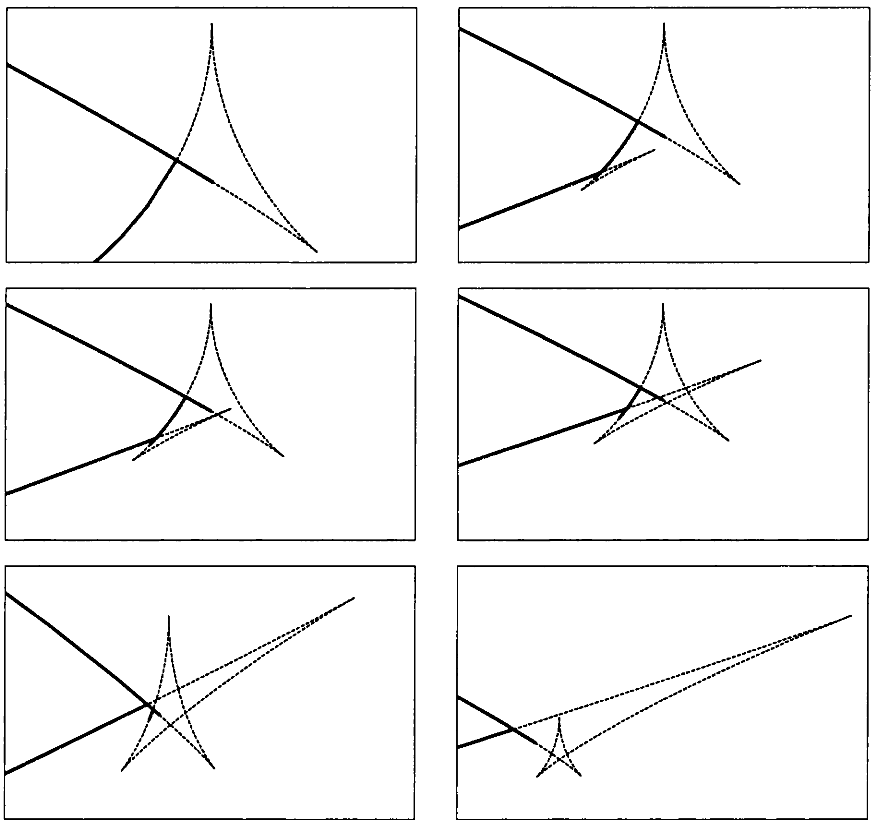

Figure 2.10: Hot and cool parts of the non-generic swallowtail.

Chapter 3

The swallowtail perestroika

Summary

In this chapter we consider how the shape of the caustic and Hamilton-Jacobi level surfaces can change spontaneously. We focus on the formation and destruction of swallowtails in the two dimensional case and investigate necessary conditions for these 'swallowtail perestroikas' to occur. We then present new geometric results, similar to those of DTZ from Chapter 1, which include these new phenomena. These ideas are then extended to the three dimensional case and we conclude by considering their implications for the Burgers fluid velocity.

3.1 Introduction

It is well known that the geometry of a caustic or wavefront can change suddenly with singularities appearing and disappearing. Arnol'd classified six such 'perestroikas' for two dimensional caustics and five for wavefronts [2]. We investigate one of these perestroikas, the formation or collapse of a swallowtail, using the much earlier works of Cayley and Klein.

In Cayley's work on plane algebraic curves, he describes the possible triple points of a curve [36]. He classified them by considering the possible combinations of double points which could collapse together to form a point at which there are three tangents. The four possibilities are shown in Figure 3.1. In each case the shape of the triple point which forms will be controlled by its tangents. Respectively, there will be:

1. three real distinct tangents,

2. three real tangents with two coincident,

3. three real tangents all of which are coincident,

4. one real tangent and two complex tangents.

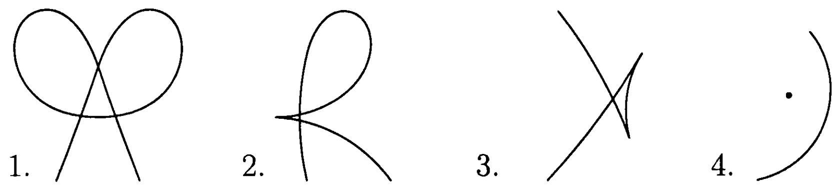

Figure 3.1: The systems of double points which collapse to form Cayley's triple points.

In his work on Riemann surfaces, Felix Klein proved that a swallowtail will form on an algebraic curve when an isolated double point (acnode) joins the main curve [23]. This event would correspond to an interchange between cases 3 and 4 in Figure 3.1, where two of the repeated real tangents from case 3 become a complex conjugate pair in case 4. This transformation from an isolated point to a swallowtail will be referred to as a 'swallowtail perestroika'.

In the analysis performed in Chapter 2, the caustic was parameterised using the pre-caustic and then the parameter was restricted to vary through only the real numbers in order to confine the pre-caustic to real values. As a result, in the examples considered so far, this produces a caustic curve with no isolated points and so we would not expect to witness a swallowtail perestroika. However, as we saw in Section 2.7, swallowtails do still form spontaneously on some of the caustics. We now examine the non-generic swallowtail from Section 2.7 in more detail.

Example 3.1. Let $V = 0$, $k_t = 0$ and

$$S_0(x_0, y_0) = x_0^5 + |x_0|^{\frac{3}{2}} y_0.$$

The pre-parameterisation of the caustic is,

$$(x_t(\lambda), y_t(\lambda)) = \\ \begin{cases} \left(\frac{\lambda}{2}(9\lambda t^2 - 70\lambda^3 t - 2), \frac{4\sqrt{\lambda}}{3t}(3\lambda t^2 - 20\lambda^3 t - 1)\right) & : \quad \lambda > 0, \\ \left(-\frac{\lambda}{2}(9\lambda t^2 + 70\lambda^3 t + 2), -\frac{4\sqrt{-\lambda}}{3t}(3\lambda t^2 + 20\lambda^3 t + 1)\right) & : \quad \lambda < 0, \end{cases}$$

where $\lambda \in \mathbb{R}$. Therefore, the caustic will have a generalised cusp when either:

$$1 + 140\lambda^3 t - 9\lambda t^2 = 0, \quad \lambda > 0; \text{ or,} \tag{3.1}$$

$$1 + 140\lambda^3 t + 9\lambda t^2 = 0, \quad \lambda < 0. \tag{3.2}$$

Let,

$$t_c = \sqrt[5]{\frac{35}{27}},$$

then equation (3.1) has one real root for times $t < t_c$ and three real roots for times $t > t_c$ since it has discriminant $-560t^2(-35 + 27t^5)$. However, by Descarte's Rule of Sign (Corollary 1.33), there is always exactly one negative root and either no or two positive roots. Thus, the part of the caustic with $\lambda > 0$ has no cusps for $t < t_c$ and two cusps for $t > t_c$.

Similarly, it can be shown that equation (3.2) always has exactly one negative root; hence, there is always one cusp on the part of the caustic corresponding to $\lambda < 0$.

As can be seen in Figure 2.10, a swallowtail forms on the part of the caustic where $\lambda > 0$ at time t_c which accounts for the appearance of two cusps. Thus, there must be some significant difference between the caustic where $\lambda > 0$ and where $\lambda < 0$ which creates a new swallowtail on one half but not the other.

Example 3.1 suggests that isolated double points should exist for pre-parameterised caustics even though they are not immediately apparent. We will find such points by allowing the pre-parameter λ to vary throughout the complex plane and then identifying when this maps to real points $x_t(\lambda) \in \mathbb{R}^2$.

3.2 Parameterised curves

We begin by considering a general parameterised curve $x(\lambda)$ of the form,

$$x(\lambda) = (x_1(\lambda), x_2(\lambda)),$$

where each $x_\alpha(\lambda)$ is a real analytic function of $\lambda \in \mathbb{C}$. It follows that,

$$\overline{x(a + \mathrm{i}\eta)} = x(a - \mathrm{i}\eta),$$

so that if $\mathrm{Im}\{x(a + \mathrm{i}\eta)\} = 0$,

$$x(a + \mathrm{i}\eta) = x(a - \mathrm{i}\eta),$$

making such a point a double point of the curve $x(\lambda)$ which we will refer to as a 'complex double point'. They are real points of the curve which have a complex conjugate pair of parameter values and will be isolated if there exists a neighbourhood of $a + \mathrm{i}\eta$ throughout which $x(\lambda) \notin \mathbb{R}^2$.

The complex parameter values have influence beyond the existence of isolated points. Following a simple idea of Klein, we can use them to interpret the definition of generalised cusps.

Lemma 3.2. *If $x(\lambda) = (x_1(\lambda), x_2(\lambda))$ is a real analytic parameterisation of a curve and λ is an intrinsic parameter, then there is a generalised cusp at $\lambda = \tilde{\lambda}$ if and only if the curves,*

$$0 = \frac{1}{\eta}\mathrm{Im}\left\{x_\alpha(a + \mathrm{i}\eta)\right\}, \qquad \alpha = 1, 2,$$

intersect at $(\tilde{\lambda}, 0)$ in the (a, η) plane.

Proof. For small η, by Taylor's Theorem,

$$\begin{aligned}
\frac{1}{\eta}\mathrm{Im}\left\{x(a + \mathrm{i}\eta)\right\} &= \frac{1}{2\mathrm{i}\eta}\left(x(a + \mathrm{i}\eta) - x(a - \mathrm{i}\eta)\right) \\
&= \frac{1}{2\mathrm{i}\eta}\left(\left\{x(a) + \mathrm{i}\eta\frac{\mathrm{d}x}{\mathrm{d}\lambda}(a) + \frac{(\mathrm{i}\eta)^2}{2}\frac{\mathrm{d}^2x}{\mathrm{d}\lambda}(a) + \mathrm{O}(\eta^3)\right\}\right. \\
&\qquad \left. - \left\{x(a) - \mathrm{i}\eta\frac{\mathrm{d}x}{\mathrm{d}\lambda}(a) + \frac{(-\mathrm{i}\eta)^2}{2}\frac{\mathrm{d}^2x}{\mathrm{d}\lambda}(a) + \mathrm{O}(\eta^3)\right\}\right) \\
&= \frac{\mathrm{d}x}{\mathrm{d}\lambda}(a) + \mathrm{O}(\eta^2).
\end{aligned}$$

Thus, when $a = \tilde{\lambda}$ and $\eta = 0$,

$$\frac{\mathrm{d}x}{\mathrm{d}\lambda}(\tilde{\lambda}) = 0. \qquad \square$$

We now consider a family of parameterised curves $x_t(\lambda) = (x_t^1(\lambda), x_t^2(\lambda))$. The geometry of the curve can change with swallowtails forming and disappearing as t varies.

Proposition 3.3. *If a swallowtail on the curve $x_t(\lambda)$ collapses to a point where $\lambda = \tilde{\lambda}$ when $t = \tilde{t}$ then,*

$$\frac{\mathrm{d}x_{\tilde{t}}}{\mathrm{d}\lambda}(\tilde{\lambda}) = \frac{\mathrm{d}^2x_{\tilde{t}}}{\mathrm{d}\lambda^2}(\tilde{\lambda}) = 0.$$

Proof. When a swallowtail collapses, the two generalised cusps will coincide producing a repeated root for,

$$\frac{\mathrm{d}x_t}{\mathrm{d}\lambda}(\lambda) = 0,$$

when $\lambda = \tilde{\lambda}$ and $t = \tilde{t}$. $\square$

Similarly, we can consider the effect of a complex double point joining the main curve.

Proposition 3.4. *Assume that there exists a neighbourhood of $\tilde{\lambda} \in \mathbb{R}$ such that,*

$$\frac{\mathrm{d}x_t^\alpha}{\mathrm{d}\lambda}(\lambda) \neq 0,$$

for $t \in (\tilde{t} - \delta, \tilde{t})$ where $\delta > 0$. If a complex double point joins the curve $x_t(\lambda)$ at $\lambda = \tilde{\lambda}$ when $t = \tilde{t}$ then,

$$\frac{\mathrm{d}x_{\tilde{t}}}{\mathrm{d}\lambda}(\tilde{\lambda}) = \frac{\mathrm{d}^2 x_{\tilde{t}}}{\mathrm{d}\lambda^2}(\tilde{\lambda}) = 0.$$

Proof. Assume a complex double point has joined the curve $x_t(\lambda)$ at $\lambda = \tilde{\lambda}$ when $t = \tilde{t}$. Then in the (a, η) plane, the curves,

$$\frac{1}{\eta}\mathrm{Im}\left\{x_{\tilde{t}}^\alpha(a + \mathrm{i}\eta)\right\} = 0,$$

must both have a point of self-intersection at $(\lambda_0, 0)$ for $\alpha = 1, 2$. These curves are the zero level contours of the surfaces,

$$z_\alpha(a, \eta) = \frac{1}{\eta}\mathrm{Im}\left\{x_{\tilde{t}}^\alpha(a + \mathrm{i}\eta)\right\}.$$

As these contours have a point of self-intersection, the surfaces themselves must have critical points (saddle points) at $(\tilde{\lambda}, 0)$ where $z_\alpha(\tilde{\lambda}, 0) = 0$.

However, for small η,

$$z_\alpha(a, \eta) = \frac{\mathrm{d}x_t^\alpha}{\mathrm{d}\lambda}(a) + \mathrm{O}(\eta^2),$$

and so,

$$\frac{\partial z_\alpha}{\partial a} = \frac{\partial^2 x_t^\alpha}{\partial \lambda^2} + O(\eta^2), \qquad \frac{\partial z_\alpha}{\partial \eta} = O(\eta).$$

Therefore, at $(a, \eta) = (\tilde{\lambda}, 0)$,

$$\frac{\mathrm{d}x_{\tilde{t}}^\alpha}{\mathrm{d}\lambda}(\tilde{\lambda}) = \frac{\mathrm{d}^2 x_{\tilde{t}}^\alpha}{\mathrm{d}\lambda^2}(\tilde{\lambda}) = 0, \qquad \alpha = 1, 2. \qquad \square$$

Propositions 3.3 and 3.4 provide a necessary condition for the formation or destruction of a swallowtail and for a complex double point to join or leave the main curve. This leads to the following definition.

Definition 3.5. *A family of parameterised curves $x_t(\lambda)$ (where λ is some intrinsic parameter) for which,*

$$\frac{\mathrm{d}x_{\tilde{t}}}{\mathrm{d}\lambda}(\tilde{\lambda}) = \frac{\mathrm{d}^2 x_{\tilde{t}}}{\mathrm{d}\lambda^2}(\tilde{\lambda}) = 0,$$

is said to have a point of swallowtail perestroika when $\lambda = \tilde{\lambda}$ and $t = \tilde{t}$.

As with the definition of a generalised cusp, we have not ruled out further degeneracy when $\lambda = \tilde{\lambda}$ and $t = \tilde{t}$. Although $x_{\tilde{t}}(\tilde{\lambda})$ will satisfy the definition of a generalised cusp, the curve will not appear cusped provided there is no further degeneracy. As Cayley highlighted, these points are barely distinguishable from an ordinary point of the curve [36].

Lemma 3.6. *If $x_t(\lambda)$ is real analytic parameterisation such that,*

$$\frac{\mathrm{d}x_{\tilde{t}}}{\mathrm{d}\lambda}(\tilde{\lambda}) = \frac{\mathrm{d}^2x_{\tilde{t}}}{\mathrm{d}\lambda^2}(\tilde{\lambda}) = 0 \quad \textit{and} \quad \frac{\mathrm{d}^3x_{\tilde{t}}}{\mathrm{d}\lambda^3}(\tilde{\lambda}) \neq 0,$$

then there is a well defined normal to the curve $x_{\tilde{t}}(\lambda)$ at $\lambda = \tilde{\lambda}$.

Proof. The normal to the curve is given by,

$$\tilde{n} = \frac{\mathrm{d}\hat{\tau}}{\mathrm{d}\lambda}(\lambda) = \frac{\mathrm{d}}{\mathrm{d}\lambda}\left(\left|\frac{\mathrm{d}x_t}{\mathrm{d}\lambda}\right|^{-1}\frac{\mathrm{d}x_t}{\mathrm{d}\lambda}\right),$$

where $\hat{\tau}$ denotes the unit tangent vector to the curve. Moreover, if $x_t(\lambda)$ is real analytic,

$$\frac{\mathrm{d}x_{\tilde{t}}}{\mathrm{d}\lambda}(\lambda) = \left((\lambda-\tilde{\lambda})^2F(\lambda), (\lambda-\tilde{\lambda})^2G(\lambda)\right),$$

where $\left(F(\tilde{\lambda}), G(\tilde{\lambda})\right) \neq 0$. □

3.3 The complex caustic in two dimensions

We now consider the pre-parameterisation of the caustic $x_t(\lambda) \in \mathbb{R}^2$ from Definition 2.1. Recall that in Chapter 2 we restricted the parameter λ to real values and thus ignored isolated points which correspond to complex parameter values. We now allow the parameter to vary over the complex plane and will refer to the full caustic as the complex caustic.

If x is a point on the caustic, that is $x = x_t(\lambda)$, then,

$$f'_{(x,t)}(\lambda) = f''_{(x,t)}(\lambda) = 0.$$

Therefore, by considering the complex caustic, we are determining solutions $a = a_t$ and $\eta = \eta_t$ to the equations,

$$f'_{(x,t)}(a + \mathrm{i}\eta) = f''_{(x,t)}(a + \mathrm{i}\eta) = 0,$$

where $x \in \mathbb{R}^2$. Thus, we can call the complex double points of the caustic 'complex critical inflexions of f'. Moreover, we are particularly interested in these points if they join the main caustic at some finite critical time $\tilde{t}$. This requires that a finite positive value $\tilde{t}$ exists such that $\eta_t \to 0$ as $t \uparrow \tilde{t}$. If this holds, a swallowtail can develop at the critical time $\tilde{t}$. If $\eta_t \to 0$ as $t \downarrow \tilde{t}$ then a swallowtail can disappear. This can be expressed in terms of derivatives of the reduced action function.

Theorem 3.7. *Let $x_t(\lambda)$ denote the pre-parameterisation of the caustic where $\lambda \in \mathbb{R}$ and $x_t(\lambda)$ is a real analytic function. If at time $\tilde{t}$ a swallowtail perestroika occurs on the caustic when $\lambda = \tilde{\lambda}$ then,*

$$f'_{(x_{\tilde{t}}(\tilde{\lambda}),\tilde{t})}(\tilde{\lambda}) = f''_{(x_{\tilde{t}}(\tilde{\lambda}),\tilde{t})}(\tilde{\lambda}) = f'''_{(x_{\tilde{t}}(\tilde{\lambda}),\tilde{t})}(\tilde{\lambda}) = f^{(4)}_{(x_{\tilde{t}}(\tilde{\lambda}),\tilde{t})}(\tilde{\lambda}) = 0.$$

Proof. The first three parts follow from Theorem 2.10. Moreover, differentiating the equation $0 = f''_{(x_t(\lambda),t)}(\lambda)$ with respect to λ gives,

$$0 = \frac{\mathrm{d}x_t}{\mathrm{d}\lambda}(\lambda) \cdot \nabla_x f''_{(x_t(\lambda),t)}(\lambda) + f'''_{(x_t(\lambda),t)}(\lambda),$$

for all $\lambda \in \mathbb{R}$. Differentiating again gives,

$$0 = \frac{\mathrm{d}x_t}{\mathrm{d}\lambda} \cdot \frac{\partial}{\partial\lambda}\{\nabla_x f''\} + \frac{\mathrm{d}^2x_t}{\mathrm{d}\lambda^2} \cdot \nabla_x f'' + \frac{\mathrm{d}x_t}{\mathrm{d}\lambda} \cdot \nabla_x f''' + f^{(4)}_{(x_t(\lambda),t)}(\lambda), \qquad (3.3)$$

and setting $\lambda = \tilde{\lambda}$ and $t = \tilde{t}$ we conclude that,

$$f^{(4)}_{(x_{\tilde{t}}(\tilde{\lambda}),\tilde{t})}(\tilde{\lambda}) = 0.$$

□

Theorem 3.8. *Let $x_t(\lambda)$ denote the pre-parameterisation of the caustic where $\lambda \in \mathbb{R}$. Assume that $x_t(\lambda)$ is a real analytic function. If*

$$f'_{(x_{\tilde{t}}(\tilde{\lambda}),\tilde{t})}(\tilde{\lambda}) = f''_{(x_{\tilde{t}}(\tilde{\lambda}),\tilde{t})}(\tilde{\lambda}) = f'''_{(x_{\tilde{t}}(\tilde{\lambda}),\tilde{t})}(\tilde{\lambda}) = f^{(4)}_{(x_{\tilde{t}}(\tilde{\lambda}),\tilde{t})}(\tilde{\lambda}) = 0,$$

and the vectors,

$$\nabla_x f'_{(x_{\tilde{t}}(\tilde{\lambda}),\tilde{t})}(\tilde{\lambda}), \qquad \nabla_x f''_{(x_{\tilde{t}}(\tilde{\lambda}),\tilde{t})}(\tilde{\lambda}),$$

are linearly independent, then $x_{\tilde{t}}(\tilde{\lambda})$ is a point of swallowtail perestroika on the caustic.

Proof. From Theorem 2.12, there is a generalised cusp on the caustic at $x_{\tilde{t}}(\tilde{\lambda})$. Therefore, equation (3.3) reduces to,

$$0 = \frac{\mathrm{d}^2x_{\tilde{t}}}{\mathrm{d}\lambda^2}(\tilde{\lambda}) \cdot \nabla_x f''_{(x_{\tilde{t}}(\tilde{\lambda}),\tilde{t})}(\tilde{\lambda}). \qquad (3.4)$$

Moreover, differentiating the equation $0 = f'_{(x_t(\lambda),t)}(\lambda)$ twice with respect to λ and then setting $\lambda = \tilde{\lambda}$ with $t = \tilde{t}$ gives,

$$0 = \frac{\mathrm{d}^2 x_{\tilde{t}}}{\mathrm{d}\lambda^2}(\tilde{\lambda}) \cdot \nabla_x f'_{(x_{\tilde{t}}(\tilde{\lambda}),\tilde{t})}(\tilde{\lambda}). \tag{3.5}$$

Combining equations (3.4) and (3.5), it follows that,

$$\frac{\mathrm{d}^2 x_{\tilde{t}}}{\mathrm{d}\lambda^2}(\tilde{\lambda}) = 0. \qquad \square$$

We now demonstrate how these ideas affect a polynomial example.

Example 3.9. Let $V = 0$, $k_t = 0$ and

$$S_0(x_0, y_0) = x_0^5 + x_0^6 y_0.$$

The pre-parameterisation of the caustic is,

$$(x_t(\lambda), y_t(\lambda)) = \left(\frac{\lambda}{5}\left(4 + 5\lambda^3 t + 36\lambda^{10}t^2\right), \frac{1}{30\lambda^4 t}\left(-1 - 20\lambda^3 t + 66\lambda^{10}t^2\right) \right).$$

This will have generalised cusps when,

$$1 + 5\lambda^3 t + 99\lambda^{10}t^2 = 0. \tag{3.6}$$

Using Sturm's Theorem (Theorem 1.35), it can be shown that equation (3.6) has no real roots for $t < \tilde{t}$ but two real roots for times $t > \tilde{t}$, where,

$$\tilde{t} = \frac{4}{7}\sqrt{2}\left(\frac{33}{7}\right)^{\frac{3}{4}} = 2.5854\ldots$$

Therefore, the geometry of the caustic changes at time $\tilde{t}$ as two cusps form on a previously smooth curve. This is an example of the above mechanism for the formation of a swallowtail and is shown in Figure 3.2 where a swallowtail forms at the critical time $\tilde{t}$.

In addition, Figure 3.3 shows the curves $\mathrm{Im}\{x_t(a + \mathrm{i}\eta)\} = 0$ (dashed) and $\mathrm{Im}\{y_t(a + \mathrm{i}\eta)\} = 0$ (solid). The pre-images of the complex double points of the caustic are represented by conjugate pairs of intersections of the curves. When two of these intersections coalesce onto the real axis, a point of self-intersection forms on each curve. At this moment, the corresponding complex double point joins the main caustic and its pre-images become real. Consequently, a swallowtail forms on the caustic at this point. After the critical time, the intersection of the curves with the real axis corresponds to cusps on the caustic. In this example there are five complex double points before the critical time $\tilde{t}$ and four after. The remaining complex double points do not join the main caustic and so do not influence its behaviour for real times.

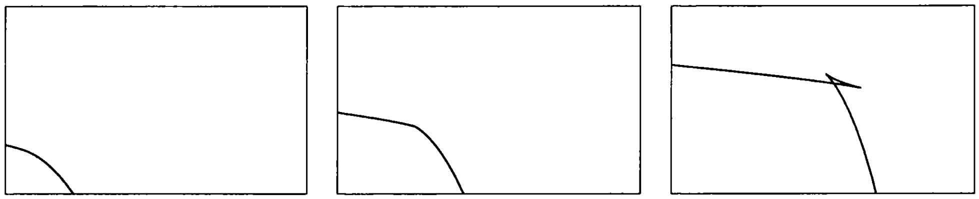

Figure 3.2: Caustic plotted as we pass through the critical time $\tilde{t}$.

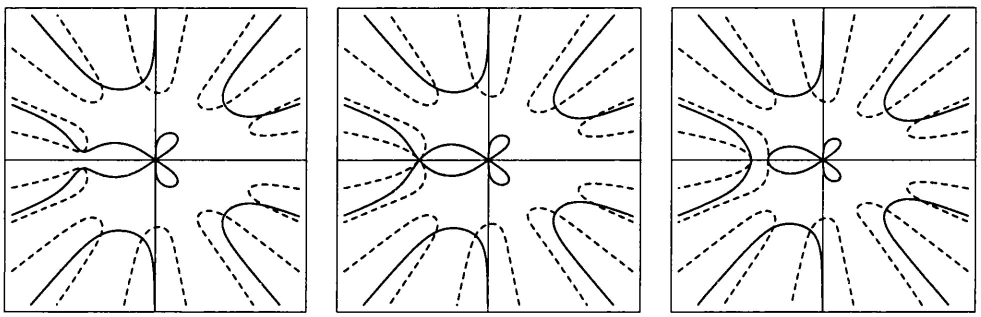

Figure 3.3: Curves $\mathrm{Im}\{x_t(a+\mathrm{i}\eta)\}=0$ (dashed) and $\mathrm{Im}\{y_t(a+\mathrm{i}\eta)\}=0$ (solid) in (a,η) plane at corresponding times to Figure 3.2.

The swallowtail perestroika is not the only way in which a swallowtail can form or disappear. Similarly, if two cusps coalesce it does not necessarily correspond to a swallowtail perestroika occurring on the caustic. We include a more complicated example to illustrate these points.

Example 3.10. Let $V=0$, $k_t=0$ and

$$S_0(x_0,y_0)=x_0^2(x_0+1)(y_0+1).$$

The reduced action function is,

$$f_{(x,y,t)}(x_0)=\frac{(x-x_0)^2}{2t}+x_0^2+x_0^3+\frac{t}{2}x_0^4(1+x_0)^2+x_0^2(1+x_0)(y-tx_0^2-tx_0^3),$$

and the pre-caustic is,

$$y_0(x_0)=\frac{1}{18}(27tx_0^3+27tx_0^2+3tx_0-t-18)+\frac{t^2-9}{18t(1+3x_0)},$$

for $x_0\neq-\frac{1}{3}$. The pre-caustic and consequently the caustic will change considerably at $t=3$. The pre-parameterisation of the caustic is,

$$x_t(\lambda) \;=\; \frac{\lambda^2}{2(1+3\lambda)}(3+8\lambda t^2+36\lambda^2t^2+54\lambda^3t^2+27\lambda^4t^2),$$

$$y_t(\lambda) = \frac{1}{2(1+3\lambda)t}(-1-2t-6\lambda t+6\lambda^2 t^2+20\lambda^3 t^2+15\lambda^4 t^2),$$

and the cusps of the caustic are given as roots of,

$$0 = 1+4t^2\lambda+26t^2\lambda^2+60t^2\lambda^3+45t^2\lambda^4.$$

Using Sturm's Theorem (Theorem 1.35), it can be shown that this polynomial has no real roots for $t < \sqrt{5}$, four real roots for $\sqrt{5} < t < 3$ and only two real roots for $3 < t$. Thus, the number of cusps changes twice, when $t = \sqrt{5}$ and $t = 3$. We investigate if either of these corresponds to a swallowtail perestroika on the caustic.

If a swallowtail perestroika did occur, then we could solve the equations,

$$f'_{(x,t)}(x_0) = f''_{(x,t)}(x_0) = f'''_{(x,t)}(x_0) = f^{(4)}_{(x,t)}(x_0) = 0,$$

which requires,

$$\begin{aligned} x &= x_0\left(1+t(2+3x_0)(1-tx_0^2-tx_0^3+y)\right), \\ y &= \frac{1}{2t(1+3x_0)}\left(-1-2t-6tx_0+6t^2x_0^2+20t^2x_0^3+15t^2x_0^4\right), \\ y &= -1+2tx_0+10tx_0^2+10tx_0^3, \\ 0 &= 1+10x_0+15x_0^2. \end{aligned}$$

These equations can be solved only for $t = \sqrt{5}$ when there are two solutions for x_0, namely $x_0 = \frac{1}{15}\left(-5 \pm \sqrt{10}\right)$. Therefore, there are two points on the caustic at which swallowtail perestroikas occur simultaneously; hence, the number of cusps jumps from 0 to 4 (see Figure 3.4).

When $t = 3$, the first four derivatives of the reduced action are not all simultaneously zero. Therefore, the two cusps that vanish do not disappear as a result of a swallowtail collapsing in on itself. In fact, as is shown in Figure 3.4, two cusps from different swallowtails coalesce to form an inflexion and then disappear. In terms of the complex contour plots shown in Figure 3.5, this corresponds to the surfaces z_1 and z_2 simultaneously having either a maximum or minimum. From the proof of Theorem 3.4, there is normally a saddle point on these surfaces when a swallowtail perestroika occurs on the caustic.

3.4 Some geometric results in two dimensions

Unsurprisingly the occurence of a swallowtail perestroika is not restricted to the caustic. As one would expect, there is an interplay between the level

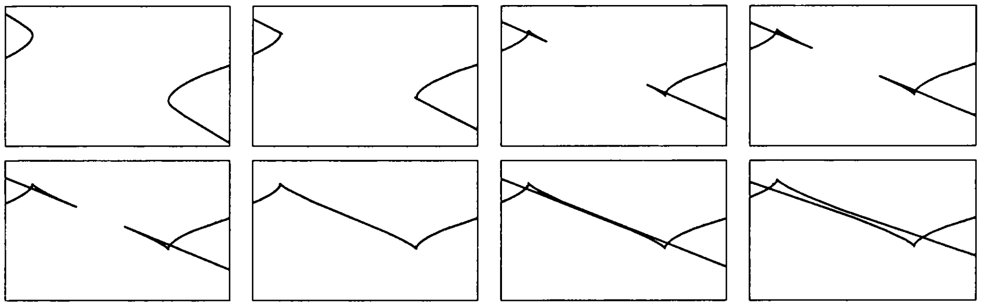

Figure 3.4: The caustic as two swallowtails form and merge.

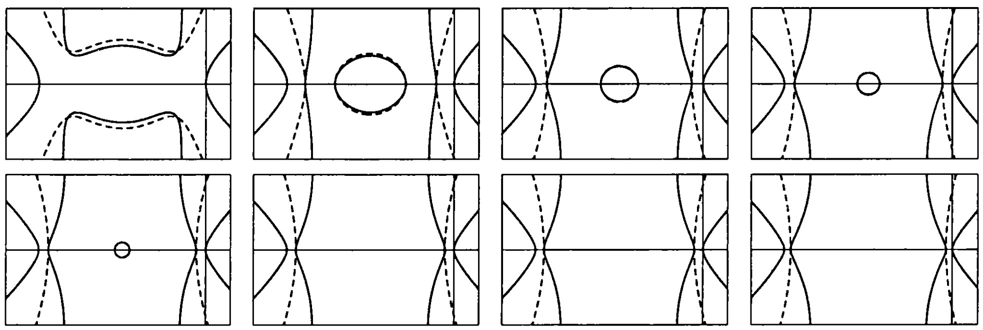

Figure 3.5: The complex curves at the corresponding times to Figure 3.4.

surfaces and the caustic characterised by both their pre-images. We begin by extending Proposition 1.11 with the assumption that,

$$\det\left(\frac{\partial^2 \mathcal{A}}{\partial x \partial x_0}(x_0, x, t)\right) \neq 0.$$

Lemma 3.11. *Let Φ_t denote the flow map and let $\Phi_t^{-1}\Gamma_t$ and Γ_t be some surfaces where if $x_0 \in \Phi_t^{-1}\Gamma_t$ then $x = \Phi_t(x_0) \in \Gamma_t$. Then, Φ_t is a differentiable map from $\Phi_t^{-1}\Gamma_t$ to Γ_t with Frechet derivative,*

$$(D\Phi_t)(x_0) = \left(-\frac{\partial^2 \mathcal{A}}{\partial x \partial x_0}(x_0, x, t)\right)^{-1} \left(\frac{\partial^2 \mathcal{A}}{(\partial x_0)^2}(x_0, x, t)\right).$$

Proof. From Theorem 1.10,

$$\Phi_t(x_0) = x \qquad \Leftrightarrow \qquad \frac{\partial \mathcal{A}}{\partial x_0^\alpha}(x_0, x, t) = 0, \quad \alpha = 1, 2, \ldots d.$$

If, at fixed time t, we move to a neighbouring point $x_0 + \delta x_0 \in \Phi_t^{-1}\Gamma_t$ and $x + \delta x \in \Gamma_t$ then,

$$\frac{\partial \mathcal{A}}{\partial x_0^\alpha}(x_0 + \delta x_0, x + \delta x, t) = 0, \quad \alpha = 1, 2, \ldots d.$$

Therefore, correct to first order,

$$\left(\frac{\partial^2 \mathcal{A}}{(\partial x_0)^2}(x_0, x, t)\right)\delta x_0 + \left(\frac{\partial^2 \mathcal{A}}{\partial x \partial x_0}(x_0, x, t)\right)\delta x = 0,$$

giving,

$$\delta x = \left(-\frac{\partial^2 \mathcal{A}}{\partial x \partial x_0}(x_0, x, t)\right)^{-1}\left(\frac{\partial^2 \mathcal{A}}{(\partial x_0)^2}(x_0, x, t)\right)\delta x_0. \qquad \square$$

We now consider the two dimensional case.

Lemma 3.12. *Let $x_0(s)$ be any two dimensional intrinsically parameterised curve, and define,*

$$x(s) = \Phi_t(x_0(s)).$$

Let e_0 denote the zero eigenvector of $\left(\frac{\partial^2 \mathcal{A}}{(\partial x_0)^2}\right)$ and assume that $\ker\left(\frac{\partial^2 \mathcal{A}}{(\partial x_0)^2}\right) = \langle e_0 \rangle$*. Then, there is a generalised cusp on $x(s)$ when $s = \sigma$ if and only if either:*

1. *there is a generalised cusp on $x_0(s)$ when $s = \sigma$; or,*
2. *$x_0(\sigma)$ is on the pre-caustic and the tangent $\frac{\mathrm{d}x_0}{\mathrm{d}s}(s)$ at $s = \sigma$ is parallel to e_0.*

Proof. Clearly,

$$\frac{\mathrm{d}x}{\mathrm{d}s}(s) = D\Phi_t(x_0(s))\frac{\mathrm{d}x_0}{\mathrm{d}s}(s),$$

where $D\Phi_t$ is the Frechet derivative of the flow map Φ_t. From Lemma 3.11 this gives,

$$\frac{\mathrm{d}x}{\mathrm{d}s}(s) = \left(-\frac{\partial^2 \mathcal{A}}{\partial x \partial x_0}(x_0(s), x(s), t)\right)^{-1}\left(\frac{\partial^2 \mathcal{A}}{(\partial x_0)^2}(x_0(s), x(s), t)\right)\frac{\mathrm{d}x_0}{\mathrm{d}s}(s).$$

Therefore, there is a generalised cusp on $x(s)$ at $s = \sigma$ if and only if

$$0 = \left(\frac{\partial^2 \mathcal{A}}{(\partial x_0)^2}(x_0(\sigma), x(\sigma), t)\right)\frac{\mathrm{d}x_0}{\mathrm{d}s}(\sigma). \tag{3.7}$$

Recall from equation (1.13) that if $x_0(\sigma)$ is on the pre-caustic,

$$\det\left(\frac{\partial^2 \mathcal{A}}{(\partial x_0)^2}(x_0(\sigma), x(\sigma), t)\right) = 0.$$

Therefore, if $x_0(\sigma)$ is on the pre-caustic, equation (3.7) will only hold if $\frac{\mathrm{d}x_0}{\mathrm{d}s}(\sigma)$ is parallel to e_0. Alternatively, if $x_0(\sigma)$ is not on the pre-caustic, we can invert the matrix in equation (3.7) giving the trivial solution,

$$\frac{\mathrm{d}x_0}{\mathrm{d}s}(\sigma) = 0. \qquad \square$$

Lemmas 3.11 and 3.12 generalise the ideas of DTZ beyond the Hamilton-Jacobi level surfaces to any two dimensional parameterised curve.

Proposition 3.13. *Assume that in two dimensions at* $x_0 \in \Phi_t^{-1} H_t^c \cap \Phi_t^{-1} C_t$ *the normal to the pre-level surface* $n(x_0) \neq 0$ *and the normal to the pre-caustic* $\tilde{n}(x_0) \neq 0$ *so that neither the pre-level surface nor the pre-caustic are cusped at* x_0. *Then* $\tilde{n}(x_0)$ *is parallel to* $n(x_0)$ *if and only if there is a generalised cusp on the caustic.*

Proof. Assume that the normal to the pre-caustic $\tilde{n}(x_0) \neq 0$ so that the pre-caustic is not cusped at x_0. Therefore, from Lemma 3.12, there is a cusp on the caustic at $\Phi_t(x_0)$ if and only if the tangent plane to the pre-caustic $\tilde{T}_{x_0}$ is spanned by the zero eigenvector e_0. However, from Lemma 1.12, the tangent plane to the pre-level surface T_{x_0} is spanned by e_0 when the pre-level surface intersects the pre-caustic. Thus, there is a cusp on the caustic if and only if the pre-caustic touches the pre-level surface. □

Corollary 3.14. *Assume that in two dimensions at* $x_0 \in \Phi_t^{-1} H_t^c \cap \Phi_t^{-1} C_t$ *the normal to the pre-level surface* $n(x_0) \neq 0$ *and the normal to the pre-caustic* $\tilde{n}(x_0) \neq 0$ *so that neither the pre-level surface nor the pre-caustic are cusped at* x_0. *Then at* $\Phi_t(x_0)$ *there is a point of swallowtail perestroika on the level surface* H_t^c *if and only if there is a generalised cusp on the caustic* C_t *at* $\Phi_t(x_0)$.

Proof. There is a double point of contact between the pre-caustic and pre-level surface when the pre-curves touch. From Proposition 1.14, there is a generalised cusp on a level surface whenever the pre-level surface intersects the pre-caustic. Thus, the double point of contact gives two cusps on the level surface which must coincide to produce a point of swallowtail perestroika. □

Corollary 3.15. *Assume that in two dimensions at* $x_0 \in \Phi_t^{-1} H_t^c \cap \Phi_t^{-1} C_t$ *the normal to the pre-level surface* $n(x_0) \neq 0$ *and the normal to the pre-caustic* $\tilde{n}(x_0) \neq 0$ *so that neither the pre-level surface nor the pre-caustic are cusped at* x_0. *Then at* $\Phi_t(x_0)$ *there is a point of swallowtail perestroika on the caustic* C_t *if and only if there is a double point of swallowtail perestroika on the level surface* H_t^c *at* $\Phi_t(x_0)$.

Proof. A swallowtail perestroika on the caustic corresponds to two generalised cusps of the caustic collapsing in on each other. Each of these cusps corresponds to a point of swallowtail perestroika on a level surface. As they collapse together they will produce a level surface with two simultaneous swallowtail perestroikas. □

3.5 Level surfaces in two dimensions

Corollary 3.14 shows that if the pre-level surface is well behaved, the only place a swallowtail can form on a Hamilton-Jacobi level surface curve is where it meets a cusp on the caustic.

The condition on the pre-image is of vital importance. Consider the example of the generic Cusp caustic and zero level surface (Example 1.5). The zero level surface meets the caustic at a cusp but does not have a point of swallowtail perestroika (consider the change in the level surfaces from Figure 1.1 to Figure 1.2). This is because the pre-image consists of the parabola $y_0 = tx_0^2 - 1/t$ and line pair $x_0^2 = 0$ with the result that the normal to the pre-level surface is not well defined at the cusp on the caustic $(0, -1/t)$ [34].

If the first two derivatives of the pre-parameterisation of the level surface are zero, then it is natural to expect the first three derivatives of the reduced action function to be zero.

Consider the pre-level surface given by $\mathcal{A}(x_0, \Phi_t(x_0), t) = c$ where $x_0 \in \mathbb{R}^2$ and $c \in \mathbb{R}$. Assuming a favoured ordering of coordinates then this equation may be solved locally to give,

$$x_0^1 = \lambda, \qquad x_0^2 = x_{0,\mathrm{H}}^2(\lambda, c),$$

where the additional subscript denotes the Hamilton-Jacobi level surface. The pre-parameterisation of the level surface is given by,

$$x_{(t,c)}(\lambda) = \Phi_t(\lambda, x_{0,\mathrm{H}}^2(\lambda, c)).$$

Therefore,

$$f_{(x_{(t,c)}(\lambda),t)}(\lambda) = c, \qquad f'_{(x_{(t,c)}(\lambda),t)}(\lambda) = 0.$$

If the level surface meets the caustic at $x_{(t,c)}(\lambda_0)$ with the pre-level surface and pre-caustic also intersecting, then $\lambda = \lambda_0$ is a root of,

$$f''_{(x_{(t,c)}(\lambda),t)}(\lambda) = 0.$$

Now set,

$$\tilde{c} = f_{(x_t(\lambda),t)}(\lambda)\big|_{\lambda=\tilde{\lambda}},$$

where $x_t(\lambda)$ is the pre-parameterisation of the caustic which has a generalised cusp when $\lambda = \tilde{\lambda}$. Assume that as $c \uparrow \tilde{c}$ there are two distinct roots for,

$$f''_{(x_{(t,c)}(\lambda),t)}(\lambda) = 0, \tag{3.8}$$

given by $\lambda = \lambda_1, \lambda_2$. These roots correspond to generalised cusps on the level surface because they are points where the pre-level surface intersects the pre-caustic. Assuming that both λ_1 and λ_2 tend to $\tilde{\lambda}$ as $c \uparrow \tilde{c}$, then the pre-surfaces will touch when $c = \tilde{c}$ and there will be a repeated root to equation (3.8). Therefore,

$$f'''_{(x(t,\tilde{c})(\lambda),t)}(\lambda) = 0.$$

Moreover, when $c > \tilde{c}$ the two roots will become complex conjugate pairs of points at which the complex caustic meets the level surface; which is in agreement with Klein's argument.

Example 3.16. Let $V = 0$, $k_t = 0$ and

$$S_0(x_0, y_0) = x_0^5 + x_0^6 y_0.$$

Consider the behaviour of the level surfaces through a given point at a fixed time as the point is moved through a cusp on the caustic. This is illustrated in Figure 3.6. Part (a) shows all of the level surfaces through a point demonstrating how three swallowtail level surfaces collapse together at the cusp to form a single level surface with a point of swallowtail perestroika. Parts (b) and (c) show how one of these swallowtails collapses on its own and how its pre-images behave.

(a)

(b)

(c)

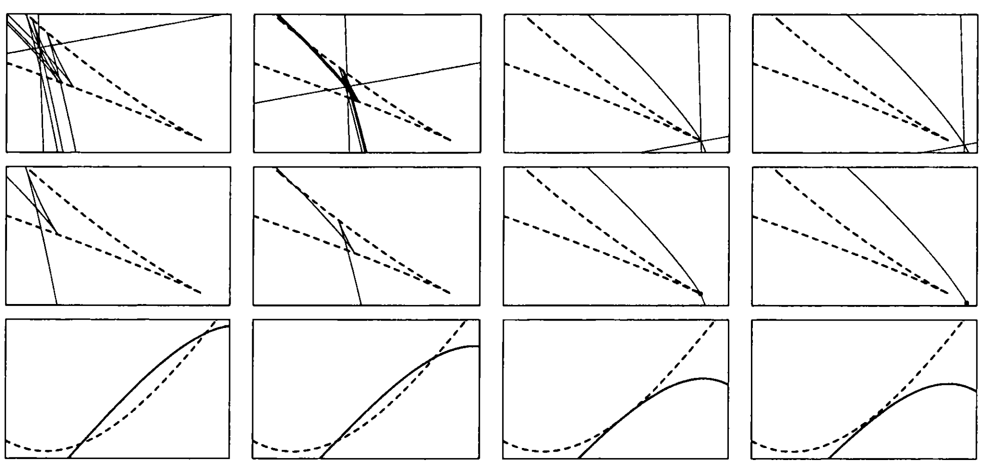

Figure 3.6: (a) All level surfaces (solid line) through a point as it crosses the caustic (dashed line) at a cusp, (b) one of these level surfaces with its complex double point, and (c) its real pre-image.

3.6 The complex caustic in three dimensions

We consider how to extend our work on the complex caustic to a three dimensional setting. There is no immediate analogue of Klein's work for three dimensions and so we consider instead what can be gained from the derivatives of the reduced action function. We have already found a geometrical interpretation for zeros of each of the first four derivatives in terms of the subcaustic (Proposition 2.15) and so our attention turns to the fifth derivative. The natural way to extend our work is to reduce the three dimensional case to a two dimensional setting so that we can again apply Klein's ideas. We achieve this by considering the subcaustic and its projection onto each of the planes $x = 0$, $y = 0$ and $z = 0$. Setting the first three derivatives of f equal to zero forces us onto the subcaustic. Thus, we need to consider when complex double points of the caustic join the subcaustic. That is, we want to solve,

$$\frac{1}{\eta}\mathrm{Im}\left\{\Phi_t\left(a+\mathrm{i}\eta, \lambda_2(a+\mathrm{i}\eta), z_t(a+\mathrm{i}\eta, \lambda_2(a+\mathrm{i}\eta))\right)\right\} = 0,$$

where $\lambda_2 = \lambda_2(\lambda_1)$ denotes the equation of the pre-subcaustic. However, this gives us three equations in the two unknowns a and η. Thus, we are forced to consider the projections of the subcaustic onto three orthogonal planes.

As in the two dimensional case, we can consider when each of these projected curves has a point of swallowtail perestroika. If we find a time $\tilde{t}$ and a parameter $\tilde{\lambda}_1$ at which a complex double point joins the projected subcaustic for each projection, then each will simultaneously have a point of swallowtail perestroika. Moreover, at such a time and position,

$$\frac{\partial x_t^{\mathrm{sc}}}{\partial \lambda_1} = \frac{\partial^2 x_t^{\mathrm{sc}}}{\partial \lambda_1^2} = 0,$$

which leads us to the following proposition.

Proposition 3.17. *If each of the projected subcaustics has a point of swallowtail perestroika at a time $\tilde{t}$ when $\lambda_1 = \tilde{\lambda}_1$ then,*

$$\begin{aligned} f'_{(x_{\tilde{t}}^{\mathrm{sc}}(\tilde{\lambda}_1),\tilde{t})}(\tilde{\lambda}_1) = f''_{(x_{\tilde{t}}^{\mathrm{sc}}(\tilde{\lambda}_1),\tilde{t})}(\tilde{\lambda}_1) &= f'''_{(x_{\tilde{t}}^{\mathrm{sc}}(\tilde{\lambda}_1),\tilde{t})}(\tilde{\lambda}_1) \\ &= f^{(4)}_{(x_{\tilde{t}}^{\mathrm{sc}}(\tilde{\lambda}_1),\tilde{t})}(\tilde{\lambda}_1) = f^{(5)}_{(x_{\tilde{t}}^{\mathrm{sc}}(\tilde{\lambda}_1),\tilde{t})}(\tilde{\lambda}_1) = 0. \end{aligned}$$

Proof. The first four parts follow from Proposition 2.15. Moreover, $0 = f'''_{(x_t^{\mathrm{sc}}(\lambda_1),t)}(\lambda_1)$ for all $\lambda_1 \in \mathbb{R}$, and differentiating with respect to λ_1 gives,

$$0 = \frac{\mathrm{d}x_t^{\mathrm{sc}}}{\mathrm{d}\lambda_1} \cdot \nabla_x f'''_{(x_t^{\mathrm{sc}}(\lambda_1),t)}(\lambda_1) + f^{(4)}_{(x_t^{\mathrm{sc}}(\lambda_1),t)}(\lambda_1).$$

Differentiating again gives,

$$0 \;=\; \frac{\mathrm{d}x_t^{\mathrm{sc}}}{\mathrm{d}\lambda_1} \cdot \frac{\partial}{\partial \lambda_1}\{\nabla_x f'''\} + \frac{\mathrm{d}^2 x_t^{\mathrm{sc}}}{\mathrm{d}\lambda_1^2} \cdot \nabla_x f''' + \frac{\mathrm{d}x_t^{\mathrm{sc}}}{\mathrm{d}\lambda_1} \cdot \nabla_x f^{(4)} + f^{(5)}_{(x_t^{\mathrm{sc}}(\lambda_1),t)}(\lambda_1).$$

Setting $\lambda_1 = \tilde{\lambda}_1$ and $t = \tilde{t}$ gives the result. □

The formation of a swallowtail on each of the projections of the subcaustic produces an interesting pyramidical shape on the caustic.

Example 3.18. Let $V = 0$, $k_t = 0$ and

$$S_0(x_0, y_0, z_0) = x_0^4 + x_0^3 + x_0^2 + x_0^5 y_0 + x_0^2 z_0.$$

Then (to 5 d.p.) at time $t = 5.98056$ when $x = -0.199789$, $y = 1.62976$, $z = -1.34006$ and $x_0 = 0.23091$, the first five derivatives of the reduced action function are zero. Therefore, from the Proposition 3.17, we would expect swallowtails to form on each of the three projections of the subcaustic (Figure 3.7). Moreover, if we consider the caustic, two dimensional swallowtails form on slices taken parallel to any of the axes. In fact a pyramid like structure forms on the caustic (Figure 3.8).

3.7 Implications for the Burgers fluid

The development of a swallowtail on a two dimensional caustic will affect the shape of the hot and cool parts of the caustic. The typical swallowtail caustic has a lambda shaped cool part as in Example 2.31. Therefore, when a swallowtail forms, the cool part will develop a new branch across which the Burgers fluid is discontinuous. If this appearance and disappearance is random as a result of the random potential k_t, then turbulent like behaviour could be produced within the fluid as the cool part of the caustic randomly changed shape. This concept will be examined in greater detail in Chapter 5.

Moreover, the creation of cusps on the caustic causes the creation of swallowtail perestroikas on the Hamilton-Jacobi level surfaces. This changes the number of cusps on the level surfaces and also creates crunodes (points of self-intersection). These crunodes are implicitly related to the existence of the Maxwell set across which the Burgers fluid velocity can be discontinuous. This link will be examined in Chapter 4.

Note should be made of the three dimensional case where a pyramid, rather than a swallowtail, forms on the caustic. One would expect similar geometric results to those in Section 3.5 to hold in this case enabling this concept to be extended to level surfaces. There may also be relationships between the other perestroikas outlined by Arnol'd and the geometry of the caustics and level surfaces.

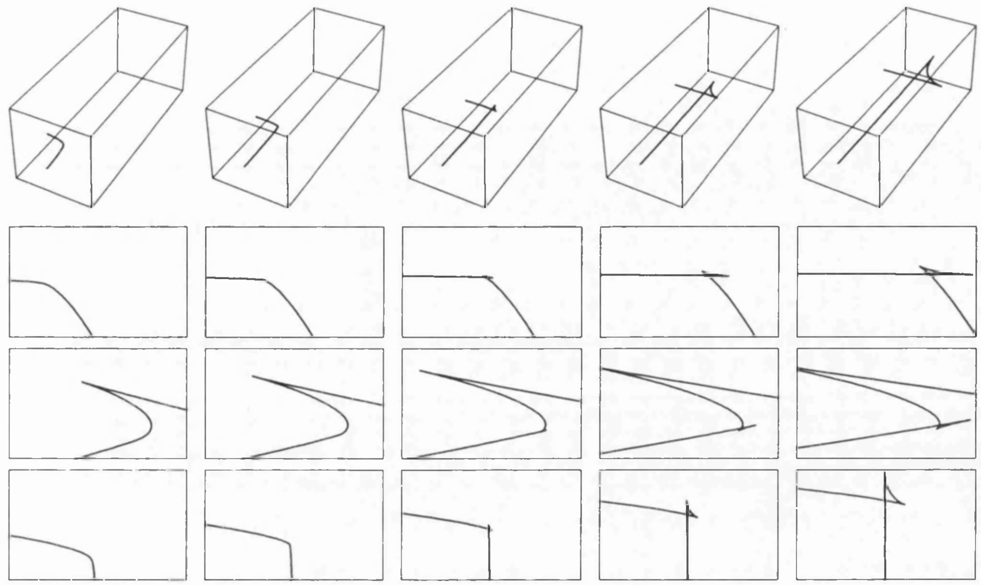

Figure 3.7: Subcaustic with projections when t=5, 6, 7, 8, 9.

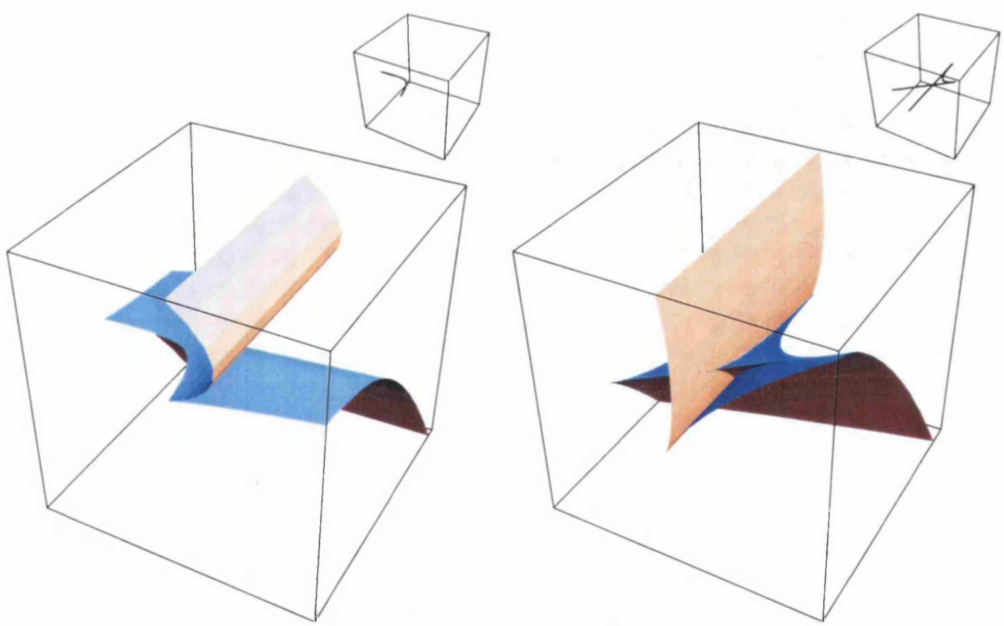

Figure 3.8: The caustic (with subcaustic inset) when $t = 5$ and $t = 9$.

Chapter 4

The Maxwell set

Summary

In this chapter we discuss several properties of the Maxwell set assuming global reducibility. We begin by considering the two dimensional case and establish an algebraic equation for the Maxwell-Klein set which contains the Maxwell set. This is then extended to produce a single algebraic equation for the set of all discontinuities of the inviscid limit of the minimal entropy solution for the stochastic Burgers equation in any dimension. We then investigate the pre-Maxwell set and use it to find the Maxwell set as a pre-parameterised surface. With this we are able to derive geometric results similar to those of DTZ. The chapter concludes with an analysis of the hot and cool parts of the Maxwell set.

4.1 Introduction

In Chapter 2 we demonstrated that there may be discontinuities in the inviscid limit of the Burgers velocity field $v^0(x,t)$ as x crosses the caustic. These jumps occur because the pre-image point $x_0(i)(x,t)$ which minimises the stochastic action coalesces with another pre-image and then becomes complex. However, this is not the only way in which the minimising pre-image value can jump. A jump will also occur if x crosses a point at which there are two distinct minimisers, $x_0(i)(x,t)$ and $x_0(j)(x,t)$, returning the same value of the action, and it is this that leads to the concept of the Maxwell set.

We begin by reiterating the definition of the Maxwell set from Section 1.1.

Definition 4.1. *The Maxwell set M_t is the set of all points $x \in \mathbb{R}^d$ where* *there exist* $x_0, \check{x}_0 \in \mathbb{R}^d$ *such that* $x = \Phi_t(x_0)$, $x = \Phi_t(\check{x}_0)$, $x_0 \neq \check{x}_0$ *and*

$$\mathcal{A}(x_0, x, t) = \mathcal{A}(\check{x}_0, x, t).$$

The cool part of the Maxwell set is made up of those regions of M_t where x_0 and $\check{x}_0$ are the global minimisers of the stochastic action. Therefore, the inviscid limit of the solution will be discontinuous as x crosses the cool Maxwell set. This will be discussed in Section 4.7.

In terms of the reduced action function, the Maxwell set corresponds to values of x for which $f_{(x,t)}(x_0^1)$ has two critical points at the same action value. If this pair of critical points also minimise the reduced action, then the inviscid limit of the solution to the Burgers equation will jump as shown in Figure 4.1.

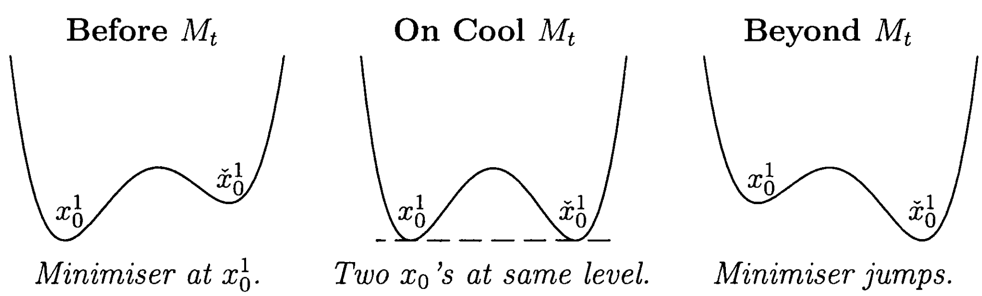

Figure 4.1: The graph of $f_{(x,t)}(x_0^1)$ as x crosses the Maxwell set.

Clearly, the Maxwell set can only exist in those regions of space in which there are sufficient real pre-images.

Lemma 4.2. *If the reduced action function* $f_{(x,t)}(x_0^1)$ *is a continuous function of* x_0^1*, then the Maxwell set* M_t *can only exist in a region where there are at least three real pre-images for each point* x.

Proof. Let x be a point with exactly two real pre-images. If x is on the Maxwell set, then $f_{(x,t)}(x_0^1)$ will have exactly two real critical points and they must be at the same action value. Therefore, these critical points must coincide and so x is on the caustic and not on the Maxwell set. □

As a point x crosses the caustic, the number of pre-images for x changes by a multiple of two. Thus, it is possible for a Maxwell set to exist on one side of a caustic but not on the other. This restriction leads to a geometrical relationship between the caustic and Maxwell set which will be shown in Section 4.5.

4.2 The Maxwell-Klein set in two dimensions

Assuming global reducibility, we now produce an algebraic equation for a surface of co-dimension one which contains the Maxwell set. We begin by considering the two dimensional polynomial case.

The algebraic equations of the caustic and Hamilton-Jacobi level surfaces can be found by eliminating the pre-variable x_0^1 from the equations (1.19) and (1.20). This can be done using the resultant as outlined in Section 1.6.

Lemma 4.3. *Let the reduced action function $f_{(x,t)}(x_0^1)$ be polynomial in x_0^1 and x. Then, the caustic is given as an algebraic equation by,*

$$R_{x_0^1}\left(f'_{(x,t)}(x_0^1), f''_{(x,t)}(x_0^1)\right) = 0,$$

and the Hamilton-Jacobi level surface associated with the value c is given as an algebraic equation by,

$$R_{x_0^1}\left(f_{(x,t)}(x_0^1) - c, f'_{(x,t)}(x_0^1)\right) = 0,$$

where R_x denotes the resultant taken with respect to x.

Proof. Recall that the caustic is found by eliminating x_0 between,

$$\det\left(\frac{\partial^2 \mathcal{A}}{(\partial x_0)^2}\right) = 0, \qquad \nabla_{x_0}\mathcal{A}(x_0, x, t) = 0,$$

and the level surface by eliminating x_0 between,

$$\mathcal{A}(x_0, x, t) = c, \qquad \nabla_{x_0}\mathcal{A}(x_0, x, t) = 0.$$

From Theorem 1.22, these are equivalent to eliminating x_0^1 between,

$$f''_{(x,t)}(x_0^1) = 0, \qquad f'_{(x,t)}(x_0^1) = 0,$$

and

$$f_{(x,t)}(x_0^1) - c = 0, \qquad f'_{(x,t)}(x_0^1) = 0,$$

respectively. □

The Maxwell set is determined using some simple geometrical properties of the Hamilton-Jacobi level surfaces. Recall the classification of the double points of an algebraic curve as acnodes, crunodes and cusps (Figure 2.4).

Lemma 4.4. *A point x is in the Maxwell set if and only if there is a Hamilton-Jacobi level surface with a point of self-intersection (crunode) at x.*

Proof. If $x_{(t,c)}(x_0^1)$ denotes the pre-parameterisation of the level surface and,

$$x_{(t,c)}(x_0^1) = x_{(t,c)}(\check{x}_0^1) \quad \text{where} \quad x_0^1 \neq \check{x}_0^1,$$

then $x_{(t,c)}(x_0^1)$ is a point of self-intersection of the level surface as there are two distinct real tangent directions at $x_{(t,c)}(x_0^1)$, namely $x'_{(t,c)}(x_0^1)$ and $x'_{(t,c)}(\check{x}_0^1)$. It follows from the definition of the Maxwell set that $x_{(t,c)}(x_0^1) \in M_t$. □

Motivated by Lemma 4.4 we have the following definition.

Definition 4.5. *In two dimensions, the Maxwell-Klein set B_t is the set of points which are non-cusp double points of some Hamilton-Jacobi level surface curve.*

A point is in the Maxwell-Klein set if it is either a complex double point (acnode) or point of self-intersection (crunode) of some Hamilton-Jacobi level surface.

If we calculate the set of all double points of the level surfaces, we find both the Maxwell-Klein set and the set of all cusps on the level surfaces. However, the geometric results of DTZ show that the cusps of the level surfaces sweep out the caustic (Proposition 1.13). Therefore, the equation of double points of the level surfaces must factorise into a product of factors corresponding to the caustic equation and the Maxwell-Klein equation, enabling us to identify the latter. The isolated points which make up the Klein part of the Maxwell-Klein set must have complex pre-images. Therefore, in simple cases, it is necessary only to perform an analysis on the multiplicity of real pre-images to extract the Maxwell set from the Maxwell-Klein set.

Theorem 4.6. *Let D_t be the set of double points of the Hamilton-Jacobi level surfaces, C_t the caustic set and B_t the Maxwell-Klein set. Then, from Cayley and Klein's classification of double points as crunodes, acnodes and cusps, by definition $D_t = C_t \cup B_t$ and the corresponding defining algebraic equations factorise as $D_t = C_t^n \cdot B_t^m$, where m, n are positive integers.*

Proof. Proposition 1.13 shows that cusps of the Hamilton-Jacobi level surfaces always occur on the caustic provided the pre-level surface is non-singular. Therefore, the equation of double points will have a factor C_t as found in Lemma 4.3. Moreover, the remaining factor will correspond to the other double points, namely the Klein complex double points (acnodes) and the Maxwell crossover points (crunodes). □

Theorem 4.7. *Let the resultant,*

$$\rho_{(t,c)}(x) = R_{x_0^1}\left(f_{(x,t)}(x_0^1) - c, f'_{(x,t)}(x_0^1)\right),$$

where $x = (x_1, x_2)$. *Then* $x \in D_t$ *if and only if for some* c,

$$\rho_{(t,c)}(x) = \frac{\partial \rho_{(t,c)}}{\partial x_1}(x) = \frac{\partial \rho_{(t,c)}}{\partial x_2}(x) = 0.$$

Further,

$$D_t(x) = \gcd\left(\rho_t^1(x), \rho_t^2(x)\right),$$

w

$$D_t(x) = \gcd\left(\rho_t^1(x), \rho_t^2(x)\right),$$

re

where $\gcd(\cdot,\cdot)$ *denotes the greatest common divisor and* ρ_t^1 *and* ρ_t^2 *are the resultants,*

$$\rho_t^1(x) = R_c\left(\rho_{(t,c)}(x), \frac{\partial \rho_{(t,c)}}{\partial x_1}(x)\right) \quad \textit{and} \quad \rho_t^2(x) = R_c\left(\frac{\partial \rho_{(t,c)}}{\partial x_1}(x), \frac{\partial \rho_{(t,c)}}{\partial x_2}(x)\right).$$

Proof. Recall from Lemma 4.3 that the equation of the Hamilton-Jacobi level surface is given by,

$$\rho_{(t,c)}(x) = R_{x_0^1}\left(f_{(x,t)}(x_0^1) - c, f'_{(x,t)}(x_0^1)\right) = 0.$$

The double points of this surface must satisfy,

$$\rho_{(t,c)}(x) = 0, \quad \frac{\partial \rho_{(t,c)}}{\partial x_1}(x) = 0 \quad \text{and} \quad \frac{\partial \rho_{(t,c)}}{\partial x_2}(x) = 0,$$

for some $c \in \mathbb{R}$. Sylvester's formula proves that all three equations are polynomial in c. To proceed, we eliminate c between pairs of these equations using resultants, giving,

$$R_c\left(\rho_{(t,c)}(x), \frac{\partial \rho_{(t,c)}}{\partial x_1}(x)\right) = \rho_t^1(x) \quad \text{and} \quad R_c\left(\frac{\partial \rho_{(t,c)}}{\partial x_1}(x), \frac{\partial \rho_{(t,c)}}{\partial x_2}(x)\right) = \rho_t^2(x).$$

Let $D_t(x) = \gcd(\rho_t^1, \rho_t^2)$ be the greatest common divisor of the algebraic ρ_t^1 and ρ_t^2 which can be found using Euclid's algorithm. Thus,

$$D_t(x) = 0,$$

is the equation of the double points of all the Hamilton-Jacobi level surfaces. $\square$

From Theorem 4.6, $D_t(x)$ factorises as $D_t(x) = C_t^n \times B_t^m$ where C_t is known explicitly. The Maxwell-Klein set of double points is characterised by $B_t = 0$ and the Maxwell set is found by removing the Klein double points from the set.

As was shown in Lemma 4.2, a Maxwell set can only exist in a region with three or more real pre-images. Typically, the formation of a swallowtail on the caustic gives rise to a region inside the swallowtail with four real pre-images and so will force the formation of a Maxwell set also typically of a swallowtail shape. Moreover, the swallowtail on the caustic leads to the formation of swallowtails on the level surfaces which are intrinsically linked to the Maxwell set. This point is illustrated in Example 4.9.

Example 4.8 (The generic Cusp). Let $V = 0$, $k_t = 0$ and

$$S_0(x_0, y_0) = x_0^2 y_0/2.$$

Using the method and notation of Theorem 4.7,

$$\begin{aligned}
&\rho_{(t,c)}(x,y) = \\
&-\frac{1}{512t^2}(8c - 32c^2t^3 + 32c^3t^6 - 40ct^2x^2 - 48c^2t^5x^2 + 24ct^4x^4 + 8ct^4y^4 \\
&-8ct^3x^2y + 48ct^2y^2 + 32ct^3y^3 + 32cty - 64c^2t^4y - 32c^2t^5y^2 + 32ct^4x^2y^2 \\
&-4x^2y + 20t^2x^4y - 12tx^2y^2 - 8t^3x^4y^2 - 12t^2x^2y^3 - 4t^3x^6 - 4t^3x^2y^4 + tx^4).
\end{aligned}$$

From Lemma 4.3, $\rho_{(t,c)}(x, y) = 0$ is the equation of the Hamilton-Jacobi level surface. Note that the zero level surface is given by,

$$0 = x^2(- 4y + 20t^2x^2y - 12ty^2 - 8t^3x^2y^2 - 12t^2y^3 - 4t^3x^4 - 4t^3y^4 + tx^2),$$

which includes the line pair $x^2 = 0$.

The equation of the double points of the Hamilton-Jacobi level surfaces $D_t(x, y)$ factorises to give,

$$x^2\left(8 - 27t^2x^2 + 24ty + 24t^2y^2 + 8t^3y^3\right)^2 = 0.$$

The second factor is the algebraic equation of the caustic. Moreover, one of the factors $x = 0$ may be ignored since it arises from the line pair $x^2 = 0$ in the zero level surface. Thus, the Maxwell-Klein set is given by the remaining factor, $x = 0$.

At a point (x, y) where $x = 0$ and $y > \frac{-1}{t}$ (above the cusp on the caustic), there are three real pre-images and no complex pre-images. Therefore, any such point is on the Maxwell set. At a point (x, y) where $x = 0$ and $y < \frac{-1}{t}$ (below the caustic), there is one real pre-image and two complex pre-images. Hence, any such point is in the Maxwell-Klein set but not in the Maxwell set (Figure 4.2).

Example 4.9 (The polynomial swallowtail). Let $V = 0$, $k_t = 0$ and

$$S_0(x_0, y_0) = x_0^5 + x_0^2 y_0.$$

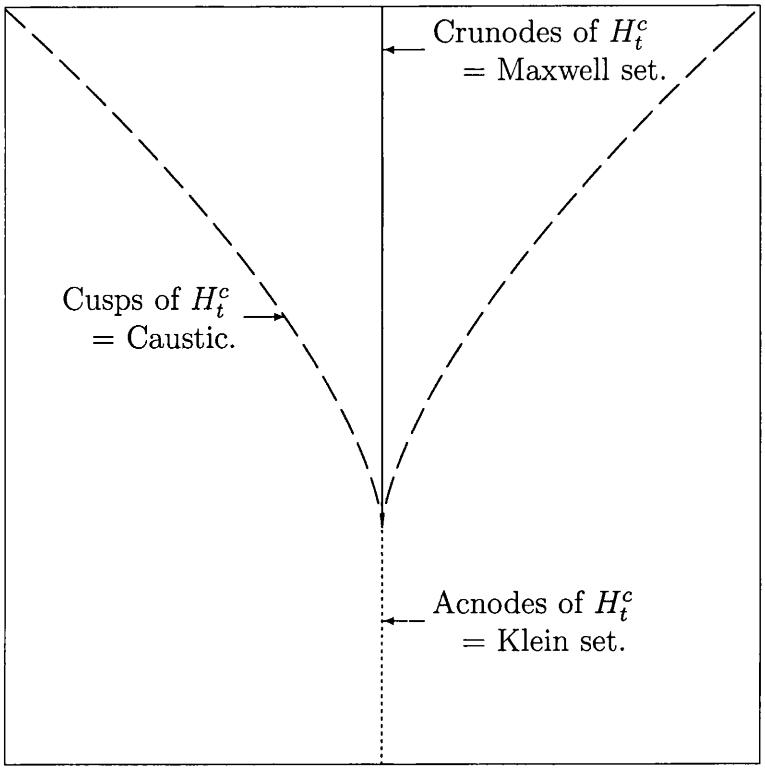

Figure 4.2: The caustic (long dash) and Maxwell set (solid line) with the curve of Klein points (dotted line) for the generic Cusp when $t = 1$.

The equation of all of the double points of the Hamilton-Jacobi level surfaces $D_t(x, y)$ factorises as,

$$\begin{aligned} 0 &= x\,(-675 + 52t^4 - t^8 + 3120t^3x - 224t^7x + 4t^{11}x - 38400t^2x^2 \\ &\quad +1408t^6x^2 + 128000tx^3 - 5400ty + 312t^5y - 4t^9y + 12480t^4xy \\ &\quad -448t^8xy - 76800t^3x^2y - 16200t^2y^2 + 624t^6y^2 - 4t^{10}y^2 + 12480t^5xy^2 \\ &\quad +416t^7y^3 - 21600t^3y^3 - 10800t^4y^4) \times (-675 + 32t^4 + 120t^3x \\ &\quad +9600t^2x^2 - 432t^6x^2 - 32000tx^3 - 5400ty + 192t^5y + 480t^4xy \\ &\quad +19200t^3x^2y - 16200t^2y^2 + 384t^6y^2 + 480t^5xy^2 - 21600t^3y^3 + 256t^7y^3 \\ &\quad -10800t^4y^4)^2, \end{aligned}$$

where again the factor x may be ignored because it arises from the zero level surface which contains the line pair $x^2 = 0$. The third factor corresponds to the caustic; hence, the second factor must be the Maxwell-Klein set.

Outside the swallowtail on the caustic there are two real and two complex pre-images, whereas inside the swallowtail there are four real and no complex pre-images. Thus, any part of the Maxwell-Klein set outside the caustic swallowtail must correspond to Klein double points and any part of the set inside the caustic swallowtail must correspond to the Maxwell set. This is shown in Figure 4.3.

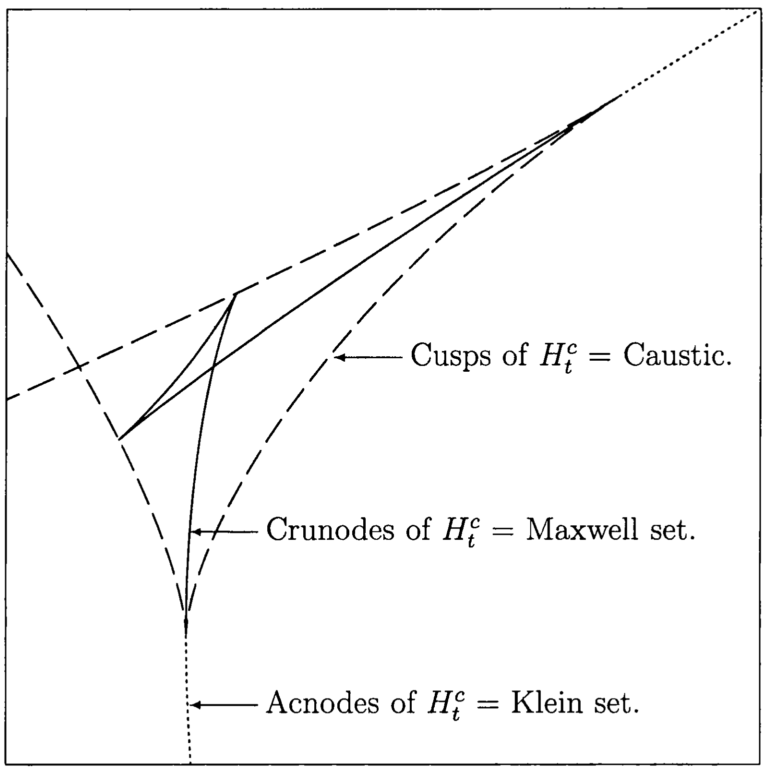

Figure 4.3: The caustic (long dash) and Maxwell set (solid line) with the curve of Klein points (dotted line) for the polynomial swallowtail when $t = 1$.

4.3 The singularity set in d-dimensions

We now extend this two dimensional geometric work to d-dimensions, again assuming global reducibility. In particular, we show how Theorems 4.6 and 4.7 can be transferred to a d-dimensional setting. This enables us to state an explicit algebraic equation for the entire set of singularities for the inviscid limit of the Burgers fluid velocity in any dimension, provided the reduced action function is polynomial in all space variables. The equation again factorises into the caustic equation and the Maxwell-Klein set.

By redefining the Maxwell-Klein set using its natural extension to d-dimensions, we are able to dispense with the need to refer to the geometry of the Hamilton-Jacobi level surfaces.

Definition 4.10. *The Maxwell-Klein set B_t is the set of all points $x \in \mathbb{R}^d$ where there exist $x_0, \check{x}_0 \in \mathbb{C}^d$ such that $x = \Phi_t(x_0)$, $x = \Phi_t(\check{x}_0)$, $x_0 \neq \check{x}_0$ and*

$$\mathcal{A}(x_0, x, t) = \mathcal{A}(\check{x}_0, x, t).$$

Theorem 4.11. *Let the reduced action function $f_{(x,t)}(x_0^1)$ be a polynomial in x_0^1. Then the set of all possible discontinuities for a d-dimensional Burgers fluid velocity field in the inviscid limit is the double discriminant,*

$$D(t) := D_c \left\{ D_\lambda \left(f_{(x,t)}(\lambda) - c \right) \right\} = 0,$$

where D_x denotes the discriminant taken with respect to x.

Proof. Let $f_{(x,t)}(\lambda)$ be a polynomial in λ of degree $(n+1)$. Then the discriminant of $f_{(x,t)}(\lambda) - c$ with respect to λ is the resultant,

$$R(c) := \frac{(n+1)!}{f_{(x,t)}^{(n+1)}(0)} \times R_\lambda \left(f_{(x,t)}(\lambda) - c, f'_{(x,t)}(\lambda) \right).$$

Therefore, using Lemma 1.24, we can rewrite $R(c)$ as,

$$\begin{aligned} R(c) &= \frac{(n+1)!}{f_{(x,t)}^{(n+1)}(0)} \times (-1)^{(n+1)n} \left(\frac{f_{(x,t)}^{(n+1)}(0)}{(n)!} \right)^{n+1} \prod_{i=1}^{n} (f_{(x,t)}(x_0^1(i)(x,t)) - c) \\ &= \frac{(n+1)!}{(n!)^{n+1}} \left(f_{(x,t)}^{(n+1)}(0) \right)^n \prod_{i=1}^{n} (f_{(x,t)}(x_0^1(i)(x,t)) - c), \end{aligned}$$

where $x_0^1(i)(x,t)$ for $i = 1, 2, \ldots, n$, is an enumeration of the real and complex roots for x_0^1 to $f'_{(x,t)}(x_0^1) = 0$. Thus, $R(c)$ is a polynomial of degree n in c with n roots $c = f_{(x,t)}(x_0^1(i)(x,t))$. Therefore, using Lemma 1.28, the discriminant of $R(c)$ can be given in terms of its zeros as,

$$D_c(R(c)) = b_0^{2n-2} \prod_{i<j} \left(f_{(x,t)}(x_0^1(i)(x,t)) - f_{(x,t)}(x_0^1(j)(x,t)) \right)^2,$$

where,

$$b_0 = \frac{(n+1)!}{(n!)^{n+1}} \left(f_{(x,t)}^{(n+1)}(0) \right)^n,$$

is the leading coefficient of c in $R(c)$. This discriminant is zero when either:

1. $x_0^1(i)(x,t) = x_0^1(j)(x,t)$ and $i \neq j$, which corresponds to the complex caustic; or,

2. $x_0^1(i)(x,t) \neq x_0^1(j)(x,t)$ but $f_{(x,t)}(x_0^1(i)(x,t)) = f_{(x,t)}(x_0^1(j)(x,t))$ which corresponds to the Maxwell-Klein set.

Hence, the equation $D(t) = 0$ contains the cool caustic and cool Maxwell set, and therefore, contains all points of discontinuity of the minimal entropy solution of the Burgers equation. □

In the two dimensional case, the curves defined by $D(t)$ in Theorem 4.11 and D_t in Theorem 4.6 coincide. However, the powers of the factors in $D(t)$ can be found explicitly.

Lemma 4.12. *If the reduced action function $f_{(x,t)}(x_0^1)$ is polynomial in x_0^1, then the equation of the caustic is,*

$$\prod_{i<j}\left(x_0^1(i)(x,t) - x_0^1(j)(x,t)\right)^2 = 0,$$

where $x_0^1(i)(x,t)$ is an enumeration of all the real and complex roots for x_0^1 to $f'_{(x,t)}(x_0^1) = 0$.

Proof. From Lemma 4.3, the equation of the caustic is given by the zeros of the discriminant of $f'_{(x,t)}(x_0^1)$ taken with respect to x_0^1, which can be found using Lemma 1.28 as,

$$\left(\frac{f^{(n)}(0)}{n!}\right)^{2n-2}\prod_{i<j}\left(x_0^1(i)(x,t) - x_0^1(j)(x,t)\right)^2,$$

where $f'_{(x,t)}(x_0^1)$ is a polynomial in x_0^1 of degree n. □

Lemma 4.13. *If F is a polynomial such that $F'(b) = F'(a) = 0$ then,*

$$F(b) - F(a) = (b-a)^3 g(a,b),$$

for some polynomial g.

Proof. Assume, without loss of generality, that $a = 0$. Then,

$$F(b) - F(0) = \int_0^b x(x-b)h(x)\,\mathrm{d}x,$$

where $F'(x) = x(x-b)h(x)$ for some polynomial $h(x)$. Differentiating this with respect to b gives,

$$F'(b) = -\int_0^b xh(x)\,\mathrm{d}x = \mathrm{O}(b^2),$$

and so $F(b) = \mathrm{O}(b^3)$. □

Theorem 4.14. *The double discriminant $D(t)$ factorises as,*

$$D(t) = b_0^{2n-2} \cdot (C_t)^3 \cdot (B_t)^2,$$

where $B_t = 0$ is the equation of the Maxwell-Klein set and $C_t = 0$ is the equation of the caustic. The expressions B_t and C_t, defining the Maxwell-Klein set and the caustic, are both algebraic in x and t.

Proof. From Theorem 4.11,

$$\begin{aligned} D(t) &= b_0^{2n-2} \prod_{i<j} \left(f_{(x,t)}(x_0^1(i)(x,t)) - f_{(x,t)}(x_0^1(j)(x,t)) \right)^2 \\ &= b_0^{2n-2} \prod_{i<j} \left\{ \left(x_0^1(i)(x,t) - x_0^1(j)(x,t) \right)^2 \right\}^3 \{p_{ij}(x,t)\}^2, \end{aligned}$$

where, from Lemma 4.12,

$$f_{(x,t)}(x_0^1(i)(x,t)) - f_{(x,t)}(x_0^1(j)(x,t)) = \left(x_0^1(i)(x,t) - x_0^1(j)(x,t) \right)^3 p_{ij}(x,t).$$

Moreover, $\prod_{i<j} p_{ij}(x,t)$ is a symmetric function of the roots of $f'_{(x,t)}(x_0^1) = 0$. Thus, by the fundamental theorem of symmetric functions [42], this product is a polynomial in the coefficients of $f'_{(x,t)}(x_0^1)$ and, as a result, is algebraic in x and t. □

We conclude this section with an example showing the complexity of the Maxwell-Klein set even in simple cases.

Example 4.15 (The Butterfly). Let $V = 0$, $k_t = 0$ and

$$S_0(x_0, y_0, z_0) = x_0^3 y_0 + x_0^2 z_0.$$

Evaluating the first discriminant gives a polynomial of degree 5 in c. Therefore, the second discriminant can be found easily using the standard formula for the discriminant of the quintic [18].

We can then perform the factorisation by dividing by the factor corresponding to the caustic to give the Maxwell-Klein equation:

$$\begin{aligned} &432(3x^2 - y^2) + 432(2xy + 25x^3y - 9xy^3 + 30x^2z - 12y^2z)t + 27(72x^2 \\ &+500x^4 + 3125x^6 - 24y^2 + 192x^2y^2 - 1125x^4y^2 - 36y^4 + 27x^2y^4 - 27y^6 \\ &+320xyz + 2400x^3yz - 1152xy^3z + 1920x^2z^2 - 960y^2z^2)t^2 + 54(24xy \\ &+510x^3y + 3750x^5y - 90xy^3 - 990x^3y^3 - 108x^3y^5 + 288x^2z + 1000x^4z \\ &-120y^2z + 576x^2y^2z - 1125x^4y^2z - 144y^4z + 54x^2y^4z - 81y^6z + 640xyz^2 \end{aligned}$$

$$
\begin{aligned}
&+2400x^3yz^2 - 1728xy^3z^2 + 1920x^2z^3 - 1280y^2z^3)t^3 + 9(129x^2 + 775x^4 \\
&-43y^2 + 1536x^2y^2 + 21150x^4y^2 - 159y^4 - 3807x^2y^4 - 81y^6 - 972x^2y^6 \\
&+1152xyz + 12240x^3yz - 3240xy^3z - 11880x^3y^3z + 5184x^2z^2 \\
&+6000x^4z^2 - 2880y^2z^2 + 6912x^2y^2z^2 - 2592y^4z^2 + 324x^2y^4z^2 - 972y^6z^2 \\
&+7680xyz^3 + 9600x^3yz^3 - 13824xy^3z^3 + 11520x^2z^4 - 11520y^2z^4)t^4 \\
&+18(43xy + 673x^3y - 6xy^3 + 4833x^3y^3 - 540xy^5 - 243xy^7 + 387x^2z \\
&+775x^4z - 172y^2z + 3072x^2y^2z - 477y^4z - 3807x^2y^4z - 162y^6z \\
&+1728xyz^2 + 6120x^3yz^2 - 3240xy^3z^2 + 3456x^2z^3 - 2880y^2z^3 \\
&+2304x^2y^2z^3 - 1728y^4z^3 - 324y^6z^3 + 3840xyz^4 - 3456xy^3z^4 + 2304x^2z^5 \\
&-4608y^2z^5)t^5 + (345x^2 + 906x^4 - 115y^2 + 6156x^2y^2 - 567y^4 + 19035x^2y^4 \\
&-1215y^6 - 729y^8 + 4644xyz + 24228x^3yz - 432xy^3z - 19440xy^5z \\
&+13932x^2z^2 - 9288y^2z^2 + 55296x^2y^2z^2 - 17172y^4z^2 - 2916y^6z^2 \\
&+41472xyz^3 - 38880xy^3z^3 + 31104x^2z^4 - 51840y^2z^4 - 15552y^4z^4 \\
&+27648xyz^5 - 27648y^2z^6)t^6 + 2(115xy + 743x^3y + 333xy^3 + 729xy^5 \\
&+690x^2z - 345y^2z + 6156x^2y^2z - 1134y^4z - 1215y^6z + 4644xyz^2 \\
&-216xy^3z^2 + 4644x^2z^3 - 6192y^2z^3 - 5724y^4z^3 + 10368xyz^4 \\
&-10368y^2z^5)t^7 + (51x^2 - 17y^2 + 762x^2y^2 - 72y^4 - 54y^6 + 920xyz \\
&+1332xy^3z + 1380x^2z^2 - 1380y^2z^2 - 2268y^4z^2 + 6192xyz^3 - 6192y^2z^4)t^8 \\
&+2(17xy + 57xy^3 + 51x^2z - 34y^2z - 72y^4z + 460xyz^2 - 460y^2z^3)t^9 \\
&+(3x^2 - y^2 - y^4 + 68xyz - 68y^2z^2)t^{10} + 2y(x - yz)t^{11} = 0.
\end{aligned}
$$

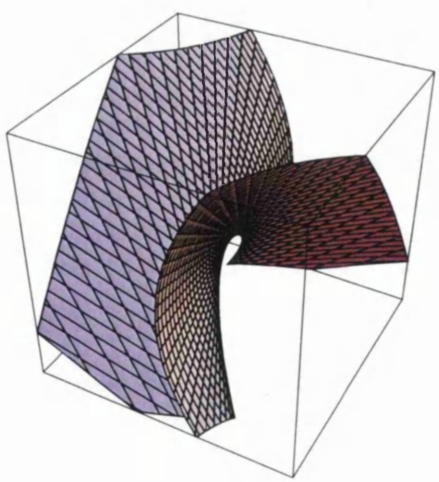

The Butterfly caustic

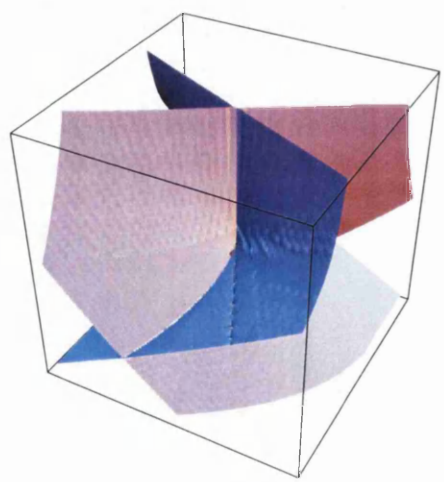

The Maxwell-Klein set

Figure 4.4: The caustic and Maxwell-Klein set for the butterfly when $t = 1$.

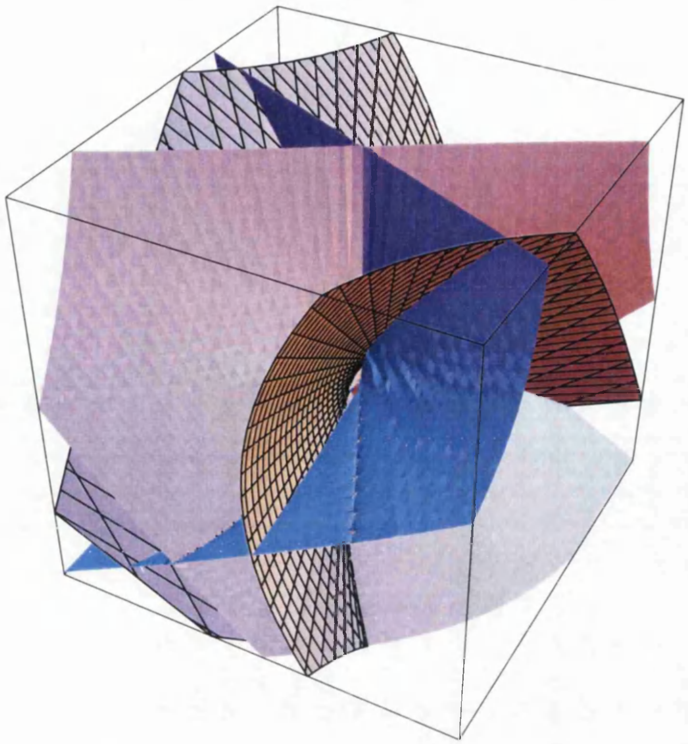

Figure 4.5: The caustic (mesh) and Maxwell-Klein set (plain) together for the butterfly when $t = 1$.

The Maxwell-Klein set and the butterfly caustic are shown in Figure 4.4. Distinguishing the Maxwell set from the Maxwell-Klein set is a more complex matter in this example as every point x has five pre-images (real and complex). We can rule out the existence of a Maxwell set below the caustic in Figure 4.5 since there is only one real pre-image in this region. However, above the caustic there are three real and two complex pre-images and so we cannot distinguish those parts of the surface that belong to the Maxwell set and those which belong to the Maxwell-Klein set.

This example illustrates how our simple method gives the algebraic equation of these complicated surfaces. This method has been applied to the three dimensional polynomial swallowtail and the Non-Generic Swallowtail which are both shown in Appendix B.

4.4 The pre-Maxwell set

In the previous sections we have established an algebraic equation which contains the Maxwell set and shown how, in simple examples, it is possible to extract the Maxwell set from this equation. However, in Example 4.15 we saw that this separation is not always possible. We overcome this limitation by considering the pre-Maxwell set which enables us to find the Maxwell set by a pre-parameterisation.

If the Maxwell set is defined as in Definition 4.1, then the pre-Maxwell set is the set of all the pre-images x_0 and $\check{x}_0$ which give rise to the Maxwell set.

Definition 4.16. *The pre-Maxwell set $\Phi_t^{-1}M_t$ is the set of all points $x_0 \in \mathbb{R}^d$ where there exists $x, \check{x}_0 \in \mathbb{R}^d$ such that $x = \Phi_t(x_0)$ and $x = \Phi_t(\check{x}_0)$ with $x_0 \neq \check{x}_0$ and*

$$\mathcal{A}(x_0, x, t) = \mathcal{A}(\check{x}_0, x, t).$$

Each regular point of a caustic or level surface is linked by Φ_t^{-1} to a single point on the relevant pre-surface. However, every point on the Maxwell set is linked by Φ_t^{-1} to at least two points on the pre-Maxwell set (x_0 and $\check{x}_0$). This pairwise correspondence leads to extensions of the geometric results found for caustics and level surfaces by DTZ [12].

We begin by establishing how to find the pre-Maxwell set. The obvious route to follow is the substitution of $x = \Phi_t(x_0)$ into the algebraic equation for the Maxwell-Klein set. However, this will produce the topological inverse image of the Maxwell-Klein set which will contain every pre-image; this is not the pre-Maxwell set. We want to determine only the two pre-images which produce the same value of the action.

Instead, we find the pre-Maxwell set by taking resultants of the reduced action function. Therefore, we assume that Φ_t is globally reducible and that $f_{(x,t)}(x_0^1)$ is polynomial in all space variables.

Lemma 4.17. *Let,*

$$G(\check{x}_0^1) = \frac{f_{(\Phi_t(x_0),t)}(x_0^1) - f_{(\Phi_t(x_0),t)}(\check{x}_0^1)}{(x_0^1 - \check{x}_0^1)^2},$$

then $G(\check{x}_0^1)$ and $G'(\check{x}_0^1)$ are polynomials in $\check{x}_0^1$.

Proof. Clearly,

$$\left[f_{(\Phi_t(x_0),t)}(x_0^1) - f_{(\Phi_t(x_0),t)}(\check{x}_0^1)\right]_{\check{x}_0^1 = x_0^1} = 0,$$

and from Theorem 1.22,

$$\left[\frac{\mathrm{d}}{\mathrm{d}\check{x}_0^1}\left(f_{(\Phi_t(x_0),t)}(x_0^1) - f_{(\Phi_t(x_0),t)}(\check{x}_0^1)\right)\right]_{\check{x}_0^1 = x_0^1} = -f'_{(\Phi_t(x_0),t)}(x_0^1) = 0.$$

Therefore, the numerator of $G(\check{x}_0^1)$ has a factor $(x_0^1 - \check{x}_0^1)^2$. □

Theorem 4.18. *The pre-Maxwell set is given by the discriminant,*

$$D_{\check{x}_0^1}\left(G(\check{x}_0^1)\right) = 0,$$

where G is as defined in Lemma 4.17.

Proof. The pre-Maxwell set is found by eliminating $\check{x}_0$ and x between the equations,

$$\mathcal{A}(x_0, x, t) - \mathcal{A}(\check{x}_0, x, t) = 0, \quad x = \Phi_t(x_0) = \Phi_t(\check{x}_0), \quad x_0 \neq \check{x}_0,$$

which is equivalent to eliminating $\check{x}_0^1$ between the equations,

$$f_{(\Phi_t(x_0),t)}(x_0^1) - f_{(\Phi_t(x_0),t)}(\check{x}_0^1) = 0, \quad f'_{(\Phi_t(x_0),t)}(\check{x}_0^1) = 0, \quad x_0^1 \neq \check{x}_0^1. \tag{4.1}$$

The first equation in (4.1) is satisfied when,

$$G(\check{x}_0^1) = \frac{f_{(\Phi_t(x_0),t)}(x_0^1) - f_{(\Phi_t(x_0),t)}(\check{x}_0^1)}{(x_0^1 - \check{x}_0^1)^2} = 0.$$

If

$$G'(\check{x}_0^1) = 2\frac{f_{(\Phi_t(x_0),t)}(x_0^1) - f_{(\Phi_t(x_0),t)}(\check{x}_0^1)}{(x_0^1 - \check{x}_0^1)^3} - \frac{f'_{(\Phi_t(x_0),t)}(\check{x}_0^1)}{(x_0^1 - \check{x}_0^1)^2},$$

then the second part of (4.1) is satisfied.

Furthermore, by dividing by $(x_0^1 - \check{x}_0^1)^2$ we automatically remove the double

then the second part of (4.1) is satisfied.

Furthermore, by dividing by $(x_0^1 - \check{x}_0^1)^2$ we automatically remove the double

root corresponding to $x_0^1 = \check{x}_0^1$. This also removes the extra zeros corresponding to the pre-caustic (when $f''_{(\Phi_t(x_0),t)}(\check{x}_0^1) = 0$) since, by Taylor's theorem,

$$G'(\check{x}_0^1) = -\frac{1}{6}f^{(3)}_{(\Phi_t(x_0),t)}(x_0^1) - \frac{1}{12}\left(\check{x}_0^1 - x_0^1\right) f^{(4)}_{(\Phi_t(x_0),t)}(x_0^1) + \mathrm{O}\left(\left(\check{x}_0^1 - x_0^1\right)^2\right),$$

which will not have a zero at such a point. □

This equation yields the pre-Maxwell set as an algebraic equation in x_0 which can be used to pre-parameterise the Maxwell set, as was done previously for the caustic and level surfaces. By restricting the parameter to real values, we obtain the Maxwell set only and not the Klein points since the latter have complex pre-images. This is the reverse of the analysis performed in Chapter 3 for caustics and level surfaces!

Example 4.19 (The generic Cusp). Let $V = 0$, $k_t = 0$ and

$$S_0(x_0, y_0) = x_0^2 y_0/2.$$

The algebraic equation of the pre-Maxwell set is,

$$-\frac{1}{2}t\,(1 + 2ty_0) = 0.$$

This can be solved to give,

$$y_{0,\mathrm{M}}(x_0) = -\frac{1}{2t}.$$

Substituting into the flow map Φ_t gives the Maxwell set parameterised as,

$$x_t^{\mathrm{M}}(x_0) = 0, \qquad y_t^{\mathrm{M}}(x_0) = -\frac{1}{2t} + tx_0^2.$$

Note that we use M to denote the Maxwell set.

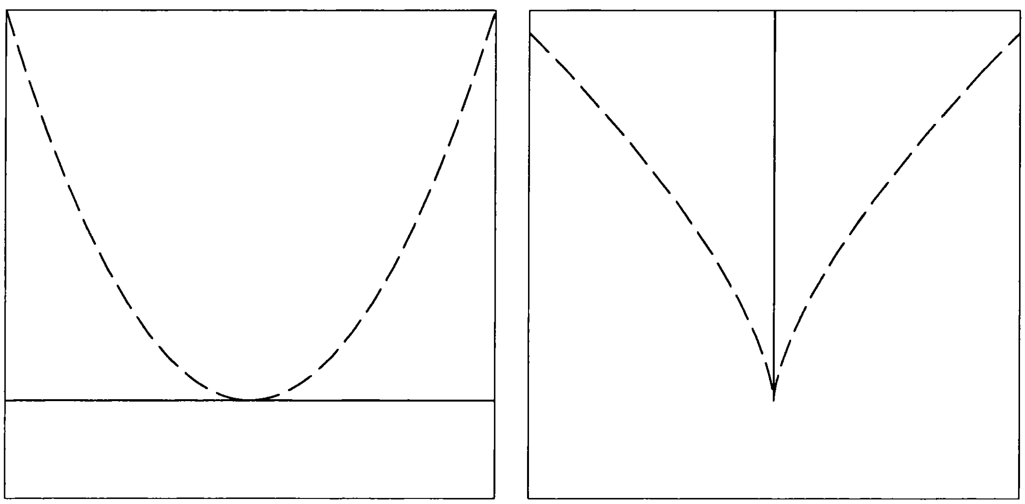

$\Phi_t^{-1}M_t$ *(solid) and* $\Phi_t^{-1}C_t$ *(dashed)* M_t *(solid) and* C_t *(dashed)*

Figure 4.6: The caustic and Maxwell set for the generic Cusp when $t = 1$.

Example 4.20 (The polynomial swallowtail). Let $V = 0$, $k_t = 0$ and

$$S_0(x_0, y_0) = x_0^5 + x_0^2 y_0.$$

Again, the pre-Maxwell set can be found as,

$$\begin{aligned} 0 \;=\; & \frac{1}{4t^2}\left(-27 + t^4 + 6t^3x_0 - 24t^2x_0^2 - 280tx_0^3 + 4t^5x_0^3 + 28t^4x_0^4 - 80t^3x_0^5\right. \\ & -800t^2x_0^6 - 108ty_0 + 2t^5y_0 + 12t^4x_0y_0 - 48t^3x_0^2y_0 - 560t^2x_0^3y_0 \\ & \left.-108t^2y_0^2\right), \end{aligned}$$

which can be solved to give,

$$y_{0,\mathrm{M}}(x_0) = \frac{1}{108t^2}\Big(-54t + t^5 + 6t^4x_0 - 24t^3x_0^2 - 280t^2x_0^3 \pm t^2\sqrt{A_t(x_0)}\Big),$$

where,

$$A_t(x_0) = (t^2 + 4tx_0 - 20x_0^2)^3.$$

Applying the flow map produces the Maxwell set,

$$\begin{aligned} x_t^{\mathrm{M}}(x_0) &= \frac{x_0}{54t}\Big(t^5 + 6t^4x_0 - 24t^3x_0^2 - 10t^2x_0^3 \pm t^2\sqrt{A_t(x_0)}\Big), \\ y_t^{\mathrm{M}}(x_0) &= \frac{1}{108t^2}\Big(t^5 + 6t^4x_0 + 84t^3x_0^2 - 280t^2x_0^3 - 54t \pm t^2\sqrt{A_t(x_0)}\Big), \end{aligned}$$

where we restrict $x_0 \in \left[\frac{t}{10}(1-\sqrt{6}), \frac{t}{10}(1+\sqrt{6})\right]$ so that $(x_0.y_{0,\mathrm{M}}(x_0)) \in \mathbb{R}^2$. This is shown in Figure 4.7 together with the caustic curves. The cusps on the pre-Maxwell set correspond to the points $x_0 = \frac{t}{10}(1-\sqrt{6})$ and $x_0 = \frac{t}{10}(1+\sqrt{6})$.

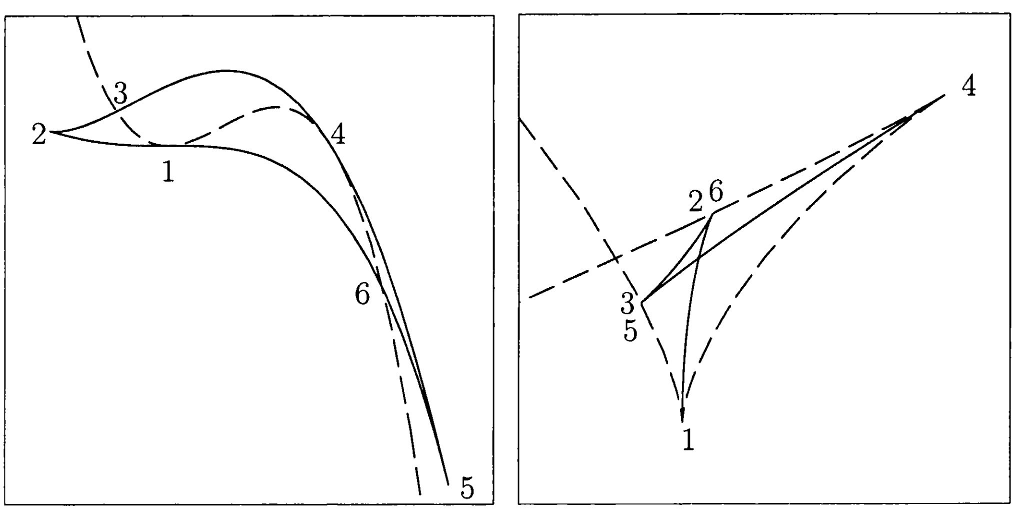

$\Phi_t^{-1}M_t$ *(solid) and* $\Phi_t^{-1}C_t$ *(dashed)* $\quad$ M_t *(solid) and* C_t *(dashed)*

Figure 4.7: The caustic and Maxwell set for the polynomial swallowtail when $t = 1$.

4.5 Geometric results

We have seen in Example 4.20 and Figure 4.7 that the cusps on the Maxwell set occur on the caustic in direct correlation to the relationships established by DTZ for level surfaces, even though the pre-Maxwell set itself has cusps. In this section we will investigate these relationships in the general stochastic case by building on the results of Sections 1.3 and 3.4.

Lemmas 3.11 and 3.12 showed that a curve has cusps when its pre-image intersects the pre-caustic at a point where the tangent to the pre-curve is parallel to e_0, the zero eigenvector of $\frac{\partial^2 \mathcal{A}}{(\partial x_0)^2}$. Therefore, in order to investigate the location of cusps on the Maxwell set, we must first consider the tangent to the pre-Maxwell set. As in Section 3.5, we assume that,

$$\det\left(\frac{\partial^2 \mathcal{A}}{\partial x \partial x_0}\right) \neq 0.$$

Lemma 4.21. *Assume that a point x on the Maxwell set corresponds to exactly two pre-images on the pre-Maxwell set, x_0 and $\check{x}_0$. Then the normal to the pre-Maxwell set at x_0 is, to within a scalar multiplier, given by,*

$$\begin{aligned} n(x_0) &= -\left(\frac{\partial^2 \mathcal{A}}{(\partial x_0)^2}(x_0, x, t)\right)\left(\frac{\partial^2 \mathcal{A}}{\partial x_0 \partial x}(x_0, x, t)\right)^{-1} \cdot \\ &\qquad \left(\dot{X}(t, x_0, \nabla S_0(x_0)) - \dot{X}(t, \check{x}_0, \nabla S_0(\check{x}_0))\right). \end{aligned}$$

Proof. Fix a point on the Maxwell set $x \in \mathbb{R}^d$. Then by Definition 4.1, there exist $x_0, \check{x}_0 \in \mathbb{R}^d$ such that,

$$x = \Phi_t(x_0) = \Phi_t(\check{x}_0), \qquad \mathcal{A}(x_0, x, t) = \mathcal{A}(\check{x}_0, x, t).$$

Therefore, by Theorem 1.10, it follows that,

$$\nabla_{x_0}\mathcal{A}(x_0, x, t) = \nabla_{x_0}\mathcal{A}(\check{x}_0, x, t) = 0, \qquad c_1 = c_2,$$

where $c_1 = \mathcal{A}(x_0, x, t)$ and $c_2 = \mathcal{A}(\check{x}_0, x, t)$. If we allow x to vary by a small amount δx so that $x \mapsto x + \delta x$, then c_1 and c_2 will also change by small amounts δc_1 and δc_2 where,

$$\delta c_1 = \nabla_x \mathcal{A}(x_0, x, t) \cdot \delta x, \qquad \delta c_2 = \nabla_x \mathcal{A}(\check{x}_0, x, t) \cdot \delta x,$$

to first order. Moreover, when $x \mapsto x + \delta x$, it follows that $x_0 \mapsto x_0 + \delta x_0$ where,

$$\delta x = D\Phi_t(x_0)\delta x_0 = \left(-\frac{\partial^2 \mathcal{A}}{\partial x \partial x_0}(x_0, x, t)\right)^{-1}\left(\frac{\partial^2 \mathcal{A}}{(\partial x_0)^2}(x_0, x, t)\right)\delta x_0.$$

For $x + \delta x$ to be on the Maxwell set we require,

$$\delta c_1 = \delta c_2 \quad \Leftrightarrow \quad (\nabla_x \mathcal{A}(x_0, x, t) - \nabla_x \mathcal{A}(\check{x}_0, x, t)) \cdot \delta x = 0.$$

It follows that,

$$\begin{aligned}(\nabla_x \mathcal{A}(x_0,x,t) \quad - \quad & \nabla_x \mathcal{A}(\check{x}_0,x,t)) \cdot \\ & \left(-\frac{\partial^2 \mathcal{A}}{\partial x \partial x_0}(x_0,x,t)\right)^{-1} \left(\frac{\partial^2 \mathcal{A}}{(\partial x_0)^2}(x_0,x,t)\right) \delta x_0 = 0,\end{aligned}$$

so that the normal to the pre-Maxwell set is,

$$\begin{aligned} n \quad = \quad & \Bigg\{ (\nabla_x \mathcal{A}(x_0,x,t) - \nabla_x \mathcal{A}(\check{x}_0,x,t)) \cdot \\ & \qquad \left(-\frac{\partial^2 \mathcal{A}}{\partial x \partial x_0}(x_0,x,t)\right)^{-1} \left(\frac{\partial^2 \mathcal{A}}{(\partial x_0)^2}(x_0,x,t)\right) \Bigg\}^T \\ = \quad & -\left(\frac{\partial^2 \mathcal{A}}{(\partial x_0)^2}(x_0,x,t)\right) \left(\frac{\partial^2 \mathcal{A}}{\partial x_0 \partial x}(x_0,x,t)\right)^{-1} \cdot \\ & \qquad \left(\dot{X}(t,x_0,\nabla S_0(x_0)) - \dot{X}(t,\check{x}_0,\nabla S_0(\check{x}_0))\right),\end{aligned}$$

where $\dot{X}(t,x_0,\nabla S_0(x_0)) = \nabla_x \mathcal{A}(x_0,x,t)$ from [12]. □

Corollary 4.22. *In two dimensions, let the pre-Maxwell set meet the pre-caustic at a point x_0 where the normal to the pre-Maxwell set $n(x_0) \neq 0$ so that the pre-Maxwell set is not cusped and,*

$$\ker \left(\frac{\partial^2 \mathcal{A}}{(\partial x_0)^2}(x_0,\Phi_t(x_0),t)\right) = \langle e_0 \rangle,$$

where e_0 is the zero eigenvector. Then T_{x_0}, the tangent plane to the pre-Maxwell set at x_0, is spanned by e_0.

Proof. By the symmetry of the matrix $\frac{\partial^2 \mathcal{A}}{(\partial x_0)^2}$,

$$\begin{aligned} & e_0 \cdot n \\ = \quad & \left(\frac{\partial^2 \mathcal{A}}{(\partial x_0)^2}\right) e_0 \cdot \left(\frac{\partial^2 \mathcal{A}}{\partial x_0 \partial x}\right)^{-1} \left(\dot{X}(t,x_0,\nabla S_0(x_0)) - \dot{X}(t,\check{x}_0,\nabla S_0(\check{x}_0))\right) \\ = \quad & 0.\end{aligned}$$

Therefore, e_0 is in the tangent plane T_{x_0} which is one dimensional. □

Proposition 4.23. *Assume that in two dimensions at $x_0 \in \Phi_t^{-1} M_t$ the normal $n(x_0) \neq 0$ so that the pre-Maxwell set does not have a generalised cusp at x_0. Then, the Maxwell set can only have a cusp at $\Phi_t(x_0)$ if $\Phi_t(x_0) \in C_t$. Moreover, if*

$$x = \Phi_t(x_0) \in \Phi_t \left\{\Phi_t^{-1} C_t \cap \Phi_t^{-1} M_t\right\},$$

the Maxwell set will have a generalised cusp at x.

Proof. From Lemma 3.12, the Maxwell set can only have a cusp at $\Phi_t(x_0)$ if the pre-Maxwell set intersects the pre-caustic.

Moreover, from Corollary 4.23, the tangent to the pre-Maxwell set at a point x_0 where it intersects the pre-caustic is parallel to the zero eigenvector e_0. Therefore, the Maxwell set will be cusped at any point $x = \Phi_t(x_0)$ if the pre-Maxwell set and pre-caustic intersect at x_0. □

Corollary 4.24. *In two dimensions, let the pre-Maxwell set intersect the pre-caustic at a point x_0 where the normal to the pre-Maxwell set $n(x_0) \neq 0$ so that the pre-Maxwell set is not cusped at x_0. Then, there is a cusp on the Maxwell set where it intersects the caustic at $x = \Phi_t(x_0)$ and the pre-Maxwell set touches the pre-level surface $\Phi_t^{-1}H_t^c$ at x_0. Moreover, if the cusp on the Maxwell set intersects the caustic at a regular point of the caustic, then there will be a cusp on the pre-Maxwell set which also intersects the same pre-level surface $\Phi_t^{-1}H_t^c$ at another point $\check{x}_0$.*

Proof. From Corollary 4.22, the tangent plane to the pre-Maxwell set is spanned by the zero eigenvector e_0. However, from Corollary 1.12, the pre-level surface is also spanned by e_0 and so the surfaces touch. Moreover, by Lemma 3.12, the second pre-image $\check{x}_0$ corresponding to the point $\Phi_t(x_0)$ on the Maxwell set must be a generalised cusp. □

Corollary 4.25. *When the pre-Maxwell set touches the pre-caustic, it must also touch a pre-level surface and the Maxwell set will have a generalised cusp which intersects a generalised cusp on the caustic.*

Proof. By Lemma 3.13, when we reach a cusp on the caustic the pre-level surface touches the pre-caustic. □

Example 4.26 (The polynomial swallowtail). Let $V = 0$, $k_t = 0$ and

$$S_0(x_0, y_0) = x_0^5 + x_0^2 y_0.$$

Recall Figure 4.7 which shows the Maxwell set and pre-Maxwell set highlighting some specific points of interest (points 1 to 6).

From Proposition 4.23, the cusps on the Maxwell set correspond to the intersections of the pre-curves (points 3 and 6). But from Corollary 4.24, the cusps on the Maxwell set also correspond to the cusps on the pre-Maxwell set (points 2 and 5). Each cusp on the pre-Maxwell set lies on the same level surface as a point of intersection between the pre-caustic and pre-Maxwell set as shown in Figure 4.8.

The Maxwell set terminates when it reaches the cusps on the caustic (points 1 and 4). These points satisfy the condition for a generalised cusp but, instead

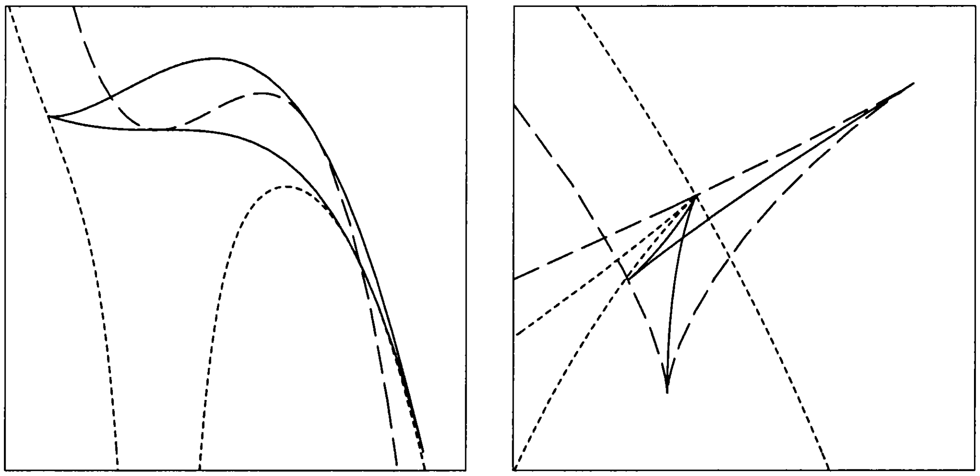

Figure 4.8: The caustic (long dash) and Maxwell set (solid line) with the level surfaces (short dash) through the cusps on the Maxwell set (points 2 and 6).

of appearing cusped, the curve stops and the parameterisation begins again in the sense that it maps back exactly onto itself. This follows because every point on the Maxwell set has at least two real pre-images, and so by pre-parameterising the Maxwell set, we effectively sweep it out twice. All of the pre-surfaces touch at the cusps on the caustic as in Figure 4.9.

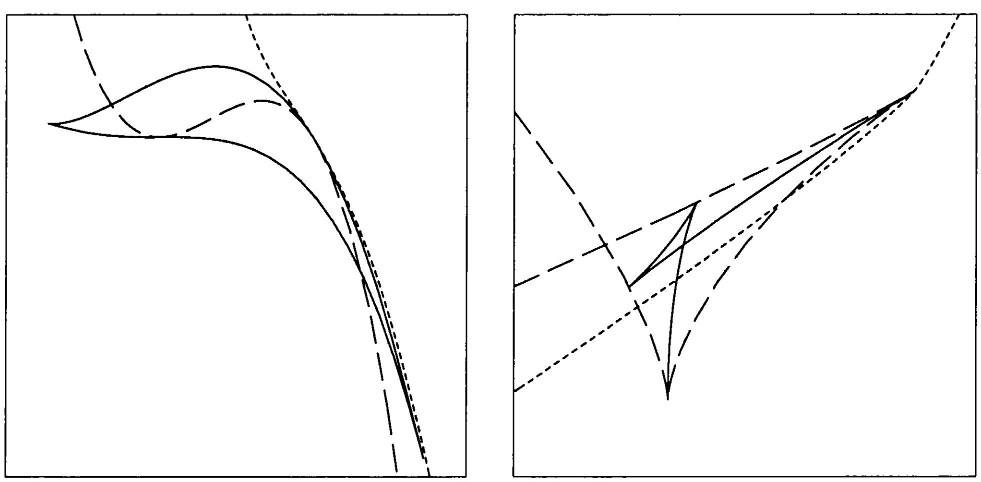

Figure 4.9: The caustic (long dash) and Maxwell set (solid line) with the level surface (short dash) through the caustic cusp (Point 4).

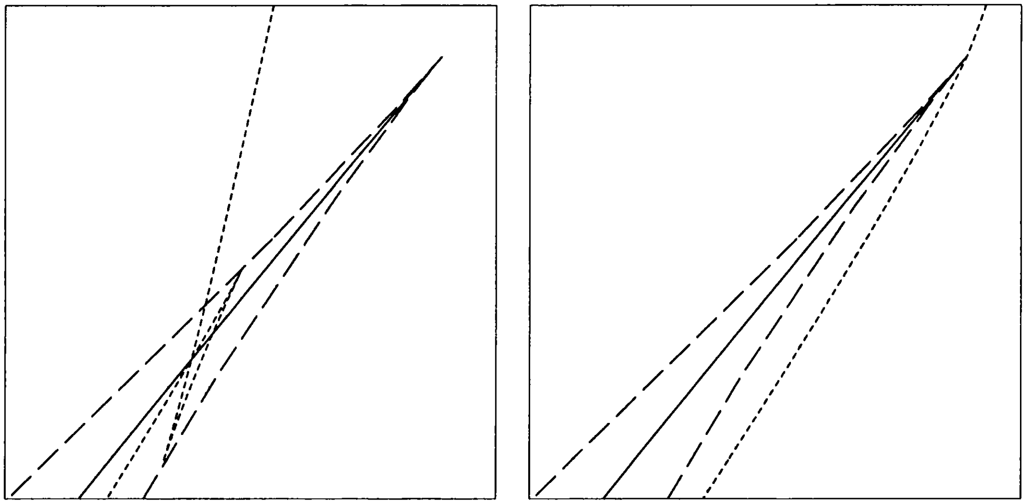

Figure 4.10: The level surface (short dash) through a point moving along the Maxwell set (solid line) towards a cusp on the caustic (long dash).

These two different forms of cusps correspond to very different geometric behaviours of the level surfaces. By Lemma 4.4, any point on the Maxwell set corresponds to a point of self-intersection on some Hamilton-Jacobi level surface. Therefore, where the Maxwell set terminates or has a cusp, the corresponding level surface must have a point of self-intersection which disappears with the variation of the parameter c.

There are two distinct ways in which this can happen. Firstly, the level surface could have a point of swallowtail perestroika. From Corollary 3.14, a cusp on the caustic corresponds to points of swallowtail perestroika on some level surface. Only one point of self-intersection will disappear at such a point and therefore, only one path of the Maxwell set can approach a cusp on the caustic. When the cusp is reached, the Maxwell set must bounce back along exactly the same path (Figure 4.10).

However, as a point $x \in M_t$ approaches a regular point of the caustic, the level surface with a point of self-intersection at x will also have a cusp but not a point of swallowtail perestroika. Therefore, this corresponds to the collapse of the second system of double points in Figure 3.1. At such a point, two different points of self-intersection have coalesced and so two paths of the Maxwell set must approach the point and produce the cusp (Figure 4.11).

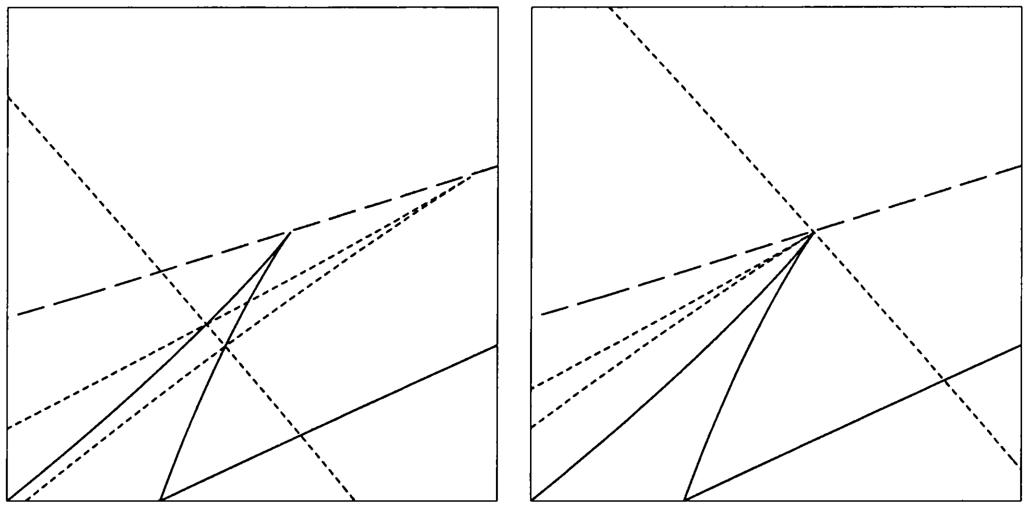

Figure 4.11: The level surface (short dash) through a point moving along the Maxwell set (solid line) towards the caustic (long dash).

4.6 Extensions to 3 dimensions

We can extend the results of the previous section to the three dimensional case by following the ideas of DTZ.

Lemma 4.27. *Let $x_0(s)$ be any 3 dimensional parameterised surface where $s = (s_1, s_2)$, and define,*

$$x(s) = \Phi_t(x_0(s)).$$

Let e_0 denote the zero eigenvector of $\left(\frac{\partial^2 \mathcal{A}}{(\partial x_0)^2}\right)$ and assume that $\ker\left(\frac{\partial^2 \mathcal{A}}{(\partial x_0)^2}\right) = \langle e_0 \rangle$*. Then the tangent space to $x(s)$ when $s = \sigma$ is at most one dimensional if and only if either:*

1. *the tangent space to $x_0(s)$ is at most one dimensional when $s = \sigma$; or,*
2. *$x_0(\sigma)$ is on the pre-caustic and the tangent space to $x_0(s)$ when $s = \sigma$ is spanned by e_0 and $(n \wedge e_0)$ where n is the normal to $x_0(s)$.*

Proof. Clearly,

$$\frac{\partial x}{\partial s_\alpha}(s) = D\Phi_t(x_0(s))\frac{\partial x_0}{\partial s_\alpha}(s),$$

where $D\Phi_t$ is the Frechet derivative of the flow map Φ_t and $\alpha = 1, 2$.

Therefore, the tangent space to $x(s)$ at $s = \sigma$ is at most one dimensional if and only if there exist scalars $\xi_1, \xi_2 \in \mathbb{R}$ not both zero such that,

$$0 = \xi_1 \frac{\partial x}{\partial s_1}(\sigma) + \xi_2 \frac{\partial x}{\partial s_2}(\sigma)$$

$$= D\Phi_t(x_0(\sigma))\left(\xi_1\frac{\partial x_0}{\partial s_1}(\sigma)+\xi_2\frac{\partial x_0}{\partial s_2}(\sigma)\right).$$

It follows from Lemma 3.11 that this is equivalent to,

$$0=\left(\frac{\partial\mathcal{A}}{(\partial x_0)^2}(x_0(\sigma),x(\sigma),t)\right)\left(\xi_1\frac{\partial x_0}{\partial s_1}(\sigma)+\xi_2\frac{\partial x_0}{\partial s_2}(\sigma)\right). \tag{4.2}$$

Recall from the proof of Lemma 3.12 that the matrix,

$$\left(\frac{\partial\mathcal{A}}{(\partial x_0)^2}(x_0(\sigma),\Phi_t(x_0(\sigma)),t)\right),$$

is only singular when $x_0(s)$ is on the pre-caustic. Therefore, if $x_0(s)\in\Phi_t^{-1}C_t$, equation (4.2) will only hold if $\left(\xi_1\frac{\partial x_0}{\partial s_1}(\sigma)+\xi_2\frac{\partial x_0}{\partial s_2}(\sigma)\right)$ is parallel to e_0. Alternatively, if $x_0(\sigma)$ is not on the pre-caustic, we can invert the matrix in equation (4.2) giving the trivial solution

$$\left(\xi_1\frac{\partial x_0}{\partial s_1}(\sigma)+\xi_2\frac{\partial x_0}{\partial s_2}(\sigma)\right)=0. \qquad \square$$

This is a generalisation of Theorem 1.15 which enables us to develop the following results.

Corollary 4.28. *In three dimensions, at any point $x_0\in\Phi_t^{-1}C_t\cap\Phi_t^{-1}M_t$ where the normal to the pre-Maxwell set $n(x_0)\neq 0$ and*

$$\ker\left(\frac{\partial^2\mathcal{A}}{(\partial x_0)^2}\right)_{x=\Phi_t(x_0)}=\langle e_0\rangle,$$

where e_0 is the zero eigenvector, the tangent plane to the pre-Maxwell set T_{x_0} is spanned by e_0 and $(n(x_0)\wedge e_0)$.

Proof. By symmetry of $\frac{\partial^2\mathcal{A}}{(\partial x_0)^2}$,

$$\begin{aligned}
&e_0\cdot n\\
&=\left(\frac{\partial^2\mathcal{A}}{(\partial x_0)^2}\right)e_0\cdot\left(\frac{\partial^2\mathcal{A}}{\partial x_0\partial x}\right)^{-1}\left(\dot X(t,x_0,\nabla S_0(x_0))-\dot X(t,\check x_0,\nabla S_0(\check x_0))\right)\\
&=0,
\end{aligned}$$

so that e_0 is in the tangent plane T_{x_0}. Setting $e_0^\perp=(n(x_0)\wedge e_0)$, it follows that $e_0^\perp\in T_{x_0}$ by definition. $\square$

Definition 4.29. *The cusped part of the Maxwell set M_t (or sub-Maxwell set) in three dimensions is defined to be the set,*

$$\begin{aligned}\mathrm{Cusp}(M_t) &= \{x \in M_t : \quad x \in \Phi_t\left(\Phi_t^{-1}C_t \cap \Phi_t^{-1}M_t\right), \\ &\qquad\qquad x = \Phi_t(x_0), \quad n(x_0) \neq 0\}.\end{aligned}$$

Proposition 4.30. *Let $x \in \mathrm{Cusp}(M_t)$. Then in three dimensions, the tangent plane to the Maxwell set at x, T_x, is at most one dimensional.*

Proof. This follows from Lemma 4.27 and Corollary 4.28 since the tangent plane to the cusped part of the Maxwell set must be $T_x = \langle D\Phi_t(x_0)(n \wedge e_0)\rangle$, which is at most one dimensional. □

The name sub-Maxwell set ties this concept into the subcaustic on which the tangent plane to the caustic dropped a dimension.

Example 4.31 (The butterfly). Let $V(x,y) \equiv 0$, $k_t(x,y) \equiv 0$ and

$$S_0(x_0, y_0, z_0) = x_0^3 y_0 + x_0^2 z_0.$$

The pre-Maxwell set can be found as

$$\begin{aligned}0 \;=\; & -16 - 8t^2 - t^4 - 12t^2{x_0}^2 - 11t^4{x_0}^2 + 9t^2{x_0}^4 - 9t^4{x_0}^4 + t^6{x_0}^4 + 9t^4{x_0}^6 \\ & +10t^6{x_0}^6 + 9t^6{x_0}^8 - 144tx_0y_0 - 12t^3x_0y_0 - 2t^5x_0y_0 - 18t^3{x_0}^3y_0 \\ & -24t^5{x_0}^3y_0 + 54t^3{x_0}^5y_0 - 54t^5{x_0}^5y_0 - 36t^2{y_0}^2 - t^4{y_0}^2 - 486t^2{x_0}^2{y_0}^2 \\ & +81t^4{x_0}^4{y_0}^2 + 108t^4{x_0}^6{y_0}^2 - 54t^3x_0{y_0}^3 - 594t^3{x_0}^3{y_0}^3 - 27t^2{y_0}^4 - 96tz_0 \\ & -32t^3z_0 - 2t^5z_0 - 48t^3{x_0}^2z_0 - 22t^5{x_0}^2z_0 + 36t^3{x_0}^4z_0 - 18t^5{x_0}^4z_0 \\ & +18t^5{x_0}^6z_0 - 576t^2x_0y_0z_0 - 24t^4x_0y_0z_0 - 36t^4{x_0}^3y_0z_0 + 108t^4{x_0}^5y_0z_0 \\ & -72t^3{y_0}^2z_0 - 972t^3{x_0}^2{y_0}^2z_0 - 192t^2{z_0}^2 - 32t^4{z_0}^2 - 48t^4{x_0}^2{z_0}^2 \\ & +36t^4{x_0}^4{z_0}^2 - 576t^3x_0y_0{z_0}^2 - 128t^3{z_0}^3.\end{aligned}$$

This is a cubic in z_0 which can be solved to find the pre-parameterisation of the Maxwell set. This solution has picked a single sheet out of the complete Maxwell-Klein set (compare Figures 4.4 and 4.5 with 4.12 and 4.13).

Example 4.32 (The 3D polynomial swallowtail). Let $V = 0$, $k_t = 0$ and

$$S_0(x_0, y_0, z_0) = x_0^7 + x_0^3 y_0 + x_0^2 z_0.$$

Then the pre-Maxwell set can be found as a quartic in z_0 which is shown in Appendix C. The equation can be solved for z_0 and, using the flow map, we can then pre-parameterise the Maxwell set.

As in the two dimensional case, the Maxwell set is a swallowtail which fits perfectly within the caustic swallowtail. The pre-Maxwell set has regions where the tangent plane is at most one dimensional, which correspond to pre-images of the cusped part of the Maxwell set (Figures 4.14 and 4.15).

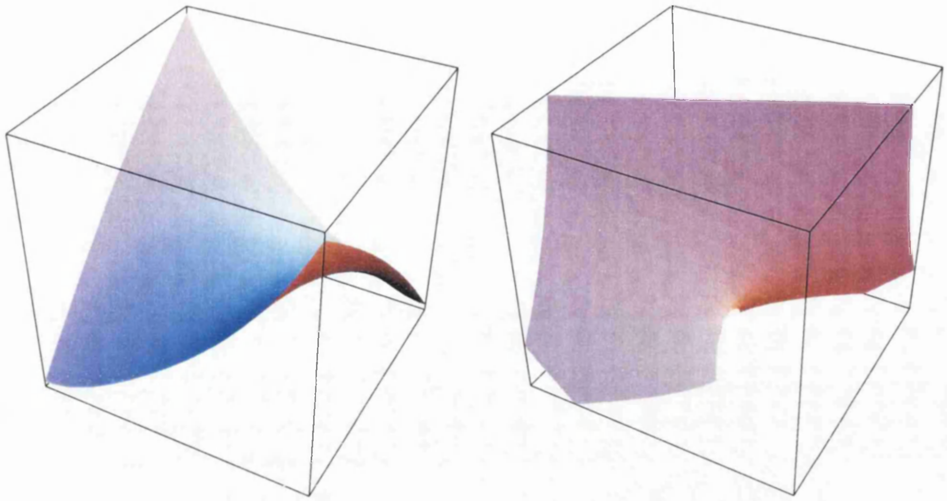

Pre-Maxwell set *Maxwell set*

Figure 4.12: The butterfly Maxwell set when $t = 1$.

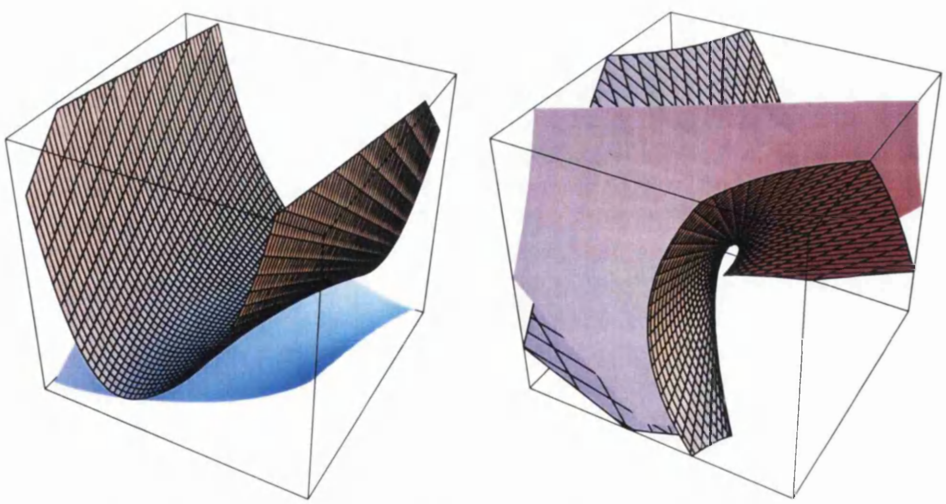

Pre-Maxwell set and pre-caustic *Maxwell set and caustic*

Figure 4.13: The butterfly Maxwell set (plain) with caustic (mesh) when $t = 1$.

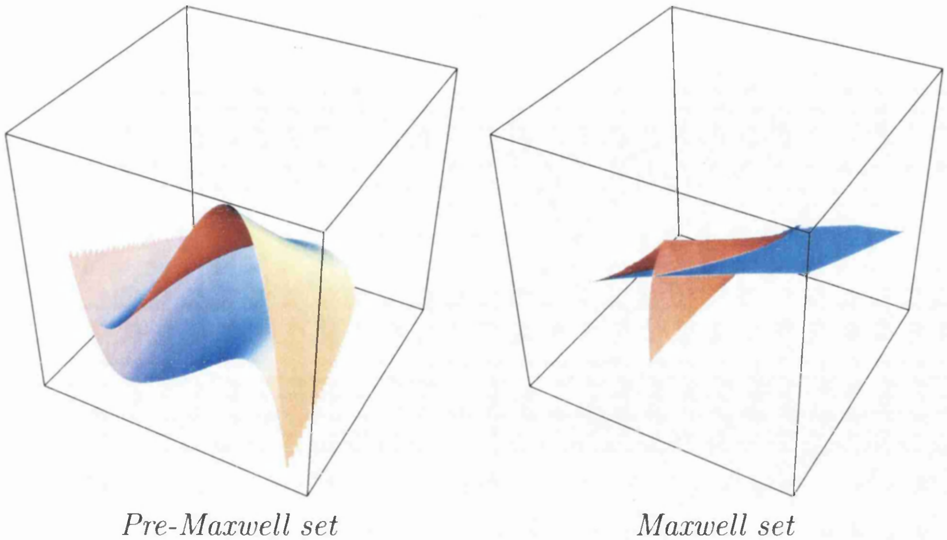

Figure 4.14: The 3D swallowtail Maxwell set when $t = 1$.

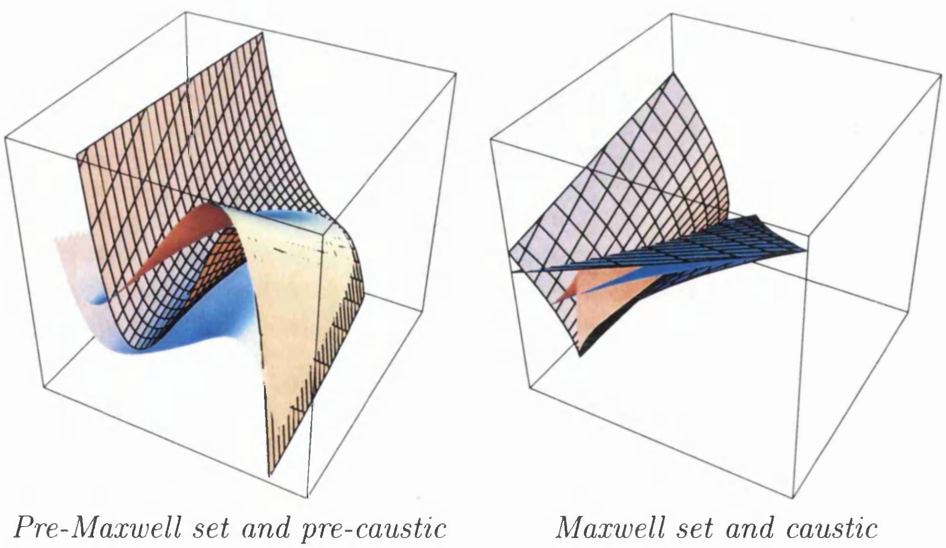

Figure 4.15: The 3D swallowtail Maxwell set (plain) and caustic (mesh) when $t = 1$.

4.7 Hot and cool parts of the Maxwell set

The only part of the Maxwell set which is singular is the region where the pre-image pair x_0 and $\check{x}_0$ are the global minimisers of the stochastic action. Therefore, following directly from our work with caustics, we can divide the Maxwell set into hot and cool parts.

Definition 4.33. *Let x be a point on the Maxwell set and let $x_0(i)(x,t)$ for $i = 1, 2, \ldots, n$ denote an enumeration of the real roots of,*

$$\nabla_{x_0}\mathcal{A}(x_0, x, t) = 0,$$

so that for some fixed i and j,

$$x_0(i)(x,t), x_0(j)(x,t) \in \Phi_t^{-1} M_t.$$

Then, the point x is said to be on the cool part of the Maxwell set if

$$\mathcal{A}(x_0(i)(x,t), x, t) \leq \mathcal{A}(x_0(k)(x,t), x, t),$$

for all $k = 1, 2, \ldots n$. If the Maxwell set is not cool it is hot.

By the definition of the Maxwell set,

$$\mathcal{A}(x_0(i)(x,t), x, t) = \mathcal{A}(x_0(j)(x,t), x, t),$$

and so it does not matter which pre-image we choose in Definition 4.33.

Lemma 4.34. *The inviscid limit of the Burgers fluid velocity field $v^0(x,t)$ will be discontinuous as x crosses a cool part of the Maxwell set, but will be continuous as x crosses a hot part of the Maxwell set.*

Lemma 4.35. *Let $x_t^M(\lambda)$ denote the pre-parameterisation of the Maxwell set where $\lambda = (\lambda_1, \lambda_2, \ldots, \lambda_{d-1}) \in \mathbb{R}^{d-1}$. Then, $x_t^M(\lambda)$ is on the cool part of the Maxwell set if and only if*

$$f_{(x_t^M(\lambda),t)}(\lambda_1) \leq f_{(x_t^M(\lambda),t)}(x_0^1(i)(x_t^M(\lambda), t)),$$

for all $i = 1, 2, \ldots, n$, where $x_0^1(i)(x,t)$ denotes an enumeration of all the real roots for x_0^1 to,

$$f'_{(x,t)}(x_0^1) = 0.$$

Proof. Follows from Definition 4.33 and Theorem 1.22. □

As in the caustic case, we will identify the hot and cool parts of the Maxwell set by finding the possible hot/cool boundaries. However, unlike the caustic case, we cannot immediately use the pre-normalised reduced action function to simplify the problem as there is no longer the guarantee of a repeated root at $x_0^1 = \lambda_1$. Instead, we are able to make the following geometric assertion.

Theorem 4.36. *A necessary condition for x to be a possible hot/cool boundary for the Maxwell set is that either:*

1. *x is a point of intersection between the Maxwell set and the caustic; or,*

2. *x is a point of self-intersection of the Maxwell set where at least three parts meet.*

Proof. For the Maxwell set to be cool, the two pre-images (which we shall now denote $x_0 = x_0(i)(x,t)$ and $\check{x}_0 = x_0(j)(x,t)$), must correspond to local minima on the reduced action function. Therefore, one way for the Maxwell set to change between being cool and hot is for one of the pre-images to become a local maximum. This can only happen if a maximum and one of the minima (either x_0 or $\check{x}_0$) coalesce to form an inflexion and then split again into a maximum and minimum pair, as shown in the first column of Figure 4.16. This will occur when one of the pre-images of the Maxwell set is also on the pre-caustic. Thus, at such a point, the Maxwell set will be cusped and will intersect the caustic.

Alternatively, the Maxwell set may become cool if a maximum and minimum occurring at a lower action value than x_0 and $\check{x}_0$ coalesce to form an inflexion and then disappear, as shown in the second column of Figure 4.16. This occurs when the Maxwell set intersects the caustic but the pre-Maxwell set does not intersect the pre-caustic. Therefore, the Maxwell set will not be cusped at this point of intersection with the caustic.

Finally, the Maxwell set will change from hot to cool if the minimising critical point rises to the same action value as x_0 and $\check{x}_0$ as shown in the final column of Figure 4.16. This will correspond to a point of self-intersection of the Maxwell set. It is important to note that not all points of self-intersection are of this form – this corresponds to points where at least three parts of the Maxwell set intersect. □

In the two dimensional case, these possible boundaries can be expressed in terms of the multiple points of the Hamilton-Jacobi level surfaces.

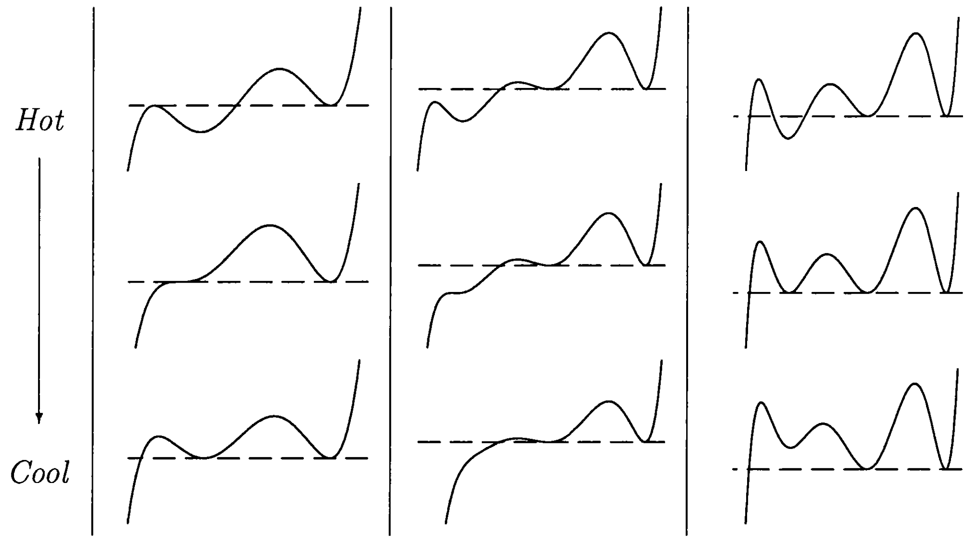

Figure 4.16: Graphs of $f_{(x,t)}(x_0^1)$ when x is on the Maxwell set.

Corollary 4.37. *In two dimensions, a necessary condition for x to be a possible hot/cool boundary for the Maxwell set is that x is a multiple point of order m of some Hamilton Jacobi level surface with either:*

1. *$m \geq 3$ where the level surface has at least three real tangents two of which are coincident; or,*

2. *$m \geq 2$ where the level surface has at least two real coincident tangents (cusp) and x is also a multiple point of order $\tilde{m} \geq 2$ of a different level surface with at least two real distinct tangents (crunode); or,*

3. *$m \geq 3$ where the level surface has at least three real distinct tangents.*

Proof. This follows from Proposition 1.14 and Lemma 4.4 since a level surface whose pre-image intersects the pre-caustic must have a cusp, and a level surface whose pre-image intersects the pre-Maxwell set must have a crunode. □

The possible boundary points from part 1 of Corollary 4.37 correspond to the possible boundaries in part 1 of Theorem 4.36 where the Maxwell set is cusped on its intersection with the caustic. Moreover, these points are also the possible hot/cool boundaries of the caustic which do not correspond to points of self-intersection of the caustic (i.e. were found from the repeated roots of the function $\tilde{F}$ in Proposition 2.29). Thus, we can find these points using the pre-normalised reduced action function. As with the caustic, we divide the results of Theorem 4.36 and Corollary 4.37 into genuine hot/cool boundaries and false positive boundaries.

Corollary 4.38. *In two dimensions, if x satisfies condition 1 in Corollary 4.37 then it will be a genuine hot/cool boundary of the Maxwell set if and only if it is a genuine hot/cool boundary of the caustic.*

Proof. If x is a genuine hot/cool boundary for the Maxwell set where the pre-Maxwell set intersects the pre-caustic, then the reduced action function has a point of inflexion and a local minimum at the same minimising level. This makes x a genuine hot/cool boundary for the caustic. □

Example 4.39 (The generic Cusp). Let $V = 0$, $k_t = 0$ and

$$S_0(x_0, y_0) = x_0^2 y_0/2.$$

Then the reduced action function is,

$$f_{(x,t)}(x_0^1) = -\frac{1}{8t}\left(t^2 x_0^4 - (4+4ty)x_0^2 + 8xx_0 - 4x^2\right).$$

Recall from Example 4.19 that the Maxwell set in this case is the line $x = 0$ for values $y > -\frac{1}{2t}$. This cuts through the region where there are three real pre-images for every point. Clearly, as $x_0^1 \to \pm\infty$, $f_{(x,t)}(x_0^1) \downarrow -\infty$. Therefore, if the reduced action function has two critical points at the same height they must both be maxima and so the whole Maxwell set is hot. This is supported by numerical simulations of $v^0(x,t)$ performed by DTZ [12] in which the curve of discontinuity for the velocity field consists solely of the semicubical parabolic caustic.

Example 4.40 (The polynomial swallowtail). Let $V = 0$, $k_t = 0$ and

$$S_0(x_0, y_0) = x_0^5 + x_0^2 y_0.$$

For this initial condition the reduced action function $f_{((x,y),t)}(x_0)$ is polynomial in x_0 with degree five and so there are at most four real pre-images for any point x. Therefore, it is impossible for any point to satisfy conditions 2 or 3 of Corollary 4.37 as these require at least five real pre-images. Thus, the only boundary points will correspond to condition 1 and, from Example 2.31 and Corollary 4.38, it follows that the only genuine boundary point is given by,

$$(x, y) = \left(-\frac{t^5(3+8\sqrt{6})}{18000}, -\frac{1}{2t} + \frac{t^3(9-\sqrt{6})}{450}\right),$$

corresponding to points 3 and 5 on Figure 4.7.

Recall from Example 4.20 that the pre-Maxwell set is given by,

$$y_{0,\mathrm{M}}^{\pm}(x_0) = \frac{1}{108t^2}\left(-54t + t^5 + 6t^4 x_0 - 24t^3 x_0^2 - 280t^2 x_0^3 \pm t^2\sqrt{A_t(x_0)}\right),$$

where,

$$A_t(x_0) = (t^2 + 4tx_0 - 20x_0^2)^3,$$

and we restrict $x_0 \in \left[\frac{t}{10}(1-\sqrt{6}), \frac{t}{10}(1+\sqrt{6})\right]$. The additional $\pm$ is to highlight the sign we take with the square root.

Thus, the hot/cool boundary has two pre-images on the pre-Maxwell set given by $(\tilde{x}_0, y_{0,\mathrm{M}}^+(\tilde{x}_0))$ (point 3 on Figure 4.7) and $(\check{x}_0, y_{0,\mathrm{M}}^+(\check{x}_0))$ (point 5 on Figure 4.7) where,

$$\tilde{x}_0 = \frac{t}{30}(3 - 2\sqrt{6}), \qquad \check{x}_0 = \frac{t}{10}(1+\sqrt{6}).$$

It does not matter which sign we choose for $y_{0,\mathrm{M}}$ for $x_0 = \check{x}_0$ as $A_t(\check{x}) = 0$.

This divides the pre-Maxwell set into two distinct pieces:

1. $\left(x_0, y_{0,\mathrm{M}}^+(x_0)\right)$ for $\tilde{x}_0 \leq x_0 \leq \check{x}_0$; and,
2. $\left(x_0, y_{0,\mathrm{M}}^-(x_0)\right)$ for $\frac{t}{10}(1-\sqrt{6}) \leq x_0 \leq \check{x}_0$ and $\left(x_0, y_{0,\mathrm{M}}^+(x_0)\right)$ for $\frac{t}{10}(1-\sqrt{6}) \leq x_0 \leq \tilde{x}_0$.

The first part of this division goes from point 3 to 5 via point 4 on Figure 4.7, and the second part goes from point 5 to 3 via points 6, 1 and 2. Therefore, we need to consider the nature of the Maxwell set at a point in each of these sectors. We choose points 1 and 4 corresponding to the two cusps on the caustic.

At $(0, -\frac{1}{2t})$ (point 1), the reduced action function has a triple critical point corresponding to the pre-Maxwell set which is a maximum, and a single additional critical point which is a minimum. Clearly, this will be on the hot part of the Maxwell set.

At $(\frac{t^5}{125}, -\frac{1}{2t} + \frac{t^3}{25})$ (point 4), the reduced action function has a triple critical point corresponding to the pre-Maxwell set which is a minimum, and a single additional critical point which is a maximum. This will be on the cool part of the Maxwell set. This is shown in Figure 4.17 where the cool parts of both the caustic and Maxwell set are indicated by a thicker line.

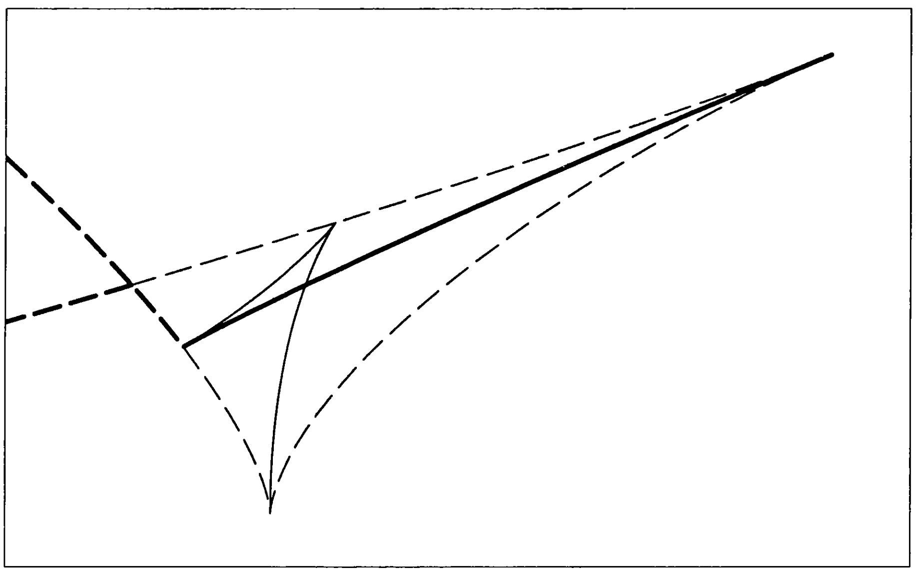

Figure 4.17: The hot (normal line) and cool (thick line) parts of the Maxwell set (solid) and caustic (long dash) for the polynomial swallowtail when $t = 1$.

Chapter 5

Real and complex turbulence

Summary

We now apply the geometrical results developed in the preceding chapters to demonstrate the existence of turbulent behaviour in the inviscid limit of the minimal entropy solution of the stochastic Burgers equation. We have shown that cusps are created and destroyed on the Hamilton-Jacobi level surfaces when the pre-level surface touches the pre-caustic. In this chapter we show that this creation and destruction occurs infinitely rapidly for short intermittent bursts as a result of the stochastic force acting upon the fluid; this causes 'real turbulence'. It is also shown that the number of swallowtails on the caustic may also change infinitely rapidly when the real part of the pre-caustic touches its complex counterpart; this causes 'complex turbulence'. We identify these turbulent times as zeros of two stochastic processes derived from the reduced action function and show that these processes may be recurrent, causing the intermittent behaviour associated with turbulence.

5.1 Real turbulence

The geometric results of DTZ show that in two dimensions a level surface will have a cusp on the caustic if the pre-level surface intersects the pre-caustic. This idea can be extended to three dimensions as in Theorem 1.14, in which case the intersections of the pre-level surface and pre-caustic force the tangent plane to the level surface to be at most one dimensional. As discussed in Section 2.2, this one dimensional tangent space gives rise to a fold in the level surface (a curve of cusps).

As time passes, the cusps or curves of cusps will appear and disappear on the level surfaces as the pre-curves move.

Definition 5.1. *Real turbulent times are defined to be times t at which there exist points where the pre-level surface $\Phi_t^{-1} H_t^c$ and pre-caustic $\Phi_t^{-1} C_t$ touch.*

Real turbulent times correspond to times at which there is a change in the number of cusps or cusped curves on the level surface H_t^c. Moreover, in two dimensions when the pre-surfaces are sufficiently well behaved, these points correspond to swallowtail perestroikas on the level surfaces (Corollary 3.14) and also consequently, to points where the Maxwell set terminates (Lemma 4.4). The turbulent times will be random when a random force acts upon the Burgers fluid.

Consider the d-dimensional case. Assuming that Φ_t is globally reducible, let $f_{(x,t)}(x_0^1)$ denote the reduced action function and $x_t(\lambda)$ the pre-parameterisation of the caustic. The number of curves of intersection between the pre-level surface $\Phi_t^{-1} H_t^c$ and the pre-caustic $\Phi_t^{-1} C_t$ will be given by the cardinality,

$$\begin{aligned}\#\{\lambda_d = \lambda_d(\lambda_1, \ldots, \lambda_{d-1}) \ \ : \ \ & \lambda = (\lambda_1, \ldots, \lambda_{d-1}, \lambda_d(\lambda_1, \ldots, \lambda_{d-1})) \\ & \text{and } f_{(x_t(\lambda),t)}(\lambda_1) = c\}.\end{aligned}$$

The real turbulent times are values of t where this cardinality changes. Therefore, the real turbulent times must satisfy the conditions,

$$f_{(x_t(\lambda),t)}(\lambda_1) - c = 0 \quad \text{and} \quad \frac{\partial f_{(x_t(\lambda),t)}(\lambda_1)}{\partial \lambda_\alpha} = 0 \quad \text{for } \alpha = 1, 2, \ldots, d.$$

Theorem 5.2. *The real turbulent times t are given by the zeros of the zeta process ζ_t^c where,*

$$\zeta_t^c := f_{(x_t(\lambda),t)}(\lambda_1) - c,$$

and λ satisfies,

$$\frac{\partial f_{(x_t(\lambda),t)}(\lambda_1)}{\partial \lambda_\alpha} = 0 \quad \textit{for } \alpha = 1, 2, \ldots, d. \tag{5.1}$$

The values of λ satisfying equation (5.1) correspond to critical points of the reduced action function evaluated on the caustic. The turbulent times will only produce genuine turbulent behaviour if the point $x_t(\lambda)$ is on the cool part of the caustic since the fluid velocity is continuous as we cross a hot part of the caustic.

Over the next five sections, we analyse the occurrence of real turbulence under the constraint that the only forces acting on the Burgers fluid are white noise in time.

5.2 The zeta process for d independent white noises acting in d orthogonal directions

Consider the Burgers fluid under the potential $V(x) = 0$ and the noise,

$$\sum_{\alpha=1}^{d} \nabla k_\alpha(x) W_\alpha(t),$$

where W_α are d independent Wiener processes. Moreover, let,

$$k_\alpha(x) = x_\alpha \quad \text{where} \quad x = (x_1, x_2, \ldots, x_d).$$

The stochastic Burgers equation is then,

$$\frac{\partial v^\mu}{\partial t} + (v^\mu \cdot \nabla) v^\mu = \frac{\mu^2}{2} \Delta v^\mu - \epsilon \dot{W}(t), \tag{5.2}$$

where $W(t) = (W_1(t), W_2(t), \ldots, W_d(t))$ so that the fluid is acted on by d orthogonal independent Wiener processes.

Theorem 5.3. *The stochastic action corresponding to the stochastic Burgers equation (5.2) is,*

$$\begin{aligned} \mathcal{A}(x_0, x, t) &= \frac{|x - x_0|^2}{2t} + \frac{\epsilon}{t}(x - x_0) \cdot \int_0^t W(s)\, \mathrm{d}s - \epsilon x \cdot W(t) \\ &\quad - \frac{\epsilon^2}{2} \int_0^t |W(s)|^2 \, \mathrm{d}s + \frac{\epsilon^2}{2t} \left| \int_0^t W(s)\, \mathrm{d}u \right|^2 + S_0(x_0). \end{aligned}$$

Proof. Recall from equation (1.16) that,

$$A(x_0, p_0, t) = \frac{1}{2} \int_0^t \dot{X}^2(s)\, \mathrm{d}s - \epsilon \int_0^t \sum_{\alpha=1}^{d} X_\alpha(s)\, \mathrm{d}W_\alpha(s),$$

where $X(s) = (X_1(s), X_2(s), \ldots, X_d(s))$ and $p_0 = (p_0^1, p_0^2, \ldots, p_0^d)$. The paths $X_\alpha(s)$ must satisfy the Euler-Lagrange equations,

$$\mathrm{d}\dot{X}_\alpha(s) = -\epsilon\, \mathrm{d}W_\alpha(s),$$

where $\dot{X}_\alpha(0) = p_0^\alpha$ and $X_\alpha(0) = x_0^\alpha$ for $\alpha = 1, 2, \ldots, d$. It follows that,

$$\dot{X}_\alpha(s) = p_0^\alpha - \epsilon W_\alpha(s),$$

giving,

$$X_\alpha(s) = x_0^\alpha + p_0^\alpha s - \epsilon \int_0^s W_\alpha(u)\, \mathrm{d}u. \tag{5.3}$$

Therefore,

$$
\begin{aligned}
&A(x_0, p_0, t)\\
&= \frac{1}{2}\int_0^t \sum_{\alpha=1}^d \dot{X}_\alpha^2(s)\,\mathrm{d}s - \epsilon \int_0^t \sum_{\alpha=1}^d X_\alpha(s)\,\mathrm{d}W_\alpha(s)\\
&= \frac{1}{2}\sum_{\alpha=1}^d \int_0^t (p_0^\alpha - \epsilon W_\alpha(s))^2\,\mathrm{d}s\\
&\qquad -\epsilon \sum_{\alpha=1}^d \int_0^t \left(x_0^\alpha + p_0^\alpha s - \epsilon \int_0^s W_\alpha(u)\,\mathrm{d}u\right)\mathrm{d}W_\alpha(s)\\
&= \sum_{\alpha=1}^d \left(\frac{1}{2}t p_0^{\alpha\,2} - \epsilon\left\{x_0^\alpha W_\alpha(t) + p_0^\alpha \int_0^t W_\alpha(s)\,\mathrm{d}s + p_0^\alpha \int_0^t s\,\mathrm{d}W_\alpha(s)\right\}\right.\\
&\qquad \left. + \frac{\epsilon^2}{2}\left\{\int_0^t W_\alpha(s)^2\,\mathrm{d}s + 2\int_0^t \int_0^s W_\alpha(u)\,\mathrm{d}u\,\mathrm{d}W_\alpha(s)\right\}\right)\\
&= \sum_{\alpha=1}^d \left(\frac{1}{2}t p_0^{\alpha\,2} - \epsilon\left\{x_0^\alpha W_\alpha(t) + p_0^\alpha \int_0^t W_\alpha(s)\,\mathrm{d}s + p_0^\alpha \int_0^t s\,\mathrm{d}W_\alpha(s)\right\}\right.\\
&\qquad \left. + \frac{\epsilon^2}{2}\left\{\int_0^t W_\alpha(s)^2\,\mathrm{d}s + 2\left(W_\alpha(t)\int_0^t W_\alpha(u)\,\mathrm{d}u - \int_0^t W_\alpha(u)^2\,\mathrm{d}u\right)\right\}\right)\\
&= \sum_{\alpha=1}^d \left(\frac{1}{2}t p_0^{\alpha\,2} - \epsilon\left\{x_0^\alpha W_\alpha(t) + p_0^\alpha t W_\alpha(t)\right\}\right.\\
&\qquad \left. + \frac{\epsilon^2}{2}\left\{2W_\alpha(t)\int_0^t W_\alpha(u)\,\mathrm{d}u - \int_0^t W_\alpha(s)^2\,\mathrm{d}s\right\}\right),
\end{aligned}
$$

where,

$$\int_0^t \int_0^s W_\alpha(u)\,\mathrm{d}u\,\mathrm{d}W_\alpha(s) = W_\alpha(t)\int_0^t W_\alpha(u)\,\mathrm{d}u - \int_0^t W_\alpha(u)^2\,\mathrm{d}u,$$

and

$$\int_0^t s\,\mathrm{d}W_\alpha(s) + \int_0^t W_\alpha(s)\,\mathrm{d}s = tW_\alpha(t).$$

From equation (5.3),

$$p_\alpha(x_0^\alpha, x_\alpha, t) = \frac{x_\alpha - x_0^\alpha}{t} + \frac{\epsilon}{t}\int_0^t W_\alpha(u)\,\mathrm{d}u.$$

Therefore,

$$\mathcal{A}(x_0, x, t) \;:=\; A(x_0, p(x_0, x, t), t) + S_0(x_0)$$

$$\begin{aligned}
&= \sum_{\alpha=1}^{d}\left\{\frac{(x_\alpha - x_0^\alpha)^2}{2t} + \frac{\epsilon}{t}(x_\alpha - x_0^\alpha)\int_0^t W_\alpha(u)\,\mathrm{d}u - \epsilon x_\alpha W_\alpha(t)\right.\\
&\quad \left. -\frac{\epsilon^2}{2}\int_0^t W_\alpha^2(s)\,\mathrm{d}s + \frac{\epsilon^2}{2t}\left(\int_0^t W_\alpha(u)\,\mathrm{d}u\right)^2\right\} + S_0(x_0)\\
&= \frac{|x-x_0|^2}{2t} + \frac{\epsilon}{t}(x-x_0)\cdot\int_0^t W(u)\,\mathrm{d}u - \epsilon x\cdot W(t)\\
&\quad -\frac{\epsilon^2}{2}\int_0^t |W(s)|^2\,\mathrm{d}s + \frac{\epsilon^2}{2t}\left|\int_0^t W(u)\,\mathrm{d}u\right|^2 + S_0(x_0). \qquad \square
\end{aligned}$$

To find the reduced action function, we must eliminate x_0^α for $\alpha = 2,\ldots,d$, using the conditions,

$$\begin{aligned}
0 = \frac{\partial \mathcal{A}}{\partial x_0^d} &\Leftrightarrow x_0^d = x_0^d(x, x_0^1, x_0^2, \ldots, x_0^{d-1}, t),\\
0 = \frac{\partial \mathcal{A}_d}{\partial x_0^{d-1}} &\Leftrightarrow x_0^{d-1} = x_0^{d-1}(x, x_0^1, x_0^2, \ldots, x_0^{d-2}, t),\\
0 = \frac{\partial \mathcal{A}_{d-1}}{\partial x_0^{d-2}} &\Leftrightarrow x_0^{d-2} = x_0^{d-2}(x, x_0^1, x_0^2, \ldots, x_0^{d-3}, t),\\
&\vdots\\
0 = \frac{\partial \mathcal{A}_3}{\partial x_0^2} &\Leftrightarrow x_0^2 = x_0^2(x, x_0^1, t).
\end{aligned}$$

Here, $\mathcal{A} = \mathcal{A}(x_0^1, x_0^2, \ldots, x_0^d, x, t)$ and $\mathcal{A}_m$ is the action evaluated with the first m substitutions,

$$\mathcal{A}_m := \mathcal{A}(x_0^1, x_0^2, \ldots, x_0^{m-1}, x_0^m(\ldots), x_0^{m+1}(\ldots), \ldots, x_0^d(\ldots), x, t).$$

Lemma 5.4. *If the stochastic action $\mathcal{A}(x_0, x, t)$ is given in Theorem 5.3, then for each integer m where $d \geq m \geq 2$,*

$$\begin{aligned}
\mathcal{A}_m &= \sum_{\alpha=1}^{m-1}\left\{\frac{(x_\alpha - x_0^\alpha)^2}{2t} + \frac{\epsilon(x_\alpha - x_0^\alpha)}{t}\int_0^t W_\alpha(s)\,\mathrm{d}s + \frac{\epsilon^2}{2t}\left(\int_0^t W_\alpha(s)\,\mathrm{d}s\right)^2\right\}\\
&\quad -\sum_{\alpha=1}^{d}\left\{\epsilon x_\alpha W_\alpha(s) + \frac{\epsilon^2}{2}\left(\int_0^t W_\alpha(s)^2\,\mathrm{d}s\right)\right\}\\
&\quad + \left[S_0(x_0) + \frac{t}{2}\sum_{i=m}^{d}\left(\frac{\partial S_0}{\partial x_0^i}\right)^2\right]_{x_0=(x_0^1,\ldots,x_0^{m-1},x_0^m(\ldots),x_0^{m+1}(\ldots),\ldots,x_0^d(\ldots))}. \qquad (5.4)
\end{aligned}$$

Proof. Firstly, set,

$$0 = \frac{\partial \mathcal{A}}{\partial x_0^d} = \frac{x_0^d - x_d}{t} - \frac{\epsilon}{t}\int_0^t W_d(u)\,\mathrm{d}u + \frac{\partial S_0}{\partial x_0^d}(x_0).$$

Therefore, if $x_0^d = x_0^d(x, x_0^1, \ldots, x_0^{d-1}, t)$ is the solution for this equation, then,

$$x_d - x_0^d(\ldots) = -\epsilon\int_0^t W_d(u)\,\mathrm{d}u + t\frac{\partial S_0}{\partial x_0^d}(x_0^1, \ldots, x_0^{d-1}, x_0^d(\ldots)). \tag{5.5}$$

This gives,

$$\begin{aligned}
\mathcal{A}_d &:= \mathcal{A}(x_0^1, x_0^2, \ldots, x_0^{d-1}, x_0^d(\ldots), x, t)\\
&= \sum_{\alpha=1}^{d-1}\left\{\frac{(x_\alpha - x_0^\alpha)^2}{2t} + \frac{\epsilon(x_\alpha - x_0^\alpha)}{t}\int_0^t W_\alpha(s)\,\mathrm{d}s + \frac{\epsilon^2}{2t}\left(\int_0^t W_\alpha(s)\,\mathrm{d}s\right)^2\right\}\\
&\quad -\sum_{\alpha=1}^{d}\left\{\epsilon x_\alpha W_\alpha(s) + \frac{\epsilon^2}{2}\left(\int_0^t W_\alpha(s)^2\,\mathrm{d}s\right)\right\}\\
&\quad + \left[S_0(x_0) + \frac{t}{2}\left\{\frac{\partial S_0}{\partial x_0^d}\right\}^2\right]_{x_0=(x_0^1,\ldots,x_0^{d-1},x_0^d(\ldots))},
\end{aligned}$$

so that equation (5.4) holds for $m = d$.

Next set,

$$\begin{aligned}
0 &= \frac{\partial \mathcal{A}_d}{\partial x_0^{d-1}}\\
&= \frac{x_0^{d-1} - x_{d-1}}{t} - \frac{\epsilon}{t}\int_0^t W_{d-1}(u)\,\mathrm{d}u\\
&\quad + \left[\frac{\partial S_0}{\partial x_0^{d-1}} + \frac{\partial S_0}{\partial x_0^d}\frac{\partial x_0^d}{\partial x_0^{d-1}}\right.\\
&\quad \left. + t\frac{\partial S_0}{\partial x_0^d}\frac{\partial}{\partial x_0^{d-1}}\left(\frac{\partial S_0}{\partial x_0^d}(x_0^1, \ldots, x_0^{d-1}, x_0^d(\ldots))\right)\right]_{x_0=(x_0^1,\ldots,x_0^{d-1},x_0^d(\ldots))}.
\end{aligned} \tag{5.6}$$

Differentiating equation (5.5) with respect to x_0^{d-1} gives,

$$\frac{\partial x_0^d}{\partial x_0^{d-1}} = -t\frac{\partial}{\partial x_0^{d-1}}\left(\frac{\partial S_0}{\partial x_0^d}(x_0^1, \ldots, x_0^{d-1}, x_0^d(\ldots))\right).$$

Substituting into equation (5.6) gives,

$$0 = \frac{x_0^{d-1} - x_{d-1}}{t} - \frac{\epsilon}{t}\int_0^t W_{d-1}(u)\,\mathrm{d}u + \frac{\partial S_0}{\partial x_0^{d-1}}(x_0^1, \ldots, x_0^{d-1}, x_0^d(\ldots)).$$

Again, if $x_0^{d-1} = x_0^{d-1}(x, x_0^1, \ldots, x_0^{d-2}, t)$ is the solution for this equation, then,

$$x_{d-1} - x_0^{d-1}(\ldots) = -\epsilon \int_0^t W_{d-1}(u)\,\mathrm{d}u + t\frac{\partial S_0}{\partial x_0^{d-1}}(x_0^1, \ldots, x_0^{d-1}(\ldots), x_0^d(\ldots)). \tag{5.7}$$

Therefore,

$$\begin{aligned}
&\mathcal{A}_{d-1} \\
&:= \mathcal{A}(x_0^1, x_0^2, \ldots, x_0^{d-2}, x_0^{d-1}(\ldots), x_0^d(\ldots), x, t) \\
&= \sum_{\alpha=1}^{d-2}\left\{\frac{(x_\alpha - x_0^\alpha)^2}{2t} + \frac{\epsilon(x_\alpha - x_0^\alpha)}{t}\int_0^t W_\alpha(s)\,\mathrm{d}s + \frac{\epsilon^2}{2t}\left(\int_0^t W_\alpha(s)\,\mathrm{d}s\right)^2\right\} \\
&\quad -\sum_{\alpha=1}^{d}\left\{\epsilon x_\alpha W_\alpha(s) + \frac{\epsilon^2}{2}\left(\int_0^t W_\alpha(s)^2\,\mathrm{d}s\right)\right\} \\
&\quad + \left[S_0(x_0) + \frac{t}{2}\sum_{\alpha=d-1}^{d}\left\{\frac{\partial S_0}{\partial x_0^\alpha}\right\}^2\right]_{x_0=(x_0^1,\ldots,x_0^{d-2},x_0^{d-1}(\ldots),x_0^d(\ldots))},
\end{aligned}$$

which is equation (5.4) for $m = d - 1$.

It follows by induction that for each integer m,

$$x^m - x_0^m(\ldots) = -\epsilon \int_0^t W_m(u)\,\mathrm{d}u + t\frac{\partial S_0}{\partial x_0^m}(x_0^1, \ldots, x_0^{m-1}, x_0^m(\ldots), \ldots, x_0^d(\ldots)), \tag{5.8}$$

and so,

$$\begin{aligned}
\mathcal{A}_m &= \sum_{\alpha=1}^{m-1}\left\{\frac{(x_\alpha - x_0^\alpha)^2}{2t} + \frac{\epsilon(x_\alpha - x_0^\alpha)}{t}\int_0^t W_\alpha(s)\,\mathrm{d}s + \frac{\epsilon^2}{2t}\left(\int_0^t W_\alpha(s)\,\mathrm{d}s\right)^2\right\} \\
&\quad -\sum_{\alpha=1}^{d}\left\{\epsilon x_\alpha W_\alpha(s) + \frac{\epsilon^2}{2}\left(\int_0^t W_\alpha(s)^2\,\mathrm{d}s\right)\right\} \\
&\quad + \left[S_0(x_0) + \frac{t}{2}\sum_{\alpha=m}^{d}\left\{\frac{\partial S_0}{\partial x_0^\alpha}\right\}^2\right]_{x_0=(x_0^1,\ldots,x_0^{m-1},x_0^m(\ldots),\ldots,x_0^d(\ldots))}. \qquad \square
\end{aligned}$$

Corollary 5.5. *The reduced action function for the stochastic Burgers equation (5.2) is,*

$$\begin{aligned}
f_{(x,t)}(x_0^1) &= \frac{(x_1 - x_0^1)^2}{2t} + \frac{\epsilon(x_1 - x_0^1)}{t}\int_0^t W_1(s)\,\mathrm{d}s + \frac{\epsilon^2}{2t}\left(\int_0^t W_1(s)\,\mathrm{d}s\right)^2 \\
&\quad -\sum_{\alpha=1}^{d}\left\{\epsilon x_\alpha W_\alpha(s) + \frac{\epsilon^2}{2}\left(\int_0^t W_\alpha(s)^2\,\mathrm{d}s\right)\right\}
\end{aligned}$$

$$+\left[S_0(x_0)+\frac{t}{2}\sum_{\alpha=2}^{d}\left\{\frac{\partial S_0}{\partial x_0^\alpha}\right\}^2\right]_{x_0=(x_0^1,x_0^2(x,x_0^1,t),\ldots,x_0^d(\ldots))}.$$

Proof. The reduced action function is $\mathcal{A}_2$ in Lemma 5.4. □

From Theorem 5.2, to find the zeta process we evaluate $f_{(x,t)}(x_0^1)$ with $x = x_t(\lambda)$ and $x_0^1 = \lambda_1$, where $x_t(\lambda)$ denotes the pre-parameterisation of the caustic.

Proposition 5.6. *If $x_t^\epsilon(\lambda)$ denotes the pre-parameterisation of the random caustic for the stochastic Burgers equation (5.2) and $x_t^0(\lambda)$ denotes the pre-parameterisation of the deterministic caustic (the $\epsilon = 0$ case) then,*

$$x_t^\epsilon(\lambda) = x_t^0(\lambda) - \epsilon\int_0^t W(u)\,\mathrm{d}u.$$

Proof. In the deterministic case, using equation (1.10), the flow map is given by,

$$\Phi_t(x_0) = x_0 + t\nabla S_0(x_0),$$

and so the pre-caustic is,

$$\det(I + tS_0''(x_0)) = 0.$$

From Theorem 5.3 and Theorem 1.10, in the stochastic case the flow map is given by,

$$\Phi_t(x_0) = x_0 + t\nabla S_0(x_0) - \epsilon\int_0^t W(u)\,\mathrm{d}u,$$

and so the pre-caustic is again,

$$\det(I + tS_0''(x_0)) = 0.$$

Therefore, in both the deterministic and stochastic cases the pre-caustics are identical and hence, the caustic is simply displaced by the noise term in the stochastic case. □

We can now express explicitly the zeta process for independent noise in d orthogonal directions.

Theorem 5.7. *In d-dimensions, the zeta process for the stochastic Burgers equation (5.2) is,*

$$\zeta_t^c = f^0_{(x_t^0(\lambda),t)}(\lambda_1) - \epsilon x_t^0(\lambda)\cdot W(t) + \epsilon^2 W(t)\cdot\int_0^t W(s)\,\mathrm{d}s - \frac{\epsilon^2}{2}\int_0^t |W(s)|^2\,\mathrm{d}s - c,$$

where $f^0_{(x,t)}(\lambda_1)$ *is the deterministic reduced action function,* $x^0_t(\lambda)$ *is the deterministic caustic and* λ *must satisfy the stochastic equation,*

$$\nabla_\lambda \left(f^0_{(x^0_t(\lambda),t)}(\lambda_1) - \epsilon x^0_t(\lambda)\cdot W(t)\right) = 0. \tag{5.9}$$

Proof. Taking the reduced action function from Corollary 5.5 and substituting in the random caustic as in Proposition 5.6 produces,

$$\begin{aligned} &f_{(x^\epsilon_t(\lambda),t)}(\lambda_1)\\ &= \frac{1}{2t}\left(x^0_t(\lambda)-\lambda_1\right)^2 - \epsilon x^0_t(\lambda)\cdot W(t) + \epsilon^2 W(t)\cdot \int_0^t W(s)\,\mathrm{d}s\\ &\quad -\frac{\epsilon^2}{2}\int_0^t |W(s)|^2\,\mathrm{d}s + \left[S_0 + \frac{t}{2}\sum_{\alpha=2}^{d}\left\{\frac{\partial S_0}{\partial x^\alpha_0}\right\}^2\right]_{x_0=(\lambda_1,x^2_0(x^\epsilon_t(\lambda),\lambda_1,t),\ldots,x^d_0(\ldots))}, \end{aligned}$$

where the substitutions $x^m_0(\ldots)$ are for the random case. However, taking the equations (5.8) we see that for each m,

$$\begin{aligned} 0 &= \frac{x^m_0 - x^{\epsilon m}_t(\lambda)}{t} + \frac{\partial S_0}{\partial x^m_0}(x^1_0,\ldots,x^{m-1}_0,x^m_0(\ldots),\ldots,x^d_0(\ldots))\\ &\quad -\frac{\epsilon}{t}\int_0^t W_m(u)\,\mathrm{d}u\\ &= \frac{x^m_0 - x^{0m}_t(\lambda)}{t} + \frac{\partial S_0}{\partial x^m_0}(x^1_0,\ldots,x^{m-1}_0,x^m_0(\ldots),\ldots,x^d_0(\ldots)), \end{aligned}$$

so that the deterministic substitutions may be used. □

Equation (5.9) shows that the value of λ used in the zeta process may be either deterministic or random. In the two dimensional case, equation (5.9) reduces to,

$$\begin{aligned} 0 &= \frac{\mathrm{d}}{\mathrm{d}\lambda}\left(f^0_{(x^0_t(\lambda),t)}(\lambda_1) - \epsilon x^0_t(\lambda)\cdot W(t)\right)\\ &= \nabla_x f^0_{(x^0_t(\lambda),t)}(\lambda_1)\cdot\frac{\mathrm{d}x^0_t}{\mathrm{d}\lambda}(\lambda) + f^{0\prime}_{(x^0_t(\lambda),t)}(\lambda_1) - \epsilon\frac{\mathrm{d}x^0_t}{\mathrm{d}\lambda}(\lambda)\cdot W(t)\\ &= \nabla_x f^0_{(x^0_t(\lambda),t)}(\lambda_1)\cdot\frac{\mathrm{d}x^0_t}{\mathrm{d}\lambda}(\lambda) - \epsilon\frac{\mathrm{d}x^0_t}{\mathrm{d}\lambda}(\lambda)\cdot W(t), \end{aligned} \tag{5.10}$$

which has a deterministic solution for λ given by,

$$\frac{\mathrm{d}x^0_t}{\mathrm{d}\lambda}(\lambda) = 0,$$

corresponding to a cusp on the deterministic caustic. This is a very important point which will be returned to in Sections 5.4 and 5.6.

5.3 Recurrence and Strassen's Law

One of the key properties associated with turbulence is the intermittent recurrence of short intervals during which the fluid velocity varies infinitely rapidly.

Using the law of the iterated logarithm, it is a simple matter to show formally that if there is a time τ such that $\zeta_t^c = 0$, then there will be infinitely many zeros of ζ_t^c in some neighbourhood of τ. This will make the set of zeros of ζ_t^c a perfect set and will result in a short period during which the fluid velocity will vary infinitely rapidly. However, this formal argument is not rigorous as it will not hold on some set of times t of measure zero. A discussion of both this formal argument and a more rigorous approach can be found in Reynolds [34].

The intermittent recurrence of turbulence will be demonstrated if we can show that there is an unbounded increasing infinite sequence of times at which the zeta process is zero. Reynolds, Truman and Williams used Strassen's form of the law of the iterated logarithm to demonstrate this recurrence in the two dimensional case where a single Wiener process acts upon the Burgers fluid. In this section we illustrate how this can be extended to the general d-dimensional setting.

We begin by indicating the derivation of Strassen's form of the law of the iterated logarithm from the theory of large deviations.

Consider a complete separable metric space X with a family of probability measures $\mathbb{P}_\epsilon$ defined on the Borel sigma field of X.

Definition 5.8. *The family of probability measures $\mathbb{P}_\epsilon$ obeys the large deviation principle with a rate function I if there exists a function $I : X \longrightarrow [0, \infty]$ where:*

1. *$I(\cdot)$ is lower semicontinuous,*
2. *for each $l \in \mathbb{R}$ the set $\{x : I(x) \leq l\}$ is compact in X,*
3. *for each closed set $C \subset X$, $\limsup_{\epsilon \longrightarrow 0} \epsilon \ln \mathbb{P}_\epsilon(C) \leq -\inf_{x \in C} I(x)$,*
4. *for each open set $G \subset X$, $\liminf_{\epsilon \longrightarrow 0} \epsilon \ln \mathbb{P}_\epsilon(G) \geq -\inf_{x \in G} I(x)$.*

We now apply the concept of large deviations to the Wiener process. Let $X = C_0[0,1]$ where $C_0[0,1]$ is the space of continuous functions $f : [0,1] \longrightarrow \mathbb{R}^d$ with $f(0) = 0$. Let $W(t)$ be a d-dimensional Wiener process and $\mathbb{P}_\epsilon$ be the distribution of $\sqrt{\epsilon} W(t)$ so that $\mathbb{P}_1$ is the Wiener measure.

Theorem 5.9. *For the measure $\mathbb{P}_\epsilon$ the large deviation principle holds with a rate function,*

$$I(f) = \begin{cases} \frac{1}{2}\int_0^1 \dot{f}(t)^2 \, \mathrm{d}t & : \ f(t) \text{ absolutely continuous and } f(0) = 0, \\ \infty & : \ \text{otherwise.} \end{cases}$$

Proof. See Varadhan [43]. □

With this bound, the Strassen form of the law of the iterated logarithm follows.

Definition 5.10. *The set of Strassen functions is defined by,*

$$K = \{f \in C_0[0,1] : \quad 2I(f) \leq 1\}.$$

Theorem 5.11 (Strassen's Law of the Iterated Logarithm). *Let,*

$$Z_n(t) = (2n \ln \ln n)^{-\frac{1}{2}} W(nt),$$

for $n \geq 2$ and $0 \leq t \leq 1$ where $W(t)$ is a d-dimensional Wiener process. For almost all paths ω the indexed subset,

$$\{Z_n(t) : \quad n = 2, 3, \ldots\},$$

is relatively compact with limit set K.

Proof. See Stroock [40]. □

Following the ideas of RTW, this theorem can be applied to the zeta process to demonstrate its recurrence.

Corollary 5.12. *There exists an unbounded increasing sequence of times t_n for which $Y_{t_n} = 0$, almost surely, where,*

$$Y_t = W(t) \cdot \int_0^t W(s)\,\mathrm{d}s - \frac{1}{2}\int_0^t |W(s)|^2\,\mathrm{d}s,$$

and $W(t)$ is a d-dimensional Wiener process.

Proof. If $h(n) = (2n \ln \ln n)^{-\frac{1}{2}}$ and $x(t) \in K$ then there exists an increasing sequence n_i such that,

$$Z_{n_i}(t) = h(n_i) W(n_i t) \rightarrow x(t),$$

as $i \rightarrow \infty$.

Consider the behaviour of each term in $h(n_i)^2 n_i^{-1} Y_t$. Firstly, following the argument of Williams,

$$\begin{aligned} h(n_i)^2 n_i^{-1} W(n_i) \cdot \int_0^{n_i} W(s)\,\mathrm{d}s &= h(n_i) W(n_i) \cdot \int_0^{n_i} h(n_i) W(s) n_i^{-1}\,\mathrm{d}s \\ &= h(n_i) W(n_i) \cdot \int_0^1 h(n_i) W(n_i r)\,\mathrm{d}r \\ &\rightarrow x(1) \cdot \int_0^1 x(r)\,\mathrm{d}r, \end{aligned} \tag{5.11}$$

and,

$$\begin{aligned} h(n_i)^2 n_i^{-1} \int_0^{n_i} |W(s)|^2 \, \mathrm{d}s &= \int_0^{n_i} |h(n_i)W(s)|^2 n_i^{-1} \, \mathrm{d}s \\ &= \int_0^1 |h(n_i)W(n_i r)|^2 \, \mathrm{d}r \\ &\to \int_0^1 |x(r)|^2 \, \mathrm{d}r, \end{aligned} \tag{5.12}$$

as $i \to \infty$.

Now let $x(t) = (x_1(t), x_2(t), \ldots, x_d(t))$ where $x_\alpha(t) = d^{-\frac{1}{2}}t$ for each $\alpha = 1, 2, \ldots, d$. Since $I(x) = \frac{1}{2}$ it follows that $x(t) \in K$. Therefore, from equations (5.11) and (5.12), there is an increasing sequence of times t_i such that,

$$h(t_i)^2 t_i^{-1} Y_{t_i} \to \frac{1}{2} - \frac{1}{6} = \frac{1}{3},$$

as $i \to \infty$.

Alternatively, let

$$x_\alpha(t) = \begin{cases} (d)^{-\frac{1}{2}}t & : \ 0 \le t \le \frac{1}{3}, \\ (d)^{-\frac{1}{2}}\left(\frac{2}{3} - t\right) & : \ \frac{1}{3} \le t \le 1, \end{cases}$$

for $\alpha = 1, 2, \ldots d$. Again, $I(x) = \frac{1}{2}$ and so $x(t) \in K$. Therefore, using equations (5.11) and (5.12) there is an increasing sequence of times τ_i such that,

$$h(\tau_i)^2 \tau_i^{-1} Y_{\tau_i} \to -\frac{1}{54} - \frac{1}{27} = -\frac{1}{18}.$$

Thus, the sequence t_i is an unbounded increasing infinite sequence of times at which $Y_t > 0$, and the sequence τ_i is an unbounded increasing infinite sequence of times at which $Y_t < 0$. Therefore, there must exist an infinite sequence of times tending to infinity at which $Y_t = 0$. □

Corollary 5.13. *If as* $t \to \infty$,

$$h(t)^2 t^{-1} f^0_{(x^0_t(\lambda),t)}(\lambda_1) \to 0, \quad \textit{and} \quad h(t)t^{-1} \sum_{\alpha=0}^{d} x^{0\alpha}_t(\lambda) \to 0,$$

then the zeta process ζ^c_t *is recurrent.*

Proof. The proof of Corollary 5.12 can be extended to include the extra terms in ζ_t. From Theorem 5.7,

$$\zeta^c_t = f^0_{(x^0_t(\lambda),t)}(\lambda_1) - \epsilon x^0_t(\lambda) \cdot W(t) + \epsilon^2 Y_t - c.$$

Making the same choices for the Strassen function $x(t)$ as in Corollary 5.12, it follows that in both cases,

$$\left(f^0_{(x^0_{n_i}(\lambda),n_i)}(\lambda_1) - c\right) h(n_i)^2 n_i^{-1} \to 0,$$

and

$$\begin{aligned} h(n_i)^2 n_i^{-1} x^0_{n_i}(\lambda) \cdot W(n_i) &= h(n_i) n_i^{-1} x^0_{n_i}(\lambda) \cdot h(n_i) W(n_i) \\ &\to 0, \end{aligned}$$

as $i \to \infty$. Therefore, the zeta process is recurrent. □

5.4 Two dimensional examples

We now consider some explicit examples in two dimensions. Since the parameter $\lambda \in \mathbb{R}$, equation (5.1) reduces to,

$$\begin{aligned} 0 &= \frac{\mathrm{d}}{\mathrm{d}\lambda} f_{(x_t(\lambda),t)}(\lambda) \\ &= \nabla_x f_{(x_t(\lambda),t)}(\lambda) \cdot \frac{\mathrm{d}x_t}{\mathrm{d}\lambda}(\lambda) + f'_{(x_t(\lambda),t)}(\lambda) \\ &= \nabla_x f_{(x_t(\lambda),t)}(\lambda) \cdot \frac{\mathrm{d}x_t}{\mathrm{d}\lambda}(\lambda). \end{aligned} \tag{5.13}$$

This gives three different forms of turbulence:

1. 'zero speed turbulence' where $\nabla f_{(x,t)}(x^1_0) = 0$. From the work of DTZ [12],
$$\nabla f_{(x,t)}(x^1_0) = \dot{X}(t),$$
where $\dot{X}(t)$ denotes the Burgers fluid velocity. Therefore, zero speed turbulence corresponds to points where the Burgers fluid has zero velocity.

2. 'orthogonal turbulence' where the vector $\nabla f_{(x_t(\lambda),t)}(\lambda)$ is orthogonal to $\frac{\mathrm{d}x_t}{\mathrm{d}\lambda}(\lambda)$. Thus, orthogonal turbulence occurs at points where the caustic tangent is orthogonal to the Burgers fluid velocity.

3. 'cusped turbulence' where,
$$\frac{\mathrm{d}x_t}{\mathrm{d}\lambda}(\lambda) = 0,$$
so there is a generalised cusp on the caustic at $x_t(\lambda)$.

As discussed in Section 5.2 and Proposition 5.6, cusped turbulence will occur at deterministic values of λ. It will also correspond to points of swallowtail perestroika on the level surfaces. As such, it is not only the simplest form to analyse, but as we will see, also the most important. Both zero and orthogonal turbulence occur at random values of λ making their analysis more complex. The categorisation of turbulence leads to a factorisation of equation (5.13).

We now consider examples with initial condition linear in y_0. Let,

$$S_0(x_0, y_0) = f(x_0) + g(x_0)y_0,$$

where f and g are twice continuously differentiable and $g''(\lambda) \neq 0$. The deterministic pre-parameterisation of the caustic is then,

$$\begin{aligned} x^0(\lambda) &= \lambda + tf'(\lambda) + \frac{g'(\lambda)}{g''(\lambda)}(-1 + t^2 g'(\lambda)^2 - tf''(\lambda)), \\ y^0(\lambda) &= \frac{-1 + t^2 g'(\lambda)^2 - tf''(\lambda)}{tg''(\lambda)} + tg(\lambda). \end{aligned}$$

Corollary 5.14. *In two dimensions, if $S_0(x_0, y_0) = f(x_0) + g(x_0)y_0$, then the zeta process for the stochastic Burgers equation (5.2) is (suppressing λ),*

$$\begin{aligned} &\zeta_t^c = \\ &\quad f + \frac{1}{2}tg^2 + \frac{1}{2}tf'^2 + \frac{1}{tg''}\left(-g - tf'g' + t^2 gg'^2 + t^3 f'g'^3 - tgf'' - t^2 f'g'f''\right) \\ &\quad + \frac{g'^2}{tg''^2}\left(\frac{1}{2} - t^2 g'^2 + \frac{1}{2}t^4 g'^4 + tf'' - t^3 g'^2 f'' + t^2 f''^2\right) \\ &\quad + \epsilon W_1(t)\left(-\lambda - tf' + \frac{g' - t^2 g'^3 + g'f''}{g''}\right) + \epsilon W_2(t)\left(-tg + \frac{1 - t^2 g'^2 + tf''}{tg''}\right) \\ &\quad + \epsilon^2\left(W(t) \cdot \int_0^t W(u)\,\mathrm{d}u - \frac{1}{2}\int_0^t |W(u)|^2\,\mathrm{d}u\right) - c, \end{aligned} \tag{5.14}$$

where λ is a root of,

$$\begin{aligned} 0 \;=\; &\frac{1}{tg''^3}\left\{g'^2(-1 + t^2 g'^2 - tf'') + g''(g - \epsilon W_2(t) + tg'f' - tg'\epsilon W_1(t))\right\} \\ &\times \left\{tg''(3tg'g'' - f''') - g'''(-1 + t^2 g'^2 - tf'')\right\}. \end{aligned} \tag{5.15}$$

Proof. This follows directly from Theorem 5.7 where $d = 2$ and $S_0(x_0, y_0) = f(x_0) + g(x_0)y_0$. □

Zeros of the second factor in equation (5.15) correspond to cusps on the caustic. Therefore, the deterministic roots λ corresponding to this factor result in cusped turbulence in which swallowtails spontaneously form and disappear on level surfaces. Moreover, the random roots λ of the first factor in (5.15) correspond to orthogonal and zero speed turbulence.

Example 5.15 (The generic Cusp). Consider the generic Cusp initial condition,

$$S_0(x_0, y_0) = \frac{1}{2}x_0^2 y_0.$$

From Corollary 5.14, the zeta process in equation (5.14) reduces to,

$$\begin{aligned}\zeta_t^c &= -\frac{3\lambda^4 t}{8} + \frac{\lambda^6 t^3}{2} - \epsilon\left(\lambda^3 t^2 W_1(t) - \frac{W_2(t)}{t} + \frac{3}{2}\lambda^2 t W_2(t)\right) \\ &\quad + \epsilon^2\left(W_1(t)\int_0^t W_1(s)\,\mathrm{d}s + W_2(t)\int_0^t W_2(s)\,\mathrm{d}s\right. \\ &\quad \left. -\frac{1}{2}\int_0^t (W_1(s)^2 + W_2(s)^2)\,\mathrm{d}s\right) - c,\end{aligned}$$

where from equation (5.15), λ must be a root of,

$$0 = \frac{3}{2}\lambda t(2\lambda^4 t^2 - \lambda^2 - 2\epsilon\{\lambda t W_1(t) + W_2(t)\}).$$

The caustic has a cusp when,

$$\begin{pmatrix}0\\0\end{pmatrix} = \begin{pmatrix}x'(\lambda)\\y'(\lambda)\end{pmatrix} = \begin{pmatrix}3\lambda^2 t\\2\lambda t\end{pmatrix},$$

which holds if $\lambda = 0$.

Thus, $\lambda = 0$ corresponds to cusped turbulence and $\lambda = \lambda_i$ for $i = 1$ to 4 corresponds to orthogonal and zero speed turbulence, where λ_i are the roots of,

$$0 = 2\lambda^4 t^2 - \lambda^2 - 2\epsilon\{\lambda t W_1(t) + W_2(t)\}. \tag{5.16}$$

Firstly, if $\lambda = 0$ then the zeta process is,

$$\begin{aligned}\zeta_t^c &= \epsilon^2\left(W_1(t)\int_0^t W_1(u)\,\mathrm{d}u + W_2(t)\int_0^t W_2(u)\,\mathrm{d}u\right. \\ &\quad \left. -\frac{1}{2}\int_0^t (W_1(u)^2 + W_2(u)^2)\,\mathrm{d}u\right) + \frac{\epsilon W_2(t)}{t} - c.\end{aligned}$$

From Corollary 5.13, this zeta process is recurrent since,

$$f^0_{(x_t^0(0),t)}(0) = 0 \quad \text{and} \quad x_t^0(0) = \left(0, \frac{1}{t}\right).$$

Therefore, the turbulence occurring at the cusp on the generic Cusp caustic is recurrent.

Alternatively, consider the roots λ_i which give rise to orthogonal and zero speed turbulence. Let,

$$\beta = -\frac{1}{2t^2}, \qquad \gamma = -\frac{\epsilon W_1(t)}{t}, \qquad \delta = -\frac{\epsilon W_2(t)}{t^2},$$

then equation (5.16) becomes,

$$0 = \lambda^4 + \beta\lambda^2 + \gamma\lambda + \delta,$$

which has solutions,

$$\lambda = \frac{Q}{2} \pm \frac{1}{2}\sqrt{-2\beta - \frac{2\gamma}{Q} - Q^2}, \qquad \lambda = -\frac{Q}{2} \pm \frac{1}{2}\sqrt{-2\beta + \frac{2\gamma}{Q} - Q^2},$$

where,

$$Q = \sqrt{-\frac{2\beta}{3} + \frac{B}{3P} + \frac{P}{3}},$$

$$P = \sqrt[3]{\frac{A + \sqrt{A^2 - 4B^3}}{2}}, \qquad A = 2\beta^3 + 27\gamma^2 - 72\beta\delta, \qquad B = \beta^2 + 12\delta.$$

Using the above values,

$$\begin{aligned} P &= \frac{\sqrt[3]{-1 + 6t\sqrt{6R} + 108t^4\epsilon^2 W_1(t)^2 - 144t^2\epsilon W_2(t)}}{2t^2}, \\ B &= \frac{1}{4t^4}\left(1 - 48\epsilon t^2 W_2(t)\right), \end{aligned}$$

where,

$$\begin{aligned} R = {} & 54\epsilon^4 t^6 W_1(t)^4 - \epsilon^2 t^2 W_1(t)^2 - 144\epsilon^3 t^4 W_1(t)^2 W_2(t) \\ & +512\epsilon^3 t^4 W_2(t)^3 + 64\epsilon^2 t^2 W_2(t)^2 + 2\epsilon W_2(t). \end{aligned}$$

We now consider how these solutions behave for large times t. By the law of the iterated logarithm, with probability one,

$$\limsup_{t\to\infty} \left| \frac{W_i(t)}{(2t\ln\ln t)^{\frac{1}{2}}} \right| = 1.$$

Formally we write this as,

$$\sup |W_i(t)| \sim (2t\ln\ln t)^{\frac{1}{2}},$$

for large t where $i = 1, 2$. Hence, formally, $\sup|R| \sim t^8(\ln\ln t)^2$, $\sup|P| \sim \sqrt[3]{\frac{\ln\ln t}{t}}$, $\sup|B| \sim \sqrt{\frac{\ln\ln t}{t^3}}$, and $\sup|\beta| \sim \frac{1}{t^2}$. Therefore,

$$\sup|Q|^2 \sim \sqrt[3]{\frac{\ln\ln t}{t}} \to 0,$$

for large t.

Moreover, $\sup\left|\frac{\gamma}{Q}\right|$ behaves like,

$$\frac{\sqrt{t\ln\ln t}}{t}\sqrt[6]{\frac{t}{\ln\ln t}} = \sqrt[3]{\frac{\ln\ln t}{t}} \to 0,$$

for large t. Therefore, using the sandwich theorem, we would expect that all four solutions will tend to zero for large times t. This is supported by a numerical solution produced using Mathematica (where $\epsilon = 1$). The Wiener processes have been simulated by replacing each $W_\alpha(t)$ by $\sqrt{t}X_\alpha$, where each X_α is a normally distributed random variable with zero mean and variance one for $\alpha = 1, 2$.

t	Roots		
10^{15}	-0.0020	-4.3×10^{-15}	0.00099 ± 0.0017i
10^{16}	-0.0015	-3.8×10^{-16}	0.00075 ± 0.0013i
10^{17}	0.0014	-1.7×10^{-17}	-0.00071 ± 0.0012i
10^{18}	-0.0013	-5.5×10^{-19}	0.00064 ± 0.0011i
10^{19}	0.00054	-2.8×10^{-19}	-0.00027 ± 0.00047i
10^{20}	0.00051	-1.7×10^{-21}	-0.00025 ± 0.00044i

The roots all tend towards zero as expected, and thus all four roots tend towards the cusp. Consequently, the zeta processes associated with each root will be recurrent. □

Example 5.16 (Polynomial swallowtail). The swallowtail initial condition is,

$$S_0(x_0, y_0) = x_0^5 + x_0^2 y_0.$$

The zeta process from equation (5.14) reduces to,

$$\begin{aligned}
\zeta_t^c \;=\;& 6\lambda^5 - \frac{3}{2}\lambda^4 t + \frac{225}{2}\lambda^8 t - 60\lambda^7 t^2 + 8\lambda^6 t^3 \\
&-\epsilon\left((4\lambda^3 t^2 - 15\lambda^4 t)W_1(t) + \left(3\lambda^2 t - 10\lambda^3 - \frac{1}{2t}\right)W_2(t)\right) \\
&+\epsilon^2\left(W_1(t)\int_0^t W_1(s)\,\mathrm{d}s + W_2(t)\int_0^t W_2(s)\,\mathrm{d}s\right. \\
&\left.-\frac{1}{2}\int_0^t (W_1(s)^2 + W_2(s)^2)\,\mathrm{d}s\right) - c,
\end{aligned}$$

where λ satisfies,

$$0 = 6\lambda(5\lambda - t)(\lambda^2 + 30\lambda^5 t - 8\lambda^4 t^2 + \epsilon\{2\lambda t W_1(t) + W_2(t)\}).$$

The caustic has a cusp when,

$$\begin{pmatrix} 0 \\ 0 \end{pmatrix} = \begin{pmatrix} x'(\lambda) \\ y'(\lambda) \end{pmatrix} = \begin{pmatrix} 12\lambda^2 t(t-5\lambda) \\ 6\lambda(t-5\lambda) \end{pmatrix},$$

giving $\lambda = 0$ or $\lambda = \frac{t}{5}$.

Hence, solutions $\lambda = 0$, $\lambda = \frac{t}{5}$ correspond to cusped turbulence whereas $\lambda = \lambda_i$ for $i = 1$ to 5, correspond to orthogonal and zero speed turbulence, where λ_i are the roots of,

$$0 = 30\lambda^5 t - 8\lambda^4 t^2 + \lambda^2 + \epsilon(2\lambda t W_1(t) + W_2(t)). \tag{5.17}$$

If $\lambda = 0$, then the turbulent times are zeros of the process,

$$\begin{aligned} \zeta_t^c \;=\; & \epsilon^2 \left(W_1(t) \int_0^t W_1(u)\,\mathrm{d}u + W_2(t) \int_0^t W_2(u)\,\mathrm{d}u \right. \\ & \left. -\frac{1}{2}\int_0^t (W_1(u)^2 + W_2(u)^2)\,\mathrm{d}u \right) + \frac{\epsilon W_2(t)}{2t} - c. \end{aligned}$$

By Corollary 5.13, this process is recurrent since,

$$f_{(x_t^0(0),t)}(0) = 0 \quad \text{and} \quad x_t^0(0) = \left(0, \frac{1}{2t}\right).$$

For $\lambda = \frac{t}{5}$, the turbulent times are zeros of the process,

$$\begin{aligned} \zeta_t^c \;=\; & \epsilon^2 \left(W_1(t) \int_0^t W_1(u)\,\mathrm{d}u + W_2(t) \int_0^t W_2(u)\,\mathrm{d}u \right. \\ & \left. -\frac{1}{2}\int_0^t (W_1(u)^2 + W_2(u)^2)\,\mathrm{d}u \right) \\ & -\epsilon\left(\frac{t^5 W_1(t)}{125} + \left\{ \frac{t^3}{25} - \frac{1}{2t} \right\} W_2(t) \right) + \frac{t^9}{31250} - \frac{3t^5}{6250} - c. \end{aligned}$$

which is not recurrent as it will be dominated by t^9 for large times.

Alternatively, we consider the roots λ_i. We cannot solve equation (5.17) directly but can perform a numerical solution for large times (where $\epsilon = 1$).

t	Roots			
10^{15}	-0.00097	-5.1×10^{-15}	$0.00048 \pm 0.00084\mathrm{i}$	2.7×10^{14}
10^{16}	0.0013	-2.0×10^{-17}	$-0.00064 \pm 0.0011\mathrm{i}$	2.7×10^{15}
10^{17}	-0.00074	-2.8×10^{-17}	$0.00037 \pm 0.00064\mathrm{i}$	2.7×10^{16}
10^{18}	0.00055	-1.4×10^{-18}	$-0.00027 \pm 0.00047\mathrm{i}$	2.7×10^{17}
10^{19}	-0.00037	-8.3×10^{-20}	$0.00018 \pm 0.00032\mathrm{i}$	2.7×10^{18}
10^{20}	-0.00029	-3.3×10^{-21}	$0.00014 \pm 0.00025\mathrm{i}$	2.7×10^{19}

In this example, four solutions tend to zero while one increases linearly with t. Thus, four roots tend towards the cusp at zero and so the processes associated with these roots will be recurrent. The process associated with the remaining root will not be recurrent. □

5.5 Small noise recurrence and Spitzer's Theorem

We can analyse the recurrence of a larger class of zeta processes in the two dimensional case by working with small values of ϵ and neglecting terms of order ϵ^2. This allows us to relax the constraints on $f^0_{(x^0_t(\lambda),t)}(\lambda_1)$ and $x^0_t(\lambda)$ in Corollary 5.13.

For small ϵ, the zeta process is (to first order in ϵ),

$$\zeta^c_t = f^0_{(x^0_t(\lambda),t)}(\lambda_1) - \epsilon x^0_t(\lambda) \cdot W(t) - c. \tag{5.18}$$

We begin by considering only the explicitly random part of this process. Let $A(t)$ be some function $A : \mathbb{R} \to \mathbb{R}^2$. We consider the behaviour of the process,

$$Y_t = A(t) \cdot W(t).$$

This is not simply a time changed Wiener process since the function $A(t)$ is t dependent. Instead, we need Spitzer's theorem to discuss its behaviour.

Let $D(t)$ denote a complex Wiener process; that is $D(t) = D_1(t) + \mathrm{i}D_2(t)$ where D_1 and D_2 are one dimensional Wiener processes. Let θ_t be the process giving the angle swept out by $D(t)$ in time t, counting anti-clockwise loops as -2π and clockwise loops as 2π (see Figure 5.1).

Theorem 5.17 (Spitzer's Theorem). *Let $D(t) = D_1(t) + iD_2(t)$ be a complex Brownian motion where D_1 and D_2 are independent, $D_1(0) = 0$ and $D_2(0) = 0$. Define the process θ_t as the continuous process where $\theta_0 = 0$ and $\sin(\theta_t) = \frac{D_2(t)}{|D(t)|}$. Then, as $t \to \infty$,*

$$\mathbb{P}\left\{\frac{2\theta_t}{\ln t} \le y\right\} \to \frac{1}{\pi}\int_{-\infty}^{y} \frac{\mathrm{d}x}{1+x^2}.$$

The proof of Spitzer's Theorem that we present is based upon the work of Durrett [14, 15] for which we need the following result of Levy.

Lemma 5.18. *Let f be a non-constant holomorphic function. If*

$$\sigma_t = \int_0^t |f'(D(s))|^2 \,\mathrm{d}s \quad \text{and} \quad \gamma_t = \inf\{s : \sigma_s \geq t\},$$

then $f(D(\gamma_t))$ has the same distribution as $D(t)$.

Proof of Theorem 5.17. From Lemma 5.18, if $f(z) = e^z$ then $C(t) = e^{D(\gamma_t)}$ is also a complex Brownian motion except with $C(0) = 1$ and $\theta_t = D_2(\gamma_t)$. Moreover,

$$\sigma_t = \int_0^t \exp(2D_1(s)) \,\mathrm{d}s,$$

so γ and D_2 are independent.

If we now define the times,

$$S_u = \gamma(e^{2u}) = \inf\left\{t : \int_0^t |e^{D(s)}|^2 \,\mathrm{d}s \geq e^{2u}\right\}, \qquad T_u = \inf\{t : D_1(t) \geq u\},$$

then for $\epsilon > 0$,

$$\mathbb{P}\left\{T_{u(1-\epsilon)} \leq S_u \leq T_{u(1+\epsilon)}\right\} \to 1, \tag{5.19}$$

as $u \to \infty$. Thus, the times S_u are approximately the same as the first hitting times T_u for the process $D_1(t)$.

Define,

$$\Delta_\epsilon(u) := \sup\left\{\frac{|D_2(t) - D_2(T_u)|}{u} : t \in [T_{u(1-\epsilon)}, T_{u(1+\epsilon)}]\right\}.$$

Then from equation 5.19, as $D_2(S_u) = \theta(e^{2u})$,

$$\mathbb{P}\left\{\frac{|D_2(t) - \theta(e^{2u})|}{u} \leq \Delta_\epsilon(u)\right\} = \mathbb{P}\left\{\frac{|D_2(t) - D_2(S_u)|}{u} \leq \Delta_\epsilon(u)\right\} \to 1,$$

as $u \to \infty$ for fixed ϵ.

Furthermore, it can be shown that $D_2(T_1)$ and $\frac{D_2(T_u)}{u}$ have the same distribution $G(y)$ where,

$$G(y) = \mathbb{P}\{D_2(T_1) \leq y\} = \mathbb{P}\left\{\frac{D_2(T_u)}{u} \leq y\right\} = \frac{1}{\pi}\int_{-\infty}^{y} \frac{\mathrm{d}x}{1 + x^2}.$$

Hence, if $\mathbb{P}\left\{\frac{\theta(e^{2u})}{u} \leq y\right\} = F_u(y)$ and $r > 0$,

$$G(y-r) - \mathbb{P}\left\{\left|\frac{D_2(T_u) - \theta(e^{2u})}{u}\right| > r\right\} \leq$$

$$F_u(y) \leq G(y+r) + \mathbb{P}\left\{\left|\frac{D_2(T_u) - \theta(e^{2u})}{u}\right| > r\right\}.$$

Then if $r = \Delta_\epsilon(u)$ and we let $u \to \infty$,

$$\lim_{u\to\infty} G(y-\Delta_\epsilon(u)) \leq \liminf_{u\to\infty} F_u(y) \leq \limsup_{u\to\infty} F_u(y) \leq \lim_{u\to\infty} G(y+\Delta_\epsilon(u)). \quad (5.20)$$

Since G is continuous, as $\epsilon \to 0$,

$$G(y) = \lim_{u\to\infty} F_u(y) = \lim_{u\to\infty} \mathbb{P}\left\{\frac{\theta(e^{2u})}{u} \leq y\right\}.$$

So, if $t = e^{2u}$, then as $u \to \infty$ it follows that $t \to \infty$ and,

$$G(y) = \int_{-\infty}^{y} \frac{\mathrm{d}x}{1+x^2} = \lim_{t\to\infty} \mathbb{P}\left\{\frac{2\theta_t}{\ln t} \leq y\right\}. \qquad \square$$

Consider replacing y in equation (5.20) with some function $y(u)$. Then the result becomes,

$$\lim_{u\to\infty} G(y(u)) = \lim_{u\to\infty} \mathbb{P}\left\{\frac{\theta(e^{2u})}{u} \leq y(u)\right\},$$

and so,

$$\lim_{t\to\infty} \int_0^{y(t)} \frac{\mathrm{d}x}{1+x^2} = \lim_{t\to\infty} \mathbb{P}\left\{\frac{2\theta_t}{\ln t} \leq y(t)\right\}.$$

We now return to considering the behaviour of the process Y_t. Assuming that $A(t) \neq 0$, let ϕ_t and θ_t measure the windings around the origin of $A(t)$ and W_t respectively. Clearly,

$$Y_t = A(t) \cdot W(t) = \epsilon |A(t)||W(t)| \cos(\phi_t - \theta_t).$$

We require Y_t to be zero, but a two dimensional brownian motion almost surely never visits the origin. Therefore, we require $\cos(\phi_t - \theta_t) = 0$, making the two vectors $A(t)$ and $W(t)$ perpendicular to each other. (Alternatively, this would be satisfied trivially if $A(t)$ were periodically zero with t.)

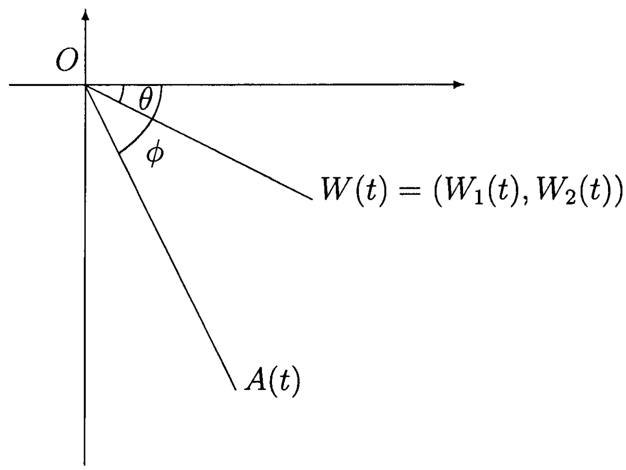

Figure 5.1: The process $Y_t = A(t) \cdot W(t)$ as vectors.

Every time 2π is added to $|\theta_t - \phi_t|$, there must be two additional times at which the vectors $A(t)$ and $W(t)$ are orthogonal. Therefore,

$$\begin{aligned}
&\mathbb{P}\left\{\sharp\{t : \cos(\phi_t - \theta_t) = 0\} > 2n_t\right\} \\
&= \mathbb{P}\left\{\sharp\left\{t : |\phi_t - \theta_t| = (2m-1)\frac{\pi}{2} \quad m \in \mathbb{N}\right\} > 2n_t\right\} \\
&\geq \mathbb{P}\left\{|\phi_t - \theta_t| > 2\pi n_t\right\},
\end{aligned}$$

where n_t denotes the number of times 2π has been added to $|\theta_t - \phi_t|$.

Proposition 5.19. *As $t \to \infty$,*

$$\mathbb{P}\left\{|\phi_t - \theta_t| > 2\pi n_t\right\} \to 1 \qquad \text{if} \qquad \frac{n_t}{\ln t} \to 0.$$

Proof. Firstly,

$$\mathbb{P}\left\{|\phi_t - \theta_t| > 2\pi n_t\right\} = \mathbb{P}\left\{\{\phi_t - \theta_t > 2\pi n_t\} \cup \{\phi_t - \theta_t < -2\pi n_t\}\right\}.$$

Using our extension of Spitzer's Theorem,

$$\begin{aligned}
\mathbb{P}\left\{\theta_t < \phi_t - 2\pi n_t\right\} &= \mathbb{P}\left\{\frac{2\theta_t}{\ln t} < \frac{2(\phi_t - 2\pi n_t)}{\ln t}\right\} \\
&\to \lim_{t\to\infty} \frac{1}{\pi} \int_{-\infty}^{\frac{2(\phi_t - 2\pi n_t)}{\ln t}} \frac{dx}{1+x^2}.
\end{aligned}$$

Similarly,

$$\begin{aligned}
\mathbb{P}\left\{\theta_t > \phi_t + 2\pi n_t\right\} &= \mathbb{P}\left\{\frac{2\theta_t}{\ln t} > \frac{2(\phi_t + 2\pi n_t)}{\ln t}\right\} \\
&\to \lim_{t\to\infty} \frac{1}{\pi} \int_{\frac{2(\phi_t + 2\pi n_t)}{\ln t}}^{\infty} \frac{dx}{1+x^2}.
\end{aligned}$$

Hence,

$$\mathbb{P}\left\{|\phi_t - \theta_t| > 2\pi n_t\right\} \quad \to \quad \lim_{t\to\infty} \frac{1}{\pi}\left[\pi - \int_{\frac{2(\phi_t-2\pi n_t)}{\ln t}}^{\frac{2(\phi_t+2\pi n_t)}{\ln t}} \frac{\mathrm{d}x}{1+x^2}\right]. \tag{5.21}$$

But,

$$\begin{aligned} 0 &\leq \int_{\frac{2(\phi_t-2\pi n_t)}{\ln t}}^{\frac{2(\phi_t+2\pi n_t)}{\ln t}} \frac{\mathrm{d}x}{1+x^2} \\ &\leq \left\{\frac{2(\phi_t+2\pi n_t)}{\ln t} - \frac{2(\phi_t-2\pi n_t)}{\ln t}\right\} \max_{x\in\mathbb{R}}\left\{\frac{1}{1+x^2}\right\} \\ &= \frac{8\pi n_t}{\ln t} \to 0 \quad \text{as} \quad t\to\infty. \end{aligned} \tag{5.22}$$

Therefore,

$$\mathbb{P}\left\{|\phi_t - \theta_t| > 2\pi n_t\right\} \to 1,$$

as $t \to \infty$. □

This condition on n_t can be improved by working with the exact integral in equation (5.22).

Theorem 5.20. *As* $t \to \infty$,

$$\mathbb{P}\left\{|\phi_t - \theta_t| > 2\pi n_t\right\} \to 1,$$

if and only if

$$\frac{4\pi^2 n_t^2 - \phi_t^2}{(\ln t)^2} < \frac{1}{4} \quad \textit{and} \quad \frac{n_t \ln t}{16\pi^2 n_t^2 - 4\phi_t^2 + (\ln t)^2} \to 0.$$

Proof. Clearly equation (5.21) holds and the integral in (5.22) can be expressed exactly as,

$$\int_{\frac{2(\phi_t-2\pi n_t)}{\ln t}}^{\frac{2(\phi_t+2\pi n_t)}{\ln t}} \frac{\mathrm{d}x}{1+x^2} = \arctan\left(\frac{2(\phi_t+2\pi n_t)}{\ln t}\right) + \arctan\left(\frac{2(2\pi n_t - \phi_t)}{\ln t}\right).$$

Since,

$$\arctan x + \arctan y = \begin{cases} \arctan\left(\frac{x+y}{1-xy}\right) & : \quad xy < 1 \\ \arctan\left(\frac{x+y}{1-xy}\right) + \pi & : \quad xy > 1 \text{ and } x, y > 0 \\ \arctan\left(\frac{x+y}{1-xy}\right) - \pi & : \quad xy > 1 \text{ and } x, y < 0, \end{cases}$$

it follows that $\arctan x + \arctan y = 0$ if and only if

$$\frac{x+y}{1-xy} = 0, \qquad xy < 1.$$

□

This theorem gives the smallest growth in n_t relative to ϕ_t necessary to guarantee by Spitzer's Theorem that the process Y_t is recurrent as $t \to \infty$.

Corollary 5.21. *The process Y_t is recurrent if there exists a function n_t such that $n_t \to \infty$ with,*

$$\frac{4\pi^2 n_t^2 - \phi_t^2}{(\ln t)^2} < \frac{1}{4} \quad \textit{and} \quad \frac{n_t \ln t}{16\pi^2 n_t^2 - 4\phi_t^2 + (\ln t)^2} \to 0,$$

as $t \to \infty$.

Corollary 5.22. *The small noise zeta process (5.18) is recurrent if there exists a bounded function $h(t)$ where $h : \mathbb{R}^+ \to \mathbb{R}^+$ such that,*

$$h(t)\left(f^0_{(x_t^0(\lambda),t)}(\lambda_1) - c\right) \to 0,$$

as $t \to \infty$ and there exists a function n_t such that $n_t \to \infty$ with,

$$\frac{4\pi^2 n_t^2 - \phi_t^2}{(\ln t)^2} < \frac{1}{4} \quad \textit{and} \quad \frac{n_t \ln t}{16\pi^2 n_t^2 - 4\phi_t^2 + (\ln t)^2} \to 0,$$

as $t \to \infty$ where $A(t) = \epsilon h(t) x_t^0(\lambda)$.

5.6 Three dimensional examples

We now consider the three dimensional case. Thus $\lambda \in \mathbb{R}^2$ and equation (5.1) becomes the pair,

$$\begin{aligned} 0 &= \nabla_\lambda f_{(x_t(\lambda),t)}(\lambda_1) \\ &= \left(\nabla_x f_{(x_t(\lambda),t)}(\lambda_1)\cdot\frac{\mathrm{d}x_t}{\mathrm{d}\lambda_1}(\lambda) + f'_{(x_t(\lambda),t)}(\lambda_1), \nabla_x f_{(x_t(\lambda),t)}(\lambda_1)\cdot\frac{\mathrm{d}x_t}{\mathrm{d}\lambda_2}(\lambda)\right) \\ &= \left(\nabla_x f_{(x_t(\lambda),t)}(\lambda_1)\cdot\frac{\mathrm{d}x_t}{\mathrm{d}\lambda_1}(\lambda), \nabla_x f_{(x_t(\lambda),t)}(\lambda_1)\cdot\frac{\mathrm{d}x_t}{\mathrm{d}\lambda_2}(\lambda)\right). \end{aligned} \tag{5.23}$$

In direct correlation to the two dimensional case, we can categorise three dimensional turbulence depending on how we solve equations (5.23).

1. If $\nabla_x f_{(x_t(\lambda),t)}(\lambda_1) = 0$ then the equations are solved trivially. This produces zero speed turbulence as in the two dimensional case.
2. Alternatively, if $\frac{\mathrm{d}x_t}{\mathrm{d}\lambda_i}(\lambda) = 0$ for $i = 1, 2$ then again the equations are solved trivially. This produces a partial analogy with cusped turbulence.

3. Finally, assume that $\nabla_x f_{(x_t(\lambda),t)}(\lambda_1) \neq 0$ and $\frac{\mathrm{d}x_t}{\mathrm{d}\lambda_i}(\lambda) \neq 0$ for i either 1 or 2. Then $\frac{\mathrm{d}x_t}{\mathrm{d}\lambda_i}(\lambda)$ must be orthogonal to $\nabla_x f_{(x_t(\lambda),t)}(\lambda_1)$ and to satisfy the equations requires either:
   (a) $\frac{\mathrm{d}x_t}{\mathrm{d}\lambda_i}(\lambda) = \kappa \frac{\mathrm{d}x_t}{\mathrm{d}\lambda_j}(\lambda)$ for some $\kappa \in \mathbb{R}$, or,
   (b) $\frac{\mathrm{d}x_t}{\mathrm{d}\lambda_j}(\lambda)$ is orthogonal to $\frac{\mathrm{d}x_t}{\mathrm{d}\lambda_i}(\lambda)$ and $\nabla_x f_{(x_t(\lambda),t)}(\lambda)$.

Therefore, as a direct extension of the two dimensional classification of turbulent times we have a new classification:

1. 'zero speed' corresponding to case 1,
2. 'orthogonal' corresponding to case 3(b),
3. 'subcaustic' (the extension of cusped turbulence to three dimensions) corresponding to cases 2 and 3(a).

As in the two dimensional case, it follows from Proposition 5.6 that the values of λ that determine the subcaustic are deterministic. However, unlike the two dimensional case, subcaustic turbulence does not occur at all points of the subcaustic. It only occurs at points where the Burgers fluid velocity is orthogonal to the subcaustic. Hence, we are selecting random points on a deterministic curve, and so subcaustic turbulence involves random values of λ.

Consider initial conditions linear in both y_0 and z_0. Let,

$$S_0(x_0, y_0, z_0) = f(x_0) + g(x_0)y_0 + h(x_0)z_0,$$

where f, g and h are twice continuously differentiable and $h''(x_0) \neq 0$. The deterministic pre-parameterisation of the caustic is (suppressing λ_1s),

$$\begin{aligned}
x_t(\lambda_1, \lambda_2) &= \lambda_1 + tf' + t\lambda_2 g' + \frac{h'}{h''}\left(t^2(g'^2 + h'^2) - 1 - t(f'' + \lambda_2 g'')\right) \\
&\quad -\epsilon \int_0^t W_1(s)\,\mathrm{d}s, \\
y_t(\lambda_1, \lambda_2) &= \lambda_2 + tg - \epsilon \int_0^t W_2(s)\,\mathrm{d}s, \\
z_t(\lambda_1, \lambda_2) &= \frac{1}{th''}\left(t^2(g'^2 + h'^2) - 1 - t(f'' + \lambda_2 g'')\right) + th - \epsilon \int_0^t W_3(s)\,\mathrm{d}s.
\end{aligned}$$

Corollary 5.23. *If $S_0(x_0, y_0, z_0) = f(x_0) + g(x_0)y_0 + h(x_0)z_0$ then the zeta process for the stochastic Burgers equation (5.2) in three dimensions is (suppressing $\lambda_1 s$),*

$$\begin{aligned}
\zeta^c(t) = &\\
& f + \lambda_2 g + \frac{1}{th''}(h + tf'h' + t\lambda_2 g'h')(-1 + t^2 g'^2 + t^2 h'^2 - tf'' - \lambda_2 tg'') \\
& + \frac{h'^2}{2th''^2}(1 - t^2 g'^2 - t^2 h'^2 + tf'' + \lambda_2 tg'')^2 + \frac{t}{2}(g^2 + h^2 + (f' + \lambda_2 g')^2) \\
& + \epsilon W_1(t)\Big(-\lambda_1 - tf' - \lambda_2 tg' + \frac{h'}{h''}(1 - t^2 g'^2 - t^2 h'^2 + tf'' + \lambda_2 tg'')\Big) \\
& - \epsilon W_2(t)\Big(\lambda_2 + tg\Big) + \epsilon W_3(t)\Big(-th + \frac{1}{th''}(1 - t^2 g'^2 - t^2 h'^2 + tf'' + \lambda_2 tg'')\Big) \\
& + \epsilon^2\left(W(t)\cdot\int_0^t W(u)\,\mathrm{d}u - \frac{1}{2}\int_0^t |W(u)|^2\,\mathrm{d}u\right) - c,
\end{aligned} \tag{5.24}$$

where $\lambda = (\lambda_1, \lambda_2)$ satisfies,

$$\begin{aligned}
0 = & -t^4 g'^4 h' h''^2 - t^3 g'^3 h''\Big(2th'^2 g'' + \lambda_2 h''^2\Big) - th''\Big(3th'h'' - f^{(3)} - \lambda_2 g^{(3)}\Big) \\
& \times\Big(h'^2(-1 + t^2 h'^2 - tf'' - t\lambda_2 g'') + h''(h - \epsilon W_3(t) - th'\epsilon W_1(t) + tf'h')\Big) \\
& + t^2 g'^2 h''\Big(-4t^2 h'^3 h'' + h'h''(1 + tf'' - \lambda_2 tg'') + th''^2(\epsilon W_1(t) - f') \\
& + th'^2(f^{(3)} + \lambda_2 g^{(3)})\Big) + t^2 g' h''\Big(-2t^2 h'^4 g'' + h''(-2g''h + 2\epsilon g'' W_3(t) \\
& - gh'' + \epsilon h'' W_2(t)) + h'^2(2g''(1 + tf'' + \lambda_2 tg'') - 3\lambda_2 th''^2) \\
& + h'h''(2t(\epsilon W_1(t) - f')g'' + \lambda_2(f^{(3)} + \lambda_2 g^{(3)}))\Big) + h^{(3)}\Big(-1 + t^2 g'^2 + t^2 h'^2 \\
& - tf'' - tbg''\Big) \times \Big(h'^2(-1 + t^2 g'^2 + t^2 h'^2 - tf'' - t\lambda_2 g'') \\
& + h''(h - \epsilon W_3(t) + th'(-\epsilon W_1(t) + f' + bg'))\Big),
\end{aligned} \tag{5.25}$$

and,

$$\begin{aligned}
0 \;=\; & -\epsilon W_2(t) + \frac{1}{h''^2}\Big(g'h'' - h'g''\Big) \\
& \times\Big(h'(-1 + t^2 g'^2 + t^2 h'^2 - tf'' - \lambda_2 tg'') + h''(tf' + \lambda_2 tg')\Big) \\
& + \frac{1}{h''}\Big(gh'' - hg'' + \epsilon W_3(t)g'' + t\epsilon W_1(t)(h'g'' - g'h'')\Big).
\end{aligned} \tag{5.26}$$

The equations (5.25) and (5.26) are polynomials in λ_2 and so we may eliminate λ_2 between the pair by assuming $h'g'' - g'h'' \neq 0$. This gives,

$$
\begin{aligned}
0 &= \Big\{hg' - \epsilon W_3(t)g' - gh' + \epsilon W_2(t)h'\Big\} \times \Big\{ -3t^2h'^3g''^2h'' + t^2h'^4g''g^{(3)} \\
&\quad +(tg''f^{(3)} - (1+tf'')g^{(3)})h'^2g'' + t(\epsilon W_1(t) - f')(-h''g^{(3)} + g''h^{(3)})h'g'' \\
&\quad +t^2g'^4h''h^{(3)} - ((h-\epsilon W_3(t))g'' - (g - \epsilon W_2(t))h'')(-h''g^{(3)} + g''h^{(3)}) \\
&\quad +g'^2\Big(t((6tg''^2h'' - 3th''^3)h' + h''^2f^{(3)} + th'^2g''g^{(3)}) + (-1 + t^2h'^2 \\
&\quad -tf'')h''h^{(3)}\Big) - 3t^2h'^2g''g'(g''^2 - 2h''^2) - t^2g'^3\Big((3h''^2 + h'h^{(3)})g'' \\
&\quad +h'h''g^{(3)}\Big) + t(\epsilon W_1(t) - f')h''g'(h''g^{(3)} - g''h^{(3)}) \\
&\quad -t^2h'^3g'\left(h''g^{(3)} + g''h^{(3)}\right) \\
&\quad +h'g'\Big(h''(-2tg''f^{(3)} + (1+tf'')g^{(3)}) + (1+tf'')g''h^{(3)}\Big)\Big\}. \qquad (5.27)
\end{aligned}
$$

It can be shown that the first factor corresponds to orthogonal and zero speed turbulence, and the second to subcaustic turbulence. A similar factorisation also occurs if $h'g'' - g'h'' = 0$ again with one factor for subcaustic turbulence and one for zero and orthogonal turbulence.

This factorisation allows us to proceed with the analysis of points of turbulence in many complex examples.

5.6.1 The butterfly

Consider the initial condition,

$$S_0(x_0, y_0, z_0) = x_0^3 y_0 + x_0^2 z_0.$$

The zeta process is (from Corollary 5.23),

$$
\begin{aligned}
\zeta_t^c &= \lambda_1^3\lambda_2 - \frac{3}{2}\lambda_1^4 t - 4\lambda_1^6 t + \frac{9}{2}\lambda_1^4\lambda_2^2 t - 12\lambda_1^5\lambda_2 t^2 - 27\lambda_1^7\lambda_2 t^2 + 8\lambda_1^6 t^3 + 36\lambda_1^8 t^3 \\
&\quad +\frac{81}{2}\lambda_1^{10}t^3 + \epsilon\Big((3\lambda_1^2\lambda_2 t - 4\lambda_1^3 t^2 - 9\lambda_1^5 t^2)W_1(t) - (\lambda_2 + \lambda_1^3 t)W_2(t) \\
&\qquad +(3\lambda_1\lambda_2 + \frac{1}{2t} - 3\lambda_1^2 t - \frac{9}{2}\lambda_1^4 t)W_3(t)\Big) \\
&\quad +\epsilon^2\Big(W_1(t)\int_0^t W_1(s)\,\mathrm{d}s + W_2(t)\int_0^t W_2(s)\,\mathrm{d}s + W_3(t)\int_0^t W_3(s)\,\mathrm{d}s \\
&\qquad -\frac{1}{2}\int_0^t (W_1(s)^2 + W_2(s)^2 + W_3(s)^2)\,\mathrm{d}s\Big) - c,
\end{aligned}
$$

where $\lambda = (\lambda_1, \lambda_2)$ must satisfy,

$$\begin{aligned}
0 &= 135t^3\lambda_1^9 + 96t^3\lambda_1^7 - 63\lambda_2 t^2\lambda_1^6 + (16t^3 - 8t)\lambda_1^5 - (20\lambda_2 + 15\epsilon W_1(t))\, t^2\lambda_1^4 \\
&\quad + \left(6\lambda_2^2 - 2 - 6\epsilon W_3(t)\right) t\lambda_1^3 + \left(\lambda_2 - 4t^2\epsilon W_1(t) - t\epsilon W_2(t)\right)\lambda_1^2 \\
&\quad + 2\left(\lambda_2 W_1(t) - W_3(t)\right)\epsilon t\lambda_1 + \epsilon\lambda_2 W_3(t), &(5.28)\\
0 &= -27t^2\lambda_1^7 - 12t^2\lambda_1^5 + 9t\lambda_1^4\lambda_2 + \lambda_1^3 + 3t\epsilon W_1(t)\lambda_1^2 + 3\epsilon W_3(t)\lambda_1 \\
&\quad - \epsilon W_2(t). &(5.29)
\end{aligned}$$

Proposition 5.24. *For all $t > 0$, there is a real solution to the equations (5.28) and (5.29) for λ_1 and λ_2, and no more than six real solutions. Moreover, there will be at most five real solutions for any time t such that $W_2(t) = 0$, and at most four for any time such that $W_3(t) < 0$.*

Proof. Assuming that $\lambda_1 \neq 0$, equation (5.29) can be solved for λ_2 and the result substituted into equation (5.28) to give the factorisation,

$$\begin{aligned}
0 &= \left(54t^2\lambda_1^7 + 6t^2\lambda_1^5 + \lambda_1^3 + 3t\epsilon W_1(t)\lambda_1^2 + 3\epsilon W_3(t)\lambda_1 - \epsilon W_2(t)\right) \\
&\quad \times \left(\lambda_1^3 - 3\epsilon W_3(t)\lambda_1 + 2\epsilon W_2(t)\right). &(5.30)
\end{aligned}$$

From equation (5.30), there is always at least one real solution for λ_1. Alternatively, if $\lambda_1 = 0$ then from equation (5.29), $W_2(t) = 0$ and so almost surely $W_3(t) \neq 0$ forcing $\lambda_2 = 0$, again producing a real solution.

Furthermore, if we let,

$$\begin{aligned}
P(\lambda_1) &= 54t^2\lambda_1^7 + 6t^2\lambda_1^5 + \lambda_1^3 + 3\epsilon t W_1(t)\lambda_1^2 + 3\epsilon W_3(t)\lambda_1 - \epsilon W_2(t), \\
Q(\lambda_1) &= \lambda_1^3 - 3\epsilon W_3(t)\lambda_1 + 2\epsilon W_2(t),
\end{aligned}$$

then by Descartes' Rule of Sign (Corollary 1.33) assuming $W_2(t) \neq 0$, there are at most three real roots for $P(\lambda_1) = 0$ and three for $Q(\lambda_1) = 0$. However, if $W_2(t) = 0$ there are at most two real roots for $P(\lambda_1) = 0$ and three for $Q(\lambda_1) = 0$. Finally, if $W_3(t) < 0$, there is only one real root for $Q(\lambda_1) = 0$. □

Corollary 5.25. *The number of real solutions for equations (5.28) and (5.29) will change infinitely often with time, almost surely.*

Proof. Follows from the proof of Proposition 5.24. □

We now consider the values of λ_1 and λ_2 which produce a recurrent zeta process. The values of λ_1 arising from $P(\lambda_1)$ are the simplest to analyse for large times. In this case, formally,

$$P(\lambda_1) \sim 54t^2\lambda_1^7 + 6t^2\lambda_1^5.$$

Consequently, for large times we expect that five roots of P will tend to zero and the remaining two roots will tend to $\pm\frac{i}{3}$. For those values where $\lambda_1 \to 0$, we would expect from equation (5.28) that $\lambda_2 \to 0$. Moreover, we may neglect the final two roots as for large times these should always be complex values for λ_1. This analysis is supported by a numerical solution performed for large times where the noise has been simulated as in Example 5.15.

t	Roots		
10^{15}	$-5.5 \times 10^{-8} \pm 0.33\mathrm{i}$	-0.0023	$-1.1 \times 10^{-15} \pm 2.0 \times 10^{-8}\mathrm{i}$ $0.0012 \pm 0.0020\mathrm{i}$
10^{16}	$5.0 \times 10^{-8} \pm 0.33\mathrm{i}$	-4.3×10^{-9} 4.3×10^{-9} 0.0022	$-0.0011 \pm 0.0019\mathrm{i}$
10^{17}	$1.3 \times 10^{-10} \pm 0.33\mathrm{i}$	-1.4×10^{-8} 1.3×10^{-8} 0.00031	$-0.00015 \pm 0.00026\mathrm{i}$
10^{18}	$-3.2 \times 10^{-9} \pm 0.33\mathrm{i}$	-0.00089	$-1.4 \times 10^{-19} \pm 2.6 \times 10^{-10}\mathrm{i}$ $0.00045 \pm 0.00077\mathrm{i}$
10^{19}	$9.1 \times 10^{-11} \pm 0.33\mathrm{i}$	-1.4×10^{-10} 1.4×10^{-10} 0.00027	$-0.00014 \pm 0.00024\mathrm{i}$
10^{20}	$-1.8 \times 10^{-10} \pm 0.33\mathrm{i}$	-0.00030	$-2.7 \times 10^{-21} \pm 1.0 \times 10^{-10}\mathrm{i}$ $0.00015 \pm 0.00026\mathrm{i}$

From Corollary 5.13, we would expect the five roots which approach zero for large times to produce a recurrent zeta process.

The roots of Q are much more difficult to analyse as the large time behaviour of this polynomial is dominated by random terms.

Corollary 5.26.

$$\begin{aligned}
&\mathbb{P}\left\{\#\{\lambda_1 \in \mathbb{R} : \quad Q(\lambda_1) = 0\} = 1\right\} \\
&= \; 2^{-1} - (2t)^{-\frac{1}{6}}\pi^{-1}\epsilon^{\frac{1}{3}}\Gamma\left(\tfrac{5}{6}\right) {}_3F_3\left(\left\{\tfrac{1}{6}, \tfrac{5}{12}, \tfrac{11}{12}\right\}, \left\{\tfrac{1}{3}, \tfrac{2}{3}, \tfrac{7}{6}\right\}, \tfrac{-2}{27}\epsilon^{-2}t^{-1}\right) \\
&\quad -(6\epsilon)^{-1}(2\pi t)^{-\frac{1}{2}} {}_3F_3\left(\left\{\tfrac{1}{2}, \tfrac{3}{4}, \tfrac{5}{4}\right\}, \left\{\tfrac{2}{3}, \tfrac{4}{3}, \tfrac{3}{2}\right\}, \tfrac{-2}{27}\epsilon^{-2}t^{-1}\right) \\
&\quad -(20\pi)^{-1}(2t^{-5})^{\frac{1}{6}}\epsilon^{\frac{5}{3}}\Gamma(\tfrac{13}{6}) {}_3F_3(\{\tfrac{5}{6}, \tfrac{13}{12}, \tfrac{19}{12}\}, \{\tfrac{4}{3}, \tfrac{5}{3}, \tfrac{11}{6}\}, \tfrac{-2}{27}\epsilon^{-2}t^{-1}),
\end{aligned}$$

where ${}_pF_q(\{a_1, a_2, \ldots, a_p\}, \{b_1, b_2, \ldots, b_q\}, z)$ *is the generalised hypergeometric function.*

Proof. From Theorem 1.30, $Q(\lambda_1) = 0$ has exactly one real root if

$$W_2(t)^2 > \epsilon W_3(t)^3.$$

Let $X = W_2(t)^2$ and $Y = \epsilon W_3(t)^3$, then these random variables have the distributions:

$$\begin{aligned} F_X(x) &= \mathbb{P}\left\{W_2(t)^2 < x\right\} \\ &= \mathbb{P}\left\{-\sqrt{x} < W_2(t) < \sqrt{x}\right\} = N_t(\sqrt{x}) - N_t(-\sqrt{x}), \\ F_Y(y) &= \mathbb{P}\left\{\epsilon W_3(t)^3 < y\right\} = \mathbb{P}\left\{W_3(t) < \sqrt[3]{\frac{y}{\epsilon}}\right\} = N_t\left(\sqrt[3]{\frac{y}{\epsilon}}\right), \end{aligned}$$

where,

$$N_t(x) = (2\pi t)^{-\frac{1}{2}} \int_{-\infty}^{x} \exp\left(-\frac{s^2}{2t}\right) \mathrm{d}s.$$

Therefore, they have density functions,

$$f_X(x) = (2\pi t x)^{-\frac{1}{2}} \exp\left(-\frac{x}{2t}\right), \quad f_Y(y) = (2\pi t x)^{-\frac{1}{2}} 3^{-1} y^{-\frac{2}{3}} \epsilon^{-\frac{1}{3}} \exp\left(-\frac{y^{\frac{2}{3}}}{2t\epsilon^{\frac{2}{3}}}\right).$$

It then follows by independence that,

$$\begin{aligned} \mathbb{P}\{X > Y\} &= \int_0^\infty \int_0^x f_X(x) f_Y(y)\, \mathrm{d}y\, \mathrm{d}x \\ &= (6\pi t\epsilon^{\frac{1}{3}})^{-1} \int_0^\infty \int_0^x y^{-\frac{2}{3}} x^{-\frac{1}{2}} \exp\left(-\frac{x\epsilon^{\frac{2}{3}} + y^{\frac{2}{3}}}{2t\epsilon^{\frac{2}{3}}}\right) \mathrm{d}y\, \mathrm{d}x. \quad (5.31) \end{aligned}$$

□

Corollary 5.27. *As $t \to \infty$,*

$$\mathbb{P}\{\textit{There is exactly one real root for } Q(\lambda_1) = 0\} \searrow \frac{1}{2}.$$

Proof. We can estimate the integral (5.31),

$$\begin{aligned} \mathbb{P}\{X > Y\} &\leq (6\pi t\epsilon^{\frac{1}{3}})^{-1} \int_0^\infty x^{-\frac{1}{6}} \exp\left(-\frac{x}{2t}\right) \mathrm{d}x \\ &= (6\pi t\epsilon^{\frac{1}{3}})^{-1} (2t)^{\frac{5}{6}} \Gamma\left(\frac{5}{6}\right) \searrow 0, \end{aligned}$$

as $t \nearrow \infty$. □

The equation $Q(\lambda_1) = 0$ can be solved explicitly to give three solutions,

$$\begin{aligned} \lambda_1 &= \epsilon^{\frac{1}{3}} \left\{X_t^{\frac{1}{3}} - \tilde{X}_t^{\frac{1}{3}}\right\}, \\ \lambda_1 &= \frac{\epsilon^{\frac{1}{3}}}{2} \left\{-(1 \mp \mathrm{i}\sqrt{3}) X_t^{\frac{1}{3}} - (1 \pm \mathrm{i}\sqrt{3}) \tilde{X}_t^{\frac{1}{3}}\right\}, \end{aligned}$$

where

$$\begin{aligned} X_t &= \left(-W_2(t) + \sqrt{W_2(t)^2 - \epsilon W_3(t)^3}\right), \\ \tilde{X}_t &= \left(W_2(t) + \sqrt{W_2(t)^2 - \epsilon W_3(t)^3}\right). \end{aligned}$$

These roots can be analysed formally using Taylor's Theorem. By estimating as in Corollary 5.27, it can be shown that,

$$\mathbb{P}\left\{|\epsilon W_3(t)^3 - W_2(t)^2| - W_2(t)^2 \geq 0\right\} \longrightarrow 1,$$

as $t \longrightarrow \infty$. Thus, we may formally assume that for large t,

$$|\epsilon W_3(t)^3 - W_2(t)^2| \geq W_2(t)^2.$$

Therefore, the roots may be expanded as,

$$\begin{aligned} \lambda_1 &= (W_2(t)^2 - \epsilon W_3(t)^3)^{\frac{1}{6}} \times \left(-\frac{2}{3}\Upsilon_t + \mathrm{O}(\Upsilon^3)\right), \\ \lambda_1 &= (W_2(t)^2 - \epsilon W_3(t)^3)^{\frac{1}{6}} \times \left(-1 \pm \frac{\mathrm{i}}{\sqrt{3}}\Upsilon_t + \mathrm{O}(\Upsilon^2)\right), \end{aligned}$$

where,

$$\Upsilon_t = \frac{W_2(t)}{\sqrt{W_2(t)^2 - \epsilon W_3(t)^3}}.$$

From this expansion and the law of the iterated logarithm, it follows that while we would expect the latter two roots to grow in modulus at a rate of $t^{\frac{1}{4}}$, we would not expect the first root to grow with time. This is supported by a numerical simulation for the roots, where two grow in modulus while one is randomly distributed about the origin.

t	Roots		
10^{15}	-0.58	13274.0	13274.6
10^{16}	0.12	$-0.059 \pm 17787.4\mathrm{i}$	
10^{17}	-0.34	-36256.2	36256.5
10^{18}	0.85	$-0.42 \pm 73359.7\mathrm{i}$	
10^{19}	1.69	$-0.85 \pm 66757.7\mathrm{i}$	
10^{20}	-1.65	-82843.6	82845.3

The zeta processes associated with these roots will not be recurrent for large t, as in all three cases the process will be dominated by the t^3 terms in the deterministic part of the reduced action function. These terms fail to satisfy the conditions on recurrence in Corollary 5.13.

5.6.2 The three dimensional swallowtail

Consider the initial condition,

$$S_0(x_0) = x_0^7 + x_0^3 y_0 + x_0^2 z_0.$$

The zeta process will be (Corollary 5.23),

$$\begin{aligned}
\zeta_t^c = {} & \\
& \frac{1225}{2} t\lambda_1^{12} - 315t^2\lambda_1^{11} + \frac{81}{2} t^3 \lambda_1^{10} - 140t^2\lambda_1^9 + (105\lambda_2 t + 36t^3)\lambda_1^8 \\
& +(15 - 27\lambda_2 t^2)\lambda_1^7 + (8t^3 - 4t)\lambda_1^6 - 12\lambda_2 t^2 \lambda_1^5 + \frac{1}{2}(9\lambda_2^2 t - 3t)\lambda_1^4 + \lambda_1^3\lambda_2 \\
& \epsilon\Big(2\lambda_1^2 t^2 (35\lambda_1^4 + 3\lambda_2 - 4\lambda_1 t - 9\lambda_1^3 t) W_1(t) - 2t(\lambda_2 + \lambda_1^3 t) W_2(t) \\
& +(1 + 42\lambda_1^5 t + 6\lambda_1\lambda_2 t - 6\lambda_1^2 t^2 - 9\lambda_1^4 t^2) W_3(t)\Big) \\
& +\epsilon^2\Big(W_1(t)\int_0^t W_1(s)\,\mathrm{d}s + W_2(t)\int_0^t W_2(s)\,\mathrm{d}s + W_3(t)\int_0^t W_3(s)\,\mathrm{d}s \\
& \quad -\frac{1}{2}\int_0^t (W_1(s)^2 + W_2(s)^2 + W_3(s)^2)\,\mathrm{d}s\Big) - c,
\end{aligned}$$

where,

$$\begin{aligned}
0 &= -2t\lambda_1^3 - 8t\lambda_1^5 + 16t^3\lambda_1^5 + 35\lambda_1^6 + 96t^3\lambda_1^7 - 420t^2\lambda_1^8 + 135t^3\lambda_1^9 \\
&\quad -1155t^2\lambda_1^{10} + 2450t\lambda_1^{11} + \lambda_1^2\lambda_2 - 20t^2\lambda_1^4\lambda_2 - 63t^2\lambda_1^6\lambda_2 + 280t\lambda_1^7\lambda_2 \\
&\quad +6t\lambda_1^3\lambda_2^2 - (4t^2\epsilon\lambda_1^2 + 15t^2\epsilon\lambda_1^4 - 70t\epsilon\lambda_1^5 - 2t\epsilon\lambda_1\lambda_2)W_1(t) - t\epsilon\lambda_1^2 W_2(t) \\
&\quad -(2t\epsilon\lambda_1 + 6t\epsilon\lambda_1^3 - 35\epsilon\lambda_1^4 - \epsilon\lambda_2)W_3(t), && (5.32) \\
0 &= \lambda_1^3 - 12t^2\lambda_1^5 - 27t^2\lambda_1^7 + 105t\lambda_1^8 + 9t\lambda_1^4\lambda_2 + 3t\epsilon\lambda_1^2 W_1(t) - \epsilon W_2(t) \\
&\quad +3\epsilon\lambda_1 W_3(t). && (5.33)
\end{aligned}$$

As in Section 5.6.1, we can solve equation (5.33) for λ_2 (assuming $\lambda_1 \neq 0$) and can then substitute into equation (5.32) to give the factorisation,

$$\begin{aligned}
0 &= \big(210t\lambda_1^8 - 54t^2\lambda_1^7 - 6t^2\lambda_1^5 - \lambda_1^3 - 3t\lambda_1^2\epsilon W_1(t) + \epsilon W_2(t) - 3\lambda_1\epsilon W_3(t)\big) \\
&\quad \times \big(\lambda_1^3 + 2\epsilon W_2(t) - 3\lambda_1\epsilon W_3(t)\big) && (5.34)
\end{aligned}$$

As previously, this factorisation also holds if $\lambda_1 = 0$ as then $W_2(t) = 0$ and so, almost surely, $\lambda_2 = 0$. The second factor in equation (5.34) is the same as the second factor in equation (5.30). Therefore, from the work of Section 5.6.1, we can conclude that none of these roots will produce recurrent behaviour in the zeta process.

Thus, we only need to analyse the roots of the second factor in equation (5.34). For large times, we expect this polynomial to behave as,

$$54t^2\lambda_1^7 - 6t^2\lambda_1^5 = 6t^2\lambda_1^5(9\lambda_1^2 - 1).$$

Hence, we expect to find five roots tending towards zero and two complex roots tending to $\pm\frac{\mathrm{i}}{3}$. This is supported by a numerical simulation.

t	Roots		
10^{15}	2.6×10^{14}	$-8.5 \times 10^{-16} \pm 2.6 \times 10^{-8}\mathrm{i}$	$6.7 \times 10^{-8} \pm 0.33\mathrm{i}$
	0.0025	$-0.0012 \pm 0.0021\mathrm{i}$	
10^{15}	2.6×10^{15}	$1.3 \times 10^{-16} - 2.2 \times 10^{-8}\mathrm{i}$	$-1.6 \times 10^{-9} \pm 0.33\mathrm{i}$
	-0.00071	$0.00036 - 0.00062\mathrm{i}$	
10^{15}	2.6×10^{16}	$-7.3 \times 10^{-18} \pm 3.1 \times 10^{-9}\mathrm{i}$	$3.4 \times 10^{-9} \pm 0.33\mathrm{i}$
	0.00091	$-0.00046 \pm 0.00079\mathrm{i}$	
10^{15}	2.6×10^{17}	$3.8 \times 10^{-18} \pm 1.4 \times 10^{-9}\mathrm{i}$	$-6.7 \times 10^{-10} \pm 0.33\mathrm{i}$
	-0.00053	$0.00027 \pm 0.00046\mathrm{i}$	
10^{15}	2.6×10^{18}	$5.4 \times 10^{-20} \pm 1.2 \times 10^{-10}\mathrm{i}$	$-7.8 \times 10^{-10} \pm 0.33\mathrm{i}$
	-0.00056	$0.00028 \pm 0.00048\mathrm{i}$	
10^{15}	2.6×10^{19}	$-8.1 \times 10^{-21} \pm 4.7 \times 10^{-11}\mathrm{i}$	$7.9 \times 10^{-11} \pm 0.33\mathrm{i}$
	0.00026	$-0.00013 \pm .00023\mathrm{i}$	

The extra root growing linearly with t is accounted for by the missing term of order eight in the above formal large time analysis. Those roots tending to $\pm\frac{\mathrm{i}}{3}$ may be discounted and so the only roots which give recurrent turbulence in this case, are the five roots tending to zero.

5.7 Complex turbulence

We now consider a completely different approach to turbulence based on the work of Chapter 3. Let $\left(\lambda, x_{0,\mathrm{C}}^2(\lambda)\right)$ denote the parameterisation of the pre-caustic at time t so that $x_t(\lambda) = \Phi_t\left(\lambda, x_{0,\mathrm{C}}^2(\lambda)\right)$ is the pre-parameterisation of the caustic. When,

$$Z_t = \mathrm{Im}\left\{\Phi_t(a + \mathrm{i}\eta, x_{0,\mathrm{C}}^2(a + \mathrm{i}\eta))\right\},$$

is random, the values of $\eta(t)$ for which $Z_t = 0$ will form a stochastic process. The zeros of this new process will correspond to points at which the real pre-caustic touches the complex pre-caustic.

Definition 5.28. *The complex turbulent times t are defined to be times t when the real and complex pre-caustics touch.*

As established in Theorems 3.7 and 3.8, the points at which these surfaces touch correspond to swallowtail perestroikas on the caustic. When such a perestroika occurs there is a solution of the equations,

$$f'_{(x,t)}(\lambda) = f''_{(x,t)}(\lambda) = f'''_{(x,t)}(\lambda) = f^{(4)}_{(x,t)}(\lambda) = 0.$$

Assuming that $f_{(x,t)}(x_0^1)$ is polynomial in x_0^1 we can use the resultant to state explicit conditions for which this holds.

Lemma 5.29. *Let g and h be polynomials of degrees m and n respectively with no common roots or zeros. Let $f = gh$ be the product polynomial. Then the resultant,*

$$R(f,f') = (-1)^{mn}\left(\frac{m!n!}{N!}\frac{f^{(N)}(0)}{g^{(m)}(0)h^{(n)}(0)}\right)^{N-1} R(g,g')R(h,h')R(g,h)^2,$$

where $N = m+n$ and $R(g,h) \neq 0$.

Proof. Recall that,

$$\begin{aligned} R(f,f') &= R(gh, gh'+hg') \\ &= \left(\frac{f^{(N)}(0)}{N!}\right)^{N-1} \prod_{\substack{w\in Z(g)\\ w\in Z(h)}} (gh'+hg')(w), \\ &= \left(\frac{f^{(N)}(0)}{N!}\right)^{N-1} \prod_{w\in Z(g)} (hg')(w) \prod_{w\in Z(h)} (gh')(w), \end{aligned}$$

where $Z(g)$ denotes the set of zeros of g, and $Z(h)$ those of h. The result then follows by evaluating the product with Lemma 1.24. □

Since $f'_{(x_t(\lambda),t)}(x_0^1)$ is a polynomial in x_0 with real coefficients, its zeros are real or occur in complex conjugate pairs. Of the real roots, $x_0 = \lambda$ is repeated. So,

$$f'_{(x_t(\lambda),t)}(x_0^1) = (x_0^1-\lambda)^2 Q_{(\lambda,t)}(x_0^1)H_{(\lambda,t)}(x_0^1),$$

where Q is the product of quadratic factors,

$$Q_{(\lambda,t)}(x_0^1) = \prod_{i=1}^{q}\left\{(x_0^1-a_t^i)^2+(\eta_t^i)^2\right\},$$

and $H_{(\lambda,t)}(x_0^1)$ the product of real factors corresponding to real zeros. This gives,

$$f'''_{(x_t(\lambda),t)}(x_0^1)\big|_{x_0^1=\lambda} = 2\prod_{i=1}^{q}\left\{(\lambda-a_t^i)^2+(\eta_t^i)^2\right\} H_{(\lambda,t)}(\lambda).$$

We now assume that the real roots of H are distinct as are the complex roots of Q. Denoting $f'''_{(x_t(\lambda),t)}(x_0^1)\Big|_{x_0^1=\lambda}$ by $f_t'''(\lambda)$ etc, a simple calculation gives

$$\begin{aligned}&\left|R_\lambda(f_t'''(\lambda), f_t^{(4)}(\lambda))\right| = \\ &\quad K_t \prod_{k=1}^{q} (\eta_t^k)^2 \prod_{j\neq k} \left\{(a_t^k - a_t^j)^4 + 2((\eta_t^k)^2 + (\eta_t^j)^2)(a_t^k - a_t^j)^2 + ((\eta_t^k)^2 - (\eta_t^j)^2)^2\right\} \\ &\qquad \times \left|R_\lambda(H, H')\right| \left|R_\lambda(Q, H)\right|^2,\end{aligned}$$

K_t being a positive constant. Thus, the condition for a swallowtail perestroika to occur is that

$$\rho_\eta(t) := \left|R_\lambda(f_t'''(\lambda), f_t^{(4)}(\lambda))\right| = 0,$$

where we call $\rho_\eta(t)$ the *resultant eta process.*

When the zeros of $\rho_\eta(t)$ form a perfect set, swallowtails will spontaneously appear and disappear on the caustic infinitely rapidly. As they do so, the geometry of the cool part of the caustic will rapidly change as the λ shaped sections typical of a swallowtail caustic appear and disappear. Moreover, Maxwell sets will be created and destroyed with each swallowtail that forms and vanishes adding to the turbulent nature of the solution in these regions. We call this 'complex turbulence' occurring at the turbulent times which are the zeros of the resultant eta process.

Complex turbulence can be seen as a special case of real turbulence which occurs at specific generalised cusps of the caustic. Recall that when a swallowtail perestroika occurs on a curve, it also satisfies the conditions for having a generalised cusp. Thus, the zeros of the resultant eta process must coincide with some of the zeros of the zeta process for certain forms of cusped turbulence. From Corollary 3.15, at points where the complex and real pre-caustic touch, the real pre-caustic and pre-level surface touch in a particular manner (a double touch) since at such a point two swallowtail perestroikas on the level surface have coalesced.

Thus, our separation of complex turbulence from real turbulence can be seen as an alternative form of categorisation to that outlined in Sections 5.4 and 5.6 which could be extended to include other perestroikas.

Appendix A

The hot and cool parts of the non-generic swallowtail

Here we list the functions used to numerically calculate the hot and cool parts of the non-generic swallowtail in Section 2.7.

$$
\left.\begin{array}{l} P_1(\lambda, t) \\ P_2(\lambda, t) \end{array}\right\} =
$$

$$
\begin{aligned}
&72900 + 6524000\lambda^3 t \mp 923400\lambda t^2 + 258720000\lambda^6 t^2 \mp 74424000\lambda^4 t^3 \\
&+4939200000\lambda^9 t^3 + 5454000\lambda^2 t^4 \mp 2105040000\lambda^7 t^4 + 38416000000\lambda^{12} t^4 \\
&\mp 14580 t^5 + 297612000\lambda^5 t^5 \mp 21403200000\lambda^{10} t^5 \mp 13786200\lambda^3 t^6 \\
&+4410000000\lambda^8 t^6 - 24300\lambda t^7 \mp 390096000\lambda^6 t^7 + 11088900\lambda^4 t^8 \\
&\pm 143370\lambda^2 t^9 + 729 t^{10},
\end{aligned}
$$

$$
\left.\begin{array}{l} Q_1(\lambda, t) \\ Q_2(\lambda, t) \end{array}\right\} =
$$

$$
\begin{aligned}
&\pm 145800 \mp 2215240000\lambda^3 t - 11542500\lambda t^2 \mp 340820960000\lambda^6 t^2 \\
&+49143048000\lambda^4 t^3 \mp 22002960000000\lambda^9 t^3 \pm 267516000\lambda^2 t^4 \\
&+6514707360000\lambda^7 t^4 \mp 775015360000000\lambda^{12} t^4 + 29160 t^5 \\
&\mp 460036656000\lambda^5 t^5 + 351347875200000\lambda^{10} t^5 \mp 16137793280000000\lambda^{15} t^5 \\
&-3002324400\lambda^3 t^6 \mp 51939044640000\lambda^8 t^6 + 10016631744000000\lambda^{13} t^6 \\
&\mp 200070528000000000\lambda^{18} t^6 \mp 1773900\lambda t^7 + 2377430136000\lambda^6 t^7 \\
&\mp 2288813284800000\lambda^{11} t^7 + 161660674560000000\lambda^{16} t^7 \\
&\mp 1385434624000000000\lambda^{21} t^7 \pm 18655855200\lambda^4 t^8 + 225463724640000\lambda^9 t^8 \\
&\mp 51054732288000000\lambda^{14} t^8 + 1444380134400000000\lambda^{19} t^8 \\
&\mp 4216540160000000000\lambda^{24} t^8 + 21102120\lambda^2 t^9 \mp 7498443456000\lambda^7 t^9
\end{aligned}
$$

$$
\begin{aligned}
&+7864271856000000\lambda^{12}t^{9} \mp 602258388480000000\lambda^{17}t^{9}\\
&+6144101376000000000\lambda^{22}t^{9} \pm 1458t^{10} - 68035237200\lambda^{5}t^{10}\\
&\mp 582215467680000\lambda^{10}t^{10} + 129634440768000000\lambda^{15}t^{10}\\
&\mp 3427014528000000000\lambda^{20}t^{10} + 6324810240000000000\lambda^{25}t^{10}\\
&\mp 117536670\lambda^{3}t^{11} + 15041318976000\lambda^{8}t^{11} \mp 1519597376640000\lambda^{13}t^{11}\\
&+99433208448000000\lambda^{18}t^{11} \mp 623445580800000000\lambda^{23}t^{11} - 85293\lambda t^{12}\\
&\pm 148334004000\lambda^{6}t^{12} + 905238180000000\lambda^{11}t^{12}\\
&\mp 165225723264000000\lambda^{16}t^{12} + 2625441638400000000\lambda^{21}t^{12}\\
&+395803260\lambda^{4}t^{13} \mp 19110892464000\lambda^{9}t^{13} + 1580331332160000\lambda^{14}t^{13}\\
&-61138603008000000\lambda^{19}t^{13} \pm 879174\lambda^{2}t^{14} - 187608733200\lambda^{7}t^{14}\\
&\mp 794303586720000\lambda^{12}t^{14} + 84781269216000000\lambda^{17}t^{14} \mp 860147100\lambda^{5}t^{15}\\
&+14435967096000\lambda^{10}t^{15} \mp 6955250198400000\lambda^{15}t^{15} - 3542940\lambda^{3}t^{16}\\
&\pm 119865533400\lambda^{8}t^{16} + 306733923360000\lambda^{13}t^{16} + 1087682580\lambda^{6}t^{17}\\
&\mp 5117580000000\lambda^{11}t^{17} \pm 6377292\lambda^{4}t^{18} - 22975965900\lambda^{9}t^{18}\\
&\mp 653672430\lambda^{7}t^{19} - 4782969\lambda^{5}t^{20}
\end{aligned}
$$

$$
\left.\begin{array}{l} R_1(\lambda,t) \\ R_2(\lambda,t) \end{array}\right\} =
$$

$$
\begin{aligned}
&531441 + 56109200\lambda^{3}t \mp 7663248\lambda t^{2} + 2574969600\lambda^{6}t^{2} \mp 706132560\lambda^{4}t^{3}\\
&+56043456000\lambda^{9}t^{3} + 48922488\lambda^{2}t^{4} \mp 22685980800\lambda^{7}t^{4}\\
&+480968320000\lambda^{12}t^{4} \mp 78732t^{5} + 3048413760\lambda^{5}t^{5} \mp 254928576000\lambda^{10}t^{5}\\
&\mp 134641440\lambda^{3}t^{6} + 50214024000\lambda^{8}t^{6} - 178848\lambda t^{7} \mp 4297285440\lambda^{6}t^{7}\\
&+125119728\lambda^{4}t^{8} \pm 968112\lambda^{2}t^{9} + 2916t^{10}
\end{aligned}
$$

$$
\left.\begin{array}{l} S_1(\lambda,t) \\ S_2(\lambda,t) \end{array}\right\} =
$$

$$
\begin{aligned}
&34012224 - 1289857510400\lambda^{3}t \mp 3659253408\lambda t^{2} - 322136483827712\lambda^{6}t^{2}\\
&\pm 445107313350144\lambda^{4}t^{3} - 35033511381401600\lambda^{9}t^{3} + 126540326196\lambda^{2}t^{4}\\
&\pm 9936485550773760\lambda^{7}t^{4} - 2184785622495232000\lambda^{12}t^{4} \pm 5038848t^{5}\\
&-684000000016992\lambda^{5}t^{5} \pm 95162692426859520\lambda^{10}t^{5}\\
&-8602599142359040000\lambda^{15}t^{5} \mp 2222011140300\lambda^{3}t^{6}\\
&-135798854001514560\lambda^{8}t^{6} \pm 5145082669362892800\lambda^{13}t^{6}\\
&-21998983478542336000\lambda^{18}t^{6} - 431132544\lambda t^{7} \pm 6188314883219280\lambda^{6}t^{7}\\
&-113383230487349760\lambda^{11}t^{7} \pm 1718238688651161600000\lambda^{16}t^{7}
\end{aligned}
$$

$$
\begin{aligned}
&-35419389069937868800000\lambda^{21}t^{7} + 23400414904689\lambda^{4}t^{8} \\
&\pm 108556468428946464 0\lambda^{9}t^{8} - 523712042134710912000\lambda^{14}t^{8} \\
&\pm 3594480185829335040000 0\lambda^{19}t^{8} - 30114342298550272000000 0\lambda^{24}t^{8} \\
&\pm 9453800304\lambda^{2}t^{9} - 3673006648482067 2\lambda^{7}t^{9} \\
&\pm 7799754269603099520 0\lambda^{12}t^{9} - 145086243163110144 00000\lambda^{17}t^{9} \\
&\pm 438630004573888512000000\lambda^{22}t^{9} + 146497736513945600000000\lambda^{27}t^{9} \\
&+186624t^{10} \mp 160390386456660\lambda^{5}t^{10} - 564015199277738016 0\lambda^{10}t^{10} \\
&\pm 3017778764786811648000\lambda^{15}t^{10} - 2390466451265109504 00000\lambda^{20}t^{10} \\
&\pm 206640016802709504 0000000\lambda^{25}t^{10} - 103891446288\lambda^{3}t^{11} \\
&+323398510575616000000000 0\lambda^{30}t^{10} \pm 150798337223372496\lambda^{8}t^{11} \\
&-342565018431306163200\lambda^{13}t^{11} \pm 672179660320992768 00000\lambda^{18}t^{11} \\
&-201995939195534131 2000000\lambda^{23}t^{11} \mp 15396480\lambda t^{12} \\
&+313864947006177280000000000\lambda^{33}t^{11} + 747432787890600\lambda^{6}t^{12} \\
&\mp 182427523841654784 00000000\lambda^{28}t^{11} \pm 1998077124288096230 4\lambda^{11}t^{12} \\
&-107966581399812844 80000\lambda^{16}t^{12} \pm 823115588978221056000000\lambda^{21}t^{12} \\
&-150041898574848000000000 0\lambda^{26}t^{12} \pm 701811528012\lambda^{4}t^{13} \\
&\mp 305258617484083200000000 00\lambda^{31}t^{12} \\
&+106219787436163072000000000 0\lambda^{36}t^{12} - 439266768128727264\lambda^{9}t^{13} \\
&\pm 9997099499704822272 00\lambda^{14}t^{13} - 184530805787533363200000\lambda^{19}t^{13} \\
&\pm 402707093607408844800000 0\lambda^{24}t^{13} + 307894608\lambda^{2}t^{14} \\
&\mp 127523070631477248000000000 0\lambda^{34}t^{13} \mp 2416478134275720\lambda^{7}t^{14} \\
&+113300058262280601600000000\lambda^{29}t^{13} - 49085863752722299200\lambda^{12}t^{14} \\
&\pm 2461367492846760960 0000\lambda^{17}t^{14} - 15258632387390429184 00000\lambda^{22}t^{14} \\
&\mp 148295186026109337600000 00\lambda^{27}t^{14} \\
&+655823115679334400000000000\lambda^{32}t^{14} - 3196746892944\lambda^{5}t^{15} \\
&\pm 9132980694120696 96\lambda^{10}t^{15} - 19449498393796826880 00\lambda^{15}t^{15} \\
&\pm 299491272544831395840000\lambda^{20}t^{15} - 25985914906546667520000 00\lambda^{25}t^{15} \\
&\mp 182355071441692262400000000\lambda^{30}t^{15} \mp 2905210800\lambda^{3}t^{16} \\
&+5421586553232660\lambda^{8}t^{16} \pm 829147205995166822 40\lambda^{13}t^{16} \\
&-349645513541079168 00000\lambda^{18}t^{16} \pm 139768960086230630 4000000\lambda^{23}t^{16} \\
&+267574525632420249600000 00\lambda^{28}t^{16} \pm 10199293794864\lambda^{6}t^{17} \\
&-133718403035656339 2\lambda^{11}t^{17} \pm 2439257073425921664000\lambda^{16}t^{17} \\
&-264514917054405427200000\lambda^{21}t^{17} \mp 827358021096387379200000\lambda^{26}t^{17} \\
&+15528706020\lambda^{4}t^{18} \mp 8247378527466048\lambda^{9}t^{18}
\end{aligned}
$$

$$
\begin{aligned}
&-9252254995144981632 0\lambda^{14}t^{18} \pm 2829869766406714982 4000\lambda^{19}t^{18} \\
&-4529352973919735808 00000\lambda^{24}t^{18} - 22758922561248\lambda^{7}t^{19} \\
&\pm 1323197250594299712\lambda^{12}t^{19} - 1793117441516252774400\lambda^{17}t^{19} \\
&\pm 96889922806035824640000\lambda^{22}t^{19} \mp 50278570128\lambda^{5}t^{20} \\
&+8012091264177312\lambda^{10}t^{20} \pm 617957613764815564 80\lambda^{15}t^{20} \\
&-9973458376083818496000\lambda^{20}t^{20} \pm 34169454008496\lambda^{8}t^{21} \\
&-803430412320321792\lambda^{13}t^{21} \pm 58905506821625671680 0\lambda^{18}t^{21} \\
&+99179645184\lambda^{6}t^{22} \mp 4341746920697856\lambda^{11}t^{22} \\
&-187965892935317030 40\lambda^{16}t^{22} - 31357297819008\lambda^{9}t^{23} \\
&\pm 22865609697425740 8\lambda^{14}t^{23} \mp 111577100832\lambda^{7}t^{24} \\
&+911105545512384\lambda^{12}t^{24} \pm 13463636833728\lambda^{10}t^{25} + 55788550416\lambda^{8}t^{26}
\end{aligned}
$$

Appendix B

Some singularity sets

This appendix contains further examples of the singularity sets calculated using the double discriminant in Theorem 4.11. As is shown in Theorem 4.14, the cubed factor corresponds to the caustic and the squared factor corresponds to the Maxwell-Klein set.

B.1 The 3D polynomial swallowtail

$$
\begin{aligned}
D(t) = &-\frac{823543}{1073741824}\times \\
&(4400789 - 8673588x - 84206250x^2 + 114946776x^3 + 129730653x^4 \\
&+784147392x^5 + 17123652y + 111444768xy - 376295220x^2y \\
&-976145580x^3y - 300056400x^4y - 6004530y^2 + 266324436xy^2 \\
&+860694822x^2y^2 - 871816932x^3y^2 + 29778084y^3 - 78958476xy^3 \\
&+286829424x^2y^3 + 896168448x^3y^3 - 4749435y^4 + 385786800xy^4 \\
&-6858432x^2y^4 + 21337344y^5 - 56993220xy^5 + 256048128xy^6 + 61918908z \\
&-61665408xz - 637621956x^2z + 126459144x^3z - 560105280x^4z \\
&+152496792yz + 1031224824xyz - 1146092976x^2yz - 2254709520x^3yz \\
&-36027504y^2z + 1355220720xy^2z + 3460144068x^2y^2z + 178750152y^3z \\
&-159063912xy^3z + 1216228608x^2y^3z - 18997740y^4z + 772553376xy^4z \\
&+85349376y^5z + 348627180z^2 - 161826336xz^2 - 1449686808x^2z^2 \\
&-6667920x^3z^2 + 534883104yz^2 + 3426314256xyz^2 - 785045520x^2yz^2 \\
&-72849456y^2z^2 + 2223030096xy^2z^2 + 3734035200x^2y^2z^2 + 357663600y^3z^2 \\
&-11811744xy^3z^2 - 18997740y^4z^2 + 85349376y^5z^2 + 1017797408z^3 \\
&-184875264xz^3 - 1041571440x^2z^3 + 919267776yz^3 + 4915827360xyz^3
\end{aligned}
$$

$$
\begin{aligned}
&-51212736y^2z^3 + 1155772800xy^2z^3 + 238551264y^3z^3 + 1637055408z^4 \\
&-76991040xz^4 + 768479040yz^4 + 2593080000xyz^4 - 3175200y^2z^4 \\
&+1382161344z^5 + 246960000yz^5 + 480200000z^6)^3 \times \\
&(- 20652406010368 + 694061061008904x - 7597733206313516x^2 \\
&+13515584820475O4x^3 + 85512922684593410x^4 - 548447305128818076x^5 \\
&+950670039353615775x^6 + 1667024505421415424x^7 \\
&+2636254465092182016x^8 - 1075992387118851686 4x^9 \\
&+9328065534185648947 2x^{10} - 367992485336928y + 7572358054658512xy \\
&-25825527874729920x^2y - 60887641455449520x^3y \\
&+179387680370284 62x^4y - 775217802201498018x^5y \\
&-9139085443371015936x^6y + 12809123068354633728x^7y \\
&-2598468911289099878 4x^8y - 5139954478020663705 6x^9y \\
&-2114815852544348y^2 + 15353075013957664xy^2 \\
&+425619814844308 56x^2y^2 + 412166101213378 32x^3y^2 \\
&+678232795113306783x^4y^2 - 562726621493252478x^5y^2 \\
&-11973695462719619328x^6y^2 - 5613532696413315072x^7y^2 \\
&-5590461322072424448x^8y^2 - 3526992634825096y^3 \\
&-25432918813910544xy^3 + 61474819751339220x^2y^3 \\
&-388722502540777 56x^3y^3 + 4717526272042131948x^4y^3 \\
&+1772173452193317792x^5y^3 + 14299681211027988 48x^6y^3 \\
&-24116068097180172288x^7y^3 + 5922581291546443776x^8y^3 \\
&+2921390583162866y^4 - 46151779971653276xy^4 \\
&-356173217422755355x^2y^4 - 1143063106605265764x^3y^4 \\
&+574669662722847369x^4y^4 + 15209549262517782528x^5y^4 \\
&+4461561923160416256x^6y^4 - 10666689775081095168x^7y^4 \\
&+7483735225645878y^5 + 115928720565748590xy^5 \\
&-396059368647078612x^2y^5 - 1550744990495714532x^3y^5 \\
&-6897974994023262336x^4y^5 + 109790654601461760x^5y^5 \\
&+4654288067499786240x^6y^5 - 4467168616224887y^6 \\
&+142702711589807378xy^6 + 699336712657628134x^2y^6 \\
&-801009724663350948x^3y^6 - 1810629463166132736x^4y^6 \\
&-9047981135978717184x^5y^6 - 3258986530798043136x^6y^6 \\
&-1681319449930552y^7 - 69831928277055588xy^7 \\
&+5500179557413657 04x^2y^7 + 1582823958677043648x^3y^7
\end{aligned}
$$

$$
\begin{aligned}
&+4220931205670215 68x^4y^7 - 17311767148489605 12x^5y^7 \\
&+3316685496629167y^8 + 670526709199488xy^8 - 458377062910771743x^2y^8 \\
&+4974323805658060 80x^3y^8 + 281401088776077312x^4y^8 \\
&-8029200593829874y^9 + 7978985211727030xy^9 - 83947688184932736x^2y^9 \\
&-793586061679394816x^3y^9 - 213993960236908544x^4y^9 \\
&-1183258131527621y^{10} - 41935003789009406xy^{10} \\
&+112904897902906 88x^2y^{10} - 213240523920506880x^3y^{10} \\
&-4559346675452228y^{11} + 5570120187528608xy^{11} \\
&-109351562838540288x^2y^{11} - 8927451170236969y^{12} \\
&-24789960744894464xy^{12} + 27791423407390720x^2y^{12} \\
&+3851903465751552y^{13} - 6550835517456384xy^{13} - 4710735003254784y^{14} \\
&+2021194429628416y^{15} - 558762207905304z + 15374695695151856xz \\
&-142430526939191616x^2z - 22593758595059168x^3z \\
&+1448897031677959902x^4z - 7601575801924345284x^5z \\
&+6966905831823857472x^6z + 10072529884924747776x^7z \\
&+13368536299903647744x^8z - 13325807905979498 4960x^9z \\
&-8746028490076448yz + 146006096689368832xyz \\
&-4031981738883750 48x^2yz - 788199675667086216x^3yz \\
&+773835479750429784x^4yz - 2742589082678466168x^5yz \\
&-8558133118060729 6512x^6yz + 8862723492538348 3392x^7yz \\
&-9042512507628945408x^8yz - 43285894694649408y^2z \\
&+236794899851192416xy^2z + 538997901533446452x^2y^2z \\
&+512585035992477600x^3y^2z + 9959555165938105050x^4y^2z \\
&+4739469716582462592x^5y^2z - 7448897596956777 6768x^6y^2z \\
&-7412533643518436 9664x^7y^2z - 56623546354336648y^3z \\
&-421006274859396536xy^3z + 413500707353701208x^2y^3z \\
&-3993339707387351160x^3y^3z + 41874900009845003784x^4y^3z \\
&+28614910764823188480x^5y^3z + 25972487079947993088x^6y^3z \\
&-7022489245690783 3344x^7y^3z + 64142653661660574y^4z \\
&-429436437553153484xy^4z - 3836163436651740896x^2y^4z \\
&-13998927470338893360x^3y^4z - 14946490685282497920x^4y^4z \\
&+74603063812667056128x^5y^4z + 18203106120028913664x^6y^4z \\
&+98946850509883944y^5z + 1739600143571752584xy^5z \\
&-2126867117564589696x^2y^5z - 9731647329223113840x^3y^5z
\end{aligned}
$$

$$
\begin{aligned}
&-4440918358191538483\,2x^4y^5z - 27582601447702167552x^5y^5z\\
&-826530208047110\,10y^6z + 13693209485276757\,04xy^6z\\
&+7642826400877090892x^2y^6z - 6098635492129451\,52x^3y^6z\\
&-2813864477107396608x^4y^6z - 22293616652986613760x^5y^6z\\
&-2208642633057888\,0y^7z - 835213600653409432xy^7z\\
&+2767355354009220688x^2y^7z + 9988320160293706752x^3y^7z\\
&+1784464217361874944x^4y^7z - 1159179430809710y^8z\\
&-56260830306706332xy^8z - 3254426493810730944x^2y^8z\\
&-1115058940719661056x^3y^8z - 71899453275879720y^9z\\
&-154327500639290264xy^9z - 491831365411606528x^2y^9z\\
&-2518787233272561664x^3y^9z - 13448042153394870y^{10}z\\
&-140047304267396992xy^{10}z - 295271668228554752x^2y^{10}z\\
&-52866084686049496y^{11}z - 57573254394019840xy^{11}z\\
&-20917278606278656y^{12}z - 60130534281445376xy^{12}z\\
&-1354928568139776y^{13}z - 68739092446456\,88z^2\\
&+151518210279213616xz^2 - 1180160671979208588x^2z^2\\
&-498430882282379664x^3z^2 + 10546840914457114116x^4z^2\\
&-42010737936451582968x^5z^2 + 18625454791760332800x^6z^2\\
&+24434106198000500736x^7z^2 + 73767865193815080960x^8z^2\\
&-93566018579536488yz^2 + 124858392492438037\,6xyz^2\\
&-2812667728514414352x^2yz^2 - 4433421184346230032x^3yz^2\\
&+6306674307460542216x^4yz^2 + 14750710700475328128x^5yz^2\\
&-29961946439316696268\,8x^6yz^2 + 11269807228989053337\,6x^7yz^2\\
&-394768680186921828y^2z^2 + 1618244717471915704xy^2z^2\\
&+2659629505621286160x^2y^2z^2 + 1086575130472946928x^3y^2z^2\\
&+51833871096380332056x^4y^2z^2 + 55533787707439245312x^5y^2z^2\\
&-115334156855580622848x^6y^2z^2 - 148064532288661094400x^7y^2z^2\\
&-391607740613482096y^3z^2 - 2857679979681340864xy^3z^2\\
&+9880331009905964\,64x^2y^3z^2 - 36555041564628235392x^3y^3z^2\\
&+129419717992537430016x^4y^3z^2 + 96435545405097443328x^5y^3z^2\\
&+58697640540506161152x^6y^3z^2 + 5673966387178644\,24y^4z^2\\
&-1126798676558028968xy^4z^2 - 14850715177193168484x^2y^4z^2\\
&-58234447609727198448x^3y^4z^2 - 97476751106829563904x^4y^4z^2\\
&+88390172633872564224x^5y^4z^2 + 5213979040659346\,08y^5z^2
\end{aligned}
$$

$$
\begin{aligned}
&+10459343542686097896xy^5z^2 + 258444489262979184x^2y^5z^2\\
&-15288985291511357184x^3y^5z^2 - 8362456526568775680 0x^4y^5z^2\\
&-5853641191856485171 2x^5y^5z^2 - 615655448181330124y^6z^2\\
&+4815295037688852056xy^6z^2 + 29825148271517577072x^2y^6z^2\\
&+10972989905831245824x^3y^6z^2 + 3635409813988442112x^4y^6z^2\\
&-155660611515315744y^7z^2 - 4079209067469532928xy^7z^2\\
&+1956223218030277632x^2y^7z^2 + 14780860277614706688x^3y^7z^2\\
&-159157807731066584y^8z^2 - 670124552869309464xy^8z^2\\
&-8111494993244762112x^2y^8z^2 - 6162495491285188608x^3y^8z^2\\
&-227150752044372216y^9z^2 - 718777346863848320xy^9z^2\\
&-1151954782211014656x^2y^9z^2 - 85527190162915464y^{10}z^2\\
&-144131175445168128xy^{10}z^2 - 127296897596538880y^{11}z^2\\
&-121776964385112064xy^{11}z^2 - 15638315160043520y^{12}z^2\\
&-508681947045870 96z^3 + 875183673401460976xz^3\\
&-5682054176023383952x^2z^3 - 3529079587617350016x^3z^3\\
&+42327016167496334184x^4z^3 - 11962130356820026368 0x^5z^3\\
&+18583138139444379648x^6z^3 + 5278576119219486720x^7z^3\\
&-594923917429063040yz^3 + 6241291054940206784xyz^3\\
&-11512259102978329088x^2yz^3 - 14390750492253927072x^3yz^3\\
&+21421718694232870176x^4yz^3 + 97349769935083450368x^5yz^3\\
&-42465041281372992307 2x^6yz^3 - 2113516150197475528y^2z^3\\
&+6521095263960694656xy^2z^3 + 6354535049347898208x^2y^2z^3\\
&-62210857467098471 04x^3y^2z^3 + 12025077811468280524 8x^4y^2z^3\\
&+13891989719606958489 6x^5y^2z^3 - 17186061783505305600x^6y^2z^3\\
&-1516425899811573568y^3z^3 - 10351139474735631680xy^3z^3\\
&+3138237114172992992x^2y^3z^3 - 13171704149294111654 4x^3y^3z^3\\
&+16309868081325944832 0x^4y^3z^3 + 91023507095184211968x^5y^3z^3\\
&+2723782792687013120y^4z^3 + 1456365907747193680xy^4z^3\\
&-22415113553118448496x^2y^4z^3 - 10192955850054525542 4x^3y^4z^3\\
&-18063585257620783104 0x^4y^4z^3 + 1316463566202763168y^5z^3\\
&+32626053758172615744xy^5z^3 + 21006603587285858496x^2y^5z^3\\
&+79678875617267834 88x^3y^5z^3 - 42824560302536785920x^4y^5z^3\\
&-2456259289796126312y^6z^3 + 6473231691558400640xy^6z^3\\
&+50077841568253279232x^2y^6z^3 + 18735406286924414976x^3y^6z^3
\end{aligned}
$$

$$-6385719585965031047y^7z^3 - 10211065910011497600xy^7z^3$$
$$-8451262168922832896x^2y^7z^3 - 6481264449394008888y^8z^3$$
$$-1978264073295046656xy^8z^3 - 7341933498590035968x^2y^8z^3$$
$$-3126884533570946624y^9z^3 - 7965256813316669944xy^9z^3$$
$$-1856867189080064007y^{10}z^3 - 854270458147635207y^{11}z^3$$
$$-252311576615725712z^4 + 3282508624192381600xz^4$$
$$-17545395499379354960x^2z^4 - 1324379049560097408x^3z^4$$
$$+10060396158960864705 6x^4z^4 - 18507332526918900940 8x^5z^4$$
$$+6150076276052459520x^6z^4 - 2498673521712688192yz^4$$
$$+2021652507611621072 0xyz^4 - 3030408873181588902 4x^2yz^4$$
$$-29910095818707943872x^3yz^4 + 32918326657126041600x^4yz^4$$
$$+17773241169773356646 4x^5yz^4 - 19279235975086080000 0x^6yz^4$$
$$-7359472505803863600y^2z^4 + 17414713755947323104xy^2z^4$$
$$+7247513499250197120x^2y^2z^4 - 31513036342655102400x^3y^2z^4$$
$$+12383468784642428928 0x^4y^2z^4 + 10038776862986403840 0x^5y^2z^4$$
$$-3559390874215525824y^3z^4 - 2152381398250162252 8xy^3z^4$$
$$+16681468848688309504x^2y^3z^4 - 22389964738309545062 4x^3y^3z^4$$
$$+67828717772589957120x^4y^3z^4 + 7883991049242631344y^4z^4$$
$$+13867099102563998880xy^4z^4 + 3911498198707590008x^2y^4z^4$$
$$-65258247940938178560x^3y^4z^4 - 98742330285096960000x^4y^4z^4$$
$$+1204394192421077152y^5z^4 + 5606050848120742905 6xy^5z^4$$
$$+44457658771838140416x^2y^5z^4 + 24346304657196318720x^3y^5z^4$$
$$-5746306858121894368y^6z^4 - 1447402685289262528xy^6z^4$$
$$+30843465833124732928x^2y^6z^4 - 1450580633914238976y^7z^4$$
$$-12994901445215169536xy^7z^4 - 11646836827330969600x^2y^7z^4$$
$$-987976208826595696y^8z^4 - 1763316222903975936xy^8z^4$$
$$-163316914057543680y^9z^4 - 119961047514742784y^{10}z^4$$
$$-884076437663406720z^5 + 8356791275257273024xz^5$$
$$-36084245984535463296x^2z^5 - 29465204249645568000x^3z^5$$
$$+141008998535220897792x^4z^5 - 148109557856260718592x^5z^5$$
$$-7280264151528079488yz^5 + 44399665346483070080xyz^5$$
$$-52431239605859083392x^2yz^5 - 40240450842754053888x^3yz^5$$
$$+190374546844522414 08x^4yz^5 + 10328162129510400000 0x^5yz^5$$
$$-17423865791194398624y^2z^5 + 32667374358677922816xy^2z^5$$

$$
\begin{aligned}
&+34361927691010112 64x^2y^2z^5 - 49720720758408032256x^3y^2z^5\\
&+43850269365977088000x^4y^2z^5 - 5059399249704107008y^3z^5\\
&-2515772314488946 7264xy^3z^5 + 45927265518252614400x^2y^3z^5\\
&-17313360026807151 8208x^3y^3z^5 + 1421875745842445 0784y^4z^5\\
&+30151572825330084992xy^4z^5 + 33753222335843211264x^2y^4z^5\\
&-12823679257804800 00x^3y^4z^5 - 1597659076663428608y^5z^5\\
&+5051551633738670 6688xy^5z^5 + 28308679607757373440x^2y^5z^5\\
&-7943936018274299072y^6z^5 - 11491420327240060928xy^6z^5\\
&-1676607233256598272y^7z^5 - 6659258302490214400xy^7z^5\\
&-531999079001227264y^8z^5 - 2244707111652252160z^6\\
&+14630921314347272832xz^6 - 49485236535220954944x^2z^6\\
&-39216058251574931712x^3z^6 + 10759943088226418 6880x^4z^6\\
&-48198089937715200000x^5z^6 - 15018519781829639680yz^6\\
&+67075985395821031040xyz^6 - 57917493565979970816x^2yz^6\\
&-32002814852743827456x^3yz^6 + 4918172442624000 00x^4yz^6\\
&-28419099431614600256y^2z^6 + 43722256650243971712xy^2z^6\\
&+27664125425124779 52x^2y^2z^6 - 26781049307787264000x^3y^2z^6\\
&-3936143860166407424y^3z^6 - 13966697618055406592xy^3z^6\\
&+56755316098226307072x^2y^3z^6 - 44882877402316800000x^3y^3z^6\\
&+15693160408719466496y^4z^6 + 29175403096647555328xy^4z^6\\
&+24269099238236160000x^2y^4z^6 - 5229414742519664896y^5z^6\\
&+18695710432587632640xy^5z^6 - 6035912866065024768y^6z^6\\
&-7767609085788160000xy^6z^6 - 768060117542502400y^7z^6\\
&-4162749594047421696z^7 + 17401200492299140352xz^7\\
&-43673022409429041408x^2z^7 - 28964964387104686080x^3z^7\\
&+34427207098368000000x^4z^7 - 21938678868984592896yz^7\\
&+68990586786157594624xyz^7 - 37086845619897658368x^2yz^7\\
&-11291629508812800000x^3yz^7 - 31548976783131985280y^2z^7\\
&+40298314964324696064xy^2z^7 + 61479232253816832 00x^2y^2z^7\\
&-9436703539858216 96y^3z^7 - 751069576064976896xy^3z^7\\
&+26066313945907200000x^2y^3z^7 + 9728365066543772928y^4z^7\\
&+10898380516782080000xy^4z^7 - 5078621913875958784y^5z^7\\
&-1949381208965120000y^6z^7 - 5597770131695302144z^8\\
&+13460185235794884096xz^8 - 22518967585246191360x^2z^8
\end{aligned}
$$

$$
\begin{aligned}
&-915326537932800000x^3z^8 - 222414948801661655044yz^8 \\
&+4637368670539816089 6xyz^8 - 104677984502784000000x^2yz^8 \\
&-2282741415139124556 8y^2z^8 + 228864065482324608000xy^2z^8 \\
&+398463045120000000 0x^2y^2z^8 + 739706705379152896y^3z^8 \\
&+176089041891840000 0xy^3z^8 + 26003397054734400 00y^4z^8 \\
&-178443979571200000 0y^5z^8 - 5324857923654045696z^9 \\
&+611681563072745984 0xz^9 - 5169448118016000000x^2z^9 \\
&-1490443777808219955 2yz^9 + 1846293109960320000 0xyz^9 \\
&-9727624170544627200y^2z^9 + 5976945676800000000xy^2z^9 \\
&+430098605753600000y^3z^9 - 340212419014674227 2z^{10} \\
&+1240496972064000000xz^{10} - 5941516757881600000yz^{10} \\
&+3320525376000000000xyz^{10} - 1855371789600000000y^2z^{10} \\
&-1311204939206400000z^{11} - 1067311728000000000yz^{11} \\
&-230592040000000000z^{12})^2.
\end{aligned}
$$

B.2 The non-generic swallowtail

In this case we have substituted $x_0^1 = \pm X_0^2$ as in Section 2.7 to make the equations polynomial in X_0.

$$
\begin{aligned}
D(t) = &\pm \frac{2048 \times 10^{47} x^6 y^8}{t^{107}} \times \\
&(\pm 1458x + 216t^5x \pm 8t^{10}x + 31104t^2x^2 \pm 4032t^7x^2 + 128t^{12}x^2 \pm 221184t^4x^3 \\
&+22528t^9x^3 \pm 512t^{14}x^3 \pm 442368tx^4 + 622592t^6x^4 \pm 32768t^{11}x^4 \\
&+4718592t^3x^5 \pm 786432t^8x^5 \pm 8388608t^5x^6 \pm 33554432t^2x^7 - 729t^2y^2 \\
&\mp 108t^7y^2 - 4t^{12}y^2 \mp 72576t^4xy^2 - 8112t^9xy^2 \mp 288t^{14}xy^2 - 483840t^6x^2y^2 \\
&\mp 18944t^{11}x^2y^2 - 5419008t^3x^3y^2 \mp 1433600t^8x^3y^2 \mp 19267584t^5x^4y^2 \\
&+27783t^6y^4 \pm 2940t^{11}y^4 + 108t^{16}y^4 \pm 625632t^8xy^4 + 7056t^{13}xy^4 \\
&\pm 11063808t^5x^2y^4 + 175616t^{10}x^2y^4 + 9834496t^7x^3y^4 - 201684t^{10}y^6 \\
&-7529536t^7xy^6 \pm 1647086t^9y^8)^2 \times \\
&(\pm 1194393600x + 238878720t^5x \pm 11943936t^{10}x + 19110297600t^2x^2 \\
&\pm 3344302080t^7x^2 + 143327232t^{12}x^2 \pm 101921587200t^4x^3 \\
&+14014218240t^9x^3 \pm 429981696t^{14}x^3 \pm 113246208000tx^4 \\
&+215167795200t^6x^4 \pm 15288238080t^{11}x^4 + 905969664000t^3x^5 \\
&\pm 203843174400t^8x^5 \pm 1207959552000t^5x^6 \pm 2684354560000t^2x^7
\end{aligned}
$$

$$
\begin{aligned}
&-671846400t^2y^2 \mp 134369280t^7y^2 - 6718464t^{12}y^2 \mp 50164531200t^4xy^2\\
&-7569469440t^9xy^2 \mp 362797056t^{14}xy^2 - 250822656000t^6x^2y^2\\
&\mp 13257768960t^{11}x^2y^2 - 1560674304000t^3x^3y^2 \mp 557383680000t^8x^3y^2\\
&\mp 4161798144000t^5x^4y^2 + 21604060800t^6y^4 \pm 3086294400t^{11}y^4\\
&+153055008t^{16}y^4 \pm 364868582400t^8xy^4 + 5555329920t^{13}xy^4\\
&\pm 3584673792000t^5x^2y^4 + 76814438400t^{10}x^2y^4 + 2389782528000t^7x^3y^4\\
&-132324872400t^{10}y^6 - 2744515872000t^7xy^6 \pm 675408202875t^9y^8)^3 \times\\
(&6537720751875000 \mp 6561934532437500t^5 + 1031238009956250t^{10}\\
&\pm 620681569171875t^{15} - 89813332170000t^{20} \mp 38277931633200t^{25}\\
&-17724147840t^{30} \pm 1107742233888t^{35} + 165269175552t^{40}\\
&\pm 11140892928t^{45} + 372874752t^{50} \pm 5038848t^{55} \pm 17433922005000000t^2x\\
&-11026955668 1625000t^7x \pm 6316639967 2725000t^{12}x\\
&+6384268270293750t^{17}x \mp 6047775354060000t^{22}x - 827903401423200t^{27}x\\
&\pm 164812240218240t^{32}x + 50889697989696t^{37}x \pm 5429832371712t^{42}x\\
&+294621442560t^{47}x \pm 8142778368t^{52}x + 90699264t^{57}x\\
&-15729271853400000000t^4x^2 \pm 6053229907020000000t^9x^2\\
&+861615953224425000t^{14}x^2 \mp 235217664604237500t^{19}x^2\\
&-10551054907692 0000t^{24}x^2 \pm 4317174017265600t^{29}x^2\\
&+5586572994693120t^{34}x^2 \pm 921555558211968t^{39}x^2 + 72715917818880t^{44}x^2\\
&\pm 3073394949120t^{49}x^2 + 65827510272t^{54}x^2 \pm 544195584t^{59}x^2\\
&-40291730856000000000tx^3 \mp 58474665806400000000t^6x^3\\
&+22304463978744000000t^{11}x^3 \mp 1556090681751000000t^{16}x^3\\
&-510128814082207 5000t^{21}x^3 \mp 368802119305296000t^{26}x^3\\
&+30596028851424 9600t^{31}x^3 \pm 79800427179440640t^{36}x^3\\
&+8746681761780480t^{41}x^3 \pm 507940579952640t^{46}x^3 + 15778559047680t^{51}x^3\\
&\pm 232673845248t^{56}x^3 + 1088391168t^{61}x^3 \mp 446308403328000000000t^3x^4\\
&+203102465065920000000t^8x^4 \pm 761085584308800000000t^{13}x^4\\
&-122827367230884000000t^{18}x^4 \mp 29307291173582400000t^{23}x^4\\
&+930046687734643 2000t^{28}x^4 \pm 415236676710251 5200t^{33}x^4\\
&+62368451683522 5600t^{38}x^4 \pm 47626642979758080t^{43}x^4\\
&+1951105905377280t^{48}x^4 \pm 39778681651200t^{53}x^4 + 301847150592t^{58}x^4\\
&+634749729177600000000t^5x^5 \pm 155415320296704000000 0t^{10}x^5\\
&-1546554586800672000000t^{15}x^5 \mp 920245307294361600000t^{20}x^5\\
&+150381285567609600000t^{25}x^5 \pm 14088015940083609 6000t^{30}x^5
\end{aligned}
$$

$$
\begin{aligned}
&+29180556691677388800t^{35}x^{5} \pm 2883884868500520960t^{40}x^{5} \\
&+150046728171061248t^{45}x^{5} \pm 3907320017190912t^{50}x^{5} \\
&+39299467051008t^{55}x^{5} + 7493573191680000000t^{2}x^{6} \\
&\pm 984368182118400000000t^{7}x^{6} - 923229682707456000000t^{12}x^{6} \\
&\mp 158621705695457280000000t^{17}x^{6} + 661757676072652800000t^{22}x^{6} \\
&\pm 324380118289010688000t^{27}x^{6} + 948089926170501120000t^{32}x^{6} \\
&\pm 121227110221794508800t^{37}x^{6} + 7901980007139901440t^{42}x^{6} \\
&\pm 254876900624695296t^{47}x^{6} + 3191009210007552t^{52}x^{6} \\
&\pm 18219668152320000000000t^{4}x^{7} - 15505764774912000000000t^{9}x^{7} \\
&\mp 15776343172841472000000t^{14}x^{7} - 21353072409944064000000t^{19}x^{7} \\
&\pm 5131937021923491840000t^{24}x^{7} + 2206805530835496960000t^{29}x^{7} \\
&\pm 3690842043335639040000t^{34}x^{7} + 301192448648321433600t^{39}x^{7} \\
&\pm 11903195068256747520t^{44}x^{7} + 181039462962167808t^{49}x^{7} \\
&+2847231295488000000000t^{6}x^{8} \mp 8640962900656128000000t^{11}x^{8} \\
&-4590696438477619200000t^{16}x^{8} \pm 5505025844584120320000t^{21}x^{8} \\
&+3731024030521098240000t^{26}x^{8} \pm 8338451858449367040000t^{31}x^{8} \\
&+858977946839443046400t^{36}x^{8} \pm 41585133148082012160t^{41}x^{8} \\
&+761946561004437504t^{46}x^{8} - 1044855521280000000000t^{3}x^{9} \\
&\mp 22420277585510400000000t^{8}x^{9} - 41189550778220544000000t^{13}x^{9} \\
&\pm 38123175823382937600000t^{18}x^{9} + 45787023973862604800000t^{23}x^{9} \\
&\pm 14140150337712947200000t^{28}x^{9} + 18689406408240660480000t^{33}x^{9} \\
&\pm 1116318460600857395200t^{38}x^{9} + 24648846067808337920t^{43}x^{9} \\
&\mp 2006122600857600000000000t^{5}x^{10} - 18029923679600640000000000t^{10}x^{10} \\
&\pm 14991092215499980800000000t^{15}x^{10} \\
&+401393303346688819200000000t^{20}x^{10} \\
&\pm 180115938856707031040000000t^{25}x^{10} \\
&+31321321699585032192000000t^{30}x^{10} \\
&\pm 233969359938964684800000t^{35}x^{10} + 6265476572728262656000t^{40}x^{10} \\
&-31206351568896000000000000t^{7}x^{11} \\
&\pm 202682409827696640000000000t^{12}x^{11} \\
&+242354108869115904000000000t^{17}x^{11} \\
&\pm 1705912280936559411200000000t^{22}x^{11} \\
&+404842218982956072960000000t^{27}x^{11} \\
&\pm 38602493014503849984000000t^{32}x^{11}
\end{aligned}
$$

$$+126833524288132218880000t^{37}x^{11} - 7925422620672000000000000t^{4}x^{12}$$
$$\mp 4496943501803520000000000t^{9}x^{12}$$
$$+9384683178767155200000000t^{14}x^{12}$$
$$\pm 11730263597991854080000000t^{19}x^{12}$$
$$+4008184104354211430400000t^{24}x^{12}$$
$$\pm 502251402273939783680000t^{29}x^{12}$$
$$+20595976733995302912000t^{34}x^{12} \mp 8453784128716800000000000t^{6}x^{13}$$
$$+20137226897719296000000000t^{11}x^{13}$$
$$\pm 56000278122253516800000000t^{16}x^{13}$$
$$+29897064457495904256000000t^{21}x^{13}$$
$$\pm 5130318323458139750400000t^{26}x^{13}$$
$$+268870523371976130560000t^{31}x^{13}$$
$$+16531844518379520000000000t^{8}x^{14}$$
$$\pm 170734433303789568000000000t^{13}x^{14}$$
$$+163003791100713369600000000t^{18}x^{14}$$
$$\pm 40674304461738344448000000t^{23}x^{14}$$
$$+2814521587520031948800000t^{28}x^{14}$$
$$+15028949562163200000000000t^{5}x^{15}$$
$$\pm 278670122548199424000000000t^{10}x^{15}$$
$$+616034869590569779200000000t^{15}x^{15}$$
$$\pm 245195614735617228800000000t^{20}x^{15}$$
$$+23445282881728937984000000t^{25}x^{15}$$
$$\pm 144277915796766720000000000t^{7}x^{16}$$
$$+1460828740849238016000000000t^{12}x^{16}$$
$$\pm 1085820948791584358400000000t^{17}x^{16}$$
$$+153284752212670545920000000t^{22}x^{16}$$
$$+173133498956120064000000000t^{9}x^{17}$$
$$\pm 3329461946394083328000000000t^{14}x^{17}$$
$$+769162479601398579200000000t^{19}x^{17}$$
$$+379991218559385600000000000t^{6}x^{18}$$
$$\pm 6312780040178237440000000000t^{11}x^{18}$$
$$+2857956176031645696000000000t^{16}x^{18}$$
$$\pm 557320453887098880000000000t^{8}x^{19}$$
$$+7404199262373806080000000000t^{13}x^{19}$$

$+1193453901253181440000000000000t^{10}x^{20}$
$+9007199254740992000000000000000t^{7}x^{21} + 3341501717625000 0t^{4}y^{2}$
$\pm 1965432568258125 00t^{9}y^{2} - 757929894293812 50t^{14}y^{2}$
$\mp 3444081437444062 5t^{19}y^{2} + 7309863551430000t^{24}y^{2}$
$\pm 2382239665213200t^{29}y^{2} + 23256517409280t^{34}y^{2} \mp 43924629619296t^{39}y^{2}$
$-5648204286720t^{44}y^{2} \mp 330687836928t^{49}y^{2} - 10128084480t^{54}y^{2}$
$\mp 136048896t^{59}y^{2} \pm 9999322821090000000t^{6}xy^{2}$
$-3397017638808000000t^{11}xy^{2} \mp 3127298609939062500t^{16}xy^{2}$
$+1978099693308000000t^{21}xy^{2} \pm 359312025048120000t^{26}xy^{2}$
$+3372366664304640 0t^{31}xy^{2} \mp 5944058792772480t^{36}xy^{2}$
$-1275361788487680t^{41}xy^{2} \mp 91437835944960t^{46}xy^{2}$
$-2989125255168t^{51}xy^{2} \mp 38275089408t^{56}xy^{2}$
$\pm 1565178775560000000 0t^{3}x^{2}y^{2} + 5590161980316000000 0t^{8}x^{2}y^{2}$
$\mp 1270133998909200000 00t^{13}x^{2}y^{2} - 1196972343513675000 0t^{18}x^{2}y^{2}$
$\pm 1849590643862160000t^{23}x^{2}y^{2} + 4348851560725536000t^{28}x^{2}y^{2}$
$\mp 154893474448358400t^{33}x^{2}y^{2} - 120530354395507200t^{38}x^{2}y^{2}$
$\mp 12497433416847360t^{43}x^{2}y^{2} - 527332702187520t^{48}x^{2}y^{2}$
$\mp 8291444539392t^{53}x^{2}y^{2} - 6530347008t^{58}x^{2}y^{2}$
$+9446861203776000000 00t^{5}x^{3}y^{2} \mp 1696052286525600000 00t^{10}x^{3}y^{2}$
$-8890355603887200000 00t^{15}x^{3}y^{2} \pm 4823094511070280000 0t^{20}x^{3}y^{2}$
$+2322674648585712000 00t^{25}x^{3}y^{2} \pm 1249015609169625600 0t^{30}x^{3}y^{2}$
$-5895116259879168000t^{35}x^{3}y^{2} \mp 9957236246406144 00t^{40}x^{3}y^{2}$
$-59438208179036160t^{45}x^{3}y^{2} \mp 1381827697459200t^{50}x^{3}y^{2}$
$-7335272742912t^{55}x^{3}y^{2} \mp 5416310623104000000 00t^{7}x^{4}y^{2}$
$-1943963390825280000 000t^{12}x^{4}y^{2} \pm 6274745868974400000 00t^{17}x^{4}y^{2}$
$+6904101569641344000 000t^{22}x^{4}y^{2} \pm 1034160665574067200 000t^{27}x^{4}y^{2}$
$-1543694223294259200 00t^{32}x^{4}y^{2} \mp 4986773568272793600 0t^{37}x^{4}y^{2}$
$-4295132761964544000t^{42}x^{4}y^{2} \mp 144196293645434880t^{47}x^{4}y^{2}$
$-1462333349560320t^{52}x^{4}y^{2} \pm 1032202973952000000 000t^{4}x^{5}y^{2}$
$-1673104834206720000 0000t^{9}x^{5}y^{2} \pm 2227451842630656000 0000t^{14}x^{5}y^{2}$
$+1260067540024995840 00000t^{19}x^{5}y^{2} \pm 3499651269177246720 0000t^{24}x^{5}y^{2}$
$-1693458075938918400 000t^{29}x^{5}y^{2} \mp 1652147460445224960 000t^{34}x^{5}y^{2}$
$-2067120095328534528 00t^{39}x^{5}y^{2} \mp 9623694044811755520t^{44}x^{5}y^{2}$
$-144328027965751296t^{49}x^{5}y^{2} - 4871802126643200000 0000t^{6}x^{6}y^{2}$

$\mp 30117162247372800000000 t^{11} x^6 y^2$
$+ 14249763011719987200000000 t^{16} x^6 y^2$
$\pm 69300631203522969600000 t^{21} x^6 y^2 + 179498179551375360000000 t^{26} x^6 y^2$
$\mp 3741659904461045760000 t^{31} x^6 y^2 - 687941328757653504000 t^{36} x^6 y^2$
$\mp 43457667122237276160 t^{41} x^6 y^2 - 884492710311886848 t^{46} x^6 y^2$
$\mp 2827291969290240000000000 t^{8} x^7 y^2$
$+ 948567389593927680000000 t^{13} x^7 y^2$
$\pm 870860037802917888000000 t^{18} x^7 y^2$
$+ 92223654138445824000000 t^{23} x^7 y^2$
$\mp 590573048852594688000000 t^{28} x^7 y^2 - 162427338049368883200000 t^{33} x^7 y^2$
$\mp 1382978116956350054400 t^{38} x^7 y^2 - 370295147523892838400 t^{43} x^7 y^2$
$\mp 659652119101440000000000 t^{5} x^8 y^2$
$+ 334738686423859200000000 t^{10} x^8 y^2$
$\pm 694771714593128448000000 t^{15} x^8 y^2$
$+ 1505941577155215360000000 t^{20} x^8 y^2$
$\mp 657900235995348992000000 t^{25} x^8 y^2$
$- 275608099721052160000000 t^{30} x^8 y^2$
$\mp 31711419366233866240000 t^{35} x^8 y^2 - 1109168011973387878400 t^{40} x^8 y^2$
$+ 528278951559168000000000 t^{7} x^9 y^2$
$\pm 3320344111428403200000000 t^{12} x^9 y^2$
$+ 1368913852225290240000000 t^{17} x^9 y^2$
$\mp 5268558506706862080000000 t^{22} x^9 y^2$
$- 336352439496081408000000 t^{27} x^9 y^2$
$\mp 526392191652724736000000 t^{32} x^9 y^2$
$- 24221274925265059840000 t^{37} x^9 y^2$
$\pm 847326745932595200000000 t^{9} x^{10} y^2$
$+ 7120699302032179200000000 t^{14} x^{10} y^2$
$\mp 3184826905861816320000000 t^{19} x^{10} y^2$
$- 2916693739796902707200000 t^{24} x^{10} y^2$
$\mp 622338875993022791680000 t^{29} x^{10} y^2$
$- 38382501119377014784000 t^{34} x^{10} y^2$
$\pm 1013133191675904000000000 t^{6} x^{11} y^2$
$\mp 16074596011946803200000000 t^{16} x^{11} y^2$
$- 17445847161718702080000000 t^{21} x^{11} y^2$

$\mp 495864201000035287040000000t^{26}x^{11}y^2$
$-42427371195006451712000000t^{31}x^{11}y^2$
$+729138881101824000000000000t^{8}x^{12}y^2$
$\mp 7327486991086387200000000000t^{13}x^{12}y^2$
$-6756038918736445440000000000t^{18}x^{12}y^2$
$\mp 2207734123967650201600000000t^{23}x^{12}y^2$
$-284374978507686543360000000t^{28}x^{12}y^2$
$\mp 27011405806829568000000000000t^{10}x^{13}y^2$
$-14317022655125913600000000000t^{15}x^{13}y^2$
$\pm 5300355574477619200000000000t^{20}x^{13}y^2$
$-3386196437149679616000000000t^{25}x^{13}y^2$
$\mp 55356630887301120000000000000t^{7}x^{14}y^2$
$-50838668889292800000000000000t^{12}x^{14}y^2$
$\pm 76453730147578675200000000000t^{17}x^{14}y^2$
$+15126530875530936320000000000t^{22}x^{14}y^2$
$+33664847019245568000000000000t^{9}x^{15}y^2$
$\pm 492363725843673907200000000000t^{14}x^{15}y^2$
$+174250228935987036160000000000t^{19}x^{15}y^2$
$\pm 1476265884103213056000000000000t^{11}x^{16}y^2$
$+982234199120202956800000000000t^{16}x^{16}y^2$
$\pm 1861956970940989440000000000000t^{8}x^{17}y^2$
$+2988982777690456064000000000000t^{13}x^{17}y^2$
$+3930798049764311040000000000000t^{10}x^{18}y^2$
$-12803009568221250000t^{8}y^4 \mp 549458271504675000t^{13}y^4$
$+4676555376233343750t^{18}y^4 \pm 633805144260210000t^{23}y^4$
$-242118215328852000t^{28}y^4 \mp 49957048682510400t^{33}y^4$
$-379264278379968t^{38}y^4 \pm 410438504602368t^{43}y^4 + 30701024165376t^{48}y^4$
$\pm 747301469184t^{53}y^4 + 816293376t^{58}y^4 - 6225979985619750000t^{5}xy^4$
$\mp 22988367868467825000t^{10}xy^4 + 6301424004685537500t^{15}xy^4$
$\pm 2230206704671860000t^{20}xy^4 - 1715836459768650000t^{25}xy^4$
$\mp 794031063481690560t^{30}xy^4 - 37804199667020352t^{35}xy^4$
$\pm 6796208002977792t^{40}xy^4 + 6713420012001792t^{45}xy^4$
$\pm 172263714674688t^{50}xy^4 + 228562145280t^{55}xy^4$
$\mp 4549434703352820000000t^{7}x^2y^4 + 1724403191784030000000t^{12}x^2y^4$

$\pm 4577359588036987500000t^{17}x^2y^4 - 662766039445550400000t^{22}x^2y^4$
$\mp 46540506170743452000 0t^{27}x^2y^4 - 58483896009975187200t^{32}x^2y^4$
$\pm 3192161935041158400t^{37}x^2y^4 + 696584266619443200t^{42}x^2y^4$
$\pm 24480347916745728t^{47}x^2y^4 + 76965460512768t^{52}x^2y^4$
$\pm 17414258688t^{57}x^2y^4 - 2061971522971200000000t^{9}x^3y^4$
$\pm 24080579605674900000000t^{14}x^3y^4 - 16313068382933542500000t^{19}x^3y^4$
$\mp 15065580056857668000000t^{24}x^3y^4 - 3577611983217462960000t^{29}x^3y^4$
$\mp 493505178099768960000t^{34}x^3y^4 + 38742898728885312000t^{39}x^3y^4$
$\pm 2302199254491955200t^{44}x^3y^4 + 22263263843530752t^{49}x^3y^4$
$\pm 30833073709056t^{54}x^3y^4 - 1633833640131840000000000t^{6}x^4y^4$
$\pm 45193140355946400000000 0t^{11}x^4y^4 - 16636216216372272000000 0t^{16}x^4y^4$
$\mp 315750149444993184000000t^{21}x^4y^4 - 117903833052720387200000t^{26}x^4y^4$
$\mp 9744954076375512320000t^{31}x^4y^4 + 1147511324773043200000t^{36}x^4y^4$
$\pm 137488485388747161600t^{41}x^4y^4 + 2737186255546859520t^{46}x^4y^4$
$\pm 5536369285890048t^{51}x^4y^4 \pm 242563483630425600000000 0t^{8}x^5y^4$
$+386541185963500800000000t^{13}x^5y^4$
$\mp 435747339099025920000000 0t^{18}x^5y^4$
$-2403094463908746566400000t^{23}x^5y^4$
$\mp 397632577317584153600000t^{28}x^5y^4 + 13547429137646868480000t^{33}x^5y^4$
$\pm 5259963063880515584000t^{38}x^5y^4 + 182566651046252544000t^{43}x^5y^4$
$\pm 459058753271365632t^{48}x^5y^4 + 15864550000911360000000000t^{10}x^6y^4$
$\mp 3652675024010231808000000 0t^{15}x^6y^4$
$-3231406958571485337600000 0t^{20}x^6y^4$
$\mp 8625286175235428864000000t^{25}x^6y^4$
$-196767966801428070400000t^{30}x^6y^4 \pm 130456921365463859200000t^{35}x^6y^4$
$+7548074492209555046400t^{40}x^6y^4 \pm 22056747624895610880t^{45}x^6y^4$
$+68379986293125120000000000t^{7}x^7y^4$
$\mp 16326141719327539200000000 0t^{12}x^7y^4$
$-28836311591400431616000000 0t^{17}x^7y^4$
$\mp 11444829093557260288000000 0t^{22}x^7y^4$
$-9907224569300080640000000t^{27}x^7y^4$
$\pm 2063409316145397760000000t^{32}x^7y^4$
$+20541653769243623424000 0t^{37}x^7y^4 \pm 645683457342622924800t^{42}x^7y^4$
$\mp 319287749958696960000000000t^{9}x^8y^4$

$-16174761126758645760000000000t^{14}x^8y^4$
$\mp9637697314229649408000000000t^{19}x^8y^4$
$-1648670743807967232000000000t^{24}x^8y^4$
$\pm190211602776545689600000000t^{29}x^8y^4$
$+3731458636859296972800000t^{34}x^8y^4 \pm 10285522199243653120000t^{39}x^8y^4$
$-51614720977836441600000000000t^{11}x^9y^4$
$\mp50105539608324341760000000000t^{16}x^9y^4$
$-14518901201025761280000000000t^{21}x^9y^4$
$\pm632854641426353356800000000t^{26}x^9y^4$
$+4361037816138602905600000000t^{31}x^9y^4 \pm 59160021917761536000000t^{36}x^9y^4$
$-834527884015042560000000000000t^8x^{10}y^4$
$\mp138167020083688243200000000000t^{13}x^{10}y^4$
$-66004308988463677440000000000t^{18}x^{10}y^4$
$\mp5602103375777759232000000000t^{23}x^{10}y^4$
$+277572469031079772160000000t^{28}x^{10}y^4$
$\mp3916435943503115059200000t^{33}x^{10}y^4$
$\mp106643846716194816000000000000t^{10}x^{11}y^4$
$-84525431110867353600000000000t^{15}x^{11}y^4$
$\mp69139232976378265600000000000t^{20}x^{11}y^4$
$+565883240244156825600000000t^{25}x^{11}y^4$
$\mp1010463311641895239680000000t^{30}x^{11}y^4$
$+5225096506716979200000000000000t^{12}x^{12}y^4$
$\mp252381190021133107200000000000t^{17}x^{12}y^4$
$-138476754850619064320000000000t^{22}x^{12}y^4$
$\mp13913674902517107916800000000t^{27}x^{12}y^4$
$+21143266346926080000000000000000t^9x^{13}y^4$
$\mp1701221084063334400000000000000t^{14}x^{13}y^4$
$-95246182872378245120000000000t^{19}x^{13}y^4$
$\mp11429629796523442176000000000t^{24}x^{13}y^4$
$\pm285854640761733120000000000000t^{11}x^{14}y^4$
$-134528314694539673600000000000t^{16}x^{14}y^4$
$\mp49404665638001049600000000000t^{21}x^{14}y^4$
$+975629961912123392000000000000t^{13}x^{15}y^4$
$\mp227073491574403891200000000000t^{18}x^{15}y^4$

$+315075337372932505600000000000t^{10}x^{16}y^4$
$\pm 7357477714774720512000000000000t^{15}x^{16}y^4$
$\pm 230201670874903347200000000000t^{12}x^{17}y^4$
$\pm 4204674434256750000t^7y^6 + 1948821498324573750000t^{12}y^6$
$\pm 4842347303189272500 0t^{17}y^6 + 277830257514773400000t^{22}y^6$
$\mp 4229152387698514000t^{27}y^6 + 413474359257669920 0t^{32}y^6$
$\pm 348276014781208640t^{37}y^6 - 9632236650439680t^{42}y^6$
$\mp 1377375380884224t^{47}y^6 - 7446994080768t^{52}y^6 \mp 1632586752t^{57}y^6$
$+615761427455307000000 0t^9xy^6 \mp 47300771891652525000 0t^{14}xy^6$
$+207529179106308480000 0t^{19}xy^6 \mp 14135341769345376000 0t^{24}xy^6$
$+3739414131223603840 00t^{29}xy^6 \pm 66072431106791744000t^{34}xy^6$
$-1081554327459901440t^{39}xy^6 \mp 241595507599073280t^{44}xy^6$
$-15707499555962 88t^{49}xy^6 \mp 475264143360t^{54}xy^6$
$\pm 289696567161648150000000t^{11}x^2y^6 + 238246930551328515000000t^{16}x^2y^6$
$\pm 139308745069578672000000t^{21}x^2y^6 + 135857868458431791200 00t^{26}x^2y^6$
$\pm 47648643422055841280 00t^{31}x^2y^6 + 976525132611321472 00t^{36}x^2y^6$
$\mp 20344979001752616960t^{41}x^2y^6 - 245443568582522880t^{46}x^2y^6$
$\mp 3053483840471 04t^{51}x^2y^6 \pm 620609073017900400000000t^8x^3y^6$
$-331143557070256560000000t^{13}x^3y^6 \pm 579165876562792617000000t^{18}x^3y^6$
$+307254805811124976000000t^{23}x^3y^6 \pm 172918755502442639520000t^{28}x^3y^6$
$+14607743026835480064000t^{33}x^3y^6 \mp 731569440107976422400t^{38}x^3y^6$
$-25682398585718538240t^{43}x^3y^6 \mp 123663560035553280t^{48}x^3y^6$
$-487706825534644800000000 0t^{10}x^4y^6$
$\pm 601712958196909944000000 0t^{15}x^4y^6$
$+5368482175092139008000000t^{20}x^4y^6$
$\pm 3618263850378646585600000t^{25}x^4y^6$
$+683333644180039383040000t^{30}x^4y^6 \mp 19184967101302579200 00t^{35}x^4y^6$
$-14881738236073426944 00t^{40}x^4y^6 \mp 13562494990650408960t^{45}x^4y^6$
$\mp 969445885568832000000000t^{12}x^5y^6$
$+6463585292682212352000000 0t^{17}x^5y^6$
$\pm 4795253848339888339200000 0t^{22}x^5y^6$
$+1664147463383667240960000 0t^{27}x^5y^6$
$\pm 687867449022918184960000 0t^{32}x^5y^6 - 48836495859455033344000t^{37}x^5y^6$
$\mp 691046167105599897600t^{42}x^5y^6 \mp 18063446092751001600000000 0t^9x^6y^6$

$+4295443941587828736000000000t^{14}x^6y^6$
$\pm 42656802189249368064000000000t^{19}x^6y^6$
$+2398457281737343324160000000t^{24}x^6y^6$
$\pm 238521031933488504832000000t^{29}x^6y^6$
$-9355344358616698060800000t^{34}x^6y^6 \mp 1768655787869011968000000t^{39}x^6y^6$
$+1211417344868548608000000000t^{11}x^7y^6$
$\pm 2494820424412857139200000000t^{16}x^7y^6$
$+2149834633164928450560000000t^{21}x^7y^6$
$\pm 389519831787789987840000000t^{26}x^7y^6$
$-1096875060783973662720000000t^{31}x^7y^6$
$\mp 132455789273543475200000t^{36}x^7y^6$
$\pm 8739181936004825088000000000t^{13}x^8y^6$
$+11917962776753759846400000000t^{18}x^8y^6$
$\pm 3518978700431012331520000000t^{23}x^8y^6$
$-1130956782030039285760000000t^{28}x^8y^6$
$\pm 54515683556790108160000000t^{33}x^8y^6$
$\pm 1771036486051037184000000000t^{10}x^9y^6$
$+3540241405529659801600000000t^{15}x^9y^6$
$\pm 17625486001416437760000000000t^{20}x^9y^6$
$-1912455974984592916480000000t^{25}x^9y^6$
$\pm 197277527651432267776000000t^{30}x^9y^6$
$+2614868269005275136000000000t^{12}x^{10}y^6$
$\pm 4559127886955754291200000000t^{17}x^{10}y^6$
$-3072779204443798241280000000t^{22}x^{10}y^6$
$\pm 315434723642081017856000000t^{27}x^{10}y^6$
$\pm 2932812050096717824000000000t^{14}x^{11}y^6$
$-2875000941156719656960000000t^{19}x^{11}y^6$
$\pm 289042260803442442240000000t^{24}x^{11}y^6$
$\mp 2367529253261541376000000000t^{11}x^{12}y^6$
$-13505455152091784806400000000t^{16}x^{12}y^6$
$\pm 1534936492079788851200000000t^{21}x^{12}y^6$
$-24165400600637341696000000000t^{13}x^{13}y^6$
$\pm 4576841391673442304000000000t^{18}x^{13}y^6$
$\pm 9960734891270209536000000000t^{15}x^{14}y^6$

$$
\begin{aligned}
&\pm 2579044092205858816000000000000 t^{12}x^{15}y^{6}\\
&\mp 263674960124927400000 t^{11}y^{8} + 538582490036759700000 t^{16}y^{8}\\
&\mp 1588488841736789985000 t^{21}y^{8} - 802072517862585840000 t^{26}y^{8}\\
&\mp 34449659970742459200 t^{31}y^{8} - 3029964194567995200 0t^{36}y^{8}\\
&\pm 345712940357063040 t^{41}y^{8} + 16007618504862720 t^{46}y^{8}\\
&\pm 27470872147968 t^{51}y^{8} + 1088391168 t^{56}y^{8}\\
&-35409486726476919000000 t^{13}xy^{8} \mp 42965977164008134950000 t^{18}xy^{8}\\
&-19167889857893266770000 t^{23}xy^{8} \pm 5368510988177055360000 t^{28}xy^{8}\\
&-377867672722026064320 0t^{33}xy^{8} \pm 248818337491407552000 t^{38}xy^{8}\\
&+2368829478083519232 t^{43}xy^{8} \pm 5601213589266432 t^{48}xy^{8}\\
&+354089926656 t^{53}xy^{8} - 8849367755449760700000000 t^{10}x^{2}y^{8}\\
&\pm 29940787229570884800000 0t^{15}x^{2}y^{8}\\
&-1014932345609962363500000 t^{20}x^{2}y^{8}\\
&\pm 1053912693302739243400000 t^{25}x^{2}y^{8} - 181015152808987247040000 t^{30}x^{2}y^{8}\\
&\mp 4406314683335560352000 t^{35}x^{2}y^{8} + 1601798000751056563200 t^{40}x^{2}y^{8}\\
&\pm 1114156609179001344 t^{45}x^{2}y^{8} + 460328514158592 t^{50}x^{2}y^{8}\\
&\pm 7548235443893764620000000 t^{12}x^{3}y^{8}\\
&-17187010099595052822000000 t^{17}x^{3}y^{8}\\
&\pm 1558553690245399608600000 t^{22}x^{3}y^{8}\\
&-420961471148961925084000 0t^{27}x^{3}y^{8}\\
&\mp 4182370666993299612160 00t^{32}x^{3}y^{8} - 166086214113586417920 0t^{37}x^{3}y^{8}\\
&\pm 100074910555246187520 t^{42}x^{3}y^{8} + 185662938936148992 t^{47}x^{3}y^{8}\\
&-8731081541854526904000000 0t^{14}x^{4}y^{8}\\
&\mp 1890907827308816576400000 0t^{19}x^{4}y^{8}\\
&-5044693101543867984800000 0t^{24}x^{4}y^{8}\\
&\mp 1418407910848014471168000 0t^{29}x^{4}y^{8}\\
&-5007919405432226252800000 t^{34}x^{4}y^{8} \pm 2305869420445958246400 t^{39}x^{4}y^{8}\\
&+118335489345128448000 t^{44}x^{4}y^{8} + 10686223471589769600000000 0t^{11}x^{5}y^{8}\\
&\mp 53057516576499110592000000 0t^{16}x^{5}y^{8}\\
&-29830442834433354724800000 0t^{21}x^{5}y^{8}\\
&\mp 2451307995503238050816000 00t^{26}x^{5}y^{8}\\
&-1892062379330142014464000 0t^{31}x^{5}y^{8}\\
&\mp 81098264328909582336000 t^{36}x^{5}y^{8} - 12876712159330713600 t^{41}x^{5}y^{8}\\
&\mp 2937768563177168716800000000 t^{13}x^{6}y^{8}
\end{aligned}
$$

$$
\begin{aligned}
&-618492439865337166080000000t^{18}x^6y^8\\
&\mp 238753010414608177868800000 0t^{23}x^6y^8\\
&-318948330365266647449600000t^{28}x^6y^8\\
&\mp 4795799273109605089280000t^{33}x^6y^8\\
&-28618490438960283648000t^{38}x^6y^8\\
&+580923975809060352000000000t^{15}x^7y^8\\
&\mp 1316935109803951038464000000 0t^{20}x^7y^8\\
&-260222151580342140313600000 0t^{25}x^7y^8\\
&\mp 706271133191765385216000000t^{30}x^7y^8\\
&-13623231599449736806400000t^{35}x^7y^8\\
&-433212980612286873600000000 0t^{12}x^8y^8\\
&\mp 314889373323889803264000000 00t^{17}x^8y^8\\
&-977958351216236888064000000 0t^{22}x^8y^8\\
&\pm 294886219529950347264000000t^{27}x^8y^8\\
&-320958938970602799104000000t^{32}x^8y^8\\
&\pm 318679944961358561280000000 0t^{14}x^9y^8\\
&-351389243658536222720000000 00t^{19}x^9y^8\\
&\pm 195693874905092771020800000 00t^{24}x^9y^8\\
&-430967476293168726016000000t^{29}x^9y^8\\
&-283111601823209750528000000 000t^{16}x^{10}y^8\\
&\pm 209839097310982491340800000 0000t^{21}x^{10}y^8\\
&-314635025340421373952000000 0t^{26}x^{10}y^8\\
&-666348771104889241600000000 000t^{13}x^{11}y^8\\
&\pm 798395714538878009344000000 000t^{18}x^{11}y^8\\
&-838291208824799887360000000 00t^{23}x^{11}y^8\\
&\pm 357815918569581445120000000 000t^{15}x^{12}y^8\\
&+322268161538491678720000000 00t^{20}x^{12}y^8\\
&+223462308704828784640000000 000t^{17}x^{13}y^8\\
&+227611757706529996800000000 000t^{14}x^{14}y^8\\
&\pm 1522024953850735425000 00t^{15}y^{10}+5405742840213325575000t^{20}y^{10}\\
&\pm 9993413736499471635000t^{25}y^{10}-1460176167724601712000t^{30}y^{10}\\
&\pm 944553413970812116800t^{35}y^{10}-79647983478544320 0t^{40}y^{10}\\
&\mp 77029123976765568t^{45}y^{10}-43641341595648t^{50}y^{10}\\
&\pm 5501899805478334650000 00t^{12}xy^{10}-5538120175184573970000 00t^{17}xy^{10}
\end{aligned}
$$

$\pm 825977448938035466100000t^{22}xy^{10} - 194831758766401014720000t^{27}xy^{10}$
$\pm 90137372460453800608000t^{32}xy^{10} + 293954474870053401600t^{37}xy^{10}$
$\mp 9512904152124864000t^{42}xy^{10} - 9127983388557312t^{47}xy^{10}$
$-7528214438512242300000000t^{14}x^2y^{10}$
$\pm + 18994832213840505918000000t^{19}x^2y^{10}$
$-6386624634806715871600000t^{24}x^2y^{10}$
$\pm 3047933084165079824000000t^{29}x^2y^{10}$
$+124983718008283166592000t^{34}x^2y^{10} \mp 280626434271535564800t^{39}x^2y^{10}$
$-2469238255406684160t^{44}x^2y^{10} \pm 141725823400257179580000000t^{16}x^3y^{10}$
$-69045314707278922740000000t^{21}x^3y^{10}$
$\pm 42395670555521108582400000t^{26}x^3y^{10}$
$+7164297806895085633280000t^{31}x^3y^{10}$
$\pm 134679835478061758976000t^{36}x^3y^{10} + 92803168669659033600t^{41}x^3y^{10}$
$\pm 92770116677151278400000000t^{13}x^4y^{10}$
$+6156598163821832160000000t^{18}x^4y^{10}$
$\pm 139448020674213262592000000t^{23}x^4y^{10}$
$+166691033095447415116800000t^{28}x^4y^{10}$
$\pm 8173720198590809497600000t^{33}x^4y^{10}$
$+31918192784677527552000t^{38}x^4y^{10}$
$+2593948091871395750400000000t^{15}x^5y^{10}$
$\mp 1958312587993727150080000000t^{20}x^5y^{10}$
$\pm 1935811686972260418048000000t^{25}x^5y^{10}$
$+173616322049508716134400000t^{30}x^5y^{10}$
$+1456706937910906142720000t^{35}x^5y^{10}$
$\mp 1492913866971848294400000000t^{17}x^6y^{10}$
$+11810608610428701050880000000t^{22}x^6y^{10}$
$\pm 1531338179427747676160000000t^{27}x^6y^{10}$
$+164078926534723551232000000t^{32}x^6y^{10}$
$\mp 4227501707179720704000000000t^{14}x^7y^{10}$
$+29829596047370890444800000000t^{19}x^7y^{10}$
$\pm 6112294846270961008640000000t^{24}x^7y^{10}$
$-389968820894743150592000000t^{29}x^7y^{10}$
$-21846407732017168384000000000t^{16}x^8y^{10}$
$\pm 50670196397870396211200000000t^{21}x^8y^{10}$

$$-1232614955650087518208000000t^{26}x^8y^{10}$$
$$\pm 45144801482931175424000000000t^{18}x^9y^{10}$$
$$-11652633708932271964160000000t^{23}x^9y^{10}$$
$$\pm 542336279819321344000000000000t^{15}x^{10}y^{10}$$
$$-32352506517781059993600000000t^{20}x^{10}y^{10}$$
$$+49541701942181363712000000000t^{17}x^{11}y^{10}$$
$$-1293423074396834220000000t^{14}y^{12} \pm 2765362305989191356000000t^{19}y^{12}$$
$$-2220325248307923505700000t^{24}y^{12} \pm 5245992540721934092000t^{29}y^{12}$$
$$-1817649743051533540800 0t^{34}y^{12} \mp 4227726544847084160 0t^{39}y^{12}$$
$$+1800049738198924 80t^{44}y^{12} \pm 25350807085056t^{49}y^{12}$$
$$\pm 33094525681033312860000000t^{16}xy^{12}$$
$$-8100259601147159638500000t^{21}xy^{12}$$
$$\pm 3659409268435127915120000t^{26}xy^{12}$$
$$-1270696958455503094544000t^{31}xy^{12} \mp 7313983071002575027200t^{36}xy^{12}$$
$$+18392931730007654400t^{41}xy^{12} \pm 5929425013800960t^{46}xy^{12}$$
$$-70721821468929009708000000t^{18}x^2y^{12}$$
$$\pm 72965952749874896537000000t^{23}x^2y^{12}$$
$$-2872230202933349100304 0000t^{28}x^2y^{12}$$
$$\mp 1573423175732521253728000t^{33}x^2y^{12}$$
$$-20370251738444719104 00t^{38}x^2y^{12}$$
$$\pm 206765121176248320 0t^{43}x^2y^{12} - 88120170540564775200000000t^{15}x^3y^{12}$$
$$\pm 42752542637579414726800000 0t^{20}x^3y^{12}$$
$$-18310625395980819936440000 0t^{25}x^3y^{12}$$
$$\mp 65600677442184753355200000t^{30}x^3y^{12}$$
$$-1296274616438158994112000t^{35}x^3y^{12} \mp 9046891882225354752 00t^{40}x^3y^{12}$$
$$\mp 180967658426103457440000000t^{17}x^4y^{12}$$
$$+109821806764109631889600000 0t^{22}x^4y^{12}$$
$$\mp 107956518855446955209600000 0t^{27}x^4y^{12}$$
$$-42501154819182553912320000t^{32}x^4y^{12}$$
$$\mp 78782691469567131648000t^{37}x^4y^{12}$$
$$+109890423069353258516800000 00t^{19}x^5y^{12}$$
$$\mp 840057549421287086400000000 0t^{24}x^5y^{12}$$
$$-32267853074773638067200000 0t^{29}x^5y^{12}$$
$$\mp 588051037957552046080000t^{34}x^5y^{12}$$

$-929221376111983619840000000t^{16}x^6y^{12}$
$\mp 25154182014290859210240000000t^{21}x^6y^{12}$
$+2477477785096454246400000000t^{26}x^6y^{12}$
$\pm 82153689068372361216000000t^{31}x^6y^{12}$
$\pm 24250678531689822822400000000t^{18}x^7y^{12}$
$-15555276564374001530880000000t^{23}x^7y^{12}$
$\pm 2393855818947517317120000000t^{28}x^7y^{12}$
$-152504610614340159078400000000t^{20}x^8y^{12}$
$\pm 22449581452516455874560000000t^{25}x^8y^{12}$
$+338464211913542270976000000000t^{17}x^9y^{12}$
$\pm 34257333114560996966400000000t^{22}x^9y^{12}$
$\mp 319159124836720050176000000000t^{19}x^{10}y^{12}$
$-3369875708477638710000000t^{18}y^{14}$
$\pm 4938927506787790582500000t^{23}y^{14} - 4402488641195457262800000t^{28}y^{14}$
$\pm 2061711141564713632560000t^{33}y^{14}$
$+3768453692797868928000t^{38}y^{14} \mp 203754897120499200t^{43}y^{14}$
$\mp 20612651112310474980000000t^{20}xy^{14}$
$-18634788152549915001600000t^{25}xy^{14}$
$\pm 9586500054729717934080000t^{30}xy^{14}$
$+450266504359990671360000t^{35}xy^{14} \mp 1737780171290311680 0t^{40}xy^{14}$
$\mp 49593101089419417600000000t^{17}x^2y^{14}$
$-210530568643223082170000000t^{22}x^2y^{14}$
$\pm 125190515120349636272000000t^{27}x^2y^{14}$
$+10693904964602091874880000t^{32}x^2y^{14}$
$\pm 112813727349971773440000t^{37}x^2y^{14}$
$-603332334190036088400000000t^{19}x^3y^{14}$
$\pm 200344270886881629284000000t^{24}x^3y^{14}$
$+30686013210977997765760000 0t^{29}x^3y^{14}$
$\pm 5087503394995612187520000t^{34}x^3y^{14}$
$\mp 917853373809619341920000000t^{21}x^4y^{14}$
$+286812789006572009126400000 0t^{26}x^4y^{14}$
$\pm 20799080324356307456000000t^{31}x^4y^{14}$
$\pm 496421696389430084000000000t^{18}x^5y^{14}$
$+652987269513706360576000000 0t^{23}x^5y^{14}$

$\mp 6355412532716039654400000000t^{28}x^5y^{14}$
$-512673567552956959744000000000t^{20}x^6y^{14}$
$\pm 117383591851933530726400000000t^{25}x^6y^{14}$
$\pm 364149917383424764928000000000t^{22}x^7y^{14}$
$\mp 1361530384892426076160000000000t^{19}x^8y^{14}$
$+594476597172974476800000000t^{22}y^{16}$
$\pm 4804680038406404677500000t^{27}y^{16} - 1343676699485124500160000t^{32}y^{16}$
$\mp 125845338343233600000t^{37}y^{16} + 8986423210007040 0t^{42}y^{16}$
$+888414421448581183800000000t^{19}xy^{16}$
$\pm 1148813730814497885060000000t^{24}xy^{16}$
$-3357511940093011991122000 0t^{29}xy^{16}$
$\mp 1277451017604174873600000t^{34}xy^{16}$
$+657703102275072000 0t^{39}xy^{16} \pm 1518347705341459497680000000t^{21}x^2y^{16}$
$-18523677017908212332560000 0t^{26}x^2y^{16}$
$\mp 4329454792521580339884000 0t^{31}x^2y^{16}$
$-168697219719845376000000t^{36}x^2y^{16}$
$-9820138747769327179440000000t^{23}x^3y^{16}$
$\mp 5186166784500013874968000000t^{28}x^3y^{16}$
$-74466034806021349999200000t^{33}x^3y^{16}$
$+41414667555394953870400000000t^{20}x^4y^{16}$
$\mp 4809704214442324990240000000t^{25}x^4y^{16}$
$+2161054424781880482624000000t^{30}x^4y^{16}$
$\pm 21786172368109215651200000000t^{22}x^5y^{16}$
$-4870189146423362043968000000 0t^{27}x^5y^{16}$
$-77894664334352409062400000000t^{24}x^6y^{16}$
$-550913418336455083392000000000t^{21}x^7y^{16}$
$\pm 2192235359277425378000000t^{21}y^{18} + 4313601426292869338600000t^{26}y^{18}$
$\pm 5071284619254014998830000t^{31}y^{18} + 1865584054099584000000t^{36}y^{18}$
$+1002242518167234912400000 0t^{23}xy^{18}$
$\pm 3429528983143326828380000 0t^{28}xy^{18}$
$+1870775799125351731200000t^{33}xy^{18}$
$\pm 215471307470589816240000000t^{25}x^2y^{18}$
$+975928824812623993192000000t^{30}x^2y^{18}$
$\mp 53910194106562185392000000 0t^{22}x^3y^{18}$

$$
\begin{aligned}
&-434953354904779478880000000t^{27}x^3y^{18}\\
&+8437325296539253692480000000t^{24}x^4y^{18}\\
&\mp820441296730081647600000t^{25}y^{20}\\
&-1086332989277873808450000t^{30}y^{20}\\
&\mp10313331334971033600000t^{35}y^{20}+620369749480524139320000000t^{27}xy^{20}\\
&\mp1225098752517771264000000t^{32}xy^{20}\\
&-683217209139307982440000000t^{24}x^2y^{20}\\
&\mp9317875659449184060800000t^{29}x^2y^{20}\\
&\pm11870483763328009030400000000t^{26}x^3y^{20}\\
&\pm1220821674353463615300000t^{29}y^{22}\\
&\mp116496708794513521460000000t^{26}xy^{22}\\
&-5585458640832840070000000t^{28}y^{24})^2.
\end{aligned}
$$

Appendix C

The pre-Maxwell set for the 3D polynomial swallowtail

The following is the algebraic equation of the pre-Maxwell set calculated using the method of Theorem 4.18. Pictures of this surface can be found in Example 4.33.

$$
\begin{aligned}
0 =& \\
&3125 - 500t^4 - 241t^6 - 35t^8 - t^{10} - 2250t^3x_0 - 1430t^5x_0 - 52t^7x_0 \\
&+750t^2{x_0}^2 - 310t^4{x_0}^2 - 548t^6{x_0}^2 - 327t^8{x_0}^2 - 11t^{10}{x_0}^2 + 1390t^3{x_0}^3 \\
&+828t^5{x_0}^3 - 476t^7{x_0}^3 - 24t^9{x_0}^3 + 6220t^2{x_0}^4 + 17907t^4{x_0}^4 + 491t^6{x_0}^4 \\
&-410t^8{x_0}^4 + 18t^{10}{x_0}^4 + t^{12}{x_0}^4 + 94584t{x_0}^5 - 6422t^5{x_0}^5 + 114t^7{x_0}^5 \\
&-188t^9{x_0}^5 - 6t^{11}{x_0}^5 - 50112t^4{x_0}^6 - 12058t^6{x_0}^6 - 289t^8{x_0}^6 + 297t^{10}{x_0}^6 \\
&+10t^{12}{x_0}^6 - 62496t^3{x_0}^7 - 8068t^5{x_0}^7 - 2354t^7{x_0}^7 - 1632t^9{x_0}^7 - 48t^{11}{x_0}^7 \\
&+20680t^4{x_0}^8 - 4512t^6{x_0}^8 - 3071t^8{x_0}^8 + 257t^{10}{x_0}^8 + 9t^{12}{x_0}^8 + 135744t^3{x_0}^9 \\
&+214704t^5{x_0}^9 + 5424t^7{x_0}^9 - 5880t^9{x_0}^9 - 138t^{11}{x_0}^9 + 1192464t^2{x_0}^{10} \\
&-37088t^6{x_0}^{10} - 1132t^8{x_0}^{10} - 56t^{10}{x_0}^{10} - 338016t^5{x_0}^{11} - 28104t^7{x_0}^{11} \\
&-4060t^9{x_0}^{11} - 945504t^4{x_0}^{12} - 66736t^6{x_0}^{12} + 21088t^8{x_0}^{12} + 288t^{10}{x_0}^{12} \\
&+109536t^5{x_0}^{13} + 5712t^7{x_0}^{13} + 768t^9{x_0}^{13} + 959616t^4{x_0}^{14} + 705600t^6{x_0}^{14} \\
&+30512t^8{x_0}^{14} + 432t^{10}{x_0}^{14} + 7112448t^3{x_0}^{15} - 127680t^7{x_0}^{15} - 4320t^9{x_0}^{15} \\
&-874944t^6{x_0}^{16} - 26496t^8{x_0}^{16} - 3556224t^5{x_0}^{17} - 198464t^7{x_0}^{17} \\
&+225792t^6{x_0}^{18} + 2370816t^5{x_0}^{19} + 16595712t^4{x_0}^{20} + 2500t^2y_0 + 2250t^4y_0 \\
&+40t^6y_0 - 6t^8y_0 + 40000tx_0y_0 - 4330t^5x_0y_0 - 486t^7x_0y_0 - 66t^9x_0y_0 \\
&-2t^{11}x_0y_0 - 18230t^4{x_0}^2y_0 - 3198t^6{x_0}^2y_0 - 158t^8{x_0}^2y_0 - 21360t^3{x_0}^3y_0 \\
&-2998t^5{x_0}^3y_0 - 1054t^7{x_0}^3y_0 - 702t^9{x_0}^3y_0 - 24t^{11}{x_0}^3y_0 + 10228t^4{x_0}^4y_0 \\
&+1762t^6{x_0}^4y_0 - 1122t^8{x_0}^4y_0 - 48t^{10}{x_0}^4y_0 + 104792t^3{x_0}^5y_0 + 82920t^5{x_0}^5y_0
\end{aligned}
$$

$$
\begin{aligned}
&+3260t^7x_0{}^5y_0 - 1846t^9x_0{}^5y_0 - 54t^{11}x_0{}^5y_0 + 987504t^2x_0{}^6y_0 - 53216t^6x_0{}^6y_0 \\
&-2754t^8x_0{}^6y_0 - 72t^{10}x_0{}^6y_0 - 285952t^5x_0{}^7y_0 - 15496t^7x_0{}^7y_0 - 1498t^9x_0{}^7y_0 \\
&-604128t^4x_0{}^8y_0 - 52896t^6x_0{}^8y_0 + 10408t^8x_0{}^8y_0 + 288t^{10}x_0{}^8y_0 \\
&+121824t^5x_0{}^9y_0 + 45728t^7x_0{}^9y_0 + 1056t^9x_0{}^9y_0 + 1172640t^4x_0{}^{10}y_0 \\
&+481488t^6x_0{}^{10}y_0 + 28208t^8x_0{}^{10}y_0 + 432t^{10}x_0{}^{10}y_0 + 8580096t^3x_0{}^{11}y_0 \\
&-210432t^7x_0{}^{11}y_0 - 6912t^9x_0{}^{11}y_0 - 1289568t^6x_0{}^{12}y_0 - 38016t^8x_0{}^{12}y_0 \\
&-3499776t^5x_0{}^{13}y_0 - 242720t^7x_0{}^{13}y_0 + 384384t^6x_0{}^{14}y_0 + 4177152t^5x_0{}^{15}y_0 \\
&+26078976t^4x_0{}^{16}y_0 - 50t^4y_0{}^2 - 1020t^6y_0{}^2 - 63t^8y_0{}^2 - t^{10}y_0{}^2 \\
&+22400t^3x_0y_0{}^2 + 2880t^5x_0y_0{}^2 + 42t^7x_0y_0{}^2 - 12t^9x_0y_0{}^2 + 203200t^2x_0{}^2y_0{}^2 \\
&-14774t^6x_0{}^2y_0{}^2 - 504t^8x_0{}^2y_0{}^2 - 57568t^5x_0{}^3y_0{}^2 - 2214t^7x_0{}^3y_0{}^2 \\
&-138t^9x_0{}^3y_0{}^2 - 78656t^4x_0{}^4y_0{}^2 - 9852t^6x_0{}^4y_0{}^2 + 1855t^8x_0{}^4y_0{}^2 \\
&+81t^{10}x_0{}^4y_0{}^2 + 30216t^5x_0{}^5y_0{}^2 + 10904t^7x_0{}^5y_0{}^2 + 162t^9x_0{}^5y_0{}^2 \\
&+502752t^4x_0{}^6y_0{}^2 + 80368t^6x_0{}^6y_0{}^2 + 6528t^8x_0{}^6y_0{}^2 + 108t^{10}x_0{}^6y_0{}^2 \\
&+3446016t^3x_0{}^7y_0{}^2 - 110208t^7x_0{}^7y_0{}^2 - 3564t^9x_0{}^7y_0{}^2 - 581664t^6x_0{}^8y_0{}^2 \\
&-18072t^8x_0{}^8y_0{}^2 - 1083264t^5x_0{}^9y_0{}^2 - 95264t^7x_0{}^9y_0{}^2 + 194448t^6x_0{}^{10}y_0{}^2 \\
&+2779392t^5x_0{}^{11}y_0{}^2 + 15466752t^4x_0{}^{12}y_0{}^2 + 6400t^4y_0{}^3 + 36t^6y_0{}^3 - 6t^8y_0{}^3 \\
&-192t^5x_0y_0{}^3 - 1536t^7x_0y_0{}^3 - 54t^9x_0y_0{}^3 + 75648t^4x_0{}^2y_0{}^3 - 576t^6x_0{}^2y_0{}^3 \\
&-18t^8x_0{}^2y_0{}^3 + 459776t^3x_0{}^3y_0{}^3 - 17904t^7x_0{}^3y_0{}^3 - 594t^9x_0{}^3y_0{}^3 \\
&-85824t^6x_0{}^4y_0{}^3 - 2916t^8x_0{}^4y_0{}^3 - 79360t^5x_0{}^5y_0{}^3 - 11736t^7x_0{}^5y_0{}^3 \\
&+28272t^6x_0{}^6y_0{}^3 + 834816t^5x_0{}^7y_0{}^3 + 4119808t^4x_0{}^8y_0{}^3 - 768t^6y_0{}^4 \\
&-27t^8y_0{}^4 + 8192t^5x_0y_0{}^4 - 576t^6x_0{}^2y_0{}^4 + 95232t^5x_0{}^3y_0{}^4 + 428032t^4x_0{}^4y_0{}^4 \\
&+4096t^4y_0{}^5 + 25000tz_0 - 3000t^5z_0 - 996t^7z_0 - 86t^9z_0 - 2t^{11}z_0 \\
&-13500t^4x_0z_0 - 5880t^6x_0z_0 - 208t^8x_0z_0 + 4500t^3x_0{}^2z_0 - 1860t^5x_0{}^2z_0 \\
&-2192t^7x_0{}^2z_0 - 678t^9x_0{}^2z_0 - 22t^{11}x_0{}^2z_0 + 8340t^4x_0{}^3z_0 + 3312t^6x_0{}^3z_0 \\
&-932t^8x_0{}^3z_0 - 48t^{10}x_0{}^3z_0 + 37320t^3x_0{}^4z_0 + 71628t^5x_0{}^4z_0 + 1964t^7x_0{}^4z_0 \\
&-802t^9x_0{}^4z_0 - 18t^{11}x_0{}^4z_0 + 567504t^2x_0{}^5z_0 - 25688t^6x_0{}^5z_0 - 336t^8x_0{}^5z_0 \\
&-52t^{10}x_0{}^5z_0 - 200448t^5x_0{}^6z_0 - 27348t^7x_0{}^6z_0 - 578t^9x_0{}^6z_0 + 18t^{11}x_0{}^6z_0 \\
&-249984t^4x_0{}^7z_0 - 32272t^6x_0{}^7z_0 - 4708t^8x_0{}^7z_0 - 132t^{10}x_0{}^7z_0 \\
&+82720t^5x_0{}^8z_0 - 9024t^7x_0{}^8z_0 + 176t^9x_0{}^8z_0 + 542976t^4x_0{}^9z_0 \\
&+429408t^6x_0{}^9z_0 + 10848t^8x_0{}^9z_0 + 216t^{10}x_0{}^9z_0 + 4769856t^3x_0{}^{10}z_0 \\
&-74176t^7x_0{}^{10}z_0 - 3600t^9x_0{}^{10}z_0 - 676032t^6x_0{}^{11}z_0 - 22272t^8x_0{}^{11}z_0 \\
&-1891008t^5x_0{}^{12}z_0 - 133472t^7x_0{}^{12}z_0 + 219072t^6x_0{}^{13}z_0 + 1919232t^5x_0{}^{14}z_0 \\
&+14224896t^4x_0{}^{15}z_0 + 15000t^3y_0z_0 + 9000t^5y_0z_0 + 160t^7y_0z_0 - 12t^9y_0z_0 \\
&+240000t^2x_0y_0z_0 - 17320t^6x_0y_0z_0 - 1260t^8x_0y_0z_0 - 24t^{10}x_0y_0z_0
\end{aligned}
$$

$$
\begin{aligned}
&-72920t^5{x_0}^2y_0z_0 - 7860t^7{x_0}^2y_0z_0 - 316t^9{x_0}^2y_0z_0 - 85440t^4{x_0}^3y_0z_0 \\
&-11992t^6{x_0}^3y_0z_0 - 2108t^8{x_0}^3y_0z_0 - 36t^{10}{x_0}^3y_0z_0 + 40912t^5{x_0}^4y_0z_0 \\
&+3524t^7{x_0}^4y_0z_0 + 24t^9{x_0}^4y_0z_0 + 419168t^4{x_0}^5y_0z_0 + 165840t^6{x_0}^5y_0z_0 \\
&+6520t^8{x_0}^5y_0z_0 + 108t^{10}{x_0}^5y_0z_0 + 3950016t^3{x_0}^6y_0z_0 - 106432t^7{x_0}^6y_0z_0 \\
&-3816t^9{x_0}^6y_0z_0 - 571904t^6{x_0}^7y_0z_0 - 20544t^8{x_0}^7y_0z_0 - 1208256t^5{x_0}^8y_0z_0 \\
&-105792t^7{x_0}^8y_0z_0 + 243648t^6{x_0}^9y_0z_0 + 2345280t^5{x_0}^{10}y_0z_0 \\
&+17160192t^4{x_0}^{11}y_0z_0 - 200t^5{y_0}^2z_0 - 2040t^7{y_0}^2z_0 - 72t^9{y_0}^2z_0 \\
&+89600t^4x_0{y_0}^2z_0 + 5760t^6x_0{y_0}^2z_0 + 84t^8x_0{y_0}^2z_0 + 812800t^3{x_0}^2{y_0}^2z_0 \\
&-29548t^7{x_0}^2{y_0}^2z_0 - 972t^9{x_0}^2{y_0}^2z_0 - 115136t^6{x_0}^3{y_0}^2z_0 - 4716t^8{x_0}^3{y_0}^2z_0 \\
&-157312t^5{x_0}^4{y_0}^2z_0 - 19704t^7{x_0}^4{y_0}^2z_0 + 60432t^6{x_0}^5{y_0}^2z_0 \\
&+1005504t^5{x_0}^6{y_0}^2z_0 + 6892032t^4{x_0}^7{y_0}^2z_0 + 12800t^5{y_0}^3z_0 + 72t^7{y_0}^3z_0 \\
&-384t^6x_0{y_0}^3z_0 + 151296t^5{x_0}^2{y_0}^3z_0 + 919552t^4{x_0}^3{y_0}^3z_0 + 75000t^2{z_0}^2 \\
&-6000t^6{z_0}^2 - 1092t^8{z_0}^2 - 32t^{10}{z_0}^2 - 27000t^5x_0{z_0}^2 - 6360t^7x_0{z_0}^2 \\
&-208t^9x_0{z_0}^2 + 9000t^4{x_0}^2{z_0}^2 - 3720t^6{x_0}^2{z_0}^2 - 2192t^8{x_0}^2{z_0}^2 - 48t^{10}{x_0}^2{z_0}^2 \\
&+16680t^5{x_0}^3{z_0}^2 + 3312t^7{x_0}^3{z_0}^2 + 40t^9{x_0}^3{z_0}^2 + 74640t^4{x_0}^4{z_0}^2 \\
&+71628t^6{x_0}^4{z_0}^2 + 1964t^8{x_0}^4{z_0}^2 + 36t^{10}{x_0}^4{z_0}^2 + 1135008t^3{x_0}^5{z_0}^2 \\
&-25688t^7{x_0}^5{z_0}^2 - 1128t^9{x_0}^5{z_0}^2 - 200448t^6{x_0}^6{z_0}^2 - 6464t^8{x_0}^6{z_0}^2 \\
&-249984t^5{x_0}^7{z_0}^2 - 32272t^7{x_0}^7{z_0}^2 + 82720t^6{x_0}^8{z_0}^2 + 542976t^5{x_0}^9{z_0}^2 \\
&+4769856t^4{x_0}^{10}{z_0}^2 + 30000t^4y_0{z_0}^2 + 9000t^6y_0{z_0}^2 + 160t^8y_0{z_0}^2 \\
&+480000t^3x_0y_0{z_0}^2 - 17320t^7x_0y_0{z_0}^2 - 576t^9x_0y_0{z_0}^2 - 72920t^6{x_0}^2y_0{z_0}^2 \\
&-2928t^8{x_0}^2y_0{z_0}^2 - 85440t^5{x_0}^3y_0{z_0}^2 - 11992t^7{x_0}^3y_0{z_0}^2 + 40912t^6{x_0}^4y_0{z_0}^2 \\
&+419168t^5{x_0}^5y_0{z_0}^2 + 3950016t^4{x_0}^6y_0{z_0}^2 - 200t^6{y_0}^2{z_0}^2 + 89600t^5x_0{y_0}^2{z_0}^2 \\
&+812800t^4{x_0}^2{y_0}^2{z_0}^2 + 100000t^3{z_0}^3 - 4000t^7{z_0}^3 - 128t^9{z_0}^3 - 18000t^6x_0{z_0}^3 \\
&-640t^8x_0{z_0}^3 + 6000t^5{x_0}^2{z_0}^3 - 2480t^7{x_0}^2{z_0}^3 + 11120t^6{x_0}^3{z_0}^3 \\
&+49760t^5{x_0}^4{z_0}^3 + 756672t^4{x_0}^5{z_0}^3 + 20000t^5y_0{z_0}^3 + 320000t^4x_0y_0{z_0}^3 \\
&+50000t^4{z_0}^4.
\end{aligned}
$$

List of Figures

Bibliography

[1] Arnol'd V I (1973) Normal forms for functions near degenerate critical points, the Weyl groups A_k, D_k, E_k and Lagrangian singularities, *Funct. Anal. Appl.* **6** 254–72.

[2] Arnol'd V I (1986) *Catastrophe Theory*, Springer-Verlag.

[3] Arnol'd V I (1989) *Mathematical Methods of Classical Mechanics*, Springer-Verlag.

[4] Arnol'd V I (1990) *Singularities of Caustics and Wave Fronts. Mathematics and its Applications (Soviet Series) 62*, Kluwer Academic Publishers Group.

[5] Arnol'd V I, Shandarin S F and Zeldovich Y B (1982) The large scale structure of the universe 1, *Geophys. Astrophys. Fluid Dynamics* **20** 111–30.

[6] Burnside W S and Panton A W (1892) *The Theory of Equations*, Dublin Univerity Press.

[7] Burgers J M (1974) *The nonlinear diffusion equation*, D Reidel Publishing.

[8] Callahan J (1974) Singularities and plane maps *Amer. Math. Monthly* **81** 211–40.

[9] Callahan J (1977) Singularities and plane maps 2. Sketching catastrophes *Amer. Math. Monthly* **84** 765–803.

[10] Coolidge J L (1931) *Treatise on algebraic plane curves*, Oxford University Press.

[11] Dafermos C (2000) *Hyperbolic Conservation Laws in Continuum Physics. Grundlehren der Mathematischen Wissenschaten 325*, Springer-Verlag.

[12] Davies I M, Truman A and Zhao H Z (2002) Stochastic heat and Burgers equations and their singularities I - geometric properties, *J. Math. Phys.* **43** 3293–328.

[13] Davies I M, Truman A and Zhao H Z (2005) Stochastic heat and Burgers equations and their singularities II. Analytical properties and limiting distributions, *J. Math. Phys.* **46** 043515.

[14] Durrett R (1982) A new proof of Spitzer's result on the winding of two dimensional Brownian motion, *Ann. Probab.* **10** 244–6.

[15] Durrett R (1984) *Brownian motion and martingales in analysis*, Wadsworth.

[16] E Weinan, Khanin K, Mazel A and Sinai Y (2000) Invariant measures for Burgers equations with stochastic forcing, *Ann. Math.* **151** 877-960.

[17] Fedoriuk M V (1971) Stationary phase method and pseudo-differential operators, *Uspekhi Mat. Nauk.* **26** No. 1 67–112.

[18] Ferrar W L (1950) *Higher Algebra*, Oxford University Press.

[19] Freedman D (1971) *Brownian motion and diffusion*, Holden-Day.

[20] Freidlin M I and Wentzell A D (1998) *Random Perturbations of Dynamical Systems*, Springer-Verlag.

[21] Gilmore R (1981) *Catastrophe Theory for Scientists and Engineers*, John Wiley.

[22] Hilton H (1920) *Plane algebraic curves*, Clarendon Press.

[23] Hwa R C and Teplitz V L (1966) *Homology and Feynman integrals*, W A Benjamin.

[24] Kac M (1959) *Probability and Related Topics in Physical Science*, Interscience Publishers.

[25] Klein F (1922) Über den Verlauf der Abelschen Integrale bei den Kurven vierten Grades, *Gesammelte Mathematische Abhandlungen II* ed Fricke R and Vermeil H, Springer.

[26] Kolokoltsov V N, Schilling R L and Tyukov A E (2004) *Rev. Mat. Iberoamericana* **20** 333-80

[27] Kreyszig E (1959) *Differential geometry*, Toronto University Press.

[28] Kunita H (1984) Stochastic differential equations and stochastic flows of homeomorphisms, *Stochastic Analysis and Applications, Advances in Probability and Related Topics. Vol. 7* ed Pinsky M A, Marcel Dekker.

[29] Maslov V P (1972) *Perturbation Theory and Asymptotic Methods*, Dunod.

[30] Maslov V P and Fedoriuk M V (1981) *Semi-Classical Approximation in Quantum Mechanics. Mathematical Physics and Applied Mathematics Vol. 7*, Riedel Publishing Company.

[31] Nickalls R W D (1993) A new approach to solving the cubic, *Mathematical Gazette*

[32] Pohst M and Zassenhaus H (1989) *Algorithmic Algebraic Number Theory*, Cambridge University Press.

[33] Reasons S (2004) *Singularities of the stochastic Burgers equation with vorticity*, PhD thesis UWS.

[34] Reynolds C (2002) *On the polynomial swallowtail and cusp singularities of stochastic Burgers equations*, PhD thesis UWS.

[35] Reynolds C N, Truman A and Williams D (2003) *Probabilistic Methods in Fluids* ed Davies I M et al, World Scientific pp 239–62

[36] Salmon G (1934) *A Treatise on the Higher Plane Curves*, G E Stechert Co.

[37] Shandarin S F and Zeldovich Y B (1989) The large scale structure of the universe 2: turbulence, intermittency, structures in a self gravitating medium, *Rev. Mod. Phys.* **6** 185-220.

[38] Springer G (1957) *Introduction to Riemann surfaces*, Addison-Wesley.

[39] Strassen V (1964) An invariance principle for the law of the iterated logarithm, *Z. Wahrscheinlichkeitstheorie* **3** 211–26.

[40] Strook D W (1984) *An introduction to the theory of large deviations*, Springer-Verlag.

[41] Truman A and Zhao H Z (1998) Stochastic Burgers equations and their semi classical expansions, *Comm. Math. Phys.* **194** 231-48.

[42] Van Der Waerden (1949) *Modern Algebra Vols. 1 and 2*, Frederick Ungar Publishing.

[43] Varadhan S R S (1984) *Large deviations and applications*, SIAM.